



UNIVERSITÀ DEGLI STUDI DI MILANO

DEPARTMENT OF CHEMISTRY

Doctorate School of Chemical Sciences and Technologies

Ph.D. course in chemistry, XXXII Cycle

**(Cyclopentadienone)iron complexes
in reactions involving hydrogen transfer**

Xishan BAI

R11712

CHIM/06 Organic Chemistry

Tutor: Prof. Cesare GENNARI

Co-Tutor: Prof. Luca PIGNATARO

Milan, 2020

Table of contents

Chapter 1 - (Cyclopentadienone)iron complexes in the context of homogeneous iron catalysis for hydrogen transfer reactions.....	1
1.1 Revival of research interest in homogeneous iron catalysis and the most important applications to transformations involving hydrogen transfer.....	1
1.1.1 General difficulties in the replacement of noble metals with iron.....	3
1.1.2 Strategies for enabling two-electron pathways with iron.....	4
1.1.3 Main applications of homogeneous iron catalysis.....	6
1.1.4 Use of iron catalysts in reactions involving hydrogen transfer.....	6
1.2 (Cyclopentadienone)iron complexes (CICs) – Discovery, preparation and properties.....	10
1.3 First catalytic applications of (hydroxycyclopentadienyl)iron complexes (HCICs) in C=O double bond hydrogenation and in Oppenauer-type oxidation of alcohols.....	13
1.4 Applications of CICs in reactions involving hydrogen transfer.....	16
1.4.1 Use in reduction of C=O double bonds.....	18
1.4.2 Use in reduction of C=N double bonds.....	24
1.4.3 Use in reduction of C=C double bonds.....	26
1.5 Use of CIC in hydrogen borrowing reactions.....	27
1.6 Chiral CICs and their applications in enantioselective catalysis.....	34
1.6.1 Chiral CICs for enantioselective catalysis.....	35
1.6.2 Dual catalysis approach combining CICs with chiral Brønsted acid for enantioselective transformation.....	37
1.7 Use of CICs in Oppenauer-type alcohol oxidation.....	40
1.8 Other applications of CICs.....	41
1.9 Conclusions on the State-of-the-Art catalytic applications of (cyclopentadienone)iron complexes.....	43
References.....	45
Chapter 2 - Applications of a highly active CIC to C=N bond reduction reactions.....	51
2.1 Introduction.....	51
2.2 Preparation of CIC 9d	52

2.3 Imine transfer hydrogenation.....	55
2.4 Reductive amination of carbonyl compounds	60
2.5 Conclusions	66
2.6 Experimental Section.....	66
2.6.1. General remarks	66
2.6.2. Synthesis of Ligands and Complexes	67
2.6.3 Synthesis of pre-isolated imines	69
2.6.4 Determination of the transfer hydrogenation Kinetics of imine S1	74
2.6.5 Catalytic Tests – Transfer Hydrogenation of Imines – General Procedure	75
References	83
Chapter 3 - Applications of a highly active CIC to alcohol amination reactions.....	87
3.1 ‘Hydrogen-Borrowing’ amination of secondary alcohols.....	88
3.2 Conclusions on the 9d -catalyzed HB amination of alcohols.....	97
3.3 Experimental Section.....	98
3.3.1 General remarks	98
3.3.2 Control experiment for elucidating the mechanism of allylic alcohol amination with concomitant C=C reduction.....	99
3.3.3 Catalytic Tests – ‘hydrogen-borrowing’ amination of secondary alcohols – General Procedure.	101
References	110
Chapter 4 - Chiral complexes for enantioselective applications	113
4.1 Chiral CICs featuring a stereogenic plane	114
4.1.1 Synthesis of chiral CICs with stereogenic plane in racemic form and test of their catalytic activity	114
4.1.2 Resolution of complexes 9cc and 9am by semipreparative enantioselective HPLC and determination of the absolute configuration of the enantiomerically pure complexes	117
4.1.3 Asymmetric hydrogenation of C=O and C=N polar bonds with chiral iron complexes.....	119
4.2 Chiral macrocyclic CICs.....	121
4.2.1 Synthesis of chiral macrocyclic iron complexes.....	122
4.2.2 Asymmetric hydrogenation of C=O double bonds with chiral macrocyclic iron complexes	126

4.3 Conclusions on chiral iron complexes	127
4.4 Experimental Section.....	128
4.4.1 General remarks	128
4.4.2 Synthesis of chiral iron complexes with stereogenic plane	129
4.4.3 General Procedure for the AH of ketones and ketimines.....	141
4.4.4 Synthesis of chiral macrocyclic complexes	143
4.4.5 Catalytic tests with chiral macrocyclic iron complexes 9ga , 9gc , and 9gd	151
References	152
Chapter 5 - MOF-supported CICs	155
5.1 Preparation of MOF-supported CICs.....	156
5.1.1 Synthesis of CICs and cyclopentadienones as linkers or active site	156
5.1.2 Synthesis of MOF-supported CICs	161
5.2 Hydrogenation of C=O double bonds with MOF-supported CICs.....	163
5.3 Conclusions on MOF-supported CICs.....	165
5.4 Experimental Section.....	165
5.4.1 General remarks	166
5.4.2 Synthesis of CICs as linkers or active site	166
5.4.3 Synthesis of activated esters featuring CICs.....	176
5.4.4 Synthesis of CICs (\pm)- 9au	177
5.4.5 Hydrogenation of C=O double bonds with MOF-supported CICs	178
References	179
Conclusions	182
List of Abbreviations	183
List of papers deriving from this work of thesis	185
Acknowledgements	186

Chapter 1 - (Cyclopentadienone)iron complexes in the context of homogeneous iron catalysis for hydrogen transfer reactions

1.1 Revival of research interest in homogeneous iron catalysis and the most important applications to transformations involving hydrogen transfer

Homogeneous catalysis is considered as a key technology to achieve sustainable, convenient, efficient, and selective chemical transformations. About 80% of all fine chemical and pharmaceutical products on industrial scale are made by catalytic processes. In particular, metal complexes are playing an important role in the synthesis of fine chemicals and a number of pre-catalysts are commercially available for chemists. A careful choice of the metal and design of surrounding ligands can effectively shape reactivity and selectivity of the active catalyst. During the last decades, complexes of noble metal such as platinum, palladium, rhodium, iridium and ruthenium have occupied a central place in homogeneous catalysis and have been used to prepare highly efficient catalysts for a large amount of applications. However, due to the high cost and potential toxicity, more environmentally friendly and cheaper alternatives are desirable for industrial applications.

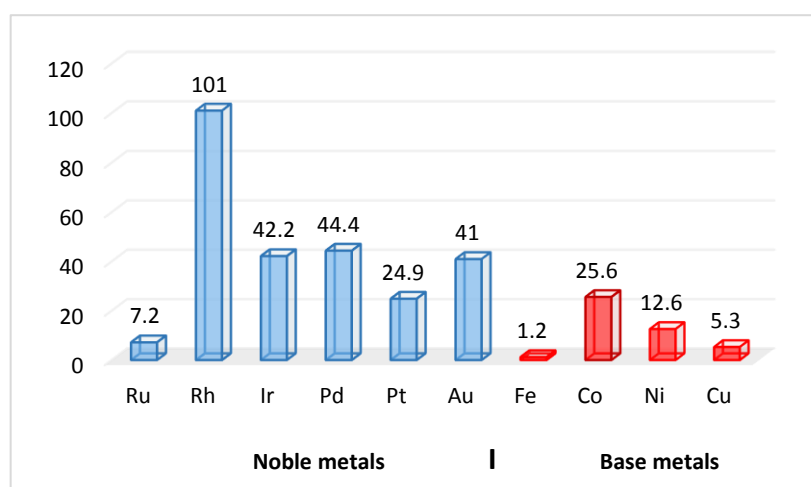


Figure 1.1. Average prices of noble and base metals 1 year. Price: €/g for noble metals (blue), €/kg for base metals (red).

To this end, replacing noble metals with more abundant and cheaper first row transition metals, such as Mn, Fe, Co, and Cu would be a possible solution. A price comparison between first-row transition metals and precious metals shows that the former are at least 1000 times cheaper (Figure 1.1).^[1] Among them, iron is the least expensive, as it is the fourth most abundant element and the second most abundant metal in the Earth crust (4.7 wt %). Owing to its rich redox chemistry and its scarce toxicity, iron is a very good candidate to be

exploited in homogeneous catalytic processes.

Use of iron in catalysis started more than 100 years ago, and the Fenton oxidation is commonly referred to as the first milestone example of iron catalysis: in 1894 Henry John Horstman Fenton reported that a solution of ferrous iron (representatively FeSO_4) in hydrogen peroxide – later called Fenton's reagent – can promote the oxidation of contaminants or waste waters.^[2] A second milestone in iron catalysis was reached in 1911, when German chemists Fritz Haber and Carl Bosch patented a very important nitrogen fixation method for the preparation of ammonia from hydrogen and nitrogen.^[3] The so-called Haber-Bosch process involves the use of a heterogeneous iron catalyst at high temperature and pressure (500 °C, 200 bar). In 1926,^[4] another important application of iron catalysis was reported, which is the Fischer-Tropsch process developed by chemists Franz Fischer and Hans Tropsch. This process involves a series of reactions which allow to obtain liquid hydrocarbons through the conversion of a mixture of carbon monoxide and hydrogen. This process, carried out at medium to high temperature (150-300 °C) under several tens bar of pressure, has been historically relevant for the production synthetic fuel in a petroleum-poor but coal-rich country such as Germany.

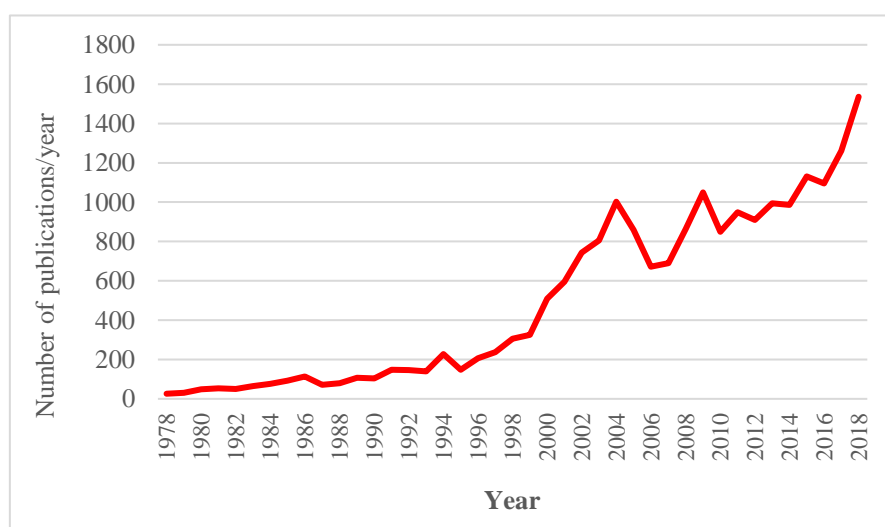


Figure 1.2. Number of iron catalysis-related publications over the last 40 years.

Another milestone in iron catalysis is homogeneous Reppe chemistry. In 1953, $\text{Fe}(\text{CO})_5$ was firstly reported by Reppe and Vetter as homogeneous catalyst for the hydroformylation of olefins and for the preparation of alcohols and aldehydes from CO and H_2O .^[5] From then on, homogeneous iron catalysis has entered chemical researcher's sight. However, in the following decades, the research on homogeneous iron catalysts was sluggish, as only few examples were explored. For instance, the first iron-catalyzed cross-coupling reaction was reported by Kochi and co-workers in 1971,^[6] iron-catalyzed epoxidation reactions were reported by Groves and co-

workers in 1979,^[7] and iron-catalyzed ethylene polymerization was reported by Brookhart and Small in 1998.^[8] Despite these and other examples, at the end of 20th century homogeneous iron catalysis could be still considered an underdeveloped research field. The explosion of research activity to develop efficient iron catalysts has happened in early 21st century (Figure 1.2, data is from SCOPUS® searching “iron catalysis”). In 2004 several reviews and highlight articles were published with a focus on the field of iron catalysis.^[9] The latter were later followed by numerous articles, accounts, reviews and books, an increasing part of which had a focus on homogeneous iron catalysis.

1.1.1 General difficulties in the replacement of noble metals with iron

In organometallic chemistry and homogeneous catalysis, two-electron processes play a very important role. For instance, oxidative addition and reductive elimination represent the key steps of the bond-activating and product-forming process in many important catalytic cycles.^[10] These transformations have been commonly promoted by the late second- and third-row transition metal complexes using strong field-ligands (e.g. cyclopentadienyl, phosphine, *N*-heterocyclic carbene, etc.). On the other hand, the control of redox chemistry to achieve such transformations with Earth-abundant metals is cumbersome, as these complexes tend to engage preferentially in single electron transfer processes.^[11]

Within these metals, the redox chemistry of iron is governed by a single-electron transfer between its most common oxidation states Fe^{II} (d^6) and Fe^{III} (d^5): to mimic the reactivity patterns typical of noble metals, iron should be diverted from one-electron reaction patterns and induced to engage in two electron patterns by use of suitable ligands (see Chapter 1.1.2).

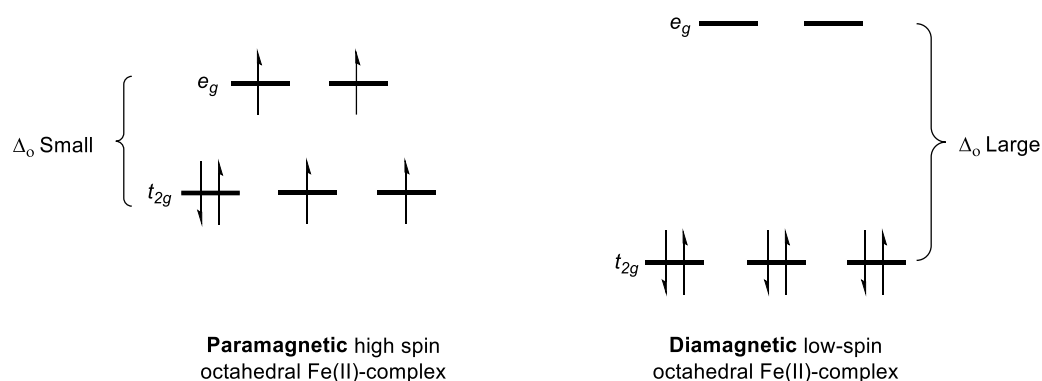


Figure 1.3. MO diagrams for octahedral crystal field: distribution of the six valence electrons in high-spin and low-spin Fe^{II}-complexes.

The use of iron as catalyst is also hampered by the difficult characterization of iron complexes. Since the latter are paramagnetic in most cases (Figure 1.3),^[12] structural characterizations are often limited to mass spectrometry and X-ray diffraction analysis, rather than NMR spectroscopy.

1.1.2 Strategies for enabling two-electron pathways with iron

The catalytic properties of iron complexes are determined by interactions between ligands and metal. Usually, tri- and tetradentate ligands containing phosphorous and/or nitrogen donors (e.g., porphyrins or polydentate phosphines) are used in order to obtain reasonably stable iron complexes. Besides enhancing complex stability, another function of these ligands is to enable two-electron pathways with iron complexes. To this end, four main strategies have been proposed:

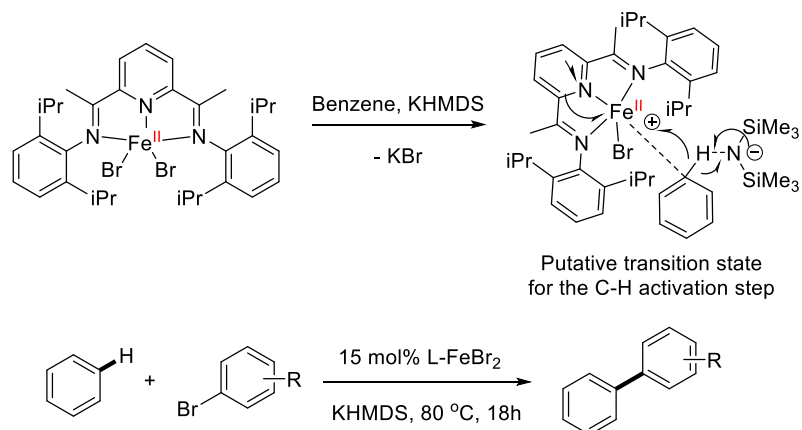
- 1) **Metal–ligand cooperativity** (Scheme 1.1 A), in which *redox non-innocent ligands* undergoing reversible electron transfer were used to form iron complexes and directly participate in redox chemistry during the catalytic transformation.^[13]

The concept of *innocent ligand* was introduced by Jørgensen and co-workers^[14] to define ligands which do not play any role in catalytic cycles. On the contrary, *redox non-innocent ligands* can affect the electronic density of the complex and reserve electrons during the catalytic cycles through resonance or inductive features. Besides enabling two-electron processes, these ligands can also initiate and control radical processes. Fensterbank and co-workers reported an example of electronic metal–ligand cooperativity, which consisted in the activation of the benzene's C-H bond to the pyridine(diimine) iron dibromide complex, (*i*PrPDI)FeBr₂ (*i*PrPDI = 2,6-(2,6-*i*Pr₂-C₆H₃N=CMe)₂C₅H₃N; Scheme 1.1 A).^[15] Combined results of IR, NMR and DFT studies provided evidence of a two-electron activation of unactivated arenes with iron(II) dibromide complex in the presence of a base (KHMDS) to a [LFe^{II}Br]⁺/HMDS⁻ ion pair with a one-electron transfer from HMDS⁻ to the ligand.

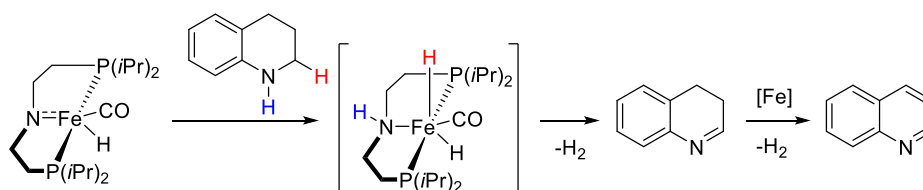
- 2) **Chemical metal-ligand cooperativity**, which relies on a supporting ligand that participates directly in the reversible bond-making and -breaking events during the catalytic cycles.^[16] One example belonging to this category is the dehydrogenation enabled by an iron complex chelating a bis(phosphino)amine pincer ligand, (*i*PrPNP)FeH(CO) (*i*PrPNP = bis(2-(*i*Pr₂-phosphanyl)ethyl)amine, Scheme 1.1 B).^[16a] Here, ligand and metal work together for catalytic cycles, with hydrogen atoms binding to both the ligand's nitrogen atom and the metal centre.

- 3) **Metal–metal cooperativity**, in which a net two-electron process stems from the ability of two different metal complexes to undergo a one-electron redox process.^[17] An illustrative example of this strategy is shown in Scheme 1.1 C.^[17b]
- 4) **Use of strong-field ligands**, a strategy proposed by Chirik and Arevalo to facilitate the oxidative addition step, that has been exploited in some examples of catalytic C-H functionalizations (Scheme 1.1 D).^[18]

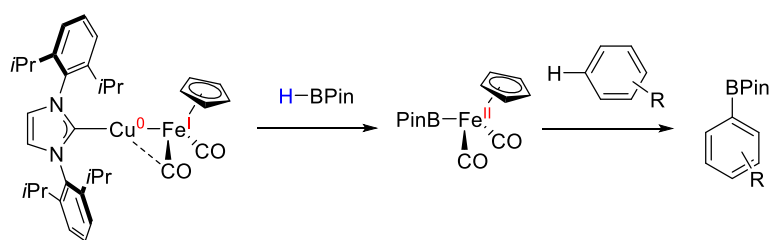
A. Activation of C-H bond enabled by electronic metal-ligand cooperativity



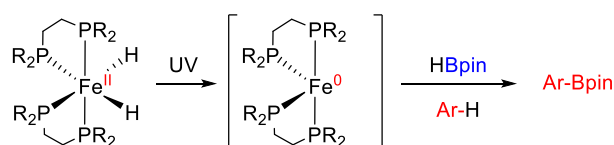
B. Dehydrogenation enabled by chemical metal-ligand cooperativity



C. C-H Borylation Enabled by Metal-Metal Cooperativity



D. C-H Borylation Enabled by strong-field ligands



Scheme 1.1. Strategies for enabling two-electron pathways with iron

1.1.3 Main applications of homogeneous iron catalysis

After entering the 21st century, numerous research groups in the world have started working on the development of effective catalytic systems based on iron. In particular, iron catalysis has been applied to a wide range of transformations,^[9,13e,19] such as:

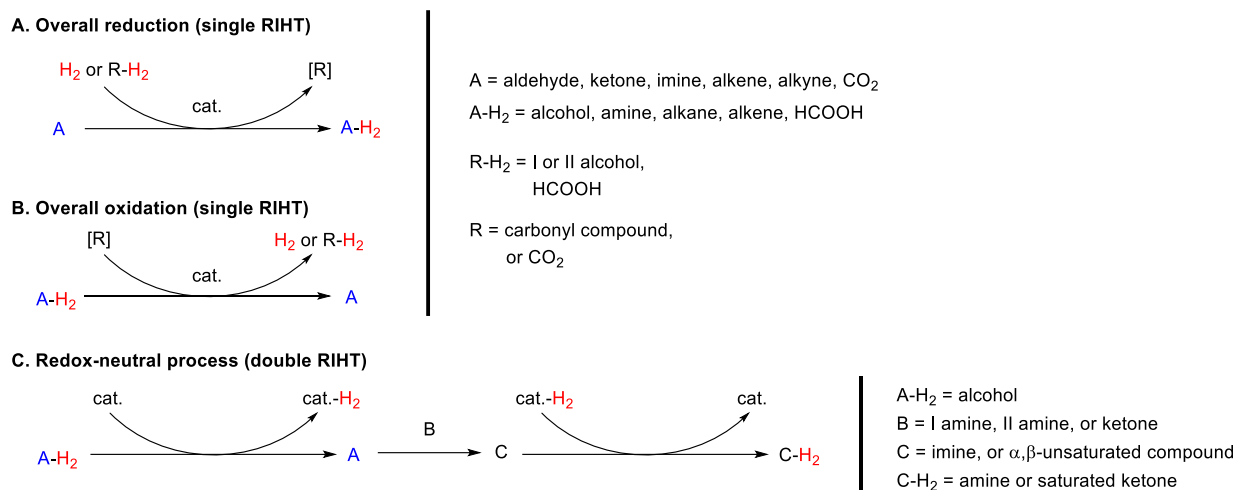
- 1) **Substitution reactions**, including nucleophilic substitution at sp³-carbon centers, electrophilic aromatic substitution, cross-coupling reactions to form C-C and C-heteroatom bonds.^[9a,b,e,19a,i,20]
- 2) **Addition reactions**, such as carbometalation, hydroalkylation, carboxylation, ring opening and ring expansion reactions, polymerizations, C-heteroatom bond forming additions, addition to carbonyl groups.^[19f,i,20g,21]
- 3) **Reductions**, including hydrogenation of alkenes and alkynes, hydrosilylation, hydrogenation and reductive amination of carbonyl compounds.^[9a,b,e,19f,22]
- 4) **Oxidations** of C(sp³)-H bonds, C(sp²)-H bonds, olefins (e.g., Wacker-type reactions), ketones (Baeyer-Villiger), alcohols (Oppenheimer).^[9a,23]
- 5) **Cycloadditions and Alder-ene-type reactions**, in particular [2 + 1], [2 + 2], [2 + 2 + 1], [3 + 2], [2 + 2 + 2], [4 + 2] and [5 + 2] cycloaddition.^[19h,24]
- 6) **Isomerizations and rearrangements**, including allyl alcohol-carbonyl isomerization, olefin isomerization, cycloisomerization, intramolecular ring expansion.^[25]

1.1.4 Use of iron catalysts in reactions involving hydrogen transfer

Among the general classes of reaction mentioned above, those involving hydrogen transfer are briefly mentioned in this Section, as they are more relevant to the topic of my work of thesis. In this thesis the reactions involving hydrogen transfer (RIHT) are defined as the ones in which a H₂ molecule is added to or abstracted from the substrate (see Scheme 1.2).

RIHT may either occur as a single transformation (thus giving rise to a net reduction or oxidation of the substrate, Scheme 1.2 A and B), or occur twice in the same catalytic cycle (thus generating a redox-neutral ‘hydrogen borrowing’ or ‘hydrogen autotransfer’ process, Scheme 1.2 C). Typical single RIHTs are the hydrogenation of multiple bonds, in which molecular H₂ is directly transferred to the substrate, and transfer

hydrogenation, in which H₂ is transferred from a donor (e.g., an alcohol or HCOOH, shown as ‘R-H₂’ in Scheme 1.2 A), just as their reverse processes (see Scheme 1.2 B). The most common ‘hydrogen-borrowing reactions’ are the amination of alcohols and the α -alkylation of ketones (see Scheme 1.2 C).

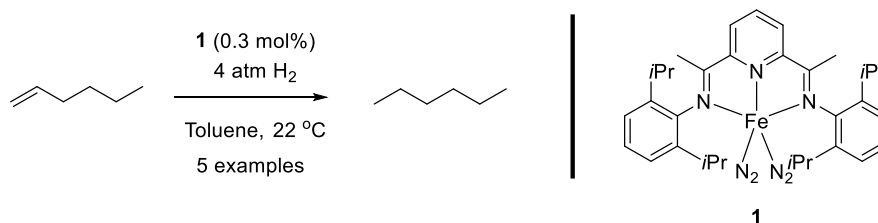


Scheme 1.2. General representation of catalytic reactions involving hydrogen transfer (RIHT): reduction (A), oxidations (B), and redox-neutral ‘hydrogen borrowing’ processes (C).

Examples of successful Fe-catalyzed hydrogenation and transfer hydrogenation have been reported by several research groups, and a number of reviews on these reactions have been published.^[9a,b,e,19f,22]

Reduction of C=O and C=C double bonds had been dominated for many years by catalysts based on noble metals such as ruthenium, rhodium and iridium, and for a long time, applications of iron catalysis lagged behind precious metal catalysts in this field. The first ground-breaking use of iron catalysts in hydrogenation of carbonyl compounds was reported in 1980s by Markó and co-workers, who used Fe(CO)₅ as pre-catalyst to hydrogenate a series of ketones and aldehydes.^[26]

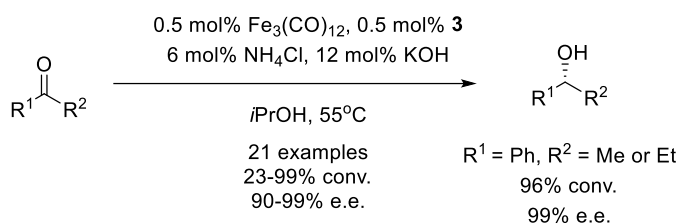
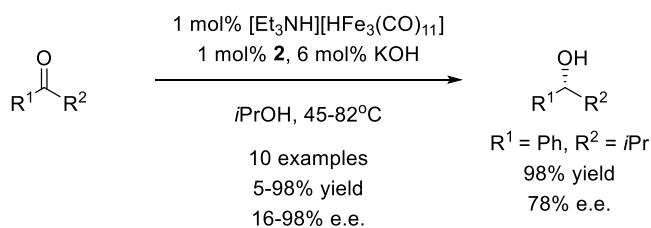
In 2004, Chirik and co-workers reported the sole example of iron catalyst for the hydrogenation of isolated C=C bonds (Scheme 1.3).^[27]



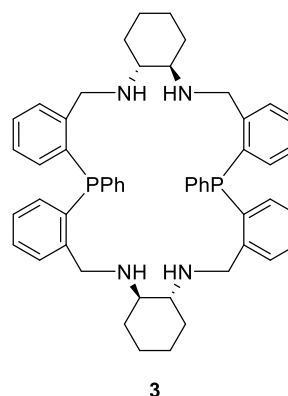
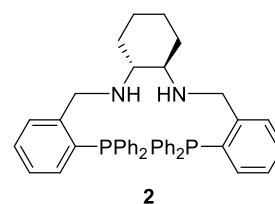
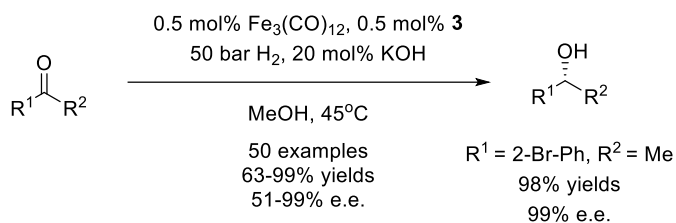
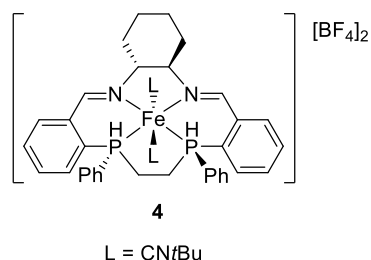
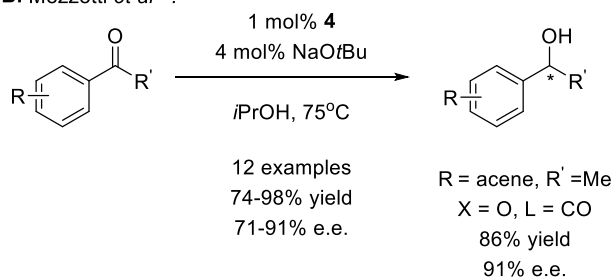
Scheme 1.3. Hydrogenations of alkenes catalyzed by iron complexes

A. Gao *et al.*^{29,30}

ATH of ketones



AH of ketones

B. Mezzetti *et al.*³¹

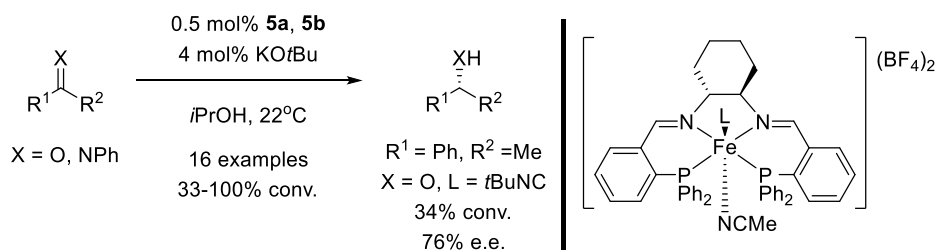
Scheme 1.4. Enantioselective hydrogenation of ketones catalyzed by *P,N,N,P*-pincer complexes and macrocyclic complexes.

A few years after the original report, the same authors demonstrated that the peculiar catalytic activity of complex **1** is due to the ‘redox non-innocent’ nature (see Section 1.1.2) of its bis(imino) pyridine ligand. Indeed, under hydrogenation conditions the ligand undergoes reduction to the corresponding radical dianion, whereas the iron center remains in the +2 oxidation state.^[28]

In the same year, Gao and co-workers reported an *in situ*-formed iron catalytic system for the Asymmetric Transfer Hydrogenation (ATH) of ketones (Scheme 1.4 A), obtaining good conversions and e.e. values in the 16-98% range.^[29] Further work of Gao and co-workers in this field led to the development of highly enantioselective catalysts for ketone ATH and Asymmetric Hydrogenation (AH) based on the use of chiral

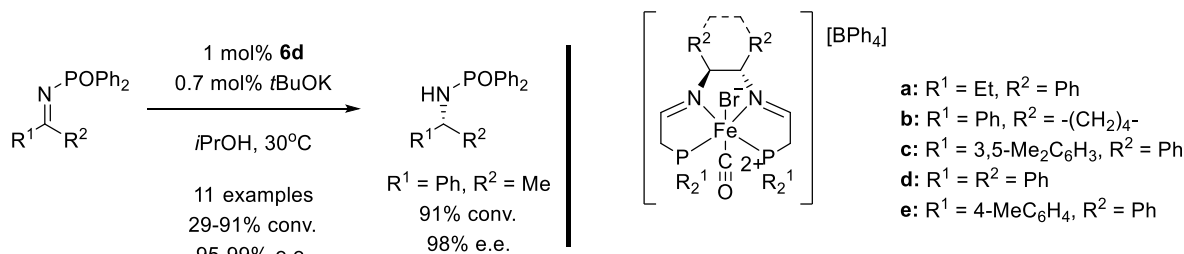
macrocyclic ligands.^[29,30] In 2014, Mezzetti and co-workers reported a bis(isonitrile) iron(II) complex bearing a chiral N₂P₂ macrocyclic ligand for the ATH of ketones: twelve ketones were reduced with excellent yields (up to 98%) and high enantioselectivity (up to 91% e.e., Scheme 1.4 B).^[31]

A. First general precatalyst



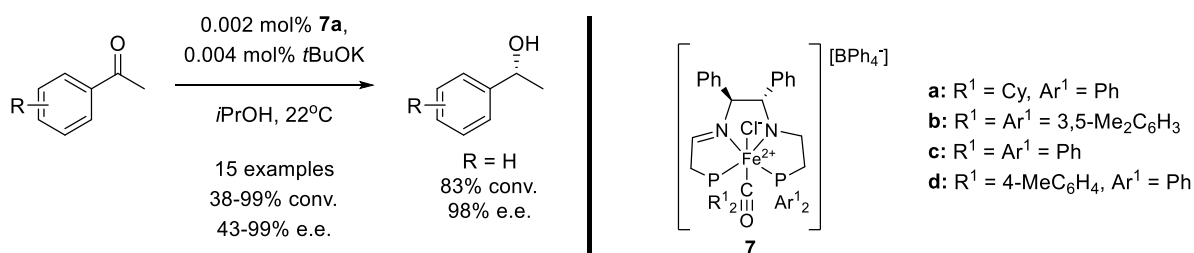
5a: L = CO
5b: L = *t*BuNC

B. Second general precatalyst



6

C. Third general precatalyst

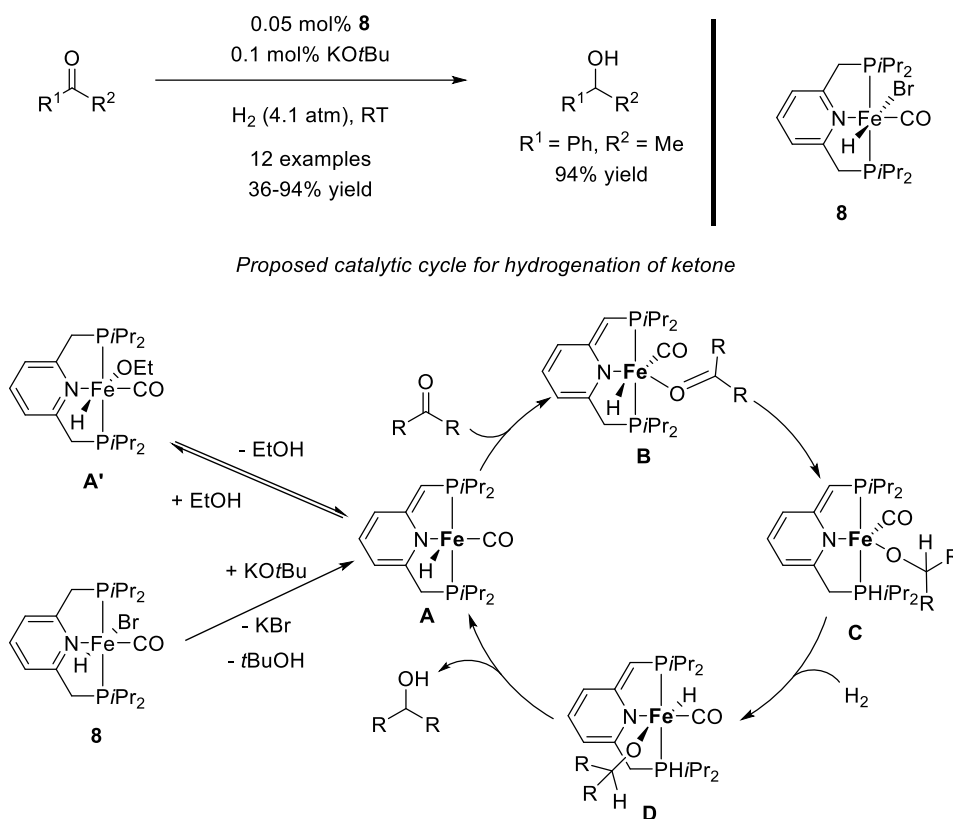


7

Scheme 1.5. Asymmetric Transfer Hydrogenation (ATH) catalyzed by the *P,N,N,P*-pincer complexes developed by Morris and co-workers.

To obtain highly efficient catalytic systems, Morris and co-workers developed a new *P,N,N,P*-pincer iron catalyst for ATH of ketones.^[32] Although excellent conversions were obtained in some cases, only moderate enantioselectivity was generally observed (e.e. values in the 18-76% range, see Scheme 1.5A). Notably, catalytic TOFs up to 907 h⁻¹ were reported, which are competitive with those obtained with ruthenium catalysts. Using related iron *P,N,N,P*-pincer complexes, the same group obtained better e.e. values and TOFs in the ATH of ketones performed in the presence of *i*PrOH.^[33] They synthesized a series of second-generation complexes possessing five membered chelate cycles, which are analogous to complexes **5** (see Scheme 1.5 B).^[34] These second generation catalysts gave an impressive TOF, up to 30,000 h⁻¹, in the ATH of ketones with high

enantiomeric excesses. Particularly, high conversions (up to 91%) and excellent enantioselectivity (95-99% e.e.) were obtained with complex **6d**.^[34c]



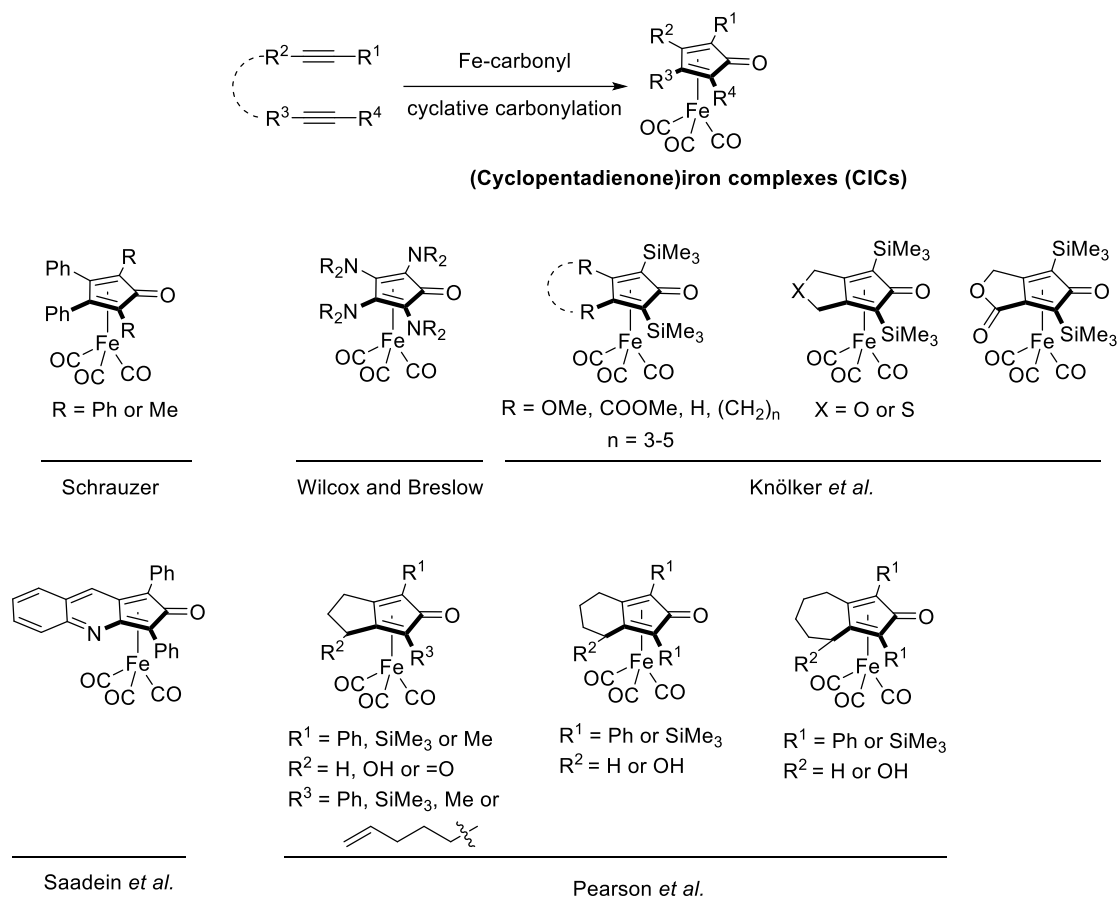
Scheme 1.6. Hydrogenation of ketones catalyzed by P,N,P -pincer complexes.

In 2011, Milstein and co-workers reported a very efficient catalytic system for the hydrogenation of ketones, based on the P,N,P -pincer iron complex **8**.^[16b-c,e,35] The high activity observed allowed a catalyst loading as low as 0.05 mol% (Scheme 1.6). Mechanistic investigations carried out by the authors revealed that this high activity is due to the non-innocent behavior of the P,N,P -ligand (chemical metal-ligand cooperation, see Section 1.1.2), which is dearomatized by the base additive and then undergoes consecutive aromatization/dearomatization steps during the catalytic cycle, with concomitant H_2 splitting and transfer to the substrate.

1.2 (Cyclopentadienone)iron complexes (CICs) – Discovery, preparation and properties

In 1953, (cyclopentadienone)iron complexes (CICs) were firstly described by Reppe and Vetter as stable organometallic intermediates.^[5] Subsequently, several similar complexes were isolated by other groups.^[36] The structure of these organometallic complexes was elucidated for the first time by Schrauazer in 1959.^[37] It was found that these complexes are formed by combination of cyclopentadienone with iron carbonyl complexes

[such as $\text{Fe}(\text{CO})_5$ and $\text{Fe}_2(\text{CO})_9$] exploiting the π orbitals of the diene. Thanks to the advances in spectroscopic techniques, the structure of these complexes was then fully elucidated by IR and NMR. Moreover, after a single-crystal X-ray study on CICs, Hoffmann and Weiss found that $\text{Fe}(\text{CO})_3$ – in the complex – can stabilize cyclopentadienone through four π -electrons of the conjugated diene system similarly to (butadiene)iron tricarbonyl.^[38] Subsequently, different research groups devoted many efforts to the synthesis of (cyclopentadienone)iron complexes (see Scheme 1.7).^[39]



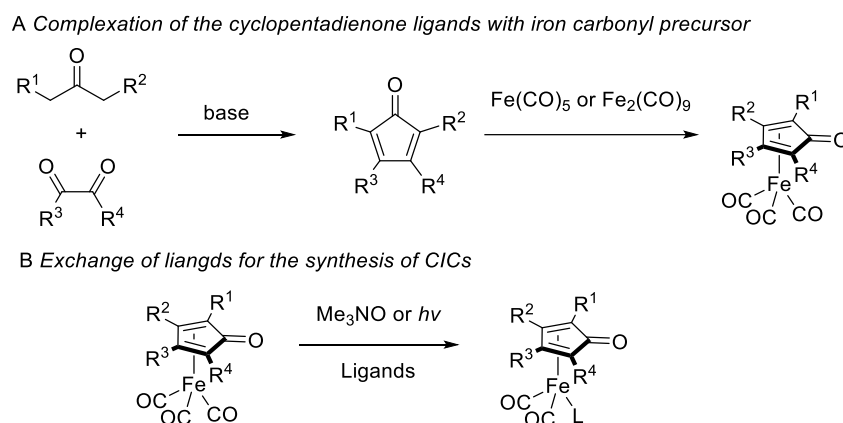
Scheme 1.7. CICs synthesized before the discovery of the catalytic applications of this kind of complexes.

In earliest reports, the synthesis of CICs was carried out by a [2+2+1] cycloaddition reaction between alkynes and iron carbonyl complexes [such as $\text{Fe}(\text{CO})_5$ or $\text{Fe}_2(\text{CO})_9$]. Monocyclic CICs can be synthesized by intermolecular alkyne cyclization, whereas bicyclic CICs could be prepared by intramolecular cyclization of a suitable diyne. Owing to the entropic gain associated to the intramolecular process, the intramolecular cyclization is often carried out in good yields, thus being the preferential strategy for the synthesis of these complexes. Various CICs could be synthesized easily by varying the alkyne substrate (Scheme 1.7).^[37,39,40] Notably, tuning the electronic and steric features of these complexes is largely possible through the modification of the substituents on the alkynes. In addition, different functional groups have been introduced

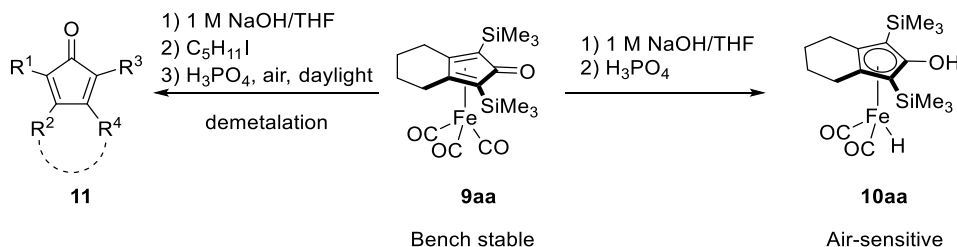
to CICs, including electron-withdrawing and donating groups, bulky substituents, etc.

Another main strategy for the synthesis of CICs is the complexation of the pre-formed cyclopentadienone ligand with an iron carbonyl precursor (such as $\text{Fe}(\text{CO})_5$ and $\text{Fe}_2(\text{CO})_9$, Scheme 1.8 A). This strategy requires previous synthesis of the cyclopentadienone ligand. This reaction is not trivial and it is mainly performed by the condensation of appropriately designed benzil derivatives with 1,3-disubstituted propanones (Scheme 1.8 A). Unfortunately, this reaction requires the presence of at least one aromatic substituent on the 1,3-disubstituted propanone, which represents a remarkable scope limitation. Similarly to the other strategy mentioned above, the reactivity of these complexes could be tuned by introducing different substituents on the cyclopentadienone ring.

A third synthetic strategy consists in exchanging one or more CO ligands of CICs with other ligands (such as CH_3CN , PhCN and chiral P-ligands). Due to the stability of the Fe-CO bond, the ligand exchange only occurs when CO is removed by treatment Me_3NO or ultraviolet light (see Scheme 1.8 B).



Scheme 1.8. Synthetic strategies of CICs



Scheme 1.9. Reactive properties of CICs

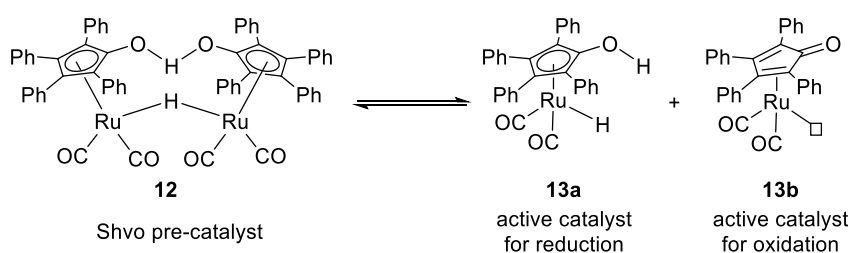
CICs may be viewed as intermediates for the synthesis of cyclopentadienones, for which demetalation is required. In 1999, studying suitable conditions to remove the $\text{Fe}(\text{CO})_3$ group, Knölker and co-workers discovered another important aspect of the reactivity of CICs.^[41] The (hydroxycyclopentadienyl)iron hydride

complex (HCIC) **10aa** was synthesized from **9aa** and isolated by a procedure involving a Hieber base reaction using NaOH and a subsequent treatment with H₃PO₄ (Scheme 1.9). However, the application of HCICs in catalytic reactions was reported only eight years later, even though all the knowledge was set for these transformations.

1.3 First catalytic applications of (hydroxycyclopentadienyl)iron complexes (HCICs) in C=O double bond hydrogenation and in Oppenauer-type oxidation of alcohols

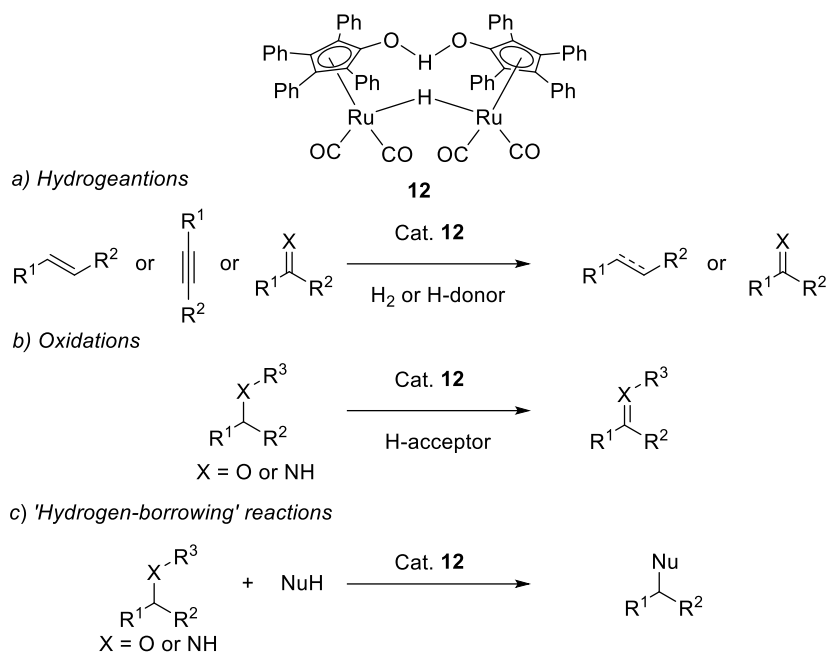
Metal-catalyzed redox processes involving hydrogen transfer (such as hydrogenations, ‘hydrogen-borrowing’ reactions and reductive aminations) have stimulated the researchers’ interest because of their intrinsic atom economy. Chemists carried out many investigations in this field, and a large number of catalysts have been discovered, some of which have been industrially applied.^[42] For a long time, simple modulation of the electronic and steric properties of the ligands has been the way to develop new catalysts. In this kind of approach, the ligand is mostly considered a simple ‘spectator’ which does not participate directly in the catalytic process. More recently, however, the concept of non-innocent ligand (see Section 1.1.2) has emerged as an effective strategy to shape reactivity and catalytic activity of metal complexes.^[13d,43]

A representative application of this concept is the Shvo’s complex **12** (Scheme 1.10), which was discovered by Shvo and co-workers in 1985 and was found to be an efficient pre-catalyst for reduction of C=C and C=X double bonds.^[44] Complex **12** can be dissociated to two complementary active catalysts **13a** and **13b**, which represent a reduction and an oxidation catalyst, respectively (see Scheme 1.10).



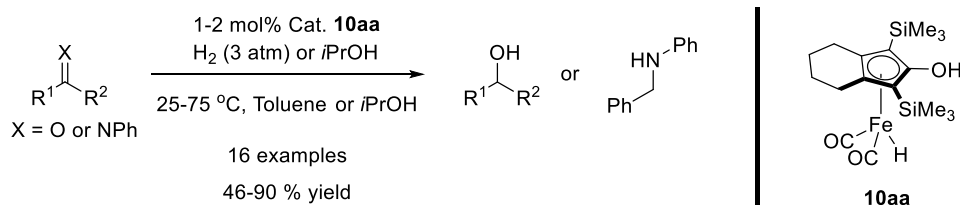
Scheme 1.10. Shvo’s ruthenium complexes

Shvo-type complexes were applied to various reactions and particularly in hydrogenation and oxidation transformations (see Scheme 1.11), and these applications were summarized by Williams in an excellent review in 2010.^[45]



Scheme 1.11. Applications of Shvo's ruthenium complexes

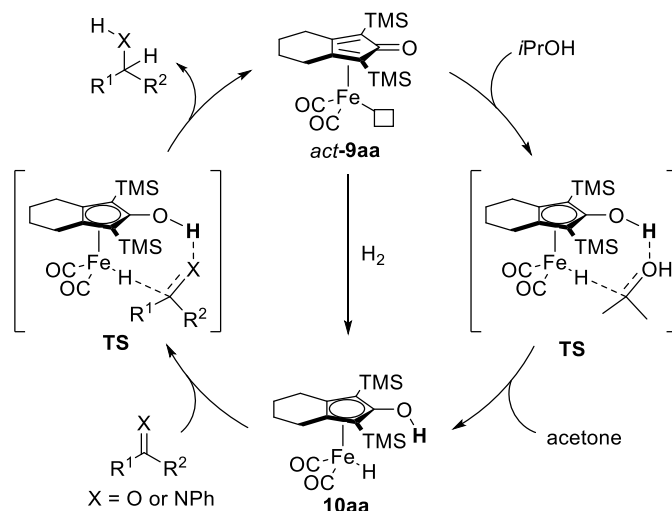
CICs **9aa** and HCICs **10aa** bear strong analogy to the species generated by dissociation of the dimeric Shvo's complex (**13a** and **13b**), whose catalytic activity had been reported in the late 1980s.^[44] Despite this, even after the successful preparation of HCICs reported by Knölker in 1999, the catalytic activity of this class of complexes remained undiscovered until 2007, when the application of complex **10aa** in hydrogenation of ketones was firstly reported. Taking advantage on their strong expertise on the use of Shvo-type catalysts, Casey and Guan moved their attention to the structurally very close complex **10aa**. As expected, complex **10aa** showed good catalytic activity and chemoselectivity in the hydrogenation of C=X double bonds (X = O or N, fifteen different carbonyl compounds and one imine, see Scheme 1.12).^[46] These hydrogenations were performed at r.t. under low hydrogen pressure (3 atm).



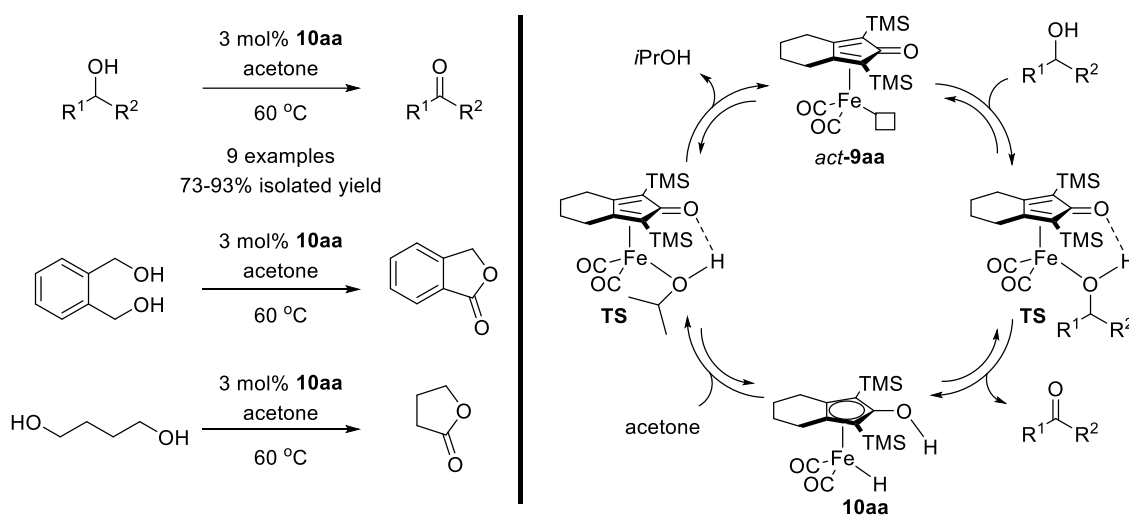
Scheme 1.12. Hydrogenation of C=X double bonds catalyzed by complex **10aa** reported by Casey and Guan.

In the catalytic cycle (Scheme 1.13), complex **10aa** reduces polar double bonds to form the coordinatively unsaturated CIC **act-9aa**, which is then re-converted into **10aa** by reaction with H_2 or *i*PrOH. An outer-sphere mechanism was proposed for this reaction: in the general catalytic cycle, reversible hydrogen transfer occurs *via* a concerted, pericyclic TS in which a hydride is transferred to the carbonyl carbon and a proton passes

from the ligand's OH to the substrate. Iron swings between oxidation states 0 (in complex **act-9aa**) and +2 (in complex **10aa**), and this two-electron pathway is enforced by the non-innocent ligand which, in turn, fluctuates between the cyclopentadienone and the hydroxycyclopentadienyl form.



Scheme 1.13. Proposed hydrogenation mechanism in hydrogenation catalyzed by catalyst **10aa**.



Scheme 1.14. Oppenauer-type oxidations catalyzed by catalyst **10** and proposed hydrogenation mechanism

Based on the reversibility of the reduction pathway, Guan and co-workers extended the use of catalyst **10aa** to the Oppenauer-type oxidation of alcohols in 2010.^[47] Several alcohols were oxidized in the presence of acetone, and good to excellent isolated yields were obtained (see Scheme 1.14). Dehydrogenation of two diols to corresponding lactones was also described in the same contribution. In addition, a mechanism involving the formation of intermediate alcohol complexes was proposed (see Scheme 1.14). HCIC **10aa** hydrogenates acetone and forms the coordinatively unsaturated intermediate complex **act-9aa**. The oxidation product is formed by dehydrogenation of the intermediate formed by complex **act-9aa** with alcohol substrates, along with

regeneration of catalyst **10aa**.

1.4 Applications of CICs in reactions involving hydrogen transfer

Following the work by Casey and Guan on the catalytic activity of HCICs in the hydrogenation of ketones, this class of iron complexes gained increasing interest among researchers. However, an evident setback of HCICs was their high sensitivity to air, which makes a glovebox indispensable to their handling. Contrary to HCICs, CICs are very stable complexes which can be handled under air and even purified by flash column chromatography. Hence, CICs can be seen as a stable pre-catalytic form of HCICs, provided that efficient activation strategies are identified. CICs possess several unique features which distinguish them from most other homogeneous iron catalysts.^[48] Indeed, these catalysts: a) can be easily synthesized from simple starting materials; b) do not require expensive P-ligands; c) are stable to air and moisture, to such extent that a number of organic reactions may be performed cyclopentadienone moiety of the complexes; d) can be purified by standard chromatography techniques.

In situ activation of CICs may be performed in two main ways, shown in Scheme 1.15:

- 1) By conversion into the corresponding HCICs by Hieber base reaction,^[49] i.e. by treating them with an aqueous base analogously to the procedure originally used by Knölker and co-workers to synthesize complex **10aa**.^[41] This activation protocol was firstly reported by Beller and co-workers.^[50]
- 2) By de-coordination of one CO ligand, leading to the corresponding activated CICs *act-9*, bearing a vacant coordination site. This may be achieved either by shining UV light,^[51] as originally reported by Knölker and co-workers,^[52] or by operating an oxidative de-coordination with Me₃NO,^[53] so that a CO₂ molecule is released.

The ability to reversibly transfer H₂ to polar double bonds is the basis of most catalytic applications of CICs. Different suitable pathways can be followed, as shown in Scheme 1.15. According to Path I, complexes *act-CICs* (*act-9*) can be directly dehydrogenate alcohols and form HCICs (**10aa**), then the substrates would be reduced by catalyst HCICs (transfer hydrogenation catalyzed by CICs).^[53d,54]

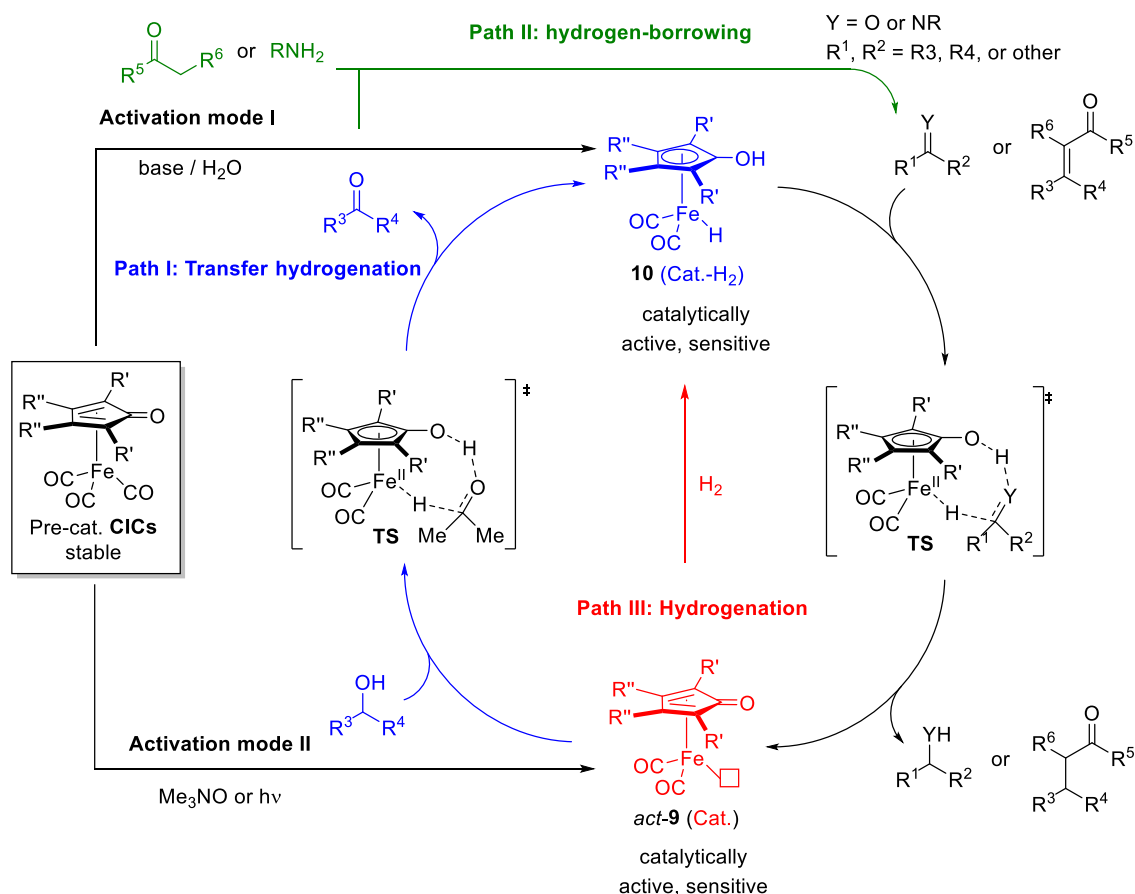
This leads to the reduction of C=O or C=N bond of the substrate (transfer hydrogenation) when the reaction is carried out in the presence of an excess of alcohol or other reductant (e.g., *i*PrOH or HCOOH). Instead, in the presence of an excess of ketone (typically acetone), the reverse path is followed, consisting in the Oppenauer-

type oxidation of an alcohol substrate.^[54b-e,55]

Additionally, redox-neutral (“hydrogen borrowing”) reactions of alcohol substrates are also possible (Scheme 1.15, Path II), in which an alcohol is oxidized and reacts with another compound (e.g., amine or ketone) to form an adduct (e.g., imine/iminium, α,β -unsaturated ketone) that is then reduced by the HCICs (**10**) formed in the oxidation stage.^[56]

Alternatively, complexes *act*-CICs (*act*-**9**) can directly split H_2 and form the HCICs (**10**), which then reduce the substrate (hydrogenation, Scheme 1.15, Path III).^[50,51,53a-c,e,57]

In Path I-III, catalysts alternatively pass from the activated CIC to the HCIC form, thus shuttling the H_2 molecule between substrate(s) and product(s). Hydrogen transfer occurs through a pericyclic transition state involving both the iron atom and the “non-innocent” ligand.^[46b,47,58]

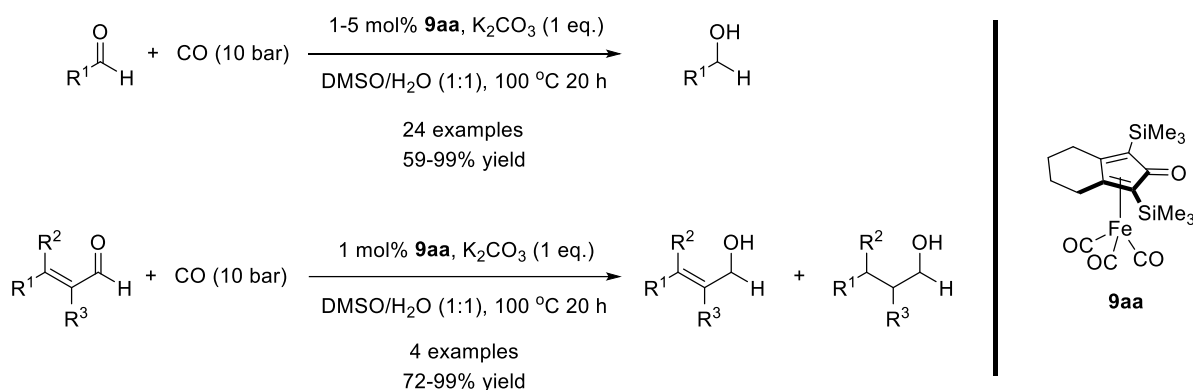


Scheme 1.15. Activation and main catalytic pathways of iron complexes (CICs) in RIHT.

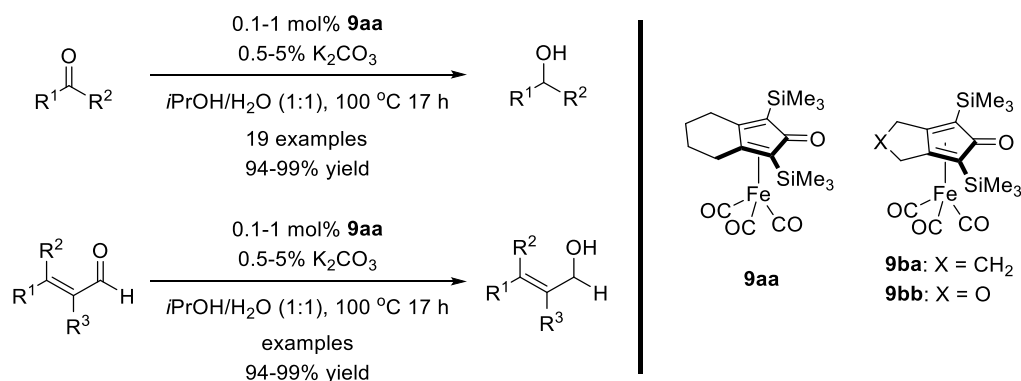
Besides RIHTs, CICs have been also used recently to promote reactions not involving hydrogen transfer, such as the formation of C–N and C–O bonds by intramolecular hydroamination and hydroalkoxylation of allenes.^[59]

1.4.1 Use in reduction of C=O double bonds

After the seminal report by Casey and Guan, who used HCICs to promote C=O bond hydrogenation,^[46] further advances consisted in the expansion of this reactivity to *in situ*-activated CICs, as these complexes are more robust and easy-to-handle. In 2012, Beller and co-workers employed the Knölker's CIC **9aa** in the catalytic reduction of aldehydes using H₂ as reducing agent formed under water-gas shift conditions in the presence of a base (Scheme 1.16).^[57o] Eighteen aromatic aldehydes and six aliphatic aldehydes could be reduced in good to excellent yields (up to 99%). Under these reaction conditions, α,β -unsaturated aldehydes could be also reduced in good yields (72-99% range), although the allylic alcohol products were obtained in mixture with the corresponding saturated alcohols deriving from C=C reduction. Significantly, this reaction could be readily scaled up, thus proving potentially useful for industrial applications.



Scheme 1.16. Hydrogenation of aldehydes catalyzed by catalyst **9aa**

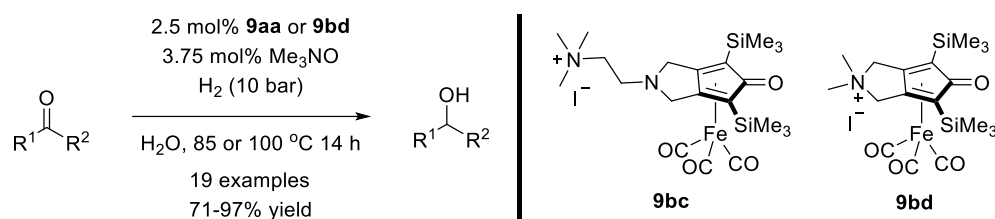


Scheme 1.17. Catalytic hydrogenation of carbonyl compounds catalyzed by CIC **9aa** under base activation conditions.

In 2013, the Beller's group reported the synthesis of nine CICs and their use in the hydrogenation of aldehydes, ketones, and α,β -unsaturated aldehydes.^[50] CIC activation was performed by adding a base additive to the reaction mixture, K₂CO₃ being the most effective. The Knölker's complex **9aa** gave the best results and, in most cases, the C=O reduction products were obtained in excellent yields with low catalyst loading (0.1-1

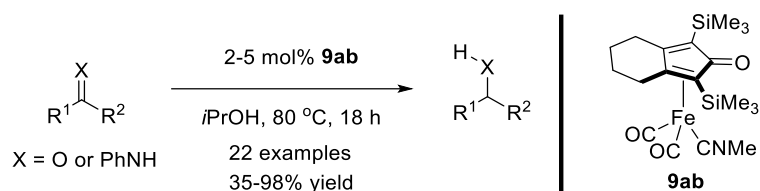
mol%, Scheme 1.17). It is worth noting that the chemoselective hydrogenation of α,β -unsaturated aldehydes was effectively performed.

In 2013, Renaud and co-workers reported that two CICs bearing ionic fragments could promote the hydrogenation of C=O bonds under mild conditions in water. The alcohol products were obtained with good to excellent yields in the 71-97% range (Scheme 1.18).^[53b] The authors found that the reaction rates can be improved if using water as solvent, and higher yields were observed in shorter reaction times using the ionic bifunctional iron complexes as catalyst.



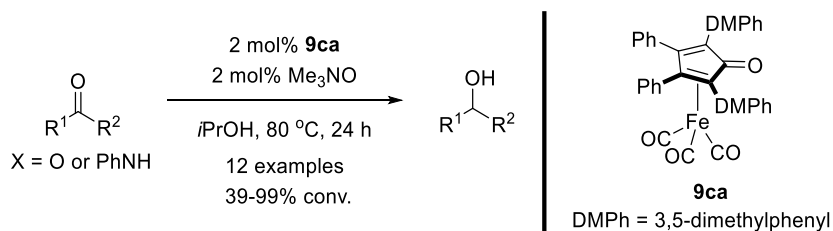
Scheme 1.18. Hydrogenation of carbonyl compounds catalyzed by ionic bifunctional CICs.

In 2012, Funk and co-workers reported the synthesis of CICs bearing a nitrile ligand instead of one CO. The lability of the nitrile ligand allows for catalyst activation by simple thermal dissociation, with no additives required. These new complexes were screened in the transfer hydrogenation of carbonyl compounds. Initial screening work was performed in transfer hydrogenation of acetophenone, and all complexes showed good catalytic activity. Complex **9ab** was chosen for further study and gave good to excellent yields (35-98%) in the transfer hydrogenation of aldehydes and ketones (Scheme 1.19).^[54e] One imine was also reduced in good yield (67%) in the presence of complex **9ab**. However, complex **9ab** was found unreactive in the hydrogenation of acetophenone.



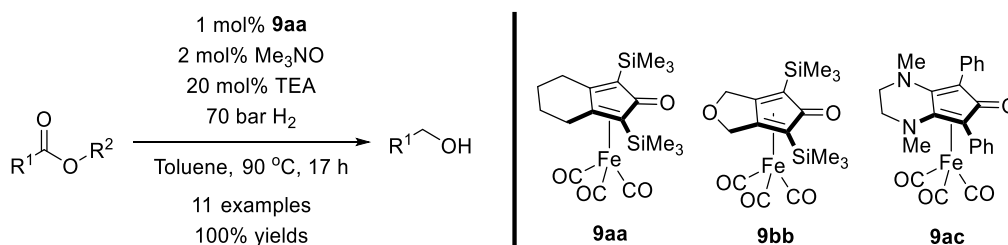
Scheme 1.19. Nitrile-ligated CICs catalyzed transfer hydrogenation of carbonyl compounds and imine

More recently, Funk and co-workers synthesized four new CICs bearing different cyclopentadienone ligands and explored their activity in the transfer hydrogenation of carbonyl compounds. Catalyst activation was performed using Me_3NO . Complex **9ca** gave the highest conversions under the reaction conditions, and was found more active than Knölker complex **9aa** with most substrates. Various alcohols were obtained through transfer hydrogenation in good to excellent conversions (up to 99%, Scheme 1.20).^[54d]



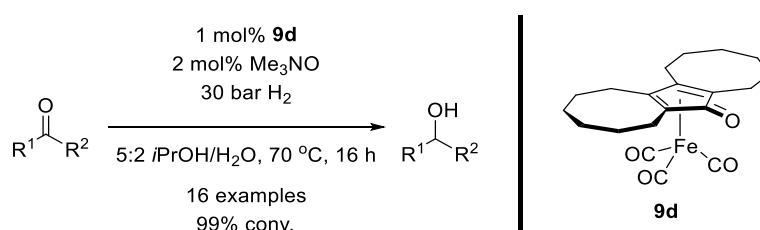
Scheme 1.20. CICs catalyzed transfer hydrogenation of carbonyl compounds

Also our group carried out investigations in this field, and the catalytic scope of CICs was expanded to the hydrogenation of activated esters. After optimizing the catalytic conditions, complex **9aa** was chosen for further studies, and 20 different esters were screened. Nearly all trifluoroacetate substrates gave full conversions, except those bearing electron-withdrawing substituents. On the contrary, all non-trifluoroacetate substrates could not be converted under the reaction conditions (Scheme 1.21).^[57c]



Scheme 1.21. Hydrogenation of activated esters catalyzed by CICs.

Recently, our group reported a CIC, [bis(hexamethylene)cyclopentadienone]iron tricarbonyl (**9d**), which was found to be more active than the Knölker complex **9aa** in the catalytic hydrogenation of C=O double bonds, and gave excellent conversions in most cases (Scheme 1.22). Complex **9d** also gave a higher conversion than **9aa** in the transfer hydrogenation of acetophenone. Kinetic studies showed that the improved activity of **9d** is due to its higher stability compared to complex **9aa** (Figure 1.4).^[57b]



Scheme 1.22. Hydrogenation of C=O bonds catalyzed by complex **9d**.

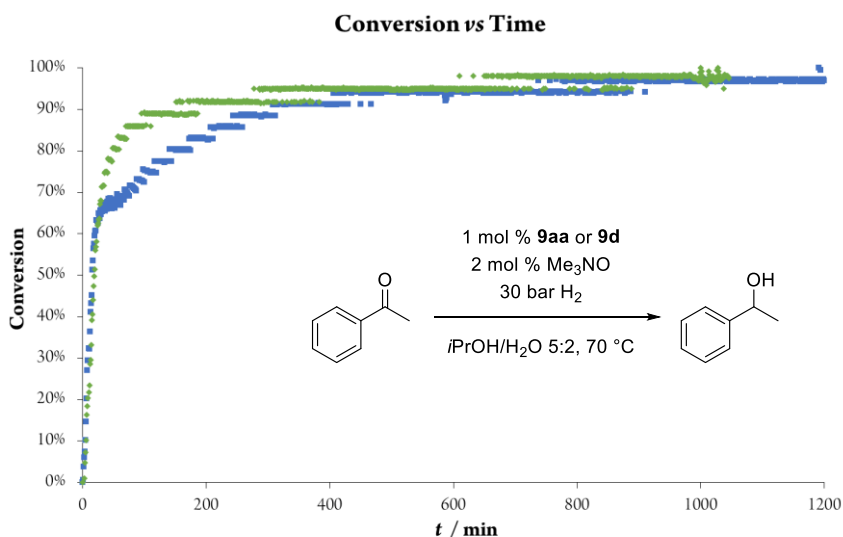
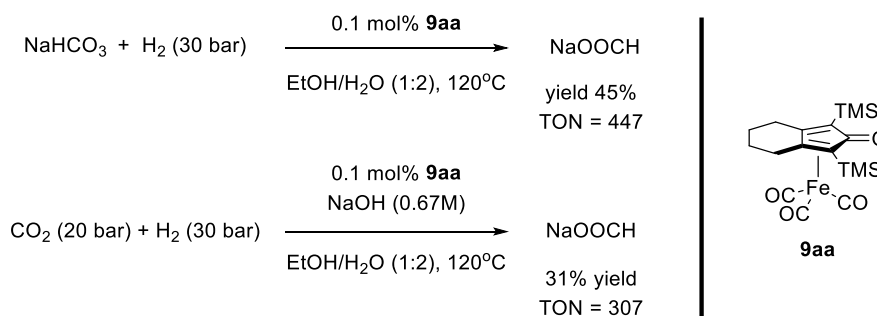


Figure 1.4. Kinetics of acetophenone hydrogenation promoted by **9aa** (■) and **9d** (◆) activated with Me₃NO. Reaction conditions: acetophenone/pre-catalyst/Me₃NO=100:1:2; solvent: 5:2 *i*PrOH/H₂O; $C_{0, \text{Sub.}} = 0.501 \text{ mol L}^{-1}$; $P_{\text{H}_2} = 30 \text{ bar}$; $T = 70 \text{ }^\circ\text{C}$; $C_{\text{cat.}} = 5 \text{ mM}$

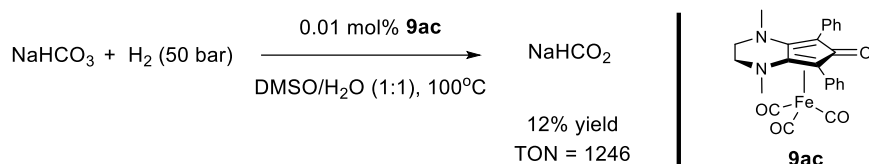
Other investigations involving chiral CICs for the enantioselective reduction of carbonyl compounds will be discussed in Section 1.6.

The reduction of bicarbonates and carbon dioxide is an extremely direct and efficient pathway for the synthesis of formic acid and methanol, both of which are important C_1 building blocks. However, direct reduction of bicarbonates and carbon dioxide to formates or methanol still poses same challenges. Hence, increasing efforts are being devoted to develop an efficient catalytic system for these transformations. While effective noble metal-based catalysts are known, replacement with base metals – and iron in particular – is a goal that is being pursued by several research groups, such as those of Beller, Milstein, and Gonsalvi. These groups used different iron catalysts to hydrogenate carbon dioxide and /or bicarbonates to formates with turnover numbers (TONs) of up to 727,^[60] 7546,^[61] 320,^[16b] and 1229,^[62] respectively. However, some drawbacks are still present, such as use of phosphorus ligands – expensive and often sensitive to air. Therefore, developing new catalyst systems is greatly desired. In addition to the hydrogenation of carbonyl compounds, CICs could also be used for catalyzing the hydrogenation of bicarbonates and carbon dioxide to the corresponding formates. The first example in this sense was reported by Zhou and co-workers in 2015.^[63] The authors applied the Knölker complex **9aa** to hydrogenate sodium bicarbonate and CO₂ to sodium formate with a good TONs (up to 450 and 307, respectively, see Scheme 1.23).

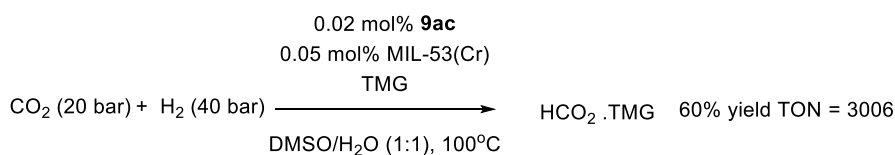


Scheme 1.23. Hydrogenation of sodium bicarbonate and CO_2 using iron complex **9aa**.

Recently, Renaud and co-workers reported that CIC **9ac** was effective for hydrogenation of sodium bicarbonate.^[53e] The reactions were performed at 100 °C under 50 bar of H_2 with an excellent TON up to 1246 (Scheme 1.24). Notably, the reduction could furnish better results without Me_3NO as activator.



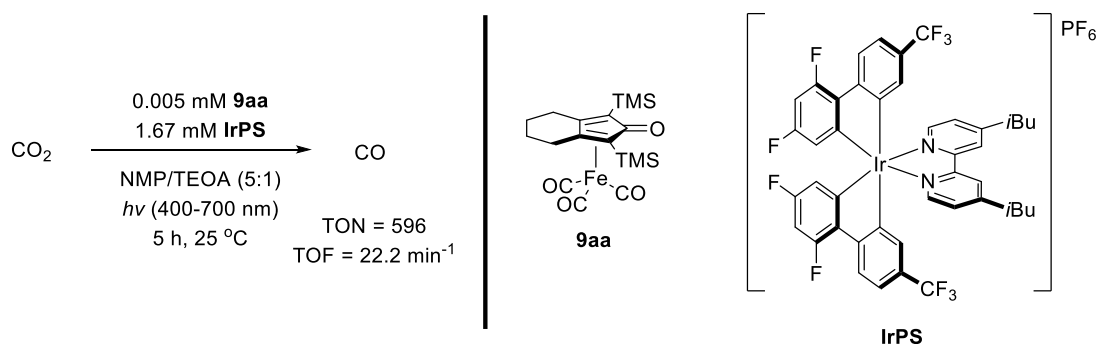
Scheme 1.24. Hydrogenation of sodium bicarbonate using iron complex **9ac**.



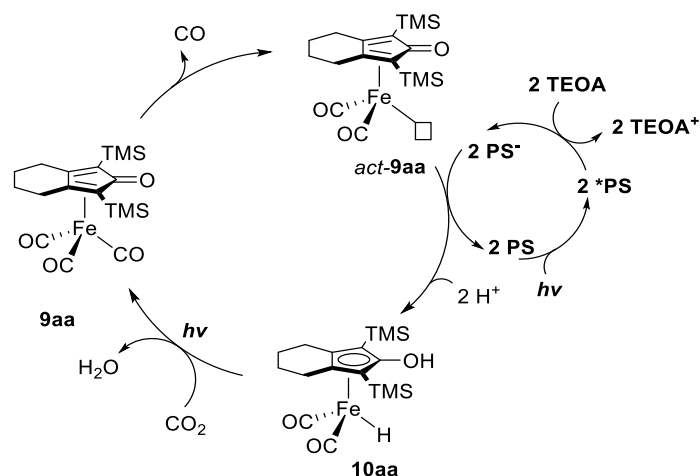
Scheme 1.25. MOF-assisted hydrogenation of CO_2 using iron complex **9ac**.

In a recent follow-up (2019), the same group disclosed a MOF-assisted iron catalyst system for the hydrogenation of CO_2 .^[64] The above mentioned iron complex **9ac** was applied in the hydrogenation of CO_2 to formate in the presence of a catalytic amount of the chromium dicarboxylate MOF MIL-53(Cr). A very high turnover number – up to 3006 – was obtained in CO_2 hydrogenation (Scheme 1.25). In addition to CO_2 , this catalyst system was also applied to hydrogenation of sodium bicarbonate and carbonate. However, in the latter case only a slight increase of TON was obtained with assistance of MIL-53(Cr) [1525 vs 1246 (without MOF)]. Moreover, investigation on controlling hydrogenation of CO_2 to CO was carried out by Beller and co-workers, and the first use of CICs as selective catalysts in this field was reported by them in 2016.^[65] Effective hydrogenation of CO_2 to CO was catalyzed by CICs through photoreduction of CO_2 , in which Ir complex and triethyl orthoacetate (TEOA) play the role of photosensitizer and electron/proton donor, respectively. Complexes **9aa** gave excellent activity (TON up to 596, TOF up to 22.2 min^{-1}) in this photoredox reaction

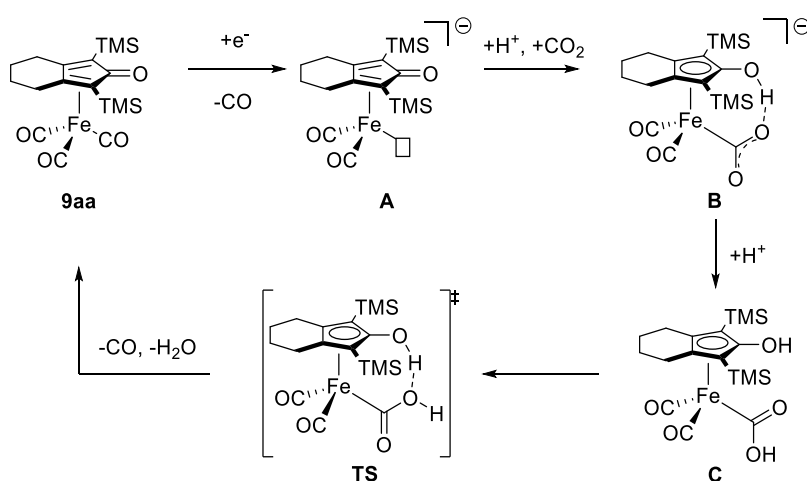
(Scheme 1.26). A mechanism of the photochemical CO₂ reduction mediated by iron complex **9aa** was also proposed (Scheme 1.27).



Scheme 1.26. Photochemical reduction of CO₂ to CO.



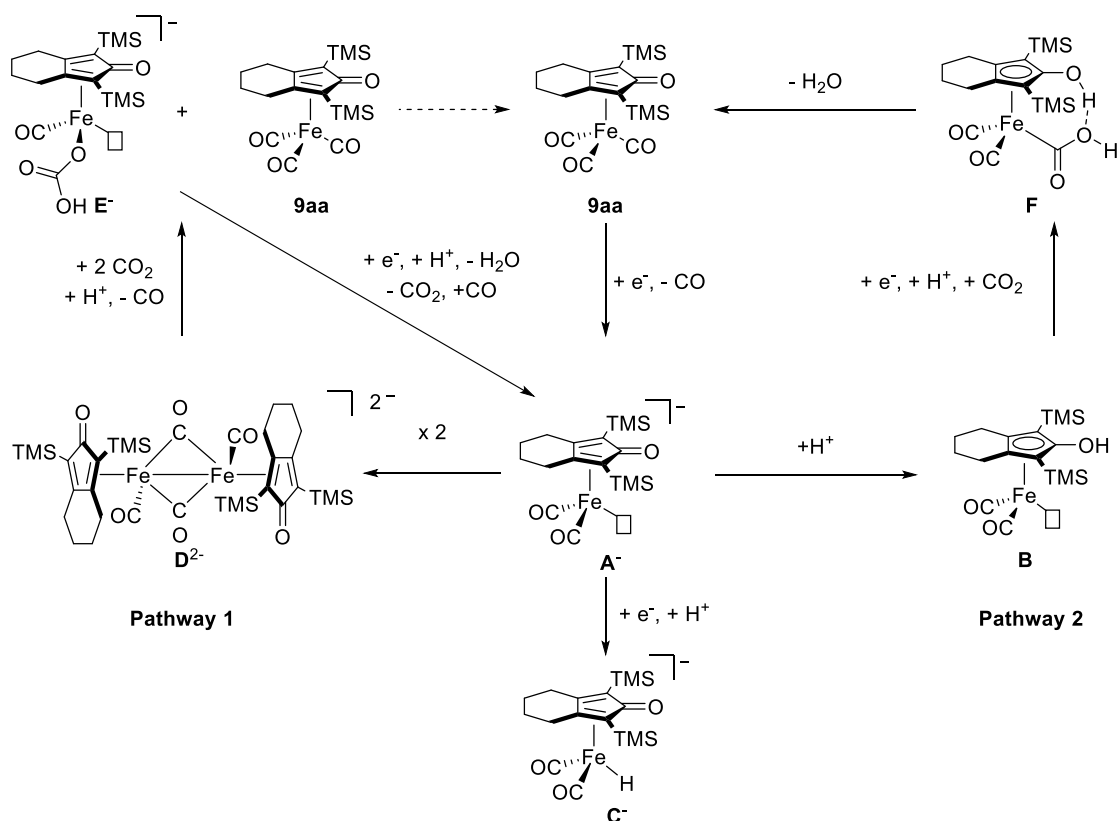
Scheme 1.27. Plausible mechanism for the photochemical reduction of carbon dioxide catalyzed by CICs.



Scheme 1.28. Plausible reaction pathway for the electrocatalytic reduction of CO₂ mediated by complex **9aa**.

The same research group also extended the use of CICs to the electrochemical conversion of CO₂ to CO. Carbon monoxide was selectively synthesized by using CICs as catalyst with a faradaic efficiency of 96%.^[66]

Through the studies of cyclic voltammetry, computational results and *in situ* experiments, a pathway of this reaction was identified (see Scheme 1.28). Cooperation between the metal center and ligand play a key role in this catalytic system. In this electroreduction pathway, no Fe–H intermediate (complex **10**, see Scheme 1.27) is formed, whereas its formation was identified in the photoreduction pathway of controlling hydrogenation of CO₂ to CO.



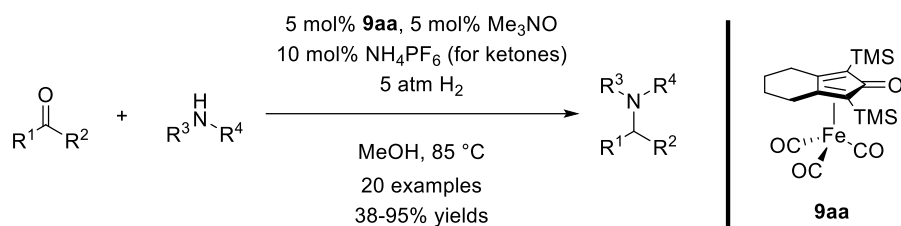
Scheme 1.29. Proposed two coexisting pathways for the electroreduction of CO₂ using Catalyst **9aa**

Further mechanistic studies were carried out, and two coexisting pathways including the terminal proton source for the electroreduction catalyzed by CICs were identified by using a combination of FTIR spectroelectrochemistry, CV, SEC, DFT calculations, and non-electrochemical control experiments. The proposed mechanistic pathways was shown in Scheme 1.29.^[67]

1.4.2 Use in reduction of C=N double bonds

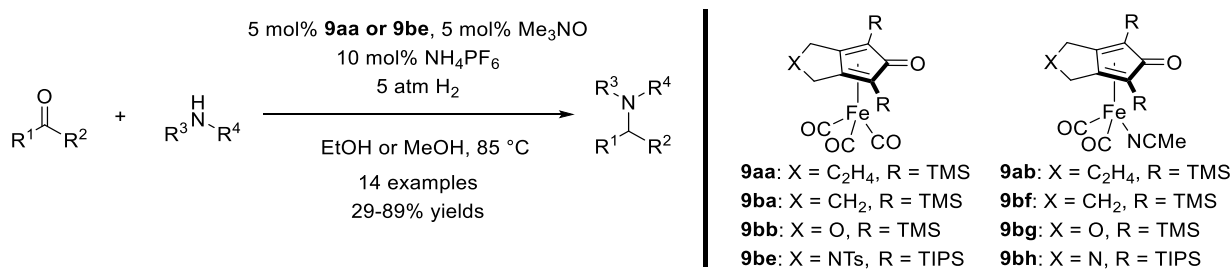
Following the first successful applications of CICs in C=O reductions (see previous Section), the next obvious step was to extend the scope of these pre-catalyst to the reduction of C=N double bonds. In 2012, Renaud and co-workers reported the first example of reductive amination of aliphatic aldehydes with aliphatic amines. These transformations were catalyzed by the well-known Knölker's complex **9aa** under low pressure of 24

hydrogen (5 bar).^[53c] A broad scope of aliphatic aldehydes, ketones and amines were screened, giving good to excellent yields in the 38-95% range (Scheme 1.30).



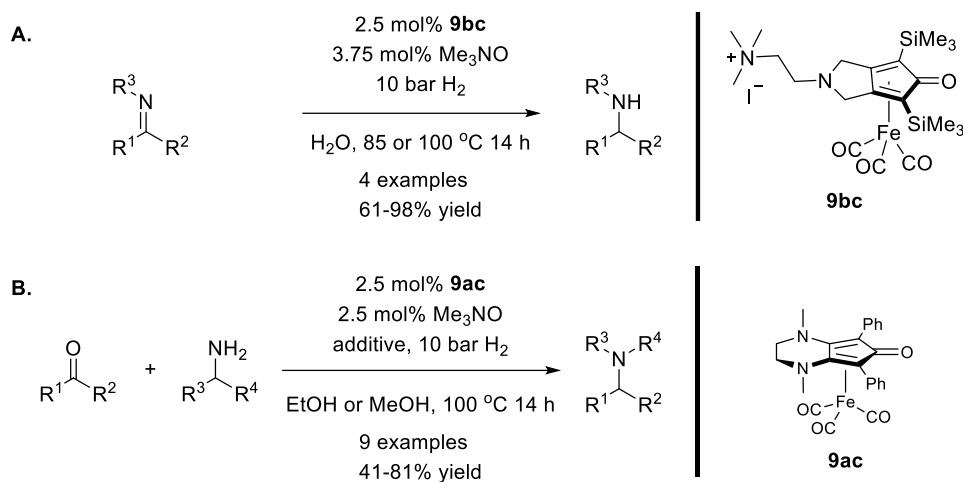
Scheme 1.30. Reductive amination of aliphatic aldehydes with aliphatic amines catalyzed by **9aa**.

In another contribution, to study the influence of the substituents on the ring of the cyclopentadienone ligand, Renaud and co-workers also synthesized a series of CICs including complexes **9aa**, **9ba-bb** and **9be** (Scheme 1.31).^[54a] Exchanging one CO ligand with acetonitrile, these iron complexes were transformed into the corresponding acetonitrile iron-dicarbonyl derivatives (Scheme 1.31). After a complex screening in a model reaction, compounds **9aa** and **9be** were chosen to explore the scope of the reductive amination, in which yields in the 29-89% range were obtained (Scheme 1.31). Both experimental and computational studies showed that the substituents close to C=O group might be useful for preventing the formation of dimers of iron complexes and maintaining their activity, whereas the substituents away from C=O group might stabilize the 16-electron iron intermediate and avoid decomposition.



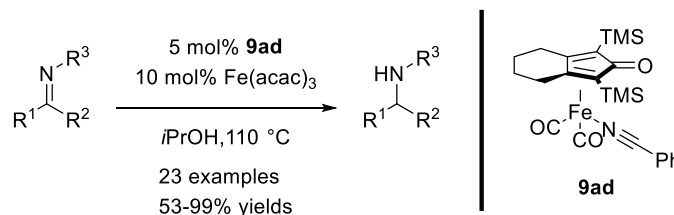
Scheme 1.31. Reductive amination of carbonyl compounds catalyzed by CIC **9aa** and **9be**.

Renaud's group also applied complex **9bc** bearing ionic fragments, already mentioned in Section 1.4.1, to the hydrogenation of imines.^[53b] Good to excellent yields (in the 61-98% range) were obtained (Scheme 1.32 A). Moreover, the same group applied the well-defined (cyclopentadienone)iron complex **9bc** (already mentioned in Section 1.4.1), bearing a more electron-rich cyclopentadienone ligand, in reductive amination of aldehydes and ketones by the same group.^[53e] This complex demonstrates better catalytic activity than Knölker's complex **9aa** under the same reaction conditions (Scheme 1.32 B).



Scheme 1.32. A: Hydrogenation of imines catalyzed by **9bc**; B: reductive amination of ketones catalyzed by **9ac**

A CIC was used for the first time as catalyst for transfer hydrogenation of imines by Zhao and co-workers in 2016.^[54f] They used a catalyst system consisting of complex **9ad** with Fe(acac)₃ as additive to reduce imines by transfer hydrogenation, obtaining yields in the 53-99% range (Scheme 1.33).



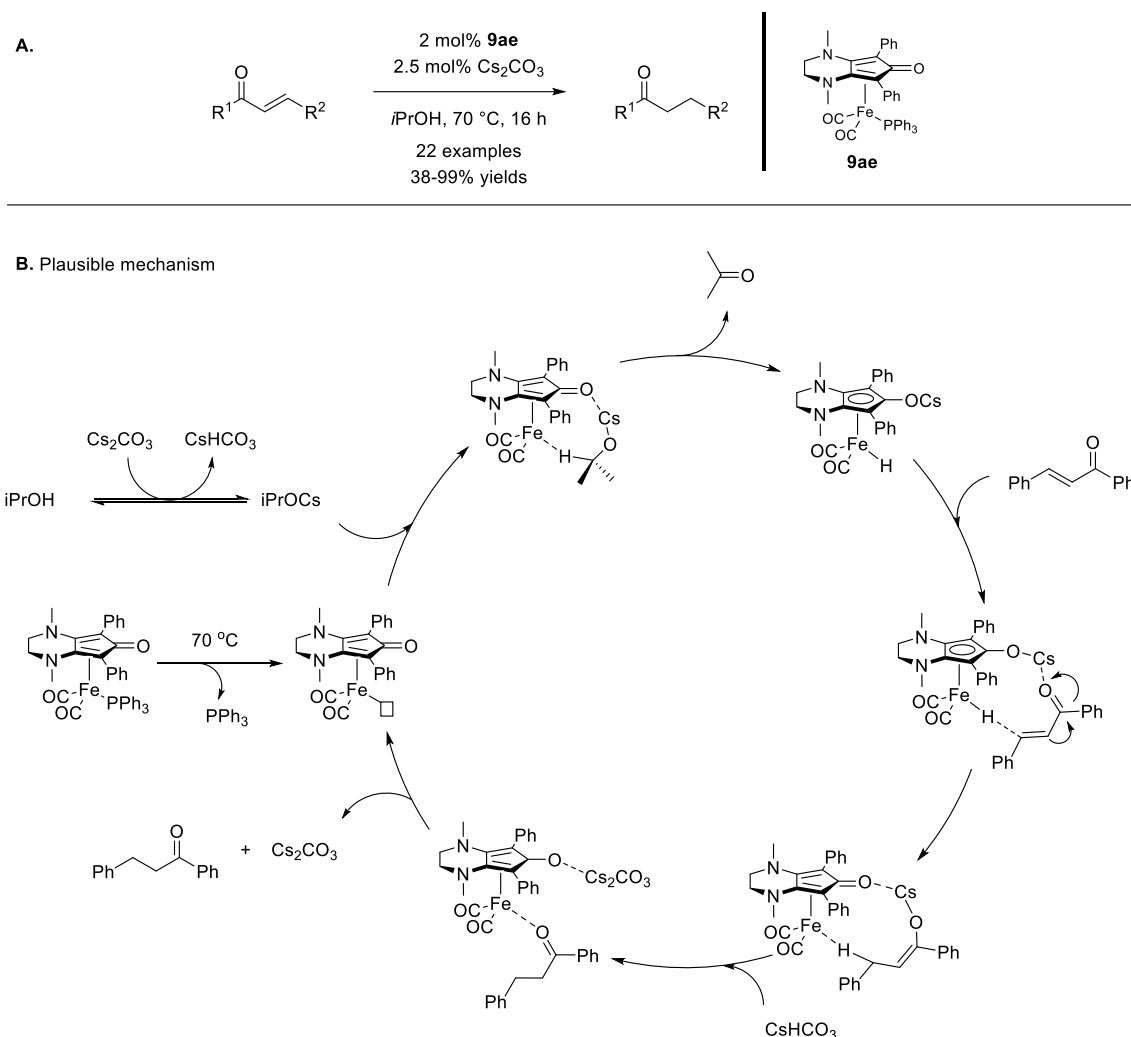
Scheme 1.33. Transfer hydrogenation of preformed imines promoted by **9ad**.

1.4.3 Use in reduction of C=C double bonds

Iron pentacarbonyl has been the first iron complex to be used as catalyst in the reduction of alkenes, with the reports of Fankel and co-workers on the hydrogenation of methyl linoleate and methyl linolenate.^[68] The monoene derivatives were obtained as main products along with a small quantity of fully reduced methyl stearate, and mechanistic investigations were also carried out.

Although iron catalyzed hydrogenation of C=C double bonds had already been reported by different groups,^[69] application of CICs in this transformations where unknown until 2018, when Renaud and co-workers showed that a chemo- and diastereoselective reduction of α,β -unsaturated ketones to the corresponding saturated ketones can be performed under mild reaction conditions using the PPh₃-substituted CIC **9ae** as catalyst.^[57f] A broad range of aromatic and aliphatic unsaturated ketones were reduced in high yields (see Scheme 1.34). A mechanism was also proposed for this transformation, supported by experimental and computational data. It

was found that the base used to activate added has a crucial effect on the reaction chemoselectivity, which is also affected by the type of cation (see Scheme 1.34).

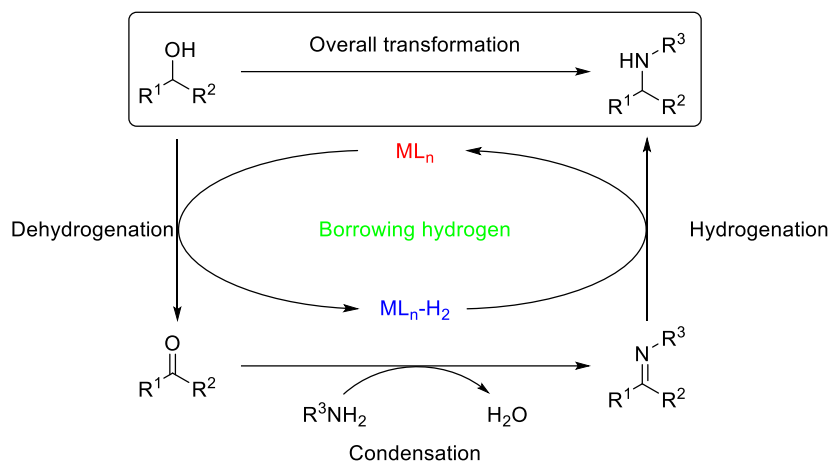


Scheme 1.34. Reduction of C=C double bonds promoted by **9ae** and plausible mechanism.

1.5 Use of CIC in hydrogen borrowing reactions

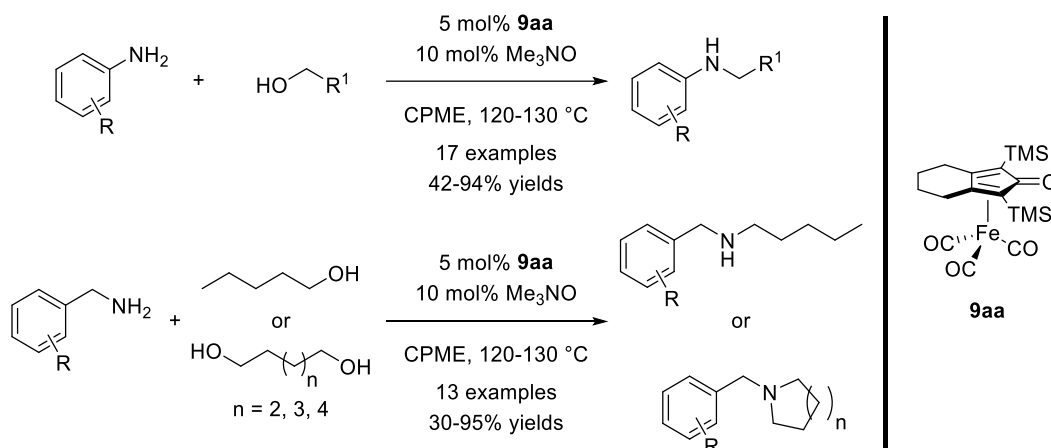
Realizing atom-economic transformations that lead to valuable compounds starting from readily available and inexpensive substrates is a main goal of modern synthetic chemistry.^[70] The so-called ‘hydrogen borrowing’ (HB) or ‘hydrogen autotransfer’ reactions are a representative example of this concept, as they may be considered an environmentally benign class of transformations, generating water is the only by-product. In HB reactions, the catalyst is able to abstract one or more H₂ molecule(s) from the substrate, generating an intermediate which then evolves through a reaction sequence ending with a reduction in which the hydrogen ‘borrowed’ is returned, thus forming the product without net change of the oxidation state.^[71] Given the important role played by amines in natural products, pharmaceuticals, agrochemicals and fine chemicals,^[71c,72]

the amination of alcohols probably represents the most well-known and developed type of HB transformation (Scheme 1.35). Therefore, different catalytic systems have been developed, and the precious metal-based catalyst were widely applied in these transformations.^[71] On the contrary, the development of efficient catalytic systems relying on non-noble metals – especially iron – is still quite limited.^[73]



Scheme 1.35. General mechanism of the HB amination of alcohols.

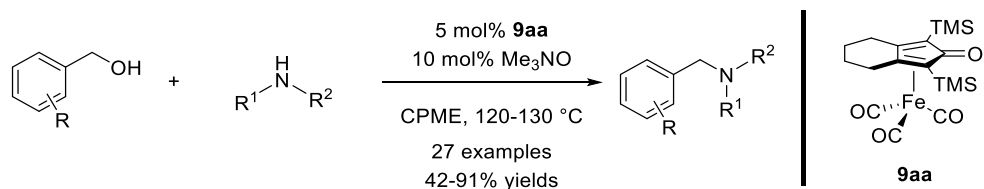
In 2014 Feringa and Barta reported a direct HB alkylation of amines with alcohols catalyzed by the Knölker complex **9aa** activated *in situ* with Me_3NO .^[56d] The direct alkylation of amines (anilines and benzylic amines) with alcohols and diols was efficiently achieved in yields ranging from 30 to 95% (see Scheme 1.36). The most evident weakness of this methodology is the scope limitation to primary alcohol substrates.



Scheme 1.36. HB alkylation of amines promoted by **9aa**.

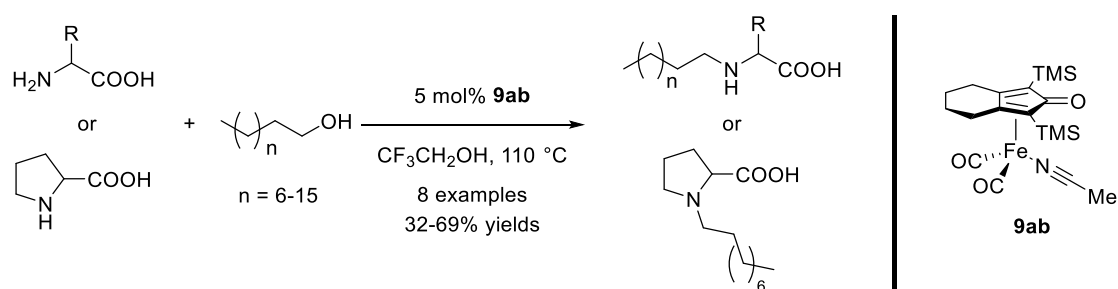
Later on, the same group devoted efforts to the formation of high-added-value benzylamines via HB amination of benzylic alcohols.^[56c] Using $\text{CIC } \mathbf{9aa} / \text{Me}_3\text{NO}$ as catalyst, several secondary and tertiary benzylamines were synthesized with yields in the 42-91% range (Scheme 1.37). The versatility of this methodology in different synthetic pathways was also demonstrated, such as the synthesis of asymmetric tertiary amines, the

sequential functionalization of diols and the synthesis of *N*-benzyl piperidines. In addition, pharmaceutically relevant compounds have been prepared directly from 2,5-furan-dimethanol using this methodology. However, also in this case, the reaction scope remained substantially limited to primary alcohols.



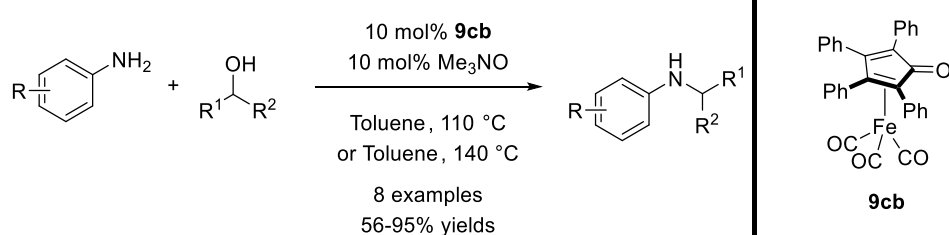
Scheme 1.37. HB amination of benzyl alcohols promoted by **9aa**.

Finally, Barta and Feringa also developed a catalytic system for the direct *N*-alkylation of unprotected amino acids with alcohols.^[56b] Mono-*N*-alkyl amino acid surfactants were obtained in moderate to good yields by *N*-alkylation of amino acids with long-chain alcohols using iron complex **9ab** as catalyst. Although the number of screened examples was limited, this work demonstrated the potential of the methodology for preparation of bio-based products (Scheme 1.38).

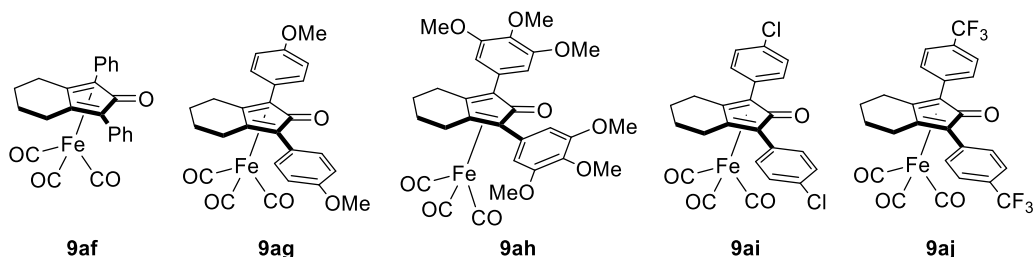


Scheme 1.38. HB *N*-alkylation of α -amino acids promoted by complex **9ab**.

A. 'Hydrogen borrowing' amination of anilines catalyzed by complex **9cb**



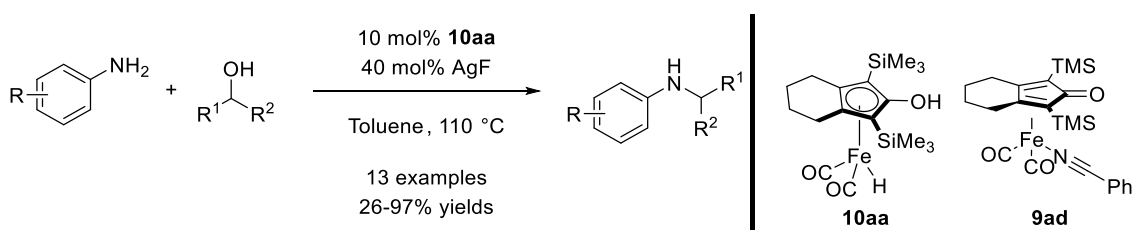
B. A series of CICs synthesized by Wills' group for HB amination



Scheme 1.39. HB amination of amines promoted by CIC **9cb** and CICs synthesized by Wills' group.

Wills and co-workers reported that the easily synthesized iron complex **9cb** has good to excellent catalytic activity in the formation of C-N bonds through HB amination of anilines with primary alcohols (Scheme 1.39 A).^[56g] In the follow-up study, the same group synthesized a series of CICs and applied them to catalyze HB amination of anilines and amines (Scheme 1.39 B).^[56f] The authors found that the efficiency of the reactions is influenced by the electronic variation of substituents on either side of carbonyl group of cyclopentadienone ligand. The Knölker catalyst **9aa** showed better reactivity when the alcohols contain unsaturated bonds, and it afforded the corresponding unsaturated amines in good yields using anilines as starting materials. Notably, the application scope also included a few secondary alcohols, *viz.* cyclopentanol, cyclohexanol, cycloheptanol and β -tetralol, whereas non-cyclic secondary alcohols were found unreactive.

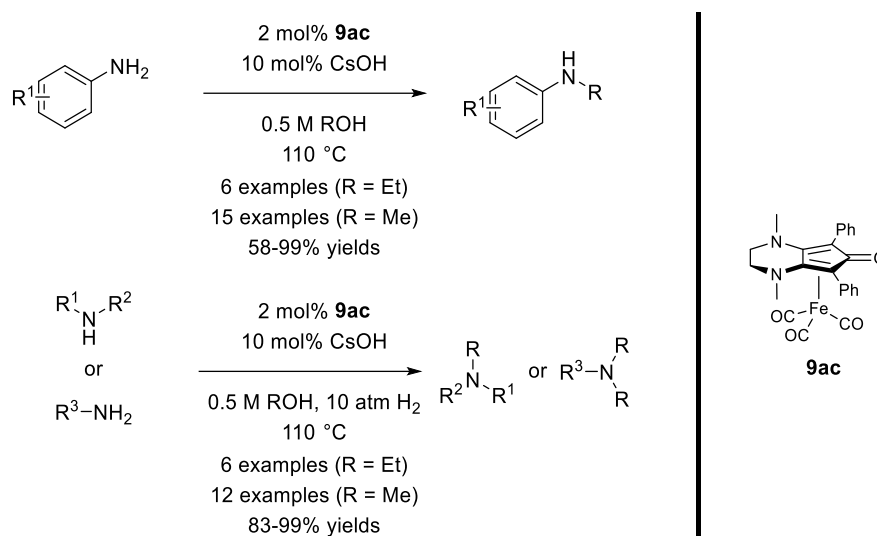
To expand the catalytic scope of CICs to the HB amination of secondary alcohols, Zhao and co-workers reported a catalyst system consisting of a CIC or HCIC assisted by a Lewis acid.^[56i] Complex **9ad** and the Knölker's HCIC **10aa** were chosen as catalysts for this transformations, which also required the presence of a Lewis acid co-catalyst (40 mol% AgF). HCIC **10aa** showed better catalytic activity than complex **9ad** in these transformations, promoting the amination of secondary alcohols in moderate to excellent yields (26-97%, Scheme 1.40). It is likely that CICs would prove inactive under these conditions, since the Me₃N byproduct generated by the standard catalyst activation with Me₃NO would result incompatible with the presence of a Lewis acid in the reaction medium. This work represents the first systematic study on the HB amination of secondary alcohols using an iron catalyst. However, some weakness remained: indeed, the HCIC catalyst is sensitive to air and moisture and use of a relatively large amount of semi-precious metal co-catalyst (AgF) is necessary.



Scheme 1.40. HB amination of secondary alcohols promoted by Knölker catalyst **10aa**.

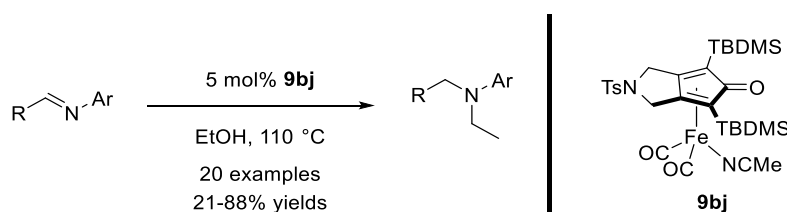
In 2018, Renaud and co-workers used their pre-catalyst **9ac** to catalyze alkylation of amines to *N*-ethyl and *N*-methylamines.^[74] A broad range of aromatic and aliphatic amines were converted in high yields (up to 99%) to mono- or dialkylamines using methanol and ethanol as alkylating agent (Scheme 1.41). Activation of the pre-catalyst in this case was performed by adding a base (CsOH) in the reaction environment. Experimental

and computational studies (DFT) were carried out in order to investigate mechanistic details and the role of the base in this reaction.



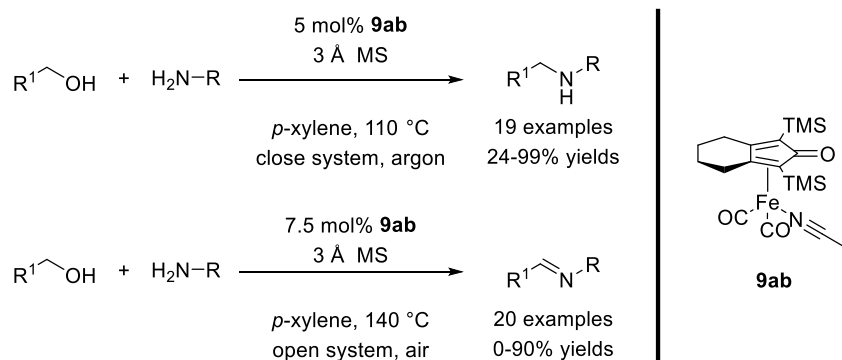
Scheme 1.41. *N*-Ethylation and *N*-methylation of amines promoted by CIC **9ac**.

The HB strategy has been used for reductive ethylation of imines by Gandon, Bour and co-workers.^[56e] Five CICs were synthesized and investigated in imine ethylations with ethanol. The acetonitrile-substituted complex **9bj** gave the best results in the first screening and thus was chosen for further study. Various imines were efficiently converted to *N*-ethylamines in moderate to good yields (21-88%, Scheme 1.42). This methodology demonstrated good chemoselectivity and allowed to perform the synthesis of unsymmetrical ethylated tertiary amines.



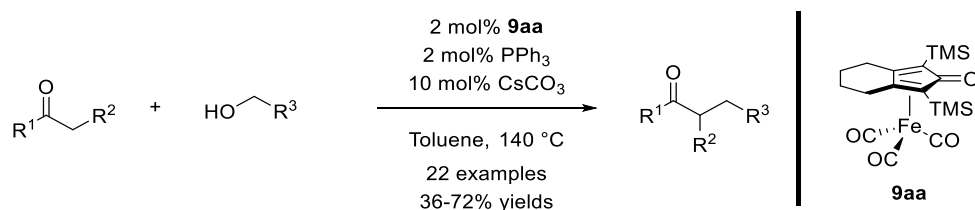
Scheme 1.42. *N*-Ethylation of imines promoted by complex **9bj**.

Hofmann and Hultsch reported a controlled CIC-catalyzed formation of imines and amines starting from arylamines with benzyl alcohols.^[75] HB *N*-alkylation of arylamines with benzylic alcohols could be easily achieved using complex **9ab** as catalyst in a sealed vessel under inert atmosphere. On the other hand, these alkylations can also be switched in favor of the dehydrogenative condensation process performing the reaction in an open system filled with air. Using this methodology, different amines were obtained in fair to excellent yields (24-99%), whereas imine formation was slightly less broad in scope (from no product to (90% yield, see Scheme 1.43).



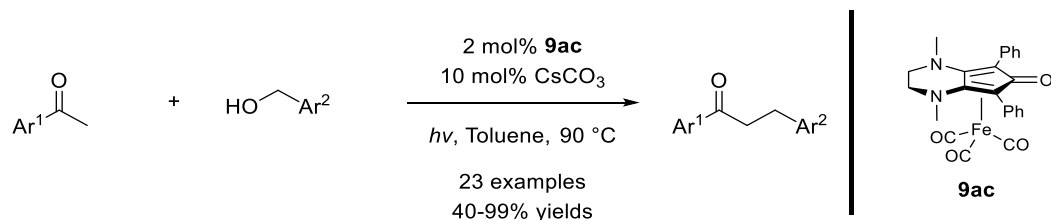
Scheme 1.43. Controlling formation of imines and amines catalyzed by **9ab**.

In 2015, Darcel and co-workers published the first report on the α -alkylation of ketones with primary alcohols promoted by CICs under HB conditions.^[76] Following a careful reaction condition optimization (2 mol% pre-catalyst **9aa**, 2 mol% PPh_3 , 10 mol% CsCO_3 at 140 °C in toluene), the authors synthesized different α -alkylated ketones in good isolated yields (36-72%, Scheme 1.44).



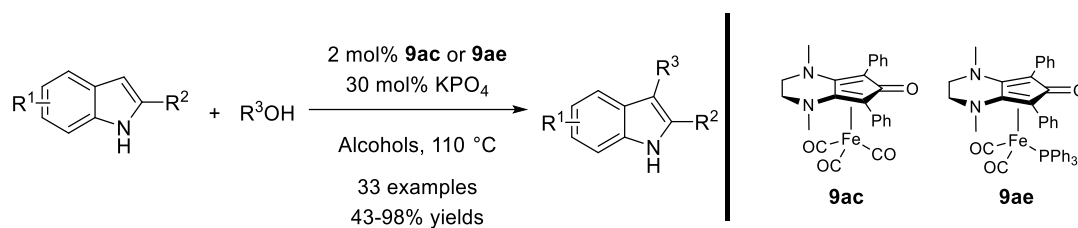
Scheme 1.44. α -Alkylation of ketones with primary alcohols promoted by **9aa**.

Renaud and co-workers also applied their CIC **9ac**, bearing an electron-rich cyclopentadienone ligand, under base activation conditions (Cs_2CO_3), to the alkylation of ketones via the HB strategy under mild reaction conditions.^[77] Both the α -alkylation of aliphatic and aromatic ketones with primary alcohols could be catalyzed by **9ac**, 40-99% yields without need of additives such as PPh_3 (Scheme 1.45).



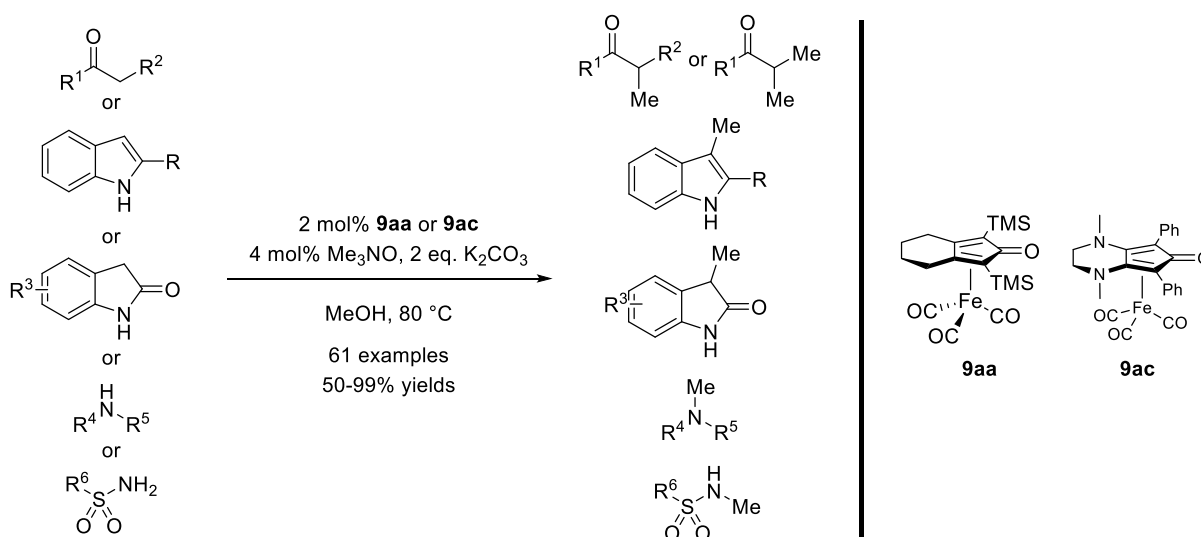
Scheme 1.45. α -Alkylation of ketones with primary alcohols promoted by **9ac**.

Later on, in 2018, the same group expanded the scope of CICs to the alkylation of indoles.^[78] Complexes **9ac** and **9ae** were chosen to promote the alkylation of indoles with different benzylic and aliphatic alcohols. Various indoles were synthesized by this alkylation procedure through the HB strategy in good to excellent yields (43-98%, Scheme 1.46).



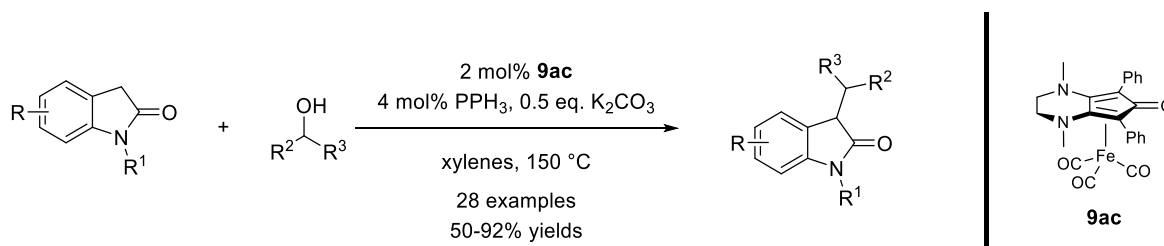
Scheme 1.46. α -Alkylation of indoles with alcohols promoted by **9ac** or **9ae**.

Morrill and co-workers reported a general and efficient methylation using CICs (complexes **9aa** and **9ac**) as pre-catalyst, and methanol as methylating agent through the HB approach.^[56a] A diverse array of ketones, indoles, oxindoles, amines, and sulfonamides were screened by this process, mono- or dimethylation products were obtained in good to excellent isolated yields (50-99%, Scheme 1.47).



Scheme 1.47. Methylation of ketones, indoles, oxindoles, amines, and sulfonamides promoted by **9aa** or **9ac**.

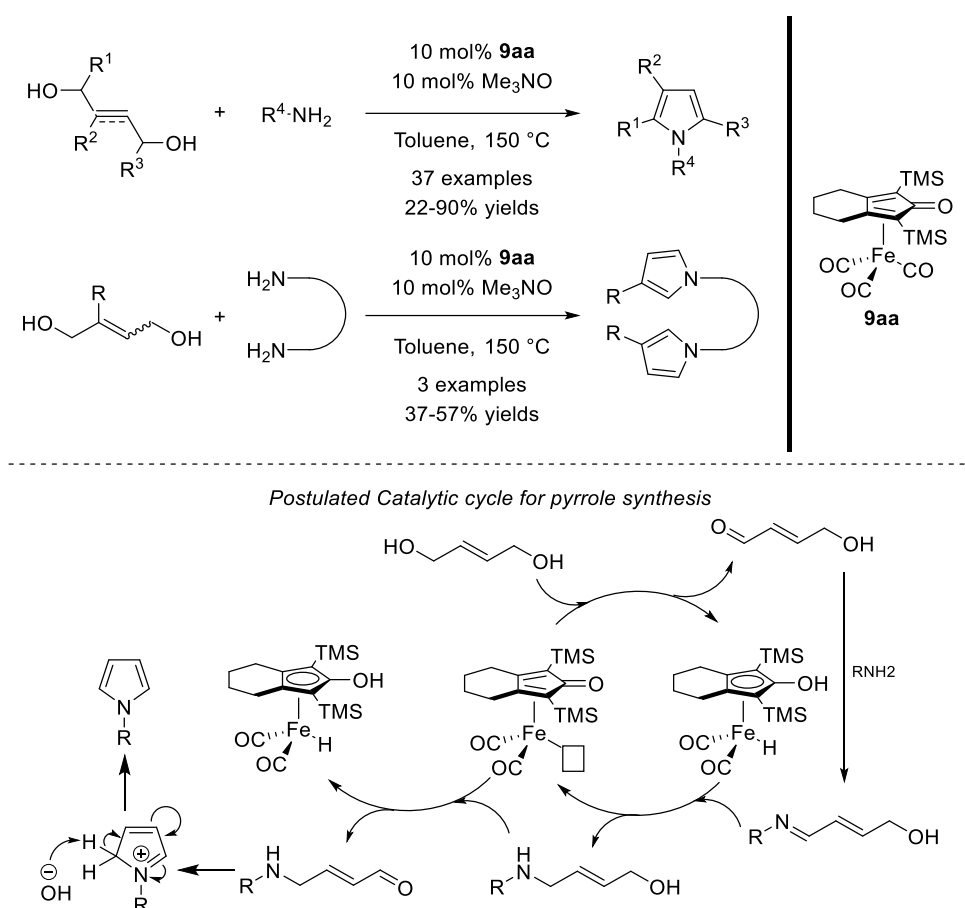
In addition, the authors investigated the C-alkylation of oxindoles with alcohols using pre-catalyst **9ac** through a HB approach.^[79] Different benzylic, primary and secondary aliphatic alcohols were employed as alkylation reagents. The corresponding alkylated oxindoles were obtained with yields in the 50-92% range (see Scheme 1.48).



Scheme 1.48. C-alkylation of Oxindoles with alcohols promoted by **9ac**.

CICs could be used for the synthesis of pyrrole via HB strategy, which was reported by Sundararaju and co-

workers in 2017.^[80] Various substituted pyrroles were synthesized employing complex **9aa** as pre-catalyst under optimized conditions with yields in the 22-90% range (see Scheme 1.49). In particular, symmetrical bis-pyrroles were prepared for the first time using CICs as catalysts. From the mechanistic point of view, the group proposed a HB pathway followed by oxidation/intermolecular condensation/reduction/second oxidation/intramolecular dehydrative condensation, to provide the desired pyrrole (Scheme 1.49).



Scheme 1.49. Synthesis of pyrroles promoted by **9aa** via HB strategy.

1.6 Chiral CICs and their applications in enantioselective catalysis

Although relatively numerous catalytic applications of CICs in RIHTs have been developed, use of CICs in enantioselective catalysis is still limited. With the aim to expand the catalytic scope of CICs to the enantioselective catalysis, two main methods have been followed: 1) using chiral CICs; 2) employing a dual catalysis approach in which common achiral CICs are combined with a chiral co-catalyst.

1.6.1 Chiral CICs for enantioselective catalysis

The use of CICs for enantioselective catalysis has been very limited so far, and only a few chiral CICs have been reported. The commonly accepted mechanism for the CIC/HCIC-mediated hydrogen transfer involves a pericyclic TS (Figure 1.5 A) with the substrate approaching from the direction of the cyclopentadienone's carbonyl group: as a consequence, it is difficult to achieve an effective transfer of the stereochemical information from the stereogenic unit(s) of the complex – usually quite remote from the cyclopentadienone's C=O. As for the ligand design, in order to develop effective chiral complexes three main strategies have been followed (Figure 1.5 B): I) chiral ligands have been employed to replace one of the CO ligands; II) chiral cyclopentadienones have been employed, bearing stereogenic units at the 2,5- or 3,4-positions of the ring; III) chiral complexes bearing a stereogenic plane have been synthesized employing achiral cyclopentadienone ligands possessing different substituents at the 2,5-positions of the ring.

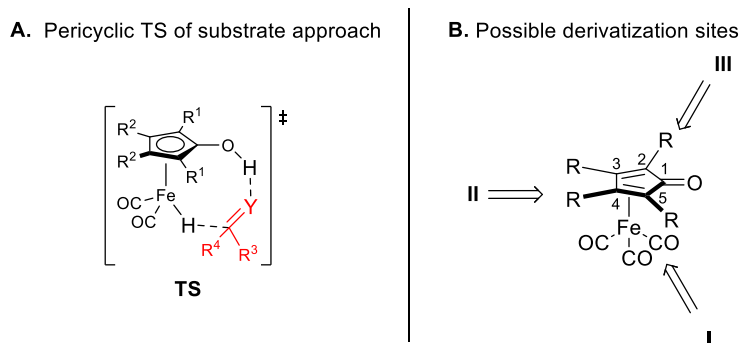
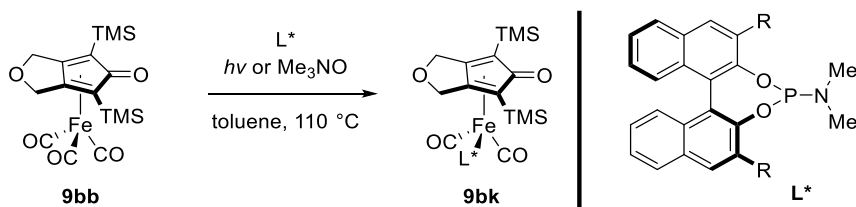


Figure 1.5. Possible derivatization sites of CICs which allow to introduce stereochemical information.

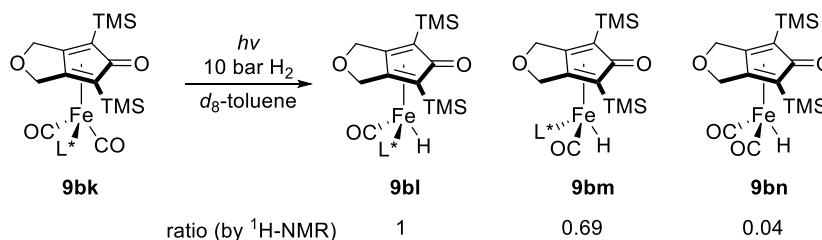
Following Approach I (Figure 1.5 B), in 2011 Berkessel and co-workers reported the first example of enantioselective catalysis using a CIC as pre-catalyst.^[51] Chiral phosphoramidite ligands were employed to replace one of the CO ligands under a mild reaction conditions – either UV irradiation or Me₃NO (Scheme 1.50) – obtaining the stable complexes **9bk**.



Scheme 1.50. Synthesis of chiral CICs through introducing a chiral ligand under photolytic conditions.

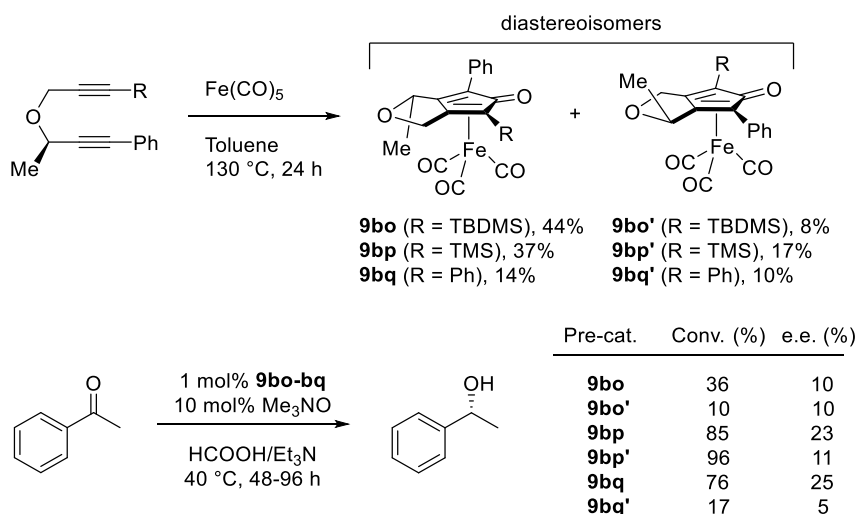
The catalytic activity and enantioselectivity of these iron phosphoramidite complexes were tested in the AH of acetophenone. Under the reaction conditions, UV irradiation was employed to generate the active catalysts

by de-coordination of another CO ligand, and up to 90% yields were obtained. However, these complexes showed only moderate enantioselectivity (up to of 31% e.e. using pre-catalyst **9bk** with R = H). To explain the low observed stereocontrol in ketone AH, an NMR study on catalyst activation was performed, which demonstrated that the formation of two diastereoisomeric hydrides, **9bl** and **9bm**, occurs with 1:0.69 ratio, together with traces of the achiral catalyst **9bn** (Scheme 1.51). The low diastereoselectivity in the formation of the active complex explains the poor observed enantioselectivity of CICs **9bk** in ketone AH.



Scheme 1.51. Formation of chiral hydride species **9bl** and **9bm** and the achiral hydride **9bn**.

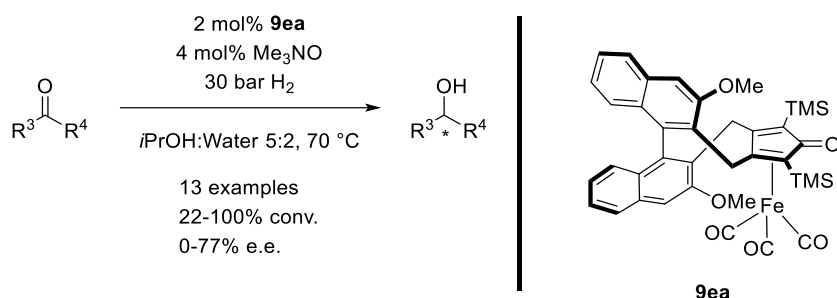
Following Approach II, Wills and co-workers synthesized a series of chiral CICs starting from chiral bis-propargyl ethers and other diynes.^[53d,5454b] These chiral complexes featuring a chiral cyclopentadienone ligand were tested in the ATH of acetophenone with formic acid and triethylamine as hydrogen donors. Poor enantioselectivity was obtained, the highest e.e. being 25% (Scheme 1.52).



Scheme 1.52. Selection of Wills' chiral CICs and their application in ATH and AH of acetophenone.

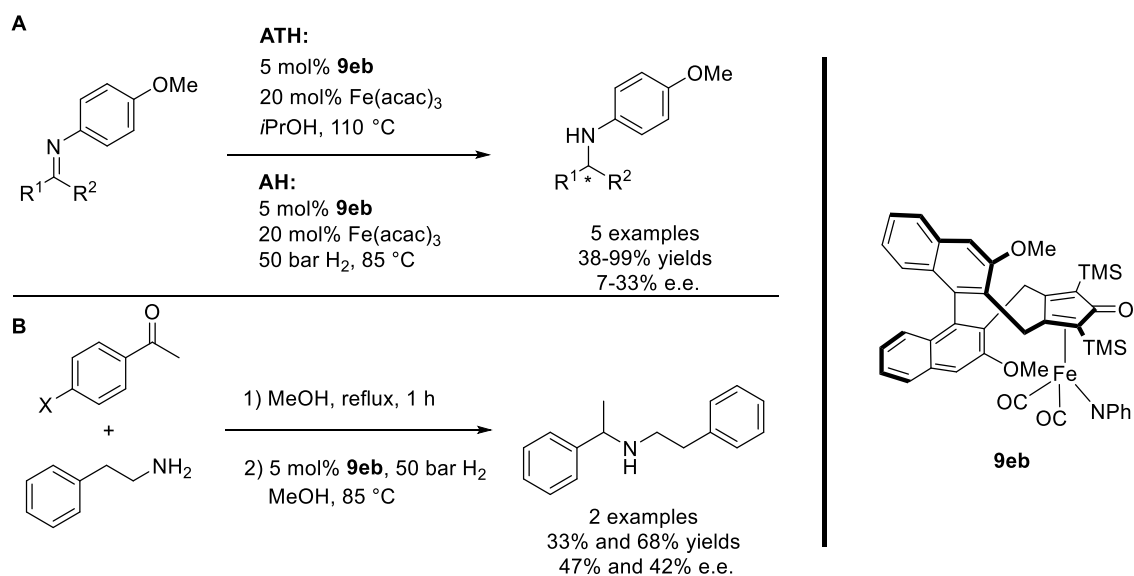
Approach II was followed also by our research group: in 2015, the synthesis of a new library of chiral CICs (Scheme 1.53) and its use in the AH of ketones was reported.^[57d,e] These chiral CICs, featuring a backbone derived from (*R*)-BINOL, were screened in AH of ketones. Complex **9ea** showed the best level of enantioselectivity and was chosen for further studies. Using this pre-catalyst, several ketones were converted to the corresponding alcohols with fair to excellent conversions (22-100%) and 13-77% e.e. (Scheme 1.53).

Even though these e.e. values were clearly inferior to those obtained with precious metal catalysts in ketone AH, they are the highest ever reported for a chiral CIC pre-catalyst (up to 77% e.e.).



Scheme 1.53. AH of ketones promoted by chiral pre-catalyst **9ea**.

The replacement of one CO ligand of complex **9ea** with PhCN led to complex **9eb** (Scheme 1.54 A), which was tested in the ATH and AH of imines giving fair to excellent yields (in a range of 33-99%) and poor to moderate e.e. values (7-47% range). Complex **9eb** was also used in reductive amination of ketones with 2-phenylethylamine, but only moderate yields and enantioselectivities were obtained (Scheme 1.54 B)

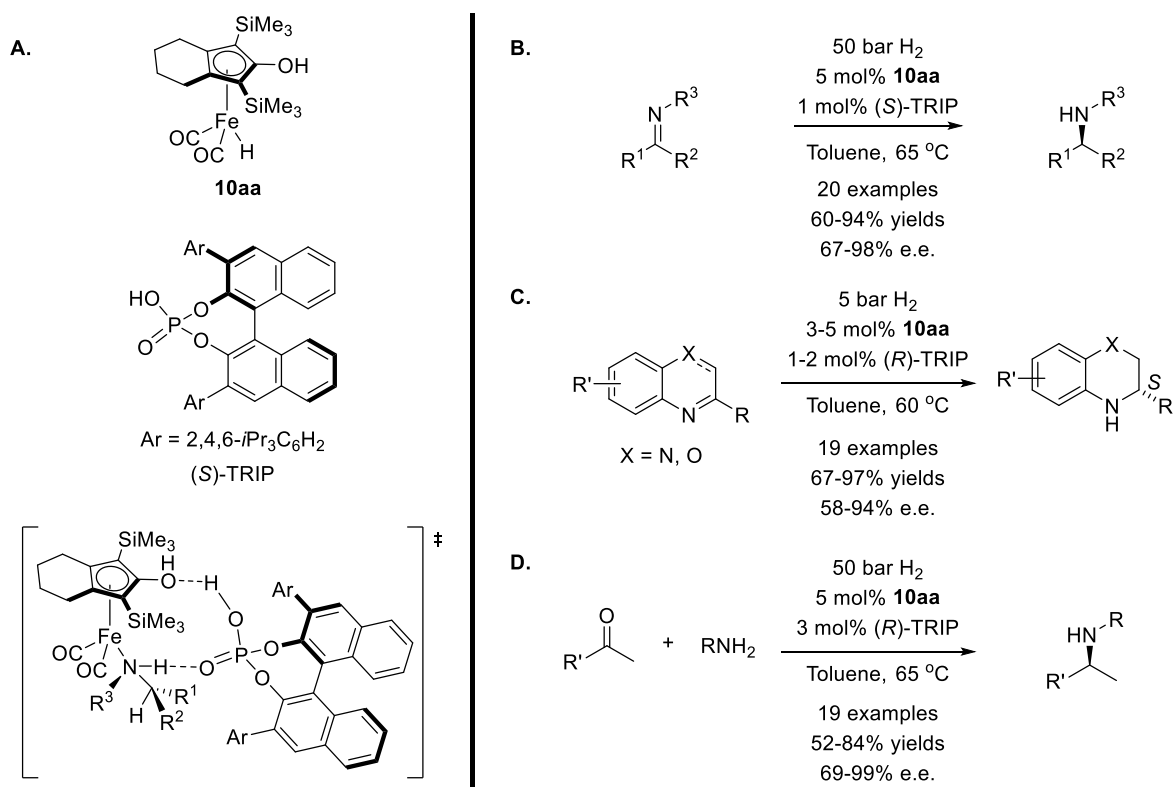


Scheme 1.54. ATH and AH of ketimines and asymmetric reductive amination of ketones promoted by the chiral pre-catalyst **9eb**.

1.6.2 Dual catalysis approach combining CICs with chiral Brønsted acid for enantioselective transformation

In 2011 Beller and co-workers reported a completely different approach to perform enantioselective reductions with CICs/HCICs. This group reported a dual catalytic procedure for the AH of ketimines employing a

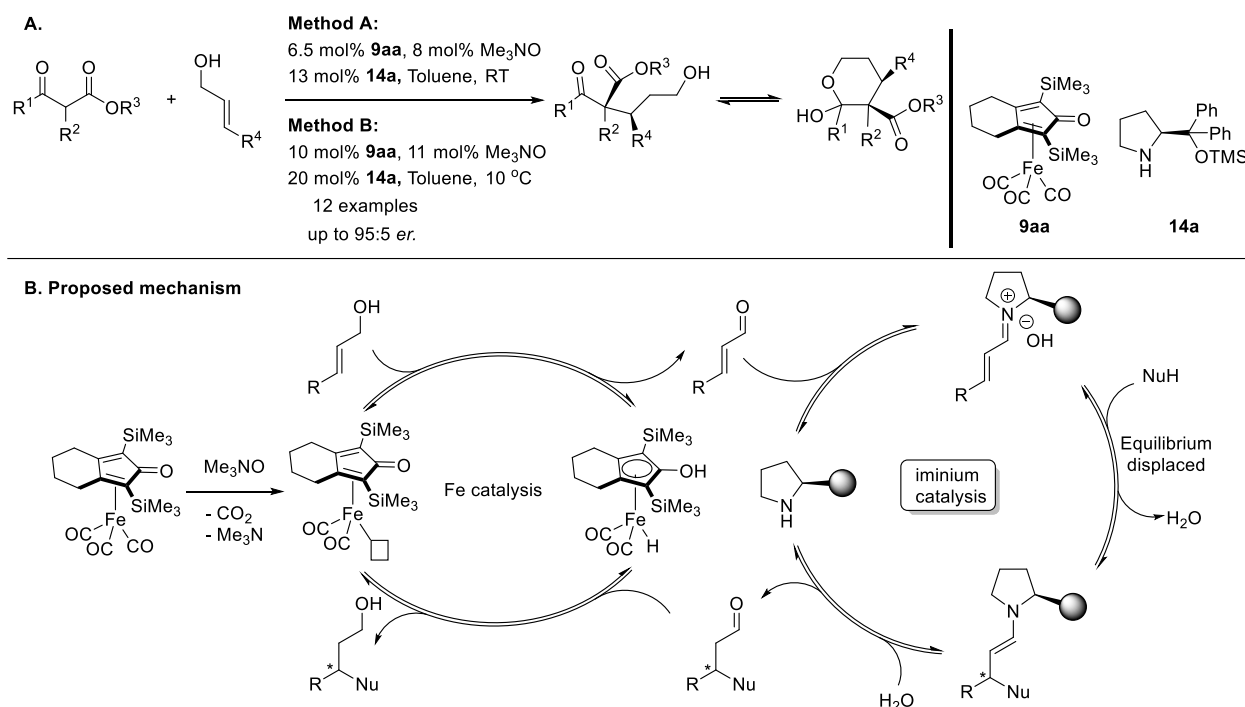
combination of the achiral Knölker's HCIC **10aa** with a chiral phosphoric acid, (*S*)-TRIP.^[50] A variety of ketimines were reduced to amines with high isolated yields (up to 93%) and excellent e.e. in most cases (up to 98%, Scheme 1.55 B). According to the proposed mechanism (Scheme 1.55 A),^[81] the Brønsted acid acts as a chiral template, forming hydrogen bonds simultaneously with the catalyst and with the substrate. The same catalytic system was also applied to the AH of quinoxalines and benzoxazines to tetrahydroquinoxalines and dihydro-2*H*-benzoxazines (Scheme 1.55 C), which was performed with good isolated yields and excellent enantioselectivity (up to 97% e.e.).^[57i] The same catalytic system was also employed in an asymmetric reductive amination (ARA) of ketones with aniline, and high isolated yields (60-80%) and e.e. values (69-94%) were obtained (Scheme 1.55 D).^[57h] Despite its high *efficiency*, this methodology has the limitation of employing the isolated HCIC complex **10aa**, which is highly sensitive to air and light and must be handled in the glovebox.



Scheme 1.55. A: proposed "chiral template" transition state with complex **10aa** and chiral acid (*S*)-TRIP; B: AH of imines; C: AH of quinoxalines and benzoxazines; D: ARA of ketones with aniline.

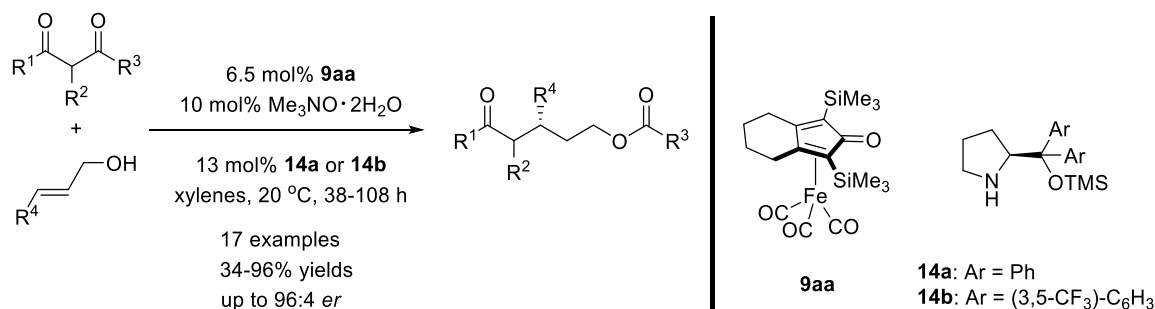
In 2013 Quintard and co-workers reported a different type of dual catalytic approach, consisting in a cascade process for the enantioselective functionalization of allylic alcohols.^[82] Combining iron-promoted HB catalysis and iminium activation, the transformation of allylic alcohols into chiral saturated alcohols was achieved under mild conditions with excellent enantioselectivities (up to 95:5 *er*, see Scheme 1.56 A). The proposed

mechanism for the iron/amine-catalyzed cascade process was supported by preliminary mechanistic experiments, which provided a better understanding of this dual catalytic system (Scheme 1.56 B).



Scheme 1.56. A: Enantioselective functionalization of allylic alcohols promoted by an iron/amine-catalyzed cascade process; B: proposed mechanism.

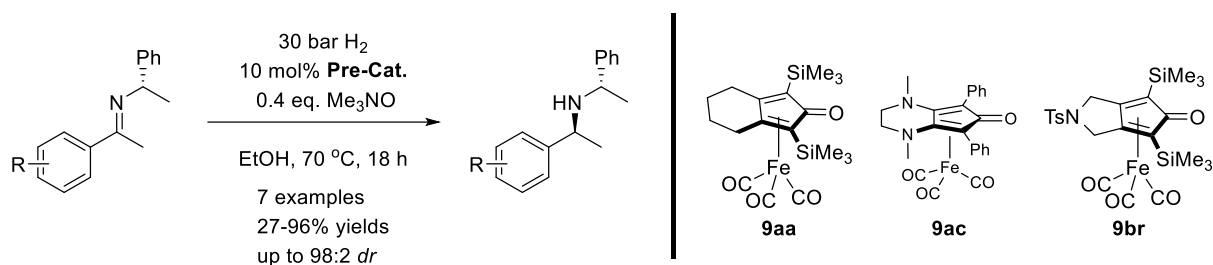
Further development of this strategy gave rise to an unprecedented cascade reaction, combining dual iron/amine-catalyzed enantioselective functionalization of allylic alcohols and acyl transfer, for the synthesis of functionalized chiral esters and alcohols from simple achiral diketones and allylic alcohols.^[83] A series of chiral esters were prepared in high yields (up to 96%) and enantioselectivities (up to 96:4 *er*) employing this cascade reaction (Scheme 1.57). Several natural product fragments or odorant molecules were rapidly synthesized, thus demonstrating the remarkable efficiency of this approach.



Scheme 1.57. Synthesis of functionalized chiral esters through a dual catalysis approach.

In 2017, Benaglia and co-workers reported an iron-catalyzed diastereoselective hydrogenation of chiral imines,

in which CICs **9aa**, **9ac** and **9br** were used as pre-catalyst to hydrogenate enantiopure imines.^[57g] Different chiral amines, including valuable biologically active products, were obtained in good yields (up to 96%) and excellent diastereomeric ratio (up to 98:2 *dr*, see Scheme 1.58). This method was employed to synthesize advanced intermediates of highly valuable APIs with good yields (up to 70%) and high diastereoisomeric ratio (up to 98:2 *dr*).



Scheme 1.58. Diastereoselective hydrogenation of chiral imines catalyzed by CICs.

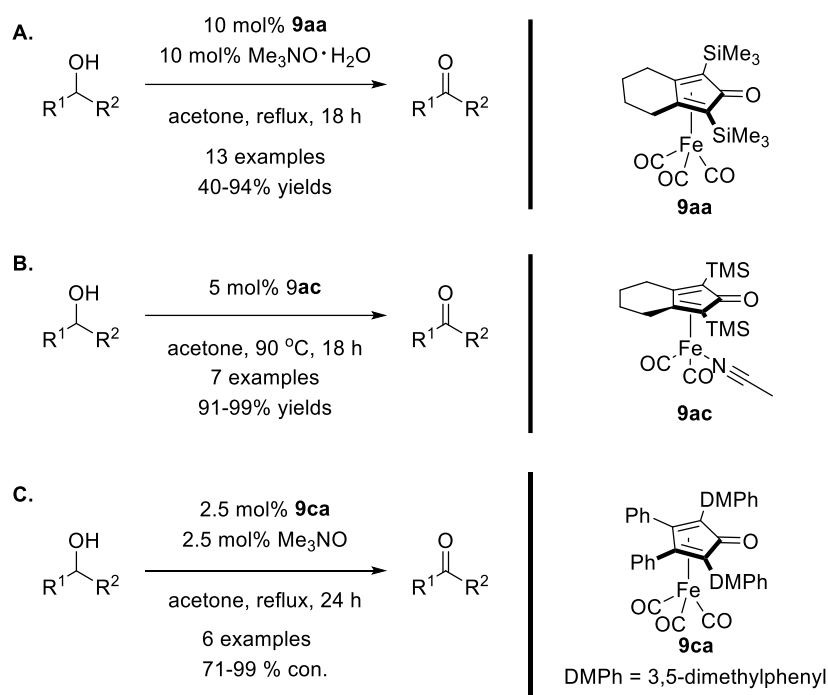
In 2016 Renaud and co-workers reported a “cofactor approach” to enantioselective reductions, consisting in the incorporation of biotinylated achiral CICs into Streptavidin. The biotinylated CICs were successfully synthesized and embedded in Streptavidin to provide the corresponding streptavidin conjugates, which were applied in AH of imines and ketones with poor yields and enantioselectivity except for one example (100% yield and 9% e.e. were obtained in AH of trifluoroacetophenone).^[84] Despite its limited success, this approach represents a conceptually innovative strategy to exploit CICs in enantioselective transformations.

1.7 Use of CICs in Oppenauer-type alcohol oxidation

In 2010, Funk and co-workers expanded for the first time the application of CICs to the Oppenauer-type oxidation of alcohols.^[55] Four air-stable CICs were synthesized and tested in Oppenauer-type oxidation of alcohols. After optimizing the reaction conditions, the Knölker’s complex **9aa** was chosen as the best pre-catalyst to extend the scope of alcohols. A variety of secondary benzylic and allylic alcohols were oxidized in high isolated yields (up to 94%) using complex **9aa** as pre-catalyst (Scheme 1.59 A). The most active complex **9ac** (already mentioned in Section 1.4.2) was also used as catalyst to oxidize secondary benzylic and allylic alcohols, and excellent isolated yields (up to 99%) were obtained in most cases (Scheme 1.59 B).^[54e]

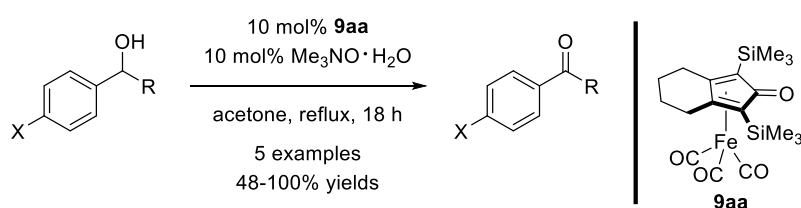
Later on, Funk and co-workers reported another example of Oppenauer-type oxidation of alcohols promoted by CICs.^[54d] They synthesized four CICs, and assessed their catalytic activity in Oppenauer-type oxidation of alcohols. Complex **9ca** was found to be a more active pre-catalyst compared to Knölker complex **9aa**. Different

alcohols were screened, and six of the corresponding products were obtained in good to excellent conversion (71-99%, see Scheme 1.59 C).



Scheme 1.59. Applications of CICs in Oppenauer-type oxidation of alcohols by Funk's group.

In 2011, Wills and co-workers reported the synthesis of a series of CICs using an intramolecular cyclization strategy, and their application in the Oppenauer-type oxidation of alcohols to aldehydes and ketones. Within the oxidation of alcohols, the screening was performed using acetone as a hydrogen acceptor and the Knölker's complex **9aa** was found to be the most active: several different alcohols were oxidized to ketones and aldehydes with up to 100% conversion (see Scheme 1.60).^[54c]



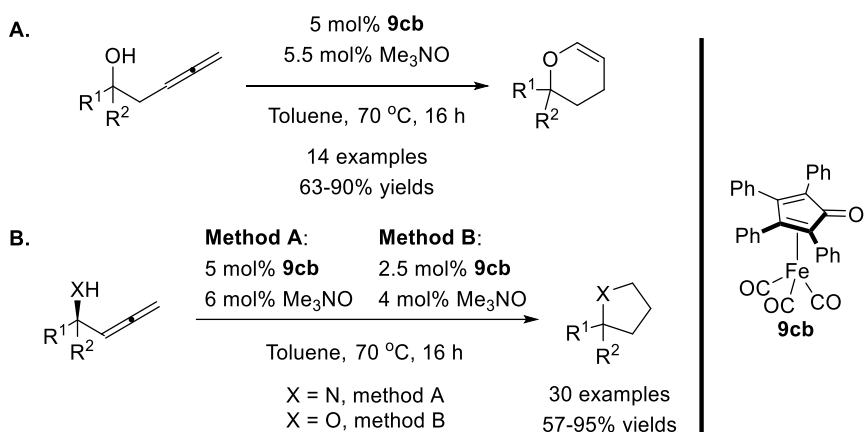
Scheme 1.60. Oppenauer-type oxidation of alcohols reported by Wills' group.

1.8 Other applications of CICs

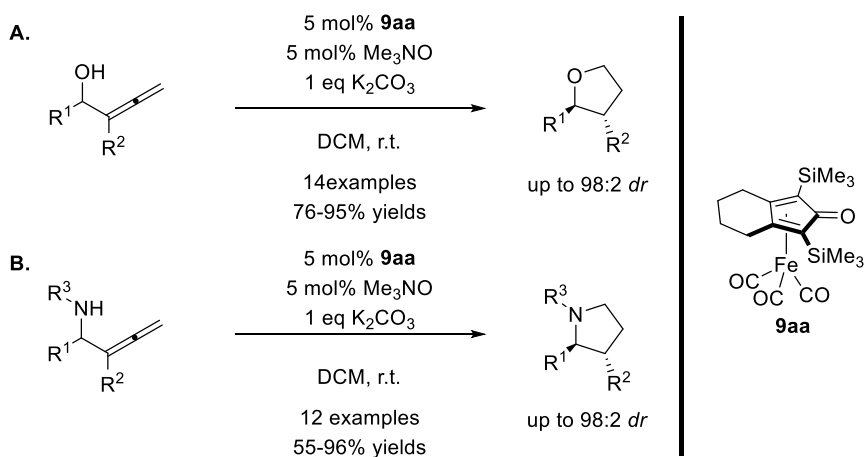
All the above-outlined applications of CICs/HCICs consist in RIHTs in which the H₂ molecule is either permanently or transiently transferred to / abstracted from the substrate. No applications of CICs to different types of reactivity were reported until the end of 2017, when the application scope of CICs was expanded to

cycloisomerization of allenols by Rueping and co-workers (Scheme 1.61 A).^[59c] CICs were found to promote the intramolecular nucleophilic cyclization of a number of β -allenols to deoxygenated pyranose glycols in good yields (up to 90%). This transformation represents an efficient method for the formation of deoxygenated pyranose glycols starting from available allenic alcohols.

Next, the same authors applied this catalytic system to cycloisomerization of α -allenic amines and alcohols. Various valuable unsaturated 5-membered heterocycles, including 2,3-dihydropyrrole and 2,3-dihydrofuran, were synthesized with yields in the 57-95% range (Scheme 1.61 B).^[59b]



Scheme 1.61. Cycloisomerization of β -allenols promoted by complex **9cb**.



Scheme 1.62. Cycloisomerization of α -allenic amines and alcohols promoted by complex **9aa**.

A very similar catalytic methodology for the formation of 2,3-dihydrofurans was simultaneously reported by Bäckvall and co-workers.^[59a] Substituted 2,3-dihydrofurans were easily synthesized by using iron complex **9aa** as pre-catalyst through intramolecular nucleophilic cyclization of α -allenols (Scheme 1.62 A) with high yields (up to 95%). These reactions showed a good diastereoselectivity (up to 98:2 *dr*). In 2019, the diastereoselective synthesis of *N*-protected 2,3-dihydropyrroles through cycloisomerization of α -allenic sulfonamides catalyzed

by CICs was reported by the same group.^[85] Employing this protocol, a variety of substituted 2,3-dihydropyrroles could be synthesized in good to excellent yields. Excellent diastereoselectivities were obtained when 1,2-disubstituted allenamide is used, which afforded *N*-protected 2,3-dihydropyrroles with > 98:2 diastereomeric ratios (Scheme 1.62 B).

1.9 Conclusions on the State-of-the-Art catalytic applications of (cyclopentadienone)iron complexes

CICs have recently gained widespread interest as cheap metal-based pre-catalysts for RIHTs due to their unique features of reactivity (i.e. iron atom ‘forced’ to undertake a two-electron catalytic cycle) and robustness (i.e. stability to air, moisture and column chromatography). In this chapter, more than 20 different CICs have been described, which can be classified by their specific reactivity and stereoselectivity (Figure 1.6). Most of these pre-catalysts have been reported in the last decade, which highlights the increasingly growing interest in homogeneous iron catalysis with CICs.

Despite the attractive features mentioned above, CICs still suffer from several important limitations:

- 1. Moderate catalytic activity:** many of the RIHTs promoted by CICs display moderate reaction rates and need to be carried out well above the r.t. to achieve substrate conversions in acceptable yields. This limits the CIC application scope, as bulky substrates (e.g., secondary alcohol in HB amination, ketimines in hydrogenation) are sluggish or do not react at all.
- 2. Limited stability of the catalytically active forms *act-9* and *10*:** once activated, CICs might undergo deactivation due to the decomposition of the catalytically active forms, which are known to be very sensitive species. Such deactivation pathway would lead to a decrease of the overall observed catalytic activity.
- 3. Lack of effective chiral complexes for enantioselective catalysis:** as discussed in Section 1.6.1, very limited success has been met so far in the development of effective chiral CICs for enantioselective catalysis.

Therefore, the aim of my PhD thesis has been to overcome these general limitations exploiting the peculiar features of CIC **9d** (Figure 1.6), previously developed by our research group, and also developing new chiral and achiral CICs.

Achiral CICs

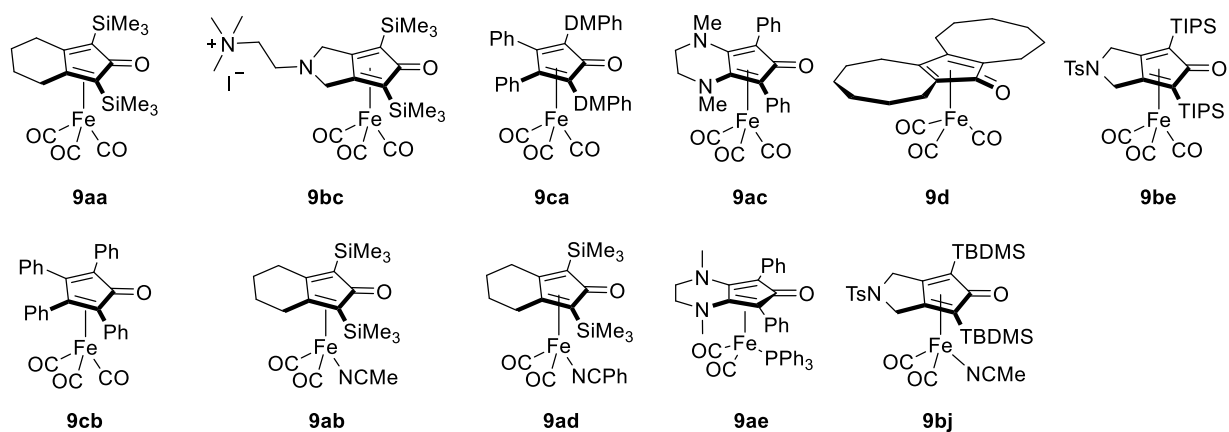


Figure 1.6. Selection of the most important CICs for hydrogen transfer reactions.

References

- [1] Prices obtained from <http://www.infomine.com/investment/metal-prices/> as for 29.7.2019.
- [2] M. A. H. J. H. Fenton, *J. Chem. Soc., Trans.*, **1894**, 65, 899-910.
- [3] C. Bosch, *Vol. US990191 (A)* BASF SE, U. S., **1908**.
- [4] a) F. Fischer, h. Tropsch, *Brennst. Chem.* **1926**, 7, 97-104; b) A. d. Klerk, in *Kirk-Othmer Encyclopedia of Chemical Technology*, pp. 1-20.
- [5] W. Reppe, H. Vetter, *Justus Liebigs Annalen der Chemie* **1953**, 582, 133-161.
- [6] a) M. Tamura, J. K. Kochi, *J. Am. Chem. Soc.* **1971**, 93, 1487-1489; b) M. Tamura, J. Kochi, *Journal of Organometallic Chemistry* **1971**, 31, 289-309; c) M. Tamura, J. Kochi, *Synthesis* **1971**, 1971, 303-305.
- [7] a) J. T. Groves, T. E. Nemo, R. S. Myers, *J. Am. Chem. Soc.* **1979**, 101, 1032-1033; b) J. T. Groves, T. E. Nemo, *J. Am. Chem. Soc.* **1983**, 105, 5786-5791.
- [8] B. L. Small, M. Brookhart, *J. Am. Chem. Soc.* **1998**, 120, 7143-7144.
- [9] a) E. B. Bauer, *Current Organic Chemistry*, **2008**, 12, 1341-1369; b) S. Enthaler, K. Junge, M. Beller, *Angew. Chem., Int. Ed.* **2008**, 47, 3317-3321; c) C. Bolm, *Nat. Chem.* **2009**, 1, 420; d) L. Liang-Xian, *Curr. Org. Chem.* **2010**, 14, 1099-1126(1028); e) H.-J. Knölker, in *Organometallics in Synthesis—Third Manual* (Ed.: M. Schlosser), Wiley: Hoboken, NJ, **2013**, p. 545; f) B. Plietker, *Iron Catalysis: Fundamentals and Applications*, Springer Berlin Heidelberg, **2011**; g) B. Plietker, *Iron Catalysis in Organic Chemistry: Reactions and Applications*, Wiley-VCH: Weinheim, Germany, **2008**.
- [10] J. A. Labinger, *Organometallics* **2015**, 34, 4784-4795.
- [11] a) P. L. Holland, *Acc. Chem. Res.* **2015**, 48, 1696-1702; b) T. Zell, R. Langer, *ChemCatChem* **2018**, 10, 1930-1940.
- [12] P. Gajewski, tutor: C. Gennari ; co-tutor: J. G. de Vries, L. Lefort ; supervisore: L. Pignataro, Doctoral thesis, Università degli Studi di Milano. DIPARTIMENTO DI CHIMICA **2016**.
- [13] a) J. M. Darmon, S. C. E. Stieber, K. T. Sylvester, I. Fernández, E. Lobkovsky, S. P. Semproni, E. Bill, K. Wiegardt, S. DeBeer, P. J. Chirik, *J. Am. Chem. Soc.* **2012**, 134, 17125-17137; b) J. Jacquet, M. Desage-El Murr, L. Fensterbank, *ChemCatChem* **2016**, 8, 3310-3316; c) D. L. J. Broere, R. Plessius, J. I. van der Vlugt, *Chem. Soc. Rev.* **2015**, 44, 6886-6915; d) O. R. Luca, R. H. Crabtree, *Chemical Society Reviews* **2013**, 42, 1440-1459; e) S. Blanchard, E. Derat, M. Desage-El Murr, L. Fensterbank, M. Malacria, V. Mouriès-Mansuy, *Eur. J. Inorg. Chem.* **2012**, 376-389; f) K. Hindson, B. de Bruin, *Eur. J. Inorg. Chem.* **2012**, 340-342; g) P. H. M. Budzelaar, *Eur. J. Inorg. Chem.* **2012**, 530-534; h) K. G. Caulton, *Eur. J. Inorg. Chem.* **2012**, 435-443; i) R. E. Cowley, G. J. Christian, W. W. Brennessel, F. Neese, P. L. Holland, *Eur. J. Inorg. Chem.* **2012**, 479-483; j) W. Kaim, *Eur. J. Inorg. Chem.* **2012**, 343-348.
- [14] C. K. Jørgensen, *Coord. Chem. Rev.* **1966**, 1, 164-178.
- [15] E. Salanouve, G. Bouzemame, S. Blanchard, E. Derat, M. Desage-El Murr, L. Fensterbank, *Chem. Eur. J.* **2014**, 20, 4754-4761.
- [16] a) S. Chakraborty, W. W. Brennessel, W. D. Jones, *J. Am. Chem. Soc.* **2014**, 136, 8564-8567; b) R. Langer, Y. Diskin-Posner, G. Leitun, L. J. W. Shimon, Y. Ben-David, D. Milstein, *Angew. Chem., Int. Ed.* **2011**, 50, 9948-9952; c) D. Oren, Y. Diskin-Posner, L. Avram, M. Feller, D. Milstein, *Organometallics* **2018**, 37, 2217-2221; d) M. K. Karunananda, N. P. Mankad, *ACS Catal.* **2017**, 7, 6110-6119; e) T. Zell, D. Milstein, *Acc. Chem. Res.* **2015**, 48, 1979-1994.
- [17] a) T. J. Mazzacano, N. P. Mankad, *J. Am. Chem. Soc.* **2013**, 135, 17258-17261; b) S. R. Parmelee, T. J. Mazzacano, Y. Zhu, N. P. Mankad, J. A. Keith, *ACS Catal.* **2015**, 5, 3689-3699; c) N. P. Mankad, *Synlett* **2014**, 25, 1197-1201.
- [18] a) R. Arevalo, P. J. Chirik, *J. Am. Chem. Soc.* **2019**, 141, 9106-9123; b) R. Pony Yu, D. Hesk, N. Rivera, I. Pelczer, P. J. Chirik, *Nature* **2016**, 529, 195.
- [19] For reviews, see: a) D. D. Diaz, P. O. Miranda, J. I. Padron, V. S. Martin, *Curr. Org. Chem.* **2006**, 10, 457-476; b) Y. Song, X. Tang, X. Hou, Y. Bai, *Chin. J. Org. Chem.* **2013**, 33, 76-89; c) K. Gopalaiah, *Chem. Rev.* **2013**, 113, 3248-3296; d) M. Darwish, M. Wills, *Catal. Sci. Technol.* **2012**, 2, 243-255; e) D. Bézier, J.-B. Sortais, C. Darcel, *Adv. Synth. Catal.* **2013**, 355, 19-33; f) K. Riener, S. Haslinger, A. Raba, M. P. Högerl, M. Cokoja, W. A. Herrmann, F. E. Kühn, *Chem. Rev.* **2014**, 114, 5215-5272; g) P. Bhattacharya, H. Guan, *Comments Inorg. Chem.* **2011**, 32, 88-112; h) C. Bolm, J. Legros, J. Le Paih, L. Zani, *Chem. Rev.* **2004**, 104, 6217-6254. For books, see: i) J. I. Padrón, V. S. Martín, in *Iron Catalysis: Fundamentals and Applications* (Ed.: B. Plietker), Springer Berlin Heidelberg, Berlin,

- Heidelberg, **2011**, pp. 1-26; j) R. Peters, D. F. Fischer, S. Jautze, in *Iron Catalysis: Fundamentals and Applications* (Ed.: B. Plietker), Springer Berlin Heidelberg, Berlin, Heidelberg, **2011**, pp. 139-175.
- [20] For reviews, see: a) B. Plietker, A. Dieskau, *Eur. J. Org. Chem.* **2009**, 775-787; b) A. Correa, O. Garcia Mancheno, C. Bolm, *Chem. Soc. Rev.* **2008**, 37, 1108-1117; c) B. Plietker, *Synlett* **2010**, 14, 2049-2058; d) E. Emer, R. Sinisi, M. G. Capdevila, D. Petruzzello, F. De Vincentiis, P. G. Cozzi, *Eur. J. Org. Chem.* **2011**, 647-666; e) X. Shang, Z. Liu, *Chin. Sci. Bull.* **2012**, 57, 2335-2337; f) D. E. Pearson, C. A. Buehler, *Synthesis* **1972**, 533-542; g) H. Shinokubo, K. Oshima, *Eur. J. Org. Chem.* **2004**, 2081-2091; h) F. Alois, M. Rubén, *Chemistry Letters* **2005**, 34, 624-629; i) B. D. Sherry, A. Fürstner, *Acc. Chem. Res.* **2008**, 41, 1500-1511; j) W. M. Czaplik, M. Mayer, J. Cvengroš, A. Jacobi von Wangelin, *ChemSusChem* **2009**, 2, 396-417; k) R. Jana, T. P. Pathak, M. S. Sigman, *Chem. Rev.* **2011**, 111, 1417-1492; l) C.-L. Sun, B.-J. Li, Z.-J. Shi, *Chem. Rev.* **2011**, 111, 1293-1314. For books, see: m) G. A. Olah, *Friedel-Crafts and Related Reactions*, Wiley-Interscience, New York, **1963-1965**; n) G. A. Olah, *riedel-Crafts Chemistry*, Wiley, New York, **1973**; o) H. Heaney, in *Comprehensive Organic Synthesis* (Eds.: B. M. Trost, I. Fleming), Pergamon, Oxford, **1991**, p. 733; p) B. Plietker, in *Iron Catalysis in Organic Chemistry* (Ed.: B. Plietker), John Wiley & Sons, Germany, **2008**, pp. 197-215; q) M. Jegelka, B. Plietker, in *Iron Catalysis: Fundamentals and Applications* (Ed.: B. Plietker), Springer Berlin Heidelberg, Berlin, Heidelberg, **2011**, pp. 177-213; r) M. Jegelka, B. Plietker, in *Asymmetric Synthesis II: More Methods and Applications* (Eds.: M. Christmann, S. Bräse), Wiley, Germany, **2013**, pp. 333-339; s) R. Taylor, *Electrophilic Aromatic Substitution*, John Wiley & Sons: Chichester, U.K., **1990**; t) J. Kischel, K. Mertins, I. Jovel, A. Zapf, M. Beller, in *Iron Catalysis in Organic Chemistry: Reactions and Applications* (Ed.: B. Plietker), John Wiley & Sons, Germany, **2008**, pp. 177-196; u) G. Cahiez, C. Duplais, in *The Chemistry of Organomagnesium Compounds* (Eds.: Z. Rappoport, I. Marek), John Wiley & Sons, U.K., **2008**, pp. 595-630; v) M. Nakamura, S. Ito, in *Modern Arylation Methods* (Ed.: L. Ackermann), Wiley, **2009**, pp. 155-179.
- [21] For reviews, see: a) M. D. Greenhalgh, S. P. Thomas, *Synlett* **2013**, 24, 531-534; b) C. Bianchini, G. Giambastiani, I. G. Rios, G. Mantovani, A. Meli, A. M. Segarra, *Coord. Chem. Rev.* **2006**, 250, 1391-1418; c) C. Bianchini, G. Giambastiani, L. Luconi, A. Meli, *Coord. Chem. Rev.* **2010**, 254, 431-455; d) V. C. Gibson, C. Redshaw, G. A. Solan, *Chem. Rev.* **2007**, 107, 1745-1776.
- [22] For reviews, see: a) S. Gaillard, J.-L. Renaud, *ChemSusChem* **2008**, 1, 505-509; b) R. H. Morris, *Chem. Soc. Rev.* **2009**, 38, 2282-2291; c) M. Zhang, A. Zhang, *Appl. Organomet. Chem.* **2010**, 24, 751-757; d) B. A. F. Le Bailly, S. P. Thomas, *RSC Adv.* **2011**, 1, 1435-1445; e) K. Junge, K. Schroder, M. Beller, *Chem. Commun.* **2011**, 47, 4849-4859. For books, see: f) S. Enthaler, K. Junge, M. Beller, in *Iron Catalysis in Organic Chemistry* (Ed.: B. Plietker), John Wiley & Sons, Germany, **2008**, pp. 125-145; g) P. J. Chirik, in *Catalysis without Precious Metals* (Ed.: R. M. Bullock), John Wiley & Sons, Germany, **2010**, pp. 83-110.
- [23] For reviews, see: a) F. Jia, Z. Li, *Org. Chem. Front.* **2014**, 1, 194-214; b) T. W.-S. Chow, G. Chen, Y. Liu, C. Zhou, C. Che, *Pure Appl. Chem.* **2012**, 84, 1685-1704; c) B. Meunier, S. P. de Visser, S. Shaik, *Chem. Rev.* **2004**, 104, 3947-3980; d) B. Meunier, *Chem. Rev.* **1992**, 92, 1411-1456; e) W. Nam, *Acc. Chem. Res.* **2007**, 40, 522-531; f) E. P. Talsi, K. P. Bryliakov, *Coord. Chem. Rev.* **2012**, 256, 1418-1434; g) S. P. de Visser, J.-U. Rohde, Y.-M. Lee, J. Cho, W. Nam, *Coord. Chem. Rev.* **2013**, 257, 381-393; h) E. Rose, B. Andrioletti, S. Zrig, M. Quelquejeu-Ethève, *Chem. Soc. Rev.* **2005**, 34, 573-583; i) C. E. I. Knappke, A. Jacobi von Wangelin, *ChemCatChem* **2010**, 2, 1381-1383; j) G. De Faveri, G. Ilyashenko, M. Watkinson, *Chem. Soc. Rev.* **2011**, 40, 1722-1760.
- [24] a) G. Hilt, J. Janikowski, in *Iron Catalysis in Organic Chemistry* (Ed.: B. Plietker), John Wiley & Sons, Germany, **2008**, pp. 245-269; b) C.-M. Che, C.-Y. Zhou, E. L.-M. Wong, in *Iron Catalysis: Fundamentals and Applications* (Ed.: B. Plietker), Springer Berlin Heidelberg, Berlin, Heidelberg, **2011**, pp. 111-138; c) C. Wang, B. Wan, *Chin. Sci. Bull.* **2012**, 57, 2338-2351.
- [25] For reviews, see: a) R. Uma, C. Crévisy, R. Grée, *Chem. Rev.* **2003**, 103, 27-52; b) R. C. van der Drift, E. Bouwman, E. Drent, *J. Organomet. Chem.* **2002**, 650, 1-24; c) Y. Yamamoto, *Chem. Rev.* **2012**, 112, 4736-4769.
- [26] a) L. Markó, M. A. Radhi, I. Ötvös, *J. Organomet. Chem.* **1981**, 218, 369-376; b) L. Markó, J. Palágyi, *Transition Met. Chem.* **1983**, 8, 207-209.
- [27] S. C. Bart, E. Lobkovsky, P. J. Chirik, *J. Am. Chem. Soc.* **2004**, 126, 13794-13807.
- [28] P. J. Chirik, K. Wieghardt, *Science* **2010**, 327, 794-795.
- [29] J. Chen, L. Chen, X. Yan, G. Chen, W. Shen, Z. Dong, Y. Li, J. Gao, *Acta Chimica Sinica (Huaxue Xuebao)* **2004**, 62, 1745-1750.
- [30] a) Y.-Y. Li, S.-L. Yu, W.-Y. Shen, J.-X. Gao, *Acc. Chem. Res.* **2015**, 48, 2587-2598; b) S. Yu, W. Shen, Y. Li, Z.

- Dong, Y. Xu, Q. Li, J. Zhang, J. Gao, *Adv. Synth. Catal.* **2012**, *354*, 818-822; c) Y. Li, S. Yu, X. Wu, J. Xiao, W. Shen, Z. Dong, J. Gao, *J. Am. Chem. Soc.* **2014**, *136*, 4031-4039.
- [31] a) R. Bigler, A. Mezzetti, *Org. Lett.* **2014**, *16*, 6460-6463; b) R. Bigler, R. Huber, A. Mezzetti, *Angew. Chem. Int. Ed.* **2015**, *54*, 5171-5174; c) L. De Luca, A. Mezzetti, *Angew. Chem. Int. Ed.* **2017**, *56*, 11949-11953; d) L. De Luca, A. Passera, A. Mezzetti, *J. Am. Chem. Soc.* **2019**, *141*, 2545-2556.
- [32] C. Sui-Seng, F. Freutel, A. J. Lough, R. H. Morris, *Angew. Chem., Int. Ed.* **2008**, *47*, 940-943.
- [33] a) A. Mikhailine, A. J. Lough, R. H. Morris, *J. Am. Chem. Soc.* **2009**, *131*, 1394-1395; b) P. O. Lagaditis, A. J. Lough, R. H. Morris, *J. Am. Chem. Soc.* **2011**, *133*, 9662-9665; c) A. A. Mikhailine, M. I. Maishan, A. J. Lough, R. H. Morris, *J. Am. Chem. Soc.* **2012**, *134*, 12266-12280; d) W. Zuo, A. J. Lough, Y. F. Li, R. H. Morris, *Science* **2013**, *342*, 1080-1083.
- [34] a) J. F. Sonnenberg, R. H. Morris, *ACS Catal.* **2013**, *3*, 1092-1102; b) J. F. Sonnenberg, N. Coombs, P. A. Dube, R. H. Morris, *J. Am. Chem. Soc.* **2012**, *134*, 5893-5899; c) A. A. Mikhailine, M. I. Maishan, R. H. Morris, *Org. Lett.* **2012**, *14*, 4638-4641; d) A. A. Mikhailine, E. Kim, C. Dingels, A. J. Lough, R. H. Morris, *Inorganic Chemistry* **2008**, *47*, 6587-6589; e) P. O. Lagaditis, A. A. Mikhailine, A. J. Lough, R. H. Morris, *Inorganic Chemistry* **2010**, *49*, 1094-1102; f) P. E. Sues, A. J. Lough, R. H. Morris, *Organometallics* **2011**, *30*, 4418-4431; g) P. O. Lagaditis, P. E. Sues, J. F. Sonnenberg, K. Y. Wan, A. J. Lough, R. H. Morris, *J. Am. Chem. Soc.* **2014**, *136*, 1367-1380.
- [35] R. Langer, G. Leitus, Y. Ben-David, D. Milstein, *Angew. Chem., Int. Ed.* **2011**, *50*, 2120-2124.
- [36] a) I. Wender, R. A. Friedel, R. Markby, H. W. Sternberg, *J. Am. Chem. Soc.* **1955**, *77*, 4946-4947; b) H. W. Sternberg, R. A. Friedel, R. Markby, I. Wender, *J. Am. Chem. Soc.* **1956**, *78*, 3621-3624; c) G. N. Schrauzer, *Chem. Ind. (London)* **1958**, 1403; d) E. Weiss, R. G. Merenyi, W. Hubel, *Chem. Ind. (London)* **1960**, 407-408.
- [37] G. N. Schrauzer, *J. Am. Chem. Soc.* **1959**, *81*, 5307-5310.
- [38] K. Hoffmann, E. Weiss, *J. Organomet. Chem.* **1977**, *128*, 237-246.
- [39] a) A. A. Ardakani, N. Maleki, M. R. Saadein, *J. Org. Chem.* **1978**, *43*, 4128-4131; b) C. Wilcox, R. Breslow, *Tetrahedron Lett.* **1980**, *21*, 3241-324; c) H.-J. Knölker, J. Heber, C. H. Mahler, *Synlett* **1992**, 1002-1004; d) A. J. Pearson, R. J. Shively, R. A. Dubbert, *Organometallics* **1992**, *11*, 4096-4104.
- [40] a) H.-J. Knölker, J. Heber, *Synlett* **1993**, 924-926; b) A. J. Pearson, R. J. Shively, *Organometallics* **1994**, *13*, 578-584; c) A. J. Pearson, A. Perosa, *Organometallics* **1995**, *14*, 5178-5183.
- [41] H.-J. Knölker, E. Baum, H. Goesmann, R. Klauss, *Angew. Chem., Int. Ed.* **1999**, *38*, 2064-2066.
- [42] For Reviews on industrial hydrogenations in the context of asymmetric catalysis: a) D J. Ager, A. H. M. de Vries, J. G. de Vries, *Chem. Soc. Rev.* **2012**, *41*, 3340-3380; b) H. Shimizu, I. Nagasaki, K. Matsumura, N. Sayo, T. Saito, *Acc. Chem. Res.* **2007**, *40*, 1385-1393; c) N. B. Johnson, I. C. Lennon, P. H. Moran, J. A. Ramsden, *Acc. Chem. Res.* **2007**, *40*, 1291-1299.
- [43] a) T. Ikariya, K. Murataa, R. Noyori, *Org. Biomol. Chem.* **2006**, *4*, 393-406; b) O. Eisenstein, R. H. Crabtree, *New J. Chem.* **2013**, *37*, 21-27; c) R. Noyori, T. Ohkuma, *Angewandte Chemie* **2001**, *113*, 40-75.
- [44] a) Y. Blum, D. Czarkie, Y. Rahamim, Y. Shvo, *Organometallics* **1985**, *4*, 1459-1461; b) Y. Shvo, D. Czarkie, Y. Rahamim, D. F. Chodosh, *J. Am. Chem. Soc.* **1986**, *108*, 7400-7402.
- [45] For Reviews on the Shvo catalyst: a) R. Prabhakaran, *Synlett* **2004**, *2004*, 2048-2049; b) R. Karvembu, R. Prabhakaran, K. Natarajan, *Coord. Chem. Rev.* **2005**, *249*, 911-918; c) B. L. Conley, M. K. Pennington-Boggio, E. Boz, T. J. Williams, *Chem. Rev.* **2010**, *110*, 2294-2312.
- [46] a) C. P. Casey, H. Guan, *J. Am. Chem. Soc.* **2007**, *129*, 5816-5817; b) C. P. Casey, H. Guan, *J. Am. Chem. Soc.* **2009**, *131*, 2499-2507.
- [47] M. G. Coleman, A. N. Brown, B. A. Bolton, H. Guan, *Adv. Synth. Catal.* **2010**, *352*, 967-970.
- [48] A. Quintard, J. Rodriguez, *Angew. Chem., Int. Ed.* **2014**, *53*, 4044-4055.
- [49] W. Hieber, F. Leutert, *Z. Anorg. Allg. Chem.* **1932**, *204*, 145-164.
- [50] S. Fleischer, S. Zhou, K. Junge, M. Beller, *Angew. Chem., Int. Ed.* **2013**, *52*, 5120-5124.
- [51] A. Berkessel, S. Reichau, A. von der Höh, N. Leconte, J.-M. Neudörfl, *Organometallics* **2011**, *30*, 3880-3887.
- [52] H.-J. Knölker, H. Goesmann, R. Klauss, *Angew. Chem. Int. Ed.* **1999**, *38*, 702-705.
- [53] See for example: a) S. Moulin, H. Dentel, A. Pagnoux-Ozherelyeva, S. Gaillard, A. Poater, L. Cavallo, J.-F. Lohier, J.-L. Renaud, *Chem. Eur. J.* **2013**, *19*, 17881-17890; b) D. S. Mérel, M. Elie, J.-F. Lohier, S. Gaillard, J.-L. Renaud, *ChemCatChem* **2013**, *5*, 2939-2945; c) A. Pagnoux-Ozherelyeva, N. Pannetier, M. D. Mbaye, S. Gaillard, J.-L. Renaud, *Angew. Chem. Int. Ed.* **2012**, *51*, 4976-4980; d) J. P. Hopewell, J. E. D. Martins, T. C. Johnson, J. Godfrey,

- M. Wills, *Org. Biomol. Chem.* **2012**, *10*, 134-145; e) T.-T. Thai, D. S. Mérel, A. Poater, S. Gaillard, J.-L. Renaud, *Chem. Eur. J.* **2015**, *21*, 7066-7070.
- [54] Examples for transfer hydrogenation: a) A. Del Grosso, A. E. Chamberlain, G. J. Clarkson, M. Wills, *Dalton Transactions* **2018**, *47*, 1451-1470; b) R. Hodgkinson, A. Del Grosso, G. Clarkson, M. Wills, *Dalton Transactions* **2016**, *45*, 3992-4005; c) T. C. Johnson, G. J. Clarkson, M. Wills, *Organometallics* **2011**, *30*, 1859-1868; d) T. W. Funk, A. R. Mahoney, R. A. Sponenborg, K. P. Zimmerman, D. K. Kim, E. E. Harrison, *Organometallics* **2018**, *37*, 1133-1140; e) T. N. Plank, J. L. Drake, D. K. Kim, T. W. Funk, *Adv. Synth. Catal.* **2012**, *354*, 597-601; f) H.-J. Pan, T. W. Ng, Y. Zhao, *Org. Biomol. Chem.* **2016**, *14*, 5490-5493.
- [55] S. A. Moyer, T. W. Funk, *Tetrahedron Lett.* **2010**, *51*, 5430-5433.
- [56] For use of (cyclopentadienone)iron complexes in the “hydrogen borrowing” alcohol aminations, see: a) K. Polidano, B. D. W. Allen, J. M. J. Williams, L. C. Morrill, *ACS Catal.* **2018**, *8*, 6440-6445; b) T. Yan, B. L. Feringa, K. Barta, *Science Advances* **2017**, *3*, eaao6494; c) T. Yan, B. L. Feringa, K. Barta, *ACS Catal.* **2016**, *6*, 381-388; d) T. Yan, B. L. Feringa, K. Barta, *Nature Communications* **2014**, *5*, 5602; e) M. Vayer, S. P. Morcillo, J. Dupont, V. Gandon, C. Bour, *Angew. Chem., Int. Ed.* **2018**, *57*, 3228-3232; f) T. J. Brown, M. Cumbes, L. J. Diorazio, G. J. Clarkson, M. Wills, *J. Org. Chem.* **2017**, *82*, 10489-10503; g) A. J. Rawlings, L. J. Diorazio, M. Wills, *Org. Lett.* **2015**, *17*, 1086-1089; h) A. Quintard, J. Rodriguez, *ChemSusChem* **2016**, *9*, 28-30; i) H.-J. Pan, T. W. Ng, Y. Zhao, *Chem. Commun.* **2015**, *51*, 11907-11910; j) X. Bai, F. Aiolfi, M. Cettolin, U. Piarulli, A. Dal Corso, L. Pignataro, C. Gennari, *Synthesis* **2019**, *51*, 3545-3555.
- [57] Examples for hydrogenation a) X. Bai, M. Cettolin, G. Mazzocanti, M. Pierini, U. Piarulli, V. Colombo, A. Dal Corso, L. Pignataro, C. Gennari, *Tetrahedron* **2019**, *75*, 1415-1424; b) S. Vailati Facchini, J.-M. Neudörfl, L. Pignataro, M. Cettolin, C. Gennari, A. Berkessel, U. Piarulli, *ChemCatChem* **2017**, *9*, 1461-1468; c) P. Gajewski, A. Gonzalez-de-Castro, M. Renom-Carrasco, U. Piarulli, C. Gennari, J. G. de Vries, L. Lefort, L. Pignataro, *ChemCatChem* **2016**, *8*, 3431-3435; d) P. Gajewski, M. Renom-Carrasco, S. Vailati Facchini, L. Pignataro, L. Lefort, J. G. de Vries, R. Ferraccioli, U. Piarulli, C. Gennari, *Eur. J. Org. Chem.* **2015**, 5526-5536; e) P. Gajewski, M. Renom-Carrasco, S. Vailati Facchini, L. Pignataro, L. Lefort, J. G. de Vries, R. Ferraccioli, A. Forni, U. Piarulli, C. Gennari, *Eur. J. Org. Chem.* **2015**, 1887-1893; f) A. Lator, S. Gaillard, A. Poater, J.-L. Renaud, *Chem. Eur. J.* **2018**, *24*, 5770-5774; g) D. Brenna, S. Rossi, F. Cozzi, M. Benaglia, *Org. Biomol. Chem.* **2017**, *15*, 5685-5688; h) S. Zhou, S. Fleischer, H. Jiao, K. Junge, M. Beller, *Adv. Synth. Catal.* **2014**, *356*, 3451-3455; i) S. Fleischer, S. Zhou, S. Werkmeister, K. Junge, M. Beller, *Chem. Eur. J.* **2013**, *19*, 4997-5003; n) S. Fleischer, S. Werkmeister, S. Zhou, K. Junge, M. Beller, *Chem. Eur. J.* **2012**, *18*, 9005-9010; o) A. Tlili, J. Schranck, H. Neumann, M. Beller, *Chem. Eur. J.* **2012**, *18*, 15935-15939.
- [58] a) H. Ge, X. Chen, X. Yang, *Chem. Commun.* **2016**, *52*, 12422-12425; b) X. Lu, Y. Zhang, P. Yun, M. Zhang, T. Li, *Org. Biomol. Chem.* **2013**, *11*, 5264-5277; c) A. von der Höh, A. Berkessel, *ChemCatChem* **2011**, *3*, 861-867; d) H. Zhang, D. Chen, Y. Zhang, G. Zhang, J. Liu, *Dalton Transactions* **2010**, *39*, 1972-1978.
- [59] a) A. Guðmundsson, K. P. J. Gustafson, B. K. Mai, B. Yang, F. Himo, J.-E. Bäckvall, *ACS Catal.* **2018**, *8*, 12-16; b) O. El-Sepelgy, A. Brzozowska, J. Sklyaruk, Y. K. Jang, V. Zubar, M. Rueping, *Org. Lett.* **2018**, *20*, 696-699; c) O. El-Sepelgy, A. Brzozowska, L. M. Azofra, Y. K. Jang, L. Cavallo, M. Rueping, *Angew. Chem., Int. Ed.* **2017**, *56*, 14863-14867.
- [60] C. Federsel, A. Boddien, R. Jackstell, R. Jennerjahn, P. J. Dyson, R. Scopelliti, G. Laurenczy, M. Beller, *Angew. Chem., Int. Ed.* **2010**, *49*, 9777-9780.
- [61] C. Ziebart, C. Federsel, P. Anbarasan, R. Jackstell, W. Baumann, A. Spannenberg, M. Beller, *J. Am. Chem. Soc.* **2012**, *134*, 20701-20704.
- [62] F. Bertini, I. Mellone, A. Ienco, M. Peruzzini, L. Gonsalvi, *ACS Catal.* **2015**, *5*, 1254-1265.
- [63] F. Zhu, L. Zhu-Ge, G. Yang, S. Zhou, *ChemSusChem* **2015**, *8*, 609-612.
- [64] S. b. Coufourier, S. Gaillard, G. Clet, C. Serre, M. Daturi, J.-L. Renaud, *Chem. Commun.* **2019**, *55*, 4977-4980.
- [65] A. Rosas-Hernández, P. G. Alsabeh, E. Barsch, H. Junge, R. Ludwig, M. Beller, *Chem. Commun.* **2016**, *52*, 8393-8396.
- [66] A. Rosas-Hernández, H. Junge, M. Beller, M. Roemelt, R. Francke, *Catal. Sci. Technol.* **2017**, *7*, 459-465
- [67] E. Oberem, A. F. Roesel, A. Rosas-Hernández, T. Kull, S. Fischer, A. Spannenberg, H. Junge, M. Beller, R. Ludwig, M. Roemelt, R. Francke, *Organometallics* **2019**, *38*, 1236-1247.
- [68] a) E. N. Frankel, E. A. Emken, H. M. Peters, V. L. Davison, R. O. Butterfield, *J. Org. Chem.* **1964**, *29*, 3292-3297;

- b) E. N. Frankel, E. A. Emken, V. L. Davison, *J. Org. Chem.* **1965**, *30*, 2739-2745.
- [69] a) S. Sakaki, T. Sagara, T. Arai, T. Kojima, T. Ogata, K. Ohkubo, *Journal of Molecular Catalysis* **1992**, *75*, L33-L37; b) E. J. Daida, J. C. Peters, *Inorganic Chemistry* **2004**, *43*, 7474-7485; c) H. Fong, M.-E. Moret, Y. Lee, J. C. Peters, *Organometallics* **2013**, *32*, 3053-3062; d) D. J. Frank, L. Guiet, A. Käslin, E. Murphy, S. P. Thomas, *RSC Adv.* **2013**, *3*, 25698-25701; e) K. Kano, M. Takeuchi, S. Hashimoto, Z.-i. Yoshida, *J. Chem. Soc., Chem. Commun.* **1991**, 1728-1729; f) H. Inoue, M. Suzuki, *J. Chem. Soc., Chem. Commun.* **1980**, 817-818; g) H. Inoue, M. Sato, *J. Chem. Soc., Chem. Commun.* **1983**, 983-984; h) S. C. Bart, K. Chłopek, E. Bill, M. W. Bouwkamp, E. Lobkovsky, F. Neese, K. Wieghardt, P. J. Chirik, *J. Am. Chem. Soc.* **2006**, *128*, 13901-13912.
- [70] a) R. A. Sheldon, I. Arends, U. Hanefeld, *Green Chemistry and Catalysis*, Wiley, **2007**; b) R. A. Sheldon, *Chem. Commun.* **2008**, 3352-3365.
- [71] For selected reviews, see: a) M. H. S. A. Hamid, P. A. Slatford, J. M. J. Williams, *Adv. Synth. Catal.* **2007**, *349*, 1555-1575; b) G. E. Dobereiner, R. H. Crabtree, *Chem. Rev.* **2010**, *110*, 681-703; c) G. Guillena, D. J. Ramón, M. Yus, *Chem. Rev.* **2010**, *110*, 1611-1641; d) C. Gunanathan, D. Milstein, *Science* **2013**, *341*, 1229712; e) Y. Obora, *ACS Catal.* **2014**, *4*, 3972-3981; f) K.-i. Shimizu, *Catal. Sci. Technol.* **2015**, *5*, 1412-1427; g) F. Huang, Z. Liu, Z. Yu, *Angew. Chem., Int. Ed.* **2016**, *55*, 862-875.
- [72] For selected reviews, see: a) A. Seayad, M. Ahmed, H. Klein, R. Jackstell, T. Gross, M. Beller, *Science* **2002**, *297*, 1676-1678; b) S. Bähn, S. Imm, L. Neubert, M. Zhang, H. Neumann, M. Beller, *ChemCatChem* **2011**, *3*, 1853-1864; c) A. J. A. Watson, J. M. J. Williams, *Science* **2010**, *329*, 635-636. For selected books, see: d) S. A. Lawrence, *Amines: Synthesis, Properties and Applications*, Cambridge University Press, **2004**; e) B. R. Brown, *The organic chemistry of aliphatic nitrogen compounds*, Clarendon Press, **1994**; f) J. L. McGuire, *Pharmaceuticals: Classes, Therapeutic Agents, Areas of Application*, Wiley-VCH, **2000**.
- [73] a) A. Corma, J. Navas, M. J. Sabater, *Chem. Rev.* **2018**, *118*, 1410-1459; b) A. Martínez-Asencio, D. J. Ramón, M. Yus, *Tetrahedron Lett.* **2010**, *51*, 325-327; c) F. Shi, M. K. Tse, X. Cui, D. Gördes, D. Michalik, K. Thurow, Y. Deng, M. Beller, *Angew. Chem., Int. Ed.* **2009**, *48*, 5912-5915; d) S. Rösler, M. Ertl, T. Irrgang, R. Kempe, *Angew. Chem., Int. Ed.* **2015**, *54*, 15046-15050; e) M. Bala, P. K. Verma, U. Sharma, N. Kumar, B. Singh, *Green Chem.* **2013**, *15*, 1687-1693; f) X. Cui, F. Shi, Y. Zhang, Y. Deng, *Tetrahedron Lett.* **2010**, *51*, 2048-2051; g) U. Jana, S. Maiti, S. Biswas, *Tetrahedron Lett.* **2008**, *49*, 858-862.
- [74] A. Lator, S. Gaillard, A. Poater, J.-L. Renaud, *Org. Lett.* **2018**, *20*, 5985-5990.
- [75] N. Hofmann, K. C. Hultsch, *Eur. J. Org. Chem.* **2019**, 3105-3111.
- [76] S. Elangovan, J.-B. Sortais, M. Beller, C. Darcel, *Angew. Chem., Int. Ed.* **2015**, *54*, 14483-14486.
- [77] C. Seck, M. D. Mbaye, S. Coufourier, A. Lator, J.-F. Lohier, A. Poater, T. R. Ward, S. Gaillard, J.-L. Renaud, *ChemCatChem* **2017**, *9*, 4410-4416.
- [78] C. Seck, M. D. Mbaye, S. Gaillard, J.-L. Renaud, *Adv. Synth. Catal.* **2018**, *360*, 4640-4645.
- [79] M. B. Dambatta, K. Polidano, A. D. Northey, J. M. J. Williams, L. C. Morrill, *ChemSusChem* **2019**, *12*, 2345-2349.
- [80] B. Emayavaramban, M. Sen, B. Sundararaju, *Org. Lett.* **2017**, *19*, 6-9.
- [81] For a computational studies on this dual catalytic system, see: K. H. Hopmann, *Chem. Eur. J.* **2015**, *21*, 10020-10030.
- [82] A. Quintard, T. Constantieux, J. Rodriguez, *Angew. Chem., Int. Ed.* **2013**, *52*, 12883-12887.
- [83] M. Roudier, T. Constantieux, A. Quintard, J. Rodriguez, *Org. Lett.* **2014**, *16*, 2802-2805.
- [84] D. S. Mérel, S. Gaillard, T. R. Ward, J.-L. Renaud, *Catalysis Letters* **2016**, *146*, 564-569.
- [85] A. Gudmundsson, K. P. J. Gustafson, B. K. Mai, V. Hobiger, F. Himo, J.-E. Bäckvall, *ACS Catal.* **2019**, 1733-1737.

Chapter 2 - Applications of a highly active CIC to C=N bond reduction reactions

2.1 Introduction

The reduction of C-N multiple bonds is an important transformation which provides access to amines, a common class of compounds used for the synthesis of bioactive compounds, dyes, fibers and materials.^[1] On lab scale, imines, iminium ions, nitriles, nitro groups, amides and azides are commonly reduced using stoichiometric reagents such as aluminum and boron hydrides (e. g., LiAlH₄, NaBH₄, NaBH₃CN), metal salts (e.g., SnCl₂) and phosphorus compounds (e.g., PPh₃). Under suitable conditions – called reductive amination conditions – imines and iminium ions may be also generated from carbonyl compounds in the same vessel where the reduction step is performed. Unfortunately, use of boron-, aluminum- or phosphorus-containing reductants is poorly atom economic, as these reactions lead to the formation of co-products in stoichiometric amounts, with associated costs of disposal.

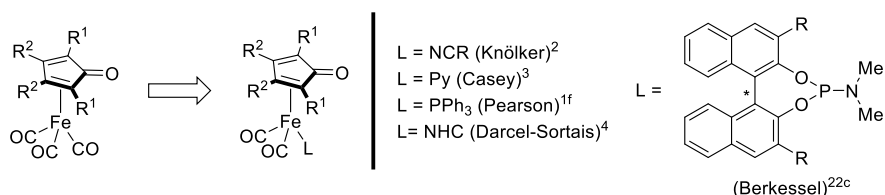
From the industrial point of view, catalytic hydrogenation (CH)^[2] and catalytic transfer hydrogenation (CTH)^[3] are much more attractive processes, because either they do not lead to co-product formations (in the case of CH) or they only result in the formation of simple materials (e.g. acetone or CO₂ in the case of CTH) that can be readily separated from the desired product. The use of noble metal catalysts has allowed to develop effective protocols for the CH of imines,^[4] nitriles,^[5] amides,^[6] azides,^[7] nitro groups,^[8] and for the CTH of imines/iminium ions.^[9] As discussed in the previous chapter, economic and environmental considerations have stimulated the development of catalytic methodologies relying on base metals.^[10] Among them, iron is particularly attractive due to its low cost and scarce toxicity.^[11] Homogeneous iron catalysts have been used in the CH of imines/iminium ions,^[12] nitriles,^[13] amides,^[14] nitro groups^[12] and, in a few instances, in the CTH of imines.^{[15],[16]} The already discussed dual catalytic system reported by Beller in 2011 (see Section 1.6.2) involved the combination of HCIC **10aa** with a chiral Brønsted acid, which allowed to perform the AH of ketimines with high enantioselectivity. As mentioned in Section 1.4.2, the first use of a CIC as the sole catalyst for the reduction of C=N bonds was reported in 2012 by Renaud and co-workers,^[12a,b,d] with the development of a CH-based protocol for the reductive amination of carbonyl compounds. However, the latter methodology had a large margin for improvement in terms of catalytic activity and application scope (it covers mostly aldehydes and only a few ketones). Later on, Zhao and co-workers reported that complexes **10aa** and **9ad** can promote the CH of isolated ketimines only in the presence of a Lewis acid co-catalyst [Fe(acac)₃].^[15e]

Remarkably, before my work of thesis no example of CIC-promoted imine CTH was known, although this kind of complexes had been reported to promote the alcohol amination,^[17] mechanistically related to CTH.^[18]

We reasoned that more efficient CIC-promoted C=N reduction protocols could be developed using a pre-catalyst more active than the Knölker's complex (**9aa**) originally employed by Renaud and co-workers.^[12a,b,d]

From the point of view of ligand design, in order to enhance the catalytic reactivity of CICs two main strategies were followed. The first approach was the replacement of one CO ligand with a different ligand, which has been mentioned in Section 1.6.1. Several ligands, such as nitriles,^[12b,19] pyridines,^[20] NHCs,^[21] phosphines,^[1f] and chiral phosphoramidites^[22] have been already used (Figure 2.1 A). The second strategy consists in modifying the cyclopentadienone ligand by variation of the substituents at the 2,5 or 3,4 positions (Scheme 2.1 B).^[12b,c,17d,22a-b,23]

A. Replacement of one CO ligand



B. Modification of the cyclopentadienone ring

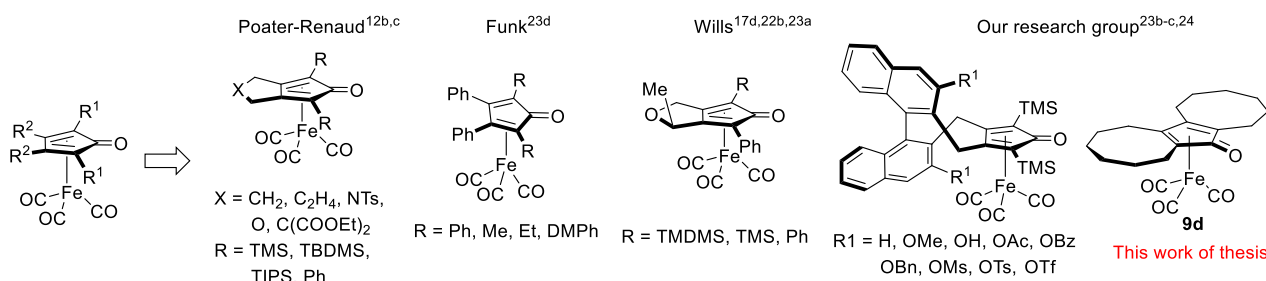


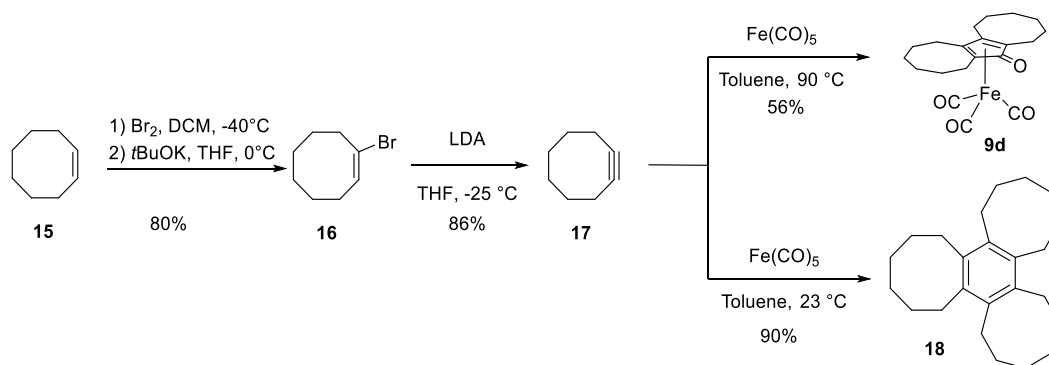
Figure 2.1. Main strategies to obtain structurally modified (cyclopentadienone)iron complexes.

As mentioned in Section 1.4.1, according to the second strategy, CIC **9d** was previously reported by our research group to have higher catalytic activity than the Knölker's complex **9aa** in the hydrogenation of ketones.^[24] Thus, I set to verify whether the high catalytic activity of **9d** could be exploited to expand the scope of C=N reductions.

2.2 Preparation of CIC **9d**

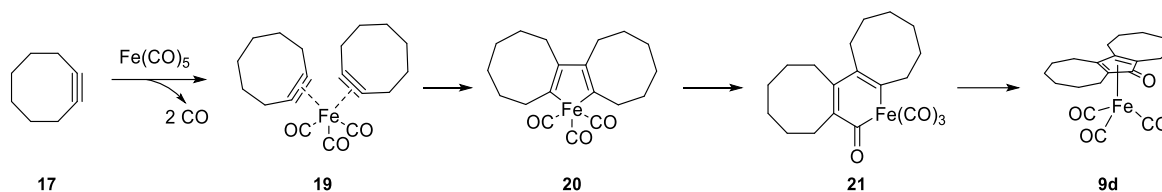
CICs can be synthesized following two main synthetic strategies: i) complexation of the cyclopentadienone ligand with iron carbonyl complexes [e.g., Fe(CO)₅ and Fe₂(CO)₉]; ii) cyclative carbonylation/complexation

of diynes or alkynes with an iron carbonyl complex. The latter route, used by our group to synthesize complex **9d**, was reported first and it is the most common synthetic strategy.^[24] For this transformation, large excesses of iron carbonyl complexes [e.g., $\text{Fe}(\text{CO})_5$] are required, but this is acceptable, due to their low cost. In this approach, the synthesis of properly functionalized diyne or alkyne precursors is an important step. Starting from two molecular alkynes, functionalized CICs could be in principle synthesized via an intermolecular cyclative carbonylation/complexation. However, the limitation of this strategy is that only alkynes bearing substituents such as silyl groups or electron-withdrawing substituents (e.g., $-\text{Cl}$, $-\text{CF}_3$ and $-\text{O}t\text{Bu}$)^[25] can lead to acceptable amount of desired CIC, whereas low yields ($< 15\%$) are commonly obtained with alkynes with other types of substituents (e.g. phenylacetylene or diphenylacetylene).^[26] Our research group performed the synthesis of complex **9d** in acceptable yields, owing to the peculiar reactivity of cyclooctyne (**17**).



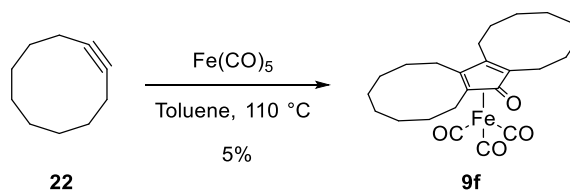
Scheme 2.1. Synthesis of [bis(hexamethylene)cyclopentadienone]iron complex **9d** from cyclooctene **15**

The synthesis of cyclooctyne **17**, the smallest cyclic alkyne ever isolated so far, was reported by Brandsma and Verkruijsse in 1978.^[27] This hydrocarbon is not commercially available, and its instability – due to ring strain – leads to the compound degradation within few days, even at $-19\text{ }^\circ\text{C}$. However, compound **17** can be easily synthesized in good yields from relatively cheap *cis*-cyclooctene (**15**). Starting from the latter, 1-bromocyclooctene **16** could be easily synthesized with high yield (up to 80%) in two steps: bromination with Br_2 and elimination of HBr from the corresponding 1,2-dibromocyclooctane upon the addition of *t*BuOK. Finally, a second elimination reaction was performed in the presence of a strong base (e.g., LDA) to afford the desired alkyne **17**. Iron complex **9d** was firstly obtained in 1971: the reaction of compound **17** with $\text{Fe}(\text{CO})_5$ led to the isolation of several products.^[28] Among them, a substantial amounts of tris(hexamethylene) benzene **18** was formed, whereas only a little quantity of the iron complex **9d** was isolated (14% yield). Optimization of cyclative carbonylation conditions performed by our group allowed to remarkably optimize the yield of **9d**: when the reaction was carried out in toluene at $90\text{ }^\circ\text{C}$ using $\text{Fe}(\text{CO})_5$, the desired complex **9d** was obtained in 56% yield, but compound **18** was still the main product at lower or higher temperatures



Scheme 2.2. Proposed mechanism for the formation of complex **9d**

The proposed mechanism for the formation of **9d** (Scheme 2.2)^[24] consists of a stepwise Fe-mediated [2+2+1] cycloaddition which is initiated by the sequential replacement of two carbonyl ligands by the two alkyne molecules, followed by formation of the tricarbonyl[bis- η^2 -alkyne] iron complex **19**. At this stage, Fe(0) promotes the coupling of the two bound alkynes to form the intermediate complex **20**. Insertion of carbonyl into the iron-carbon bond followed by a subsequent rearrangement of the complex **21** affords CIC **9d**. The release of the ring strain present in the cyclooctyne ring probably favors the intermolecular cyclative carbonylation/complexation process. To demonstrate this hypothesis, cyclododecyne **22** (which has lower ring strain than cyclooctyne **17**)^[29] was reacted with $\text{Fe}(\text{CO})_5$ under the same reaction conditions employed in the synthesis of **9f**. As expected, the related Fe-complex **9f** was formed in very low yields (only 5%).



Scheme 2.3. Synthesis of [bis(decamethylene)cyclopentadienone]iron complex **9f**.

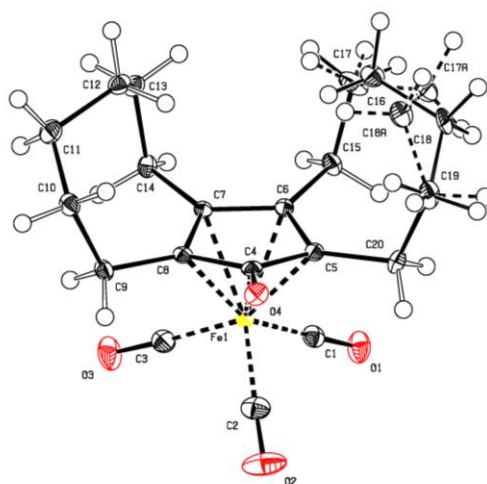


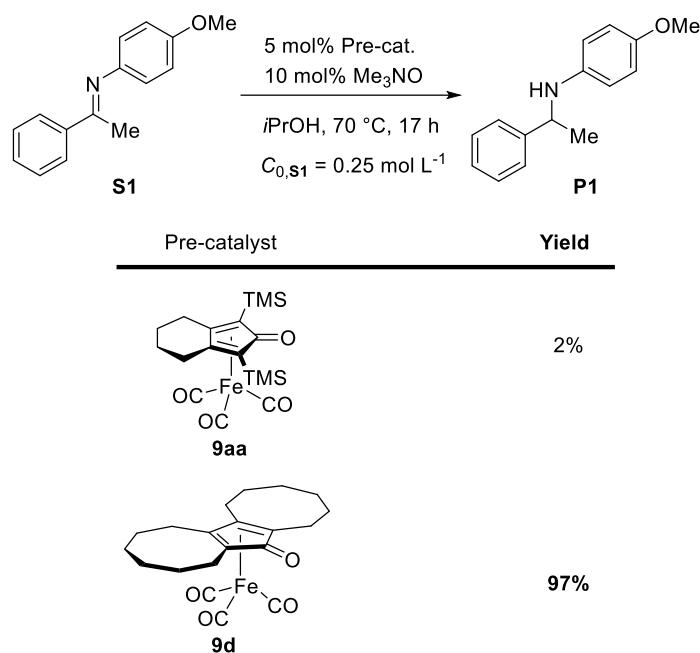
Figure 2.2. X-ray structure of CIC **9d**.

CIC **9d** was fully characterized, and suitable crystals for XRD analysis were grown.^[24] The X-ray structure reveals the usual piano-stool geometry with a significant deviation from planarity of the cyclopentadienone

ring (Figure 2.2).

2.3 Imine transfer hydrogenation

Encouraged by the remarkable catalytic activity of complex **9d** in hydrogenation of ketones and aldehydes,^[24] which is more active than Knölker complex **9aa**, we extended the use of this catalyst to the reduction of imines to amines. In an initial experiment, the classical ‘Knölker complex’ **9aa** and complex **9d** were tested in the CTH of *N*-(1-phenylethylidene)-*p*-anisidine **S1** under same reaction conditions (Scheme 2.4).

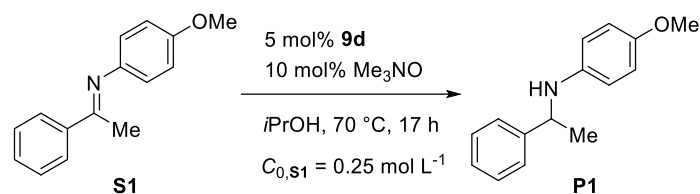


Scheme 2.4. Preliminary tests of pre-catalysts **9aa** and **9d** in the CTH of a ketimine.

According to previous reports and experience, CICs **9aa** and **9d** were activated by de-complexation of one CO ligand with Me_3NO .^[12a-d,17a,d,18b,23b,c,24,30] We found that catalyst activation is crucial for reaction reproducibility. Optimization of this step led to the definition of the following optimized conditions: to a solution of the pre-catalyst in *i*PrOH ($C_{\text{CIC}} \geq 0.1 \text{ M}$) Me_3NO was added, and the resulting mixture was reacted for 20–30 min at r.t., followed by substrate addition. The catalyst formed *in situ* from **9d** efficiently promoted the reaction (97% yield, Scheme 2.4), whereas the one derived from **9aa** was nearly inactive (2% yield). This difference in terms of catalytic activity is more remarkable than the one observed in ketone CH and CTH.^[24] Moreover, these results are in agreement Zhao’s report that pre-catalyst **9ad**, whose activated form is the same as the one generated from **9aa**, can promote ketimine CTH only in the presence of a substantial amount of a Lewis acid co-catalyst.^[15e]

Different hydrogen donors were also screened to further optimize the applicability of **9d** in the reduction of ketimine **S1** (Table 2.1).

Table 2.1. Reduction of ketimine **S1** promoted by pre-catalysts **9d**^[a]



#	Hydrogen donor	Cat. loading (mol%)	Conc. (mol L ⁻¹)	Solvent	Conv. (%)
1	H ₂ (20 atm)	10	0.5	Toluene	98
2	H ₂ (20 atm)	10	0.5	MeOH	>99
3	H ₂ (20 atm)	5	0.5	Toluene	22
4	H ₂ (20 atm)	5	0.5	MeOH	60
5	FA/TEA	5	0.5	5:2 FA/TEA	38
6	<i>i</i> PrOH	5	0.5	<i>i</i> PrOH	70

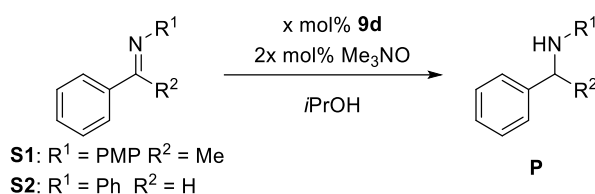
[a] Conversion was determined by ¹H-NMR of the crude reaction mixture, FA: Formic Acid, TEA: Triethylamine

Excellent conversions were obtained with a catalyst loading of 10% in both MeOH and toluene (Table 2.1, entries 1-2). However, decreasing the catalyst loading led to lower conversions to amine **P1** in both solvents (Table 2.1, entries 3-4). Using the FA/TEA mixture (5:2 v/v) as hydrogen donor and solvent, the TH of **S1** took place with a moderate conversion with 5 mol% catalyst loading (Table 2.1, entry 5). By replacing FA/TEA mixture with isopropanol, the conversion increased up to 70% (Table 2.1, entry 6). Encouraged by the promising results obtained with pre-catalyst **9d**, we set to optimize the reaction conditions using two different model substrates: ketimine **S1** and aldimine **S2**. Various parameters (e.g., catalyst loading, concentration and temperature) were varied as shown in Table 2.2.

Since only the reduced product and/or starting material signals were observed in the crude reaction mixtures, conversions were determined by ¹H NMR analysis. The initial substrate concentration ($C_{0,\text{sub.}}$) remarkably influenced the conversion in the reduction of **S1**, 0.25 M representing the optimal value (Table 2.2, entry 2 vs. entries 1 and 3). Conversion remained excellent when the catalyst loading was reduced to 2 mol% (Table 2.2, entries 4 and 5). At 1 mol% and at 0.5 mol% the reaction became sluggish (Table 2.2, entry 6 and 8). However, increasing temperature to 100 °C could restore a high conversion even with 1 mol% catalyst loading (Table 2.2, entry 7). When the loading was further lowered to 0.5 mol%, very low conversion was obtained, and only a slight improvement was observed increasing the temperature to 100 °C (Table 2.2, entry 9). When the catalyst

loading was further lowered to 0.1 mol%, no conversion was observed (Table 2.2, entry 10). As expected, the more active aldimine **S2** was reduced with higher conversions under the same reaction conditions (Table 2.2, entry 11-20 vs. 1-10, respectively). With three different $C_{0,\text{sub}}$ values, full conversion was observed with 5 mol% catalyst loading (Table 2.2, entry 11-13). The optimal $C_{0,\text{sub}}$ value (0.25 M) was confirmed by running experiments at 2 mol% catalyst loading (Table 2.2, entries 14 vs. 15). Although further lowering the catalyst loading down to 1 mol% and 0.5 mol% led to slower reactions, full conversion could still be obtained operating at 100 °C (Table 2.2, entries 17 and 19 vs. 16 and 18) and the rate decrease was less evident than in the case of **S1** (Table 2.2, entries 16 and 18 vs. 6 and 8). At 0.1 mol% catalyst loading, only a modest conversion (17%) was obtained (Table 2.2, entry 20).

Table 2.2. Imine CTH promoted by pre-catalyst **9d**: optimization of the reaction conditions.^[a]



#	Sub.	Cat. loading (mol%)	$C_{0,\text{sub}}$ (mol L ⁻¹)	Conv. ^[b] (%)
1	S1	5	0.4	72
2	S1	5	0.25	97
3	S1	5	0.13	89
4	S1	2	0.4	71
5	S1	2	0.25	>99
6	S1	1	0.25	8
7	S1	1	0.25	88 ^[c]
8	S1	0.5	0.25	4
9	S1	0.5	0.25	16 ^[c]
10	S1	0.1	0.25	0 ^[c]
11	S2	5	0.4	>99
12	S2	5	0.25	>99
13	S2	5	0.13	>99
14	S2	2	0.4	90
15	S2	2	0.25	>99
16	S2	1	0.25	74
17	S2	1	0.25	>99 ^[c]
18	S2	0.5	0.25	28
19	S2	0.5	0.25	>99 ^[c]
20	S2	0.1	0.25	17 ^[c]

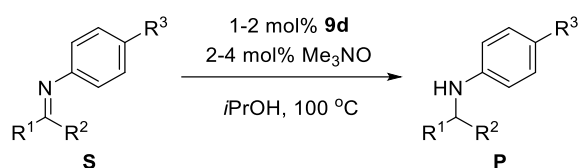
[a] Reaction conditions: **9d**/Me₃NO = 1:2, $T = 70$ °C, 18 h, solvent: *i*PrOH.

[b] Conversion was determined by ¹H-NMR of the crude reaction mixture.

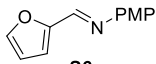
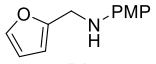
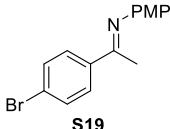
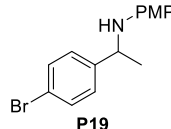
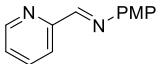
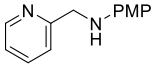
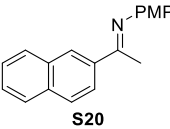
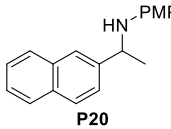
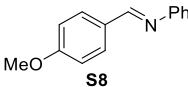
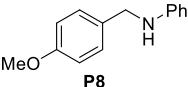
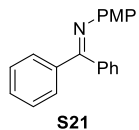
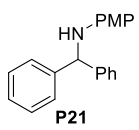
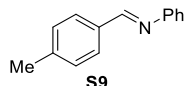
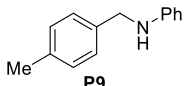
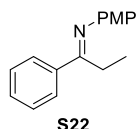
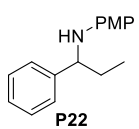
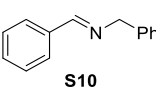
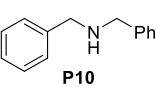
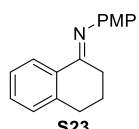
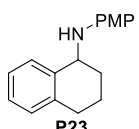
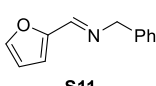
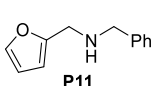
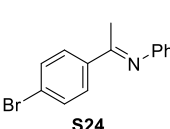
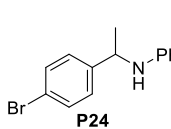
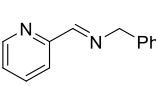
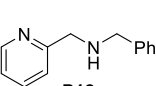
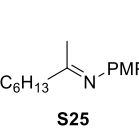
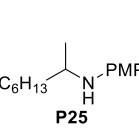
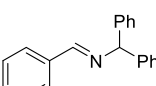
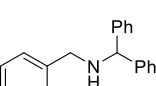
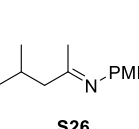
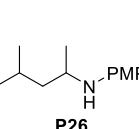
[c] Reaction run at 100 °C.

Following this optimization work, $C_{0,\text{sub.}} = 0.25 \text{ M}$ in *i*PrOH, 2 mol% catalyst **9d** loading, and $T = 100 \text{ }^\circ\text{C}$ were selected as optimal conditions for extending the substrate scope. The screening (Table 2.3) was carried out on a lab-scale (0.5 mmol) and the isolated yield of every product was determined with the exception of product **P11** (NMR yield). Delightfully, excellent yields (83% to quantitative) were obtained with all substrates except ketimines **S23**, **S24** and aldimines **S4**, **S10-13** (Table 2.3, entries 4, 10-13, 23 and 24), which gave moderate yields.

Table 2.3. CTH-based reduction of imines promoted by pre-catalyst **9d**.^[a]



#	Substrate	Product	Yield (%) ^[b]	#	Substrate	Product	Yield (%) ^[b]
1			99	14			99
2			99	15			99
3			99	16			99
4			46	17			95
5			99	18			98

6			99	19			99
7			99	20			99
8			99	21			83
9			99	22			99
10			66	23			57
11			36 ^[c]	24			68
12			66	25			99
13			67	26			99

[a] Reaction conditions: substrate/**9d**/Me₃NO = 100:1:2 (Entry 2 to 13), Substrate/**9d**/Me₃NO = 100:2:4 (Entry 1 and 14-26), C_{0,sub.} = 0.25 M (0.5 mmol), T = 100 °C, 18 h, solvent: *i*PrOH, PMP = *p*-methoxyphenyl.

[b] Isolated yields.

[c] NMR yield.

All the aniline-derived aldimines were reduced in nearly quantitative yields except for the 4-nitro-substituted aldimine **S4** (Table 2.3, entry 4). Remarkably, aldimines **S4** and **S5** were reduced chemoselectively to amines while their -NO₂ and -CN – potentially amenable to be reduced – remained unaffected. Despite the heteroatom present in aldimines **S6** and **S7** which could possibly poison the Fe center, nearly quantitative yields were obtained (Table 2.3, entries 6 and 7), The benzylamine-derived aldimines were reduced in lower yields than those obtained from the aniline-derived aldimines (Table 2.3, entry 10-12 vs. entry 2, 6 and 7). The sterically

encumbered aldimine **S13** gave a similar yield to benzylamine-derived aldimines (Table 2.3, entry 13 vs. entry 10 and 12). A number of ketimine substrates were tested (Table 2.3, entry 1 and entry 14-26) and found to react with very high yields. Exceptions to this trend were the α -tetralone-derived ketimine **S23** and ketimine **S24** bearing a bromine substituent, which were partially reduced (57% and 68% yield, respectively; see Table 2.3, entries 23 and 24).

Kinetic studies on the CTH of ketimine **S1** (Figure 2.3) promoted by complex **9d** were carried out to get additional information on its catalytic properties in the reduction of C=N double bonds. The reaction was performed in *i*PrOH at 100 °C in the presence of 5 mol% **9d** and 10 mol% Me₃NO, and the conversion was determined by GC analysis of samples taken at regular intervals (every 15 min in the first 3 h, and later every 30 min). As shown in Figure 2.3, a pseudo-first order dependence on starting substrate concentration was observed, the half-life of **S1** was found to be 98.9 min, corresponding to an average TOF of 6.07 h⁻¹ at 50% conversion. As low conversion (2%) was obtained with complex **9aa** in imine CTH, the kinetics of imine **S1** could not be taken as a term of comparison.

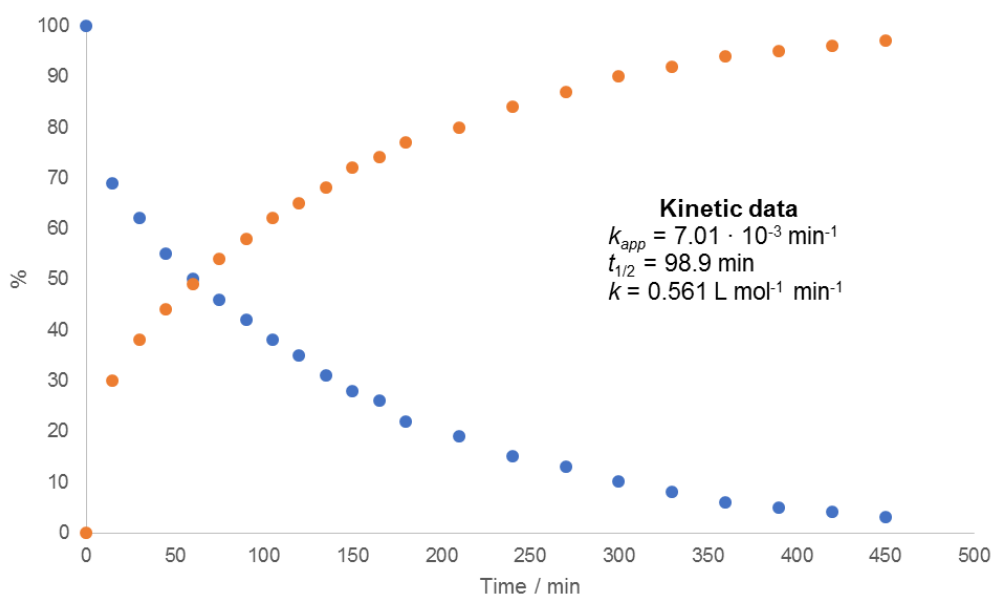


Figure 2.3. Kinetics of the CTH of **S1** promoted by complex **9d**: • Conversion to of **P1** (GC); • Percent of unreacted **S1**.

Conditions: **S1/1b**/Me₃NO = 100:5:10; solvent: *i*PrOH; C_{0,S1} = 0.25 M (0.5 mmol); T = 100 °C; C_{cat.} = 12.5 mM.

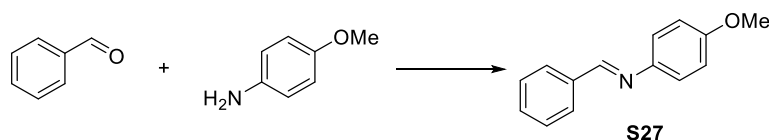
2.4 Reductive amination of carbonyl compounds

Encouraged by the remarkable results obtained in imine CTH, we focused our attention on the more

challenging reductive amination of carbonyl compounds, involving imine formation and CTH in one pot. In principle, this methodology extends the substrate scope to those imines that cannot be easily isolated due to their poor stability. The first CIC-catalyzed version of this transformation was reported in 2012 by Renaud and co-workers using CH in the imine reduction stage.^[12a,b,d] As mentioned above (see Section 1.4.2), the methodology reported by Renaud had remarkable margins for improvement, as the substrate scope was rather narrow and covered mostly aldehydes and only a few ketones.

Based on the results obtained in imine CTH, we set to develop a CTH-based protocol for the reductive amination of carbonyl compounds, and aldehydes were selected for the first investigations. We found that – similarly to the protocol developed by Renaud^[12a-d] – imine formation and reduction had to be performed sequentially and not simultaneously, arguably because the C=N bond is reduced with rate similar or higher than the C=O bond. The imine formation step was found crucial to obtain a clean reaction. Indeed, whenever imines were formed with yields lower than 90%, the CTH gave complex mixtures. Therefore, the formation of a model aldimine from benzaldehyde and 4-methoxyaniline was monitored by ¹H-NMR and we detected formation of aldimine **S27** (Table 2.4) with full conversions in a 1-hour reaction, run in toluene and in the presence of 3 Å molecular sieves (MS).

Table 2.4. *In situ* formation of imine **S27** monitored by ¹H-NMR.^[a]



#	Anisidine (eq.)	Time (h)	<i>T</i> (°C)	Solvent	Additive [amount]	Conv. (%) ^[a]
1	1	1	r.t.	CD ₃ OD		0
2	1	18	r.t.	CD ₃ OD		0
3	1	1	r.t.	CD ₃ OD	NH ₄ PF ₆	96
4	1	1	100	<i>d</i> ₈ -Toluene	4 Å MS ^[a] [200 mg]	91
5	1.5	1	100	<i>d</i>₈-Toluene	3 Å MS^[a] [200 mg]	>99
6	1	1	50	CD ₃ OD	3 Å MS ^[a] [200 mg]	87

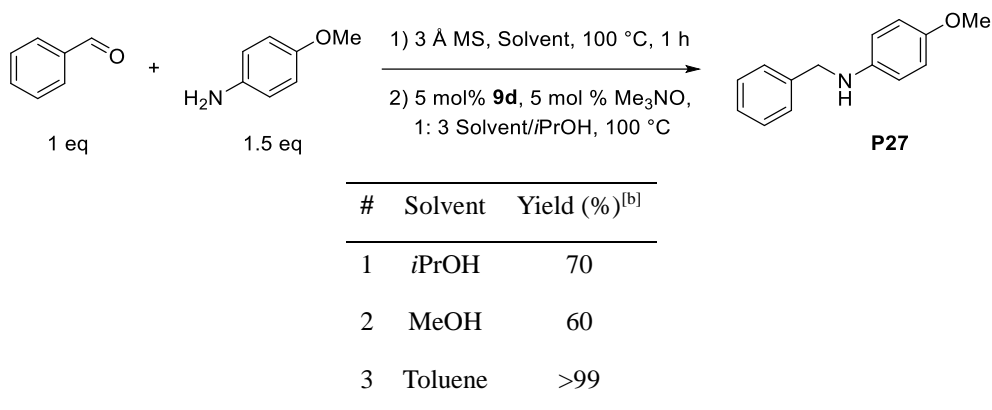
[a] Reactions run on a 0.5 mmol scale (benzaldehyde).

[b] Under vacuum overnight activated molecular sieves (MS) and kept under argon.

Later on, we carried out the first tests of aldehyde reductive amination (see Table 2.5). The catalyst loading was increased to 5 mol%, given the more challenging nature of reductive amination. Substrates benzaldehyde

and anisidine were dissolved in several different solvents for *in situ* imine formation, then a solution of catalyst **act-9d** – generated *in situ* treating **9d** with Me₃NO in *i*PrOH – was added. As expected, the best yield was obtained when imine formation was performed in toluene, which is in accordance with the results of the NMR studies shown in Table 2.4. When the imine formation was performed in *i*PrOH or MeOH, lower yields were obtained (70% and 60%, respectively).

Table 2.5. Optimization of the CTH-based reductive amination of benzaldehyde promoted by pre-catalyst **9d**.^[a]



[a] Reaction conditions: benzaldehyde/anisidine/**9d**/Me₃NO = 100:150:5:5. Imine formation: toluene, 100 °C, 3 Å MS (400 mg), 1 h. Catalyst activation: solvent, Me₃NO, r.t., 20 min. CTH: 3:1 *i*PrOH/solvent, C_{0,sub} in CTH = 0.25 M (0.5 mmol), *T* = 100 °C, 18 h; benzaldehyde was freshly distilled before use.

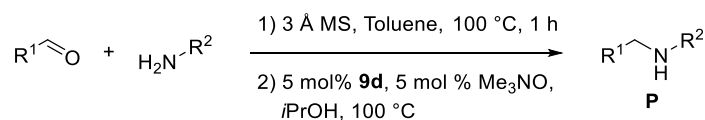
[b] Isolated yield.

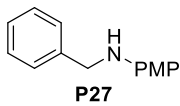
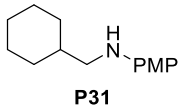
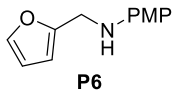
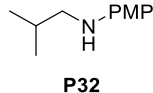
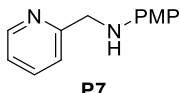
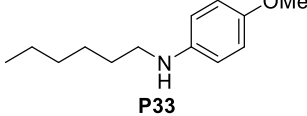
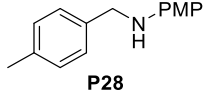
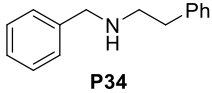
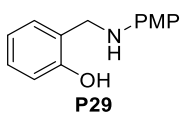
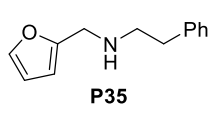
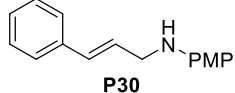
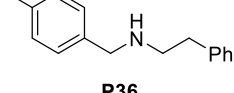
Once the reaction conditions were optimized, the aldehyde scope of the new methodology was investigated. Different aldehydes were tested in combination with *p*-anisidine or phenethylamine, and the results obtained are shown in Table 2.6. Firstly, a series of different aldehydes were screened in combination with *p*-anisidine and phenethylamine, giving the results shown in Table 2.6. Aromatic (Table 2.6, entries 1, 4) and heteroaromatic aldehydes (entries 2, 3) were converted into the corresponding *N*-PMP amines in excellent yields, with the exception of the sterically hindered salicylaldehyde, which formed product **P29** in only 44% yield (entry 5). Cinnamaldehyde and cyclohexanecarboxaldehyde were converted into products **P30** and **P31** in good yields (Table 2.6, entries 6 and 7), whereas isobutyraldehyde showed poor reactivity (entry 8). Notably, also the *in situ* formed *N*-alkyl imines proved reactive and formed the corresponding products **P34-P36** in fair to good yield (Table 2.6, entries 10-12).

Next, we investigated also the reductive amination of ketones, which is particularly challenging due to the difficulty to achieve quantitative imine formation in a reasonable time. NMR studies of *in situ* formation of ketimines were carried out on a model reaction between acetophenone and *p*-anisidine to form imine **S1**. The results of these studies (Table 2.7) demonstrate that, besides the molecular sieves, an acid catalyst is also

needed to warrant high-yielding formation of imine **S1**: the best conversion to ketimine **S1** was obtained using TFA (10 mol%) in the presence of smashed 3 Å MS (Table 2.7, entry 15).

Table 2.6. Substrate scope evaluation in reductive amination of aldehydes promoted by pre-catalyst **9d**.^[a]



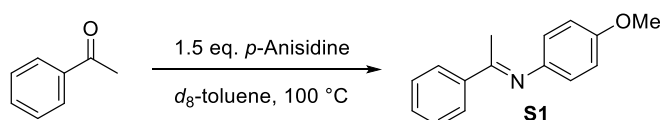
	Product	Yield (%) ^[b]		Product	Yield (%) ^[b]
1	 P27	>99	7	 P31	74
2	 P6	98	8	 P32	17 ^[c]
3	 P7	93	9	 P33	0
4	 P28	99	10	 P34	38
5	 P29	44	11	 P35	67
6	 P30	75	12	 P36	90

[a] Reaction conditions: aldehyde /amine/**9d**/Me₃NO = 100:150:5:5. Imine formation: toluene, 100 °C, 3 Å MS (400 mg), 1 h. Catalyst activation: *i*PrOH, Me₃NO, r.t., 20 min. CTH: 3:1 *i*PrOH/toluene, C_{0,substrate} in CTH = 0.25 M (0.5 mmol), *T* = 100 °C, 18 h; all the aldehydes were freshly distilled over PPh₃, before use.

[b] Isolated yields.

[c] Yield determined by ¹H NMR.

Table 2.7. NMR studies *in situ* formation of imine **S1** starting from acetophenone.^[a]



#	Time (h)	Acid [mol%]	MS [amount, mg]	Conv. (%) ^[b]
1	1	-	3 Å [200]	37
2	o.n.	-	3 Å [200]	71
3	1	NH ₄ PF ₆ [2]	3 Å [200]	35
4	o.n.	NH ₄ PF ₆ [2]	3 Å [200]	63
5	1	NH ₄ PF ₆ [5]	3 Å [200]	52
6	1	NH ₄ PF ₆ [10]	3 Å [200]	53
7	1	NH ₄ PF ₆ [10]	3 Å [400]	71
8	1	NH ₄ PF ₆ [10]	3 Å, smashed [400]	71
9	1	NH ₄ PF ₆ [5]	3 Å, smashed [400]	89
10	2	NH ₄ PF ₆ [5]	3 Å, smashed [400]	88
11	1	PTSA [5]	3 Å, smashed [400]	86
12	1	HCl, 1M in methanol [5]	3 Å, smashed [400]	80
13	1	CH ₃ COOH [5]	3 Å, smashed [400]	57
14	1	HCl 4M in dioxane [5]	3 Å, smashed [400]	85
15	2	TFA [10]	3 Å, smashed [400]	93
16	2	TFA [5]	3 Å, smashed [400]	86
17	1	TFA [5]	4 Å, smashed [400]	68
18	1	NH ₄ PF ₆ [5]	4 Å, smashed [400]	71
19	1	TFA [5]	3 Å [500]	71
20	1	NH ₄ PF ₆ [5]	3 Å [500]	79

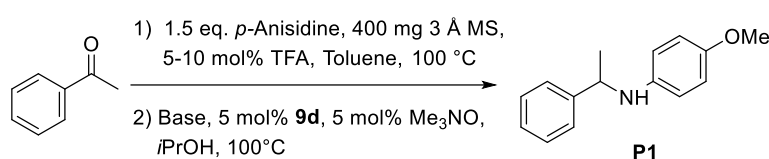
[a] Acetophenone/*p*-anisidine = 1:1.5, solvent: *d*₈-toluene, *T* = 100 °C, *C*_{0,substrate} = 0.25 M (0.5 mmol). The employed molecular sieves were activated under vacuum and kept in an oven at 110 °C.

[b] Determined by ¹H-NMR.

As in the case of aldehydes, we investigated ketone reductive amination by adding the solution of activated pre-catalyst **9d** to the newly formed imine. However, only poor to moderate yields were obtained under these

conditions (Table 2.8, entries 1-3), even when the reaction time was extended to 48 h. A possible explanation of this outcome is that the sensitive active catalyst **act-9d/10d** undergoes a progressive decomposition in the presence of the acid used to promote imine formation. To address this issue, a slight excess of base (with respect to the catalyst) was added after imine formation had taken place to quench the catalytic amount (10 mol%) of TFA. The base displayed the expected beneficial effect, and an excellent isolated yield (see Table 2.8, entry 4) was obtained after adding 15 mol% of *N,N*-diisopropylethylamine (DIPEA), whereas solid K_2CO_3 was less effective (Table 2.8, entry 5 vs. entry 4).

Table 2.8. Optimization of the CTH-based reductive amination of acetophenone promoted by pre-catalyst **9d**.^[a]

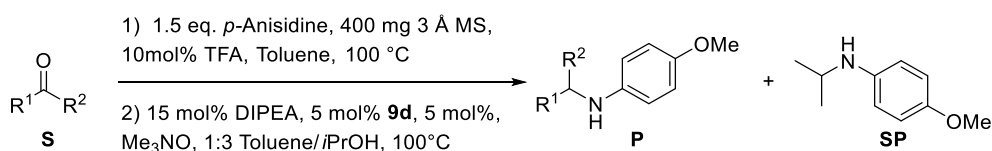


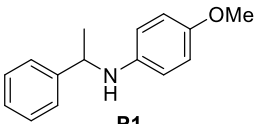
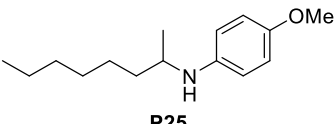
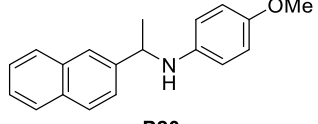
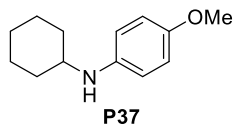
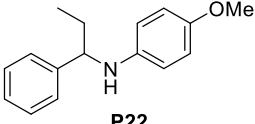
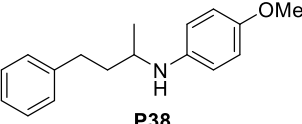
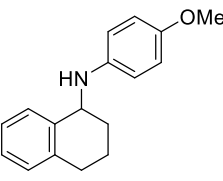
#	TFA (mol%)	Base	Time (h)	Conv. NMR (%)	Isolated Yield (%)
1	5		o/n	40	40
2	10		o/n	10	10
3	10		48	22 (60% imine left)	22 (60% imine left)
4	10	DIPEA (15 mol%)	o/n	>99	98
5	10	K_2CO_3 (15 mol%)	o/n	89	70
6	10	K_2CO_3 (aq) (15 mol%)	o/n	nd	Nd

[a] 1) Acetophenone/anisidine/TFA = 1:1.5:10; 3 Å M.S. 400 mg; 2) acetophenone/**9d**/ Me_3NO /Base = 100:5:5:15, $C_{0,substrate}$ = 0.25 M (0.5 mmol), 3:1 *iPrOH*:toluene, T = 100 °C, 22 h.

With the optimized catalytic conditions in hand, extension of substrate scope was carried out. Different aromatic (Table 2.9, entries 1-3) and aliphatic ketones (Table 2.9, entries 4-7) were screened with *p*-anisidine, and moderate to excellent yields (ranging from 31% to 98%) were obtained. Delightfully, also the amines deriving from hindered cyclic ketones were obtained in acceptable yields (Table 2.9, entries 4 and 6). The side product **SP** was formed in these transformations because the excess *p*-anisidine used to promote the imine formation reacted with the acetone deriving from the oxidation of *iPrOH*, and the resulting imine underwent **9d**-mediated CTH.

Table 2.9. Substrate scope evaluation in reductive amination of ketones promoted by pre-catalyst **9d**.^[a, b]



#	Product	Yield (%) ^[c]	#	Product	Yield (%) ^[c]
1	 P1	98	5	 P25	60
2	 P20	31	6	 P37	41
3	 P22	68	7	 P38	52
4	 P23	51			

[a] Reaction conditions: ketone/amine/**9d**/Me₃NO = 100:150:5:5. Imine formation: toluene, 100 °C, 3 Å MS (400 mg), TFA (10 mol%), 2 h. Catalyst activation: *i*PrOH, Me₃NO, r.t., 20 min. CTH: 3:1 *i*PrOH / toluene, C_{0,substrate}. in CTH = 0.25 M (0.5 mmol), DIPEA (15 mol%), *T* = 100 °C, 18 h.

[b] Toluene and DIPEA were freshly distilled over sodium/benzophenone and CaH₂, respectively.

[c] Isolated yields.

2.5 Conclusions

The highly active CIC **9d**, previously developed by our group,^[24] has been tested as pre-catalyst in CTH of imines, with a low catalyst loading (in the 1-2 mol% range). Compared to the literature precedents of CIC/HCIC-promoted imine CTH and CH, the scope of imines has been remarkably expanded, covering also ketimine substrates without need of co-catalysts. The kinetics of ketimine **S1** CTH (see Scheme Table 2.1) promoted by complex **9d** have been studied, showing a pseudo-first order dependence on substrate concentration. Finally, a CTH-based reductive amination protocol relying on pre-catalyst **9d** has been developed, which can be applied to both aldehyde and ketone substrates and allows to reduce imines that cannot be readily isolated.

2.6 Experimental Section

2.6.1. General remarks

All reactions were carried out in flame-dried glassware with magnetic stirring under inert atmosphere (nitrogen

or argon), unless otherwise stated. Solvents for reactions were distilled over the following drying agents and transferred under nitrogen: CH₂Cl₂ (CaH₂), MeOH (CaH₂), THF (Na), dioxane (Na), toluene (Na), Et₃N (CaH₂); 2-propanol, ethanol and acetone (over molecular sieves in bottles with crown cap) were purchased from Sigma Aldrich and stored under nitrogen. The reactions were monitored by analytical thin-layer chromatography (TLC) using silica gel 60 F254 pre-coated glass plates (0.25 mm thickness). Visualization was accomplished by irradiation with a UV lamp and/or staining with a potassium permanganate alkaline solution. Flash Column Chromatography was performed using silica gel (60 Å, particle size 40-64 μm) as stationary phase, following the procedure by Still and co-workers.^[31]

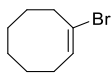
¹H-NMR spectra were recorded on a spectrometer operating at 400.13 MHz. Proton chemical shifts are reported in ppm (δ) with the solvent reference relative to tetramethylsilane (TMS) employed as the internal standard (CDCl₃, δ = 7.26 ppm; CD₂Cl₂ δ = 5.32 ppm; *d*₆-acetone, δ = 2.05 ppm). The following abbreviations are used to describe spin multiplicity: s = singlet, d = doublet, t = triplet, q = quartet, m = multiplet, br = broad signal, dd = doublet-doublet, ddd = doublet-doublet-doublet, td = triplet-doublet. ¹³C-NMR spectra were recorded on a 400 MHz spectrometer operating at 100.56 MHz, with complete proton decoupling. Carbon chemical shifts are reported in ppm (δ) relative to TMS with the respective solvent resonance as the internal standard (CDCl₃ δ = 77.16 ppm; CD₂Cl₂ δ = 54.00 ppm; *d*₆-acetone δ = 29.84 ppm, 206.26 ppm). The coupling constant values are given in Hz. Infrared spectra were recorded on a standard FT/IR spectrometer. High resolution mass spectra (HRMS) were performed on a Fourier Transform Ion Cyclotron Resonance (FT-ICR) Mass Spectrometer APEX II & Xmass software (Bruker Daltonics) – 4.7 T Magnet (MagneX) equipped with ESI source, available at CIGA (Centro Interdipartimentale Grandi Apparecchiature) c/o Università degli Studi di Milano.

Materials: commercially available reagents were used as received. The ketones used in the substrate screening were purchased from commercial suppliers (TCI Chemicals, ACROS, Sigma Aldrich) and distilled over PPh₃ before use. The other commercially available reagents were used as received.

2.6.2. Synthesis of Ligands and Complexes

Pre-catalyst **9d** was prepared by a procedure previously reported by our research group.^[24]

(E)-1-Bromocyclooct-1-ene (16):



A solution of bromine (0.25 mol, 1 eq.) in dichloromethane (12 mL) was added dropwise to a solution of cyclooctene (33.2 mL, 0.25 mol, 1 eq.) in dichloromethane (100 mL) at $-40\text{ }^{\circ}\text{C}$ until the yellow color persisted. The reaction mixture was quenched with 10% aq. $\text{Na}_2\text{S}_2\text{O}_3$ solution (50 mL) and extracted with dichloromethane ($2 \times 100\text{ mL}$). The combined organic layer was dried over MgSO_4 and concentrated under reduced pressure to give *trans*-1,2-dibromocyclooctane in quantitative yield, which was used in the following step without further purification.

^1H NMR (400 MHz, CDCl_3): δ 4.59-4.57 (m, 2H, CHBr), 2.46-2.37 (m, 2H), 2.15-2.05 (m, 2H), 1.88-1.81 (m, 2H), 1.70-1.56 (m, 4H), 1.54-1.46 (m, 2H). ^{13}C NMR (100 MHz, CDCl_3): 61.6, 33.3, 26.0, 25.5.

A solution of *Trans*-1,2-dibromocyclooctane (65.78 g, 244 mmol, 1 eq.) in THF (100 mL) was added to a suspension solution of *t*BuOK (41.07 g, 370 mmol, 1.52 eq.) in THF (40 mL) at $0\text{ }^{\circ}\text{C}$. After finishing the addition, the reaction mixture was quenched with a saturated aq. ammonium chloride solution (100 mL), and THF was evaporated off. The resulting crude was extracted with dichloromethane ($2 \times 100\text{ mL}$). The combined organic layer was dried over Na_2SO_4 and concentrated under reduced pressure. The residue was purified by distillation (b.p.: $73\text{-}80\text{ }^{\circ}\text{C} / 10\text{ mbar}$), and the product 1-bromocyclooctene was obtained as a colorless liquid. Yield: 36.8 g (80%).

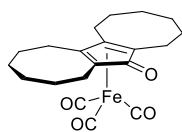
^1H NMR (400 MHz, CDCl_3): δ 6.03 (t, $J = 8.5\text{ Hz}$, 1H), 2.58-2.64 (m, 2H), 2.08-2.19 (m, 2H), 1.51-1.62 (m, 8H). ^{13}C NMR (100 MHz, CDCl_3): 131.7, 35.2, 29.9, 28.6, 27.5, 26.4, 25.5.

Cyclooctyne (17):^[24]



A lithium diisopropylamide (LDA) solution was prepared by adding dropwise *n*-butyllithium (1.58 M hexane solution, 26.7 mL, 43 mmol, 1 eq.) to a solution of dry diisopropylamine (4.77 g, 47 mmol, 1.1 eq.) in dry THF (20 mL) stirred at $-78\text{ }^{\circ}\text{C}$. The resulting mixture was allowed to warm up to $0\text{ }^{\circ}\text{C}$ and then cooled down to $-25\text{ }^{\circ}\text{C}$. 1-Bromocyclooctene **16** (8.1 g, 43 mmol, 1 eq.) was added to the LDA solution at $-25\text{ }^{\circ}\text{C}$. The temperature of the reaction mixture was allowed to rise to $15\text{ }^{\circ}\text{C}$ gradually over a period of 45 min and was kept at this level for another 90 min. It was then poured into a cold solution of 3 N HCl. The solution was extracted with hexane and the combined extracts were washed several times with water to remove the THF. The organic layer was dried over Na_2SO_4 and concentrated under reduced pressure. The residue was purified by distillation to give cyclooctyne (b.p. $50\text{-}55\text{ }^{\circ}\text{C} / 20\text{ torr}$). Yield: 3.9 g (86%).

^1H NMR (400 MHz, CD_2Cl_2): δ 2.13 (m, 4H), 1.85 (m, 4H), 1.61 (m, 4H). ^{13}C NMR (100 MHz, CD_2Cl_2): δ 94.90, 35.13, 30.32, 21.90. IR (Nujol, selected band): $\nu = 2216\text{ cm}^{-1}$ ($\text{C}\equiv\text{C}$ stretch).

[Bis(hexamethylene)cyclopentadienone] iron tricarbonyl (9d):^[24]

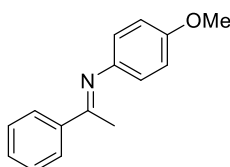
Fe(CO)₅ (14.6 mL, 111 mmol, 5.3 eq.) was added to a solution of cyclooctyne **17** (2.7 mL, 21 mmol, 1 eq.) in dry toluene (20 mL) under argon. The reaction mixture was heated to 90 °C overnight in a sealed Schlenk tube. The resulting mixture was cooled down to r.t. and concentrated under reduced pressure. The residue was purified by flash chromatography (7:3 hexane/AcOEt) to afford the product as yellow crystals. Yield: 1.55 g (38%). M.p. = 156 °C; ¹H NMR (400 MHz CDCl₃): δ 1.44-1.59 (m, 10H), 1.74-1.92 (m, 8H), 2.40-2.49 (m, 2H), 2.59-2.64 (m, 2H), 2.76-2.78 (m, 2H). ¹³C NMR (100 MHz CDCl₃): δ 23.43, 23.70, 25.77, 26.24, 28.81, 31.29, 85.54, 102.42, 171.42, 209.35; FT-IR: ν = 2924.1, 2856.6, 2050.3, 1978.9, 1950.0, 1620.2, 1585.5, 1456.3, 1354.0, 1278.8, 1203.6, 1118.7, 1097.5, 1031.9, 987.5, 817.8, 736.8, 648.1, 621.1 cm⁻¹; HRMS (ESI⁺): *m/z* 385.1098 [M+H]⁺; *m/z* 407.0919 [M + Na]⁺ (calcd. for C₂₁H₂₄O₄Fe: 385.1102; C₂₀H₂₄O₄FeNa: 407.0922).

2.6.3 Synthesis of pre-isolated imines**2.6.3.1 General Procedure**

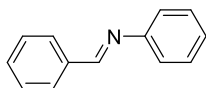
Aldehyde/ketone (4.5 mmol, 1.5 eq.) and amine (3 mmol, 1 eq.) were dissolved in anhydrous toluene (5 mL). The reaction mixture was added 3 Å molecular sieves (0.6 g) and heated to 110 °C, then stirred overnight and monitored by ¹H-NMR. The resulting mixture was cooled down to r.t. and filtrated. The filtrate was concentrated under reduced pressure to afford the crude imine. The imine was purified by reduced pressure distillation (Kugelrohr).

2.6.3.2 Characterization data

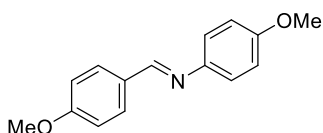
Imine (name, chemical formula)	¹ H NMR
--------------------------------	--------------------

***N*-(4-Methoxy-phenyl)-(1-phenyl-ethylidene)-amine (S1):**^[40]

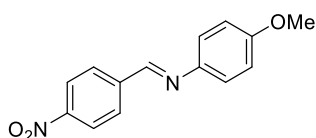
¹H NMR (400 MHz, CD₂Cl₂) δ 7.98-7.95 (m, 2H), 7.48-7.41 (m, 3H), 6.91 (d, *J* = 8.8, 2H), 6.73 (d, *J* = 8.8, 2H), 3.80, (s, 3H), 2.23 (s, 3H).

(E)-N-Benzylidenebenzenamine (S2):^[32]

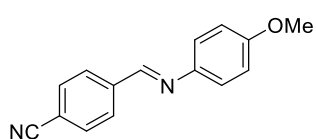
¹H NMR (300 MHz, CD₂Cl₂) δ 8.47 (s, 1H), 7.90-7.90 (m, 2H), 7.51-7.47 (m, 3H), 7.42-7.38 (m, 2H), 7.26-7.20 (m, 3H).

N-(4-Methoxybenzylidene)-4-methoxyaniline (S3):^[35]

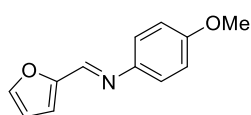
¹H NMR (400 MHz, *d*₆-acetone) δ 8.52 (s, 1H), 7.89 (d, *J* = 8.8 Hz, 2H), 7.24 (d, *J* = 9.0 Hz, 2H), 7.04 (d, *J* = 8.8 Hz, 2H), 6.96 (d, *J* = 9.0 Hz, 2H), 3.88 (s, 3H), 3.81 (s, 3H).

(E)-N-(4-Methoxyphenyl)-1-(4-nitrophenyl)methanimine (S4):^[33]

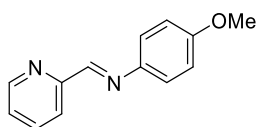
¹H NMR (400 MHz, CD₂Cl₂) δ 8.55 (s, 1H), 8.00 (d, *J* = 8.3 Hz, 2H), 7.76 (d, *J* = 8.3 Hz, 2H), 7.29 (d, *J* = 8.9 Hz, 2H), 6.96 (d, *J* = 8.9 Hz, 2H), 3.83 (s, 3H).

(E)-4-(((4-Methoxyphenyl)imino)methyl)benzonitrile (S5):^[34]

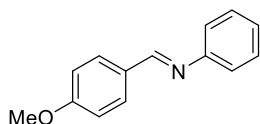
¹H NMR (400 MHz, CD₂Cl₂) δ 8.61 (s, 1H), 8.30 (d, *J* = 8.8 Hz, 2H), 8.07 (d, *J* = 8.8 Hz, 2H), 7.32 (d, *J* = 8.9 Hz, 2H), 6.97 (d, *J* = 8.9 Hz, 2H), 3.84 (s, 3H).

N-(Furan-2-ylmethylene)-4-methoxyaniline (S6):^[35]

¹H NMR (400 MHz, *d*₆-acetone) δ 8.43 (s, 1H), 7.76 (dd, *J* = 1.7, 0.8 Hz, 1H), 7.26 (d, *J* = 8.9 Hz, 2H), 7.03 (dd, *J* = 3.5, 0.8 Hz, 1H), 6.96 (d, *J* = 8.9 Hz, 2H), 6.64 (dd, *J* = 3.5, 1.8 Hz, 1H), 3.82 (s, 3H).

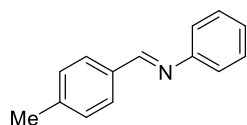
(E)-N-(4-Methoxyphenyl)-1-(pyridin-2-yl)methanimine (S7):^[35]

¹H NMR (400 MHz, *d*₆-acetone) δ 8.70-7.68 (m, 1H), 8.61 (d, *J* = 0.7 Hz, 1H), 8.20 (dt, *J* = 7.9, 1.1 Hz, 1H), 7.93-7.88 (m, 1H), 7.47-7.34 (m, 1H), 7.38 (d, *J* = 9.0 Hz, 2H), 7.01 (d, *J* = 9.0 Hz, 2H), 3.84 (s, 3H).

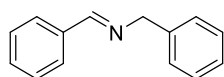
(p-Methoxybenzylidene)aniline (S8):^[36]

¹H-NMR (400 MHz, *d*₆-acetone) δ 8.50 (s, 1H), 7.92 (d, *J* = 8.8 Hz, 2H), 7.39 (dd, *J* = 8.6, 7.0 Hz, 2H), 7.22-7.20 (m, 3H), 7.07 (d, *J* = 8.8 Hz, 2H), 3.89

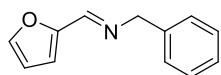
(s, 3H).

(E)-N-(4-Methylbenzylidene)benzenamine (S9):^[32]

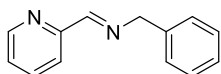
¹H NMR (400 MHz, *d*₆-acetone) δ 8.54 (s, 1H), 7.86 (d, *J* = 8.1 Hz, 2H), 7.42-7.38 (m, 2H), 7.33 (d, *J* = 7.9 Hz, 2H), 7.25-7.20 (m, 3H), 2.41 (s, 3H).

(E)-N-Benzyl-1-phenylmethanimine (S10):^[37]

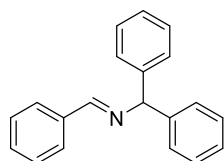
¹H NMR (400 MHz, *d*₆-acetone) δ 8.50 (s, 1H), 7.84-7.82 (m, 2H), 7.46-7.44 (m, 3H), 7.38-7.31 (m, 4H), 7.27-7.23 (m, 1H), 4.81 (d, *J* = 1.4 Hz, 2H).

N-Furfurylidenebenzylamine (S11):^[38]

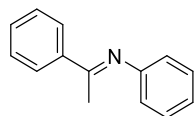
¹H NMR (400 MHz, *d*₆-acetone) δ 8.30 (t, *J* = 1.5 Hz, 1H), 7.68 (d, *J* = 1.7 Hz, 1H), 7.36-7.31 (m, 4H), 7.26-7.22 (m, 1H), 6.90 (dd, *J* = 3.4, 0.7 Hz, 1H), 6.57 (dd, *J* = 3.4, 1.8 Hz, 1H), 4.75 (d, *J* = 1.4 Hz, 2H).

(E)-N-Benzyl-1-(pyridin-2-yl)methanimine (S12):^[39]

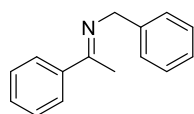
¹H NMR (400 MHz, *d*₆-acetone) δ 8.65-8.63 (m, 1H), 8.49 (q, *J* = 0.9 Hz, 1H), 8.07 (dt, *J* = 7.9, 1.1 Hz, 1H), 7.87-7.82 (m, 1H), 7.44-7.33 (m, 1H), 7.29-7.24 (m, 1H), 4.88 (d, *J* = 0.7 Hz, 2H).

(E)-N-Benzyl-1-phenylmethanimine (S13):^[37]

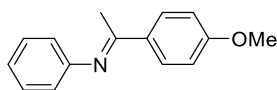
¹H NMR (400 MHz, CDCl₃) δ 8.46 (s, 1H), 7.88-7.86 (m, 2H), 7.50-7.19 (m, 13H), 5.64 (s, 1H).

(E)-(Phenyl)(1-phenylethylidene)amine (S14):^[40]

¹H NMR (400 MHz, CD₂Cl₂) δ 7.99-7.97 (m, 2H), 7.48-7.43 (m, 3H), 7.38-7.34 (m, 2H), 7.11-7.07 (m, 1H), 6.79-6.77 (m, 2H), 2.22 (s, 3H).

N-(1-Phenylethylidene)benzenemethanamine (S15):^[41]

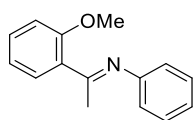
¹H NMR (400 MHz, *d*₆-acetone) δ 7.95 (dd, *J* = 6.7, 3.1 Hz, 2H), 7.48-7.46 (m, 2H), 7.41-7.39 (m, 3H), 7.36-7.32 (m, 2H), 7.25-7.23 (m, 1H), 4.73 (s, 2H), 2.37 (s, 3H).

(E)-1-(4-Methoxyphenyl)-N-phenylethan-1-imine (S16):^[42]

¹H NMR (400 MHz, *d*₆-acetone) δ 8.00 (d, *J* = 8.9 Hz, 2H), 7.34 (dd, *J* = 8.2, 7.4 Hz, 2H), 7.07-7.03 (m, 1H), 6.01 (d, *J* = 8.9 Hz, 2H), 6.77 (dd, *J* = 8.4, 1.2 Hz, 2H), 3.87 (s, 3H), 2.20 (s, 3H).

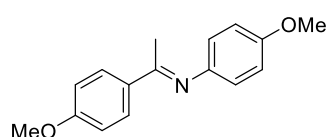
(E)-1-(2-Methoxyphenyl)-N-phenylethan-1-imine (S17):

Ratio: *E/Z* = 7:3

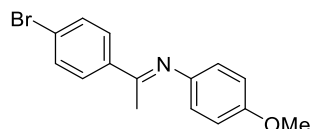


E: ¹H NMR (400 MHz, *d*₆-acetone) δ 7.57 (dd, *J* = 7.6, 1.8 Hz, 1H), 7.37-7.33 (m, 2H), 7.11-6.99 (m, 4H), 6.81-6.78 (m, 2H), 3.92 (s, 3H), 2.15 (s, 3H);

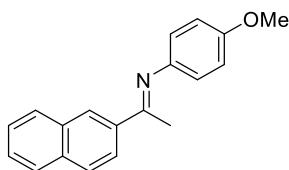
Z: ¹H NMR (400 MHz, *d*₆-acetone) δ 7.41 (ddd, *J* = 8.3, 7.4, 1.8 Hz, 2H), 7.17 (ddd, *J* = 8.4, 7.4, 1.8 Hz, 1H), 6.91-6.87 (m, 2H), 6.81-6.74 (m, 2H), 6.61-6.59 (m, 2H), 3.77 (s, 3H), 2.37 (s, 3H).

(E)-N,1-Bis(4-methoxyphenyl)ethan-1-imine (S18):^[43]

¹H NMR (400 MHz, CD₂Cl₂) δ 7.93 (d, *J* = 8.8 Hz, 2H), 6.95 (d, *J* = 8.8 Hz, 2H), 6.90 (d, *J* = 8.7 Hz, 2H), 6.71 (d, *J* = 8.7 Hz, 2H), 3.86 (s, 3H), 3.80 (s, 3H), 2.20 (s, 3H).

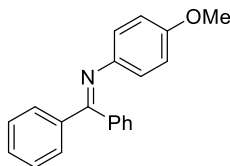
N-(1-(4-Bromophenyl)ethylidene)-4-methoxyanil (S19):^[44]

¹H NMR (400 MHz, CD₂Cl₂) δ 7.86 (d, *J* = 8.6 Hz, 2H), 7.58 (d, *J* = 8.6 Hz, 2H), 6.91 (d, *J* = 8.8 Hz, 2H), 6.73 (d, *J* = 8.8 Hz, 2H), 3.80 (s, 3H), 2.22 (s, 3H).

(4-Methoxy-phenyl)-[1-naphthalen-2-yl-ethylidene]-amine (S20):⁴³

¹H NMR (400 MHz, CD₂Cl₂) δ 8.35 (d, *J* = 1.7 Hz, 1H), 8.24 (dd, *J* = 8.7, 1.8 Hz, 1H), 7.97-7.95 (m, 1H), 7.89 (dd, *J* = 7.66, 3.3 Hz, 2H), 7.58-7.52 (m, 2H), 6.94 (d, *J* = 8.8 Hz, 2H), 6.79 (d, *J* = 8.8 Hz, 2H), 3.82 (s, 3H) 2.37 (s, 3H).

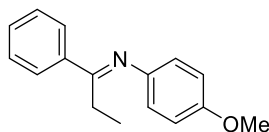
N-(4-Methoxyphenyl)-1,1-diphenylmethanimine (S21):^[45]



$^1\text{H NMR}$ (400 MHz, d_6 -acetone) δ 7.73-7.70 (m, 2 H), 7.51-7.41 (m, 3 H), 7.35-7.33 (m, 3 H), 7.17-7.15 (m, 2 H), 6.71 (d, $J = 9.1$ Hz, 2H), 6.65 (d, $J = 9.1$ Hz, 2H), 3.69 (s, 3 H).

[1-Phenylpropylidene]-(4-methoxyphenyl)-amine (S22):^[43]

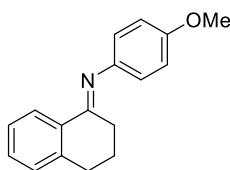
$E/Z = 88:12$



E : $^1\text{H NMR}$ (400 MHz, d_6 -acetone) δ 7.99-7.97 (m, 2H), 7.48-7.45 (m, 3H), 6.94 (d, $J = 8.8$ Hz, 2H), 6.72 (d, $J = 9.1$ Hz, 2H), 3.79 (s, 3H), 2.72 (q, $J = 7.6$ Hz, 2H), 1.06 (t, $J = 7.7$ Hz, 3H);

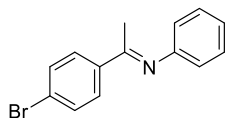
Z : $^1\text{H NMR}$ (400 MHz, d_6 -acetone) δ 7.17-7.11 (m, 3H), 7.03-7.00 (m, 2H), 6.66 (d, $J = 9.1$ Hz, 2H), 6.52 (d, $J = 9.1$ Hz, 2H), 3.67 (s, 3H), 2.75 (q, $J = 7.4$ Hz, 2H), 1.17 (t, $J = 7.4$ Hz, 3H).

[3,4-Dihydro-2H-naphthalenylidene]-(4-methoxyphenyl)amine (S23):^[46]



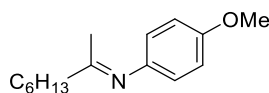
$^1\text{H NMR}$ (400 MHz, CD_2Cl_2) δ 8.27 (dd, $J = 8.0, 1.5$ Hz, 1 H), 7.36-7.33 (m, 1 H), 7.29-7.25 (m, 1 H), 7.22-7.20 (m, 1 H), 6.90 (d, $J = 8.9$ Hz, 2 H), 6.73 (d, $J = 8.9$ Hz, 2 H), 3.80 (s, 3 H), 2.90 (t, $J = 6.1$ Hz, 2 H), 2.56-2.53 (m, 2 H), 1.91-1.88 (m, 2 H).

(E)-1-(4-Bromophenyl)-N-phenylethan-1-imine (S24):^[44]



$^1\text{H NMR}$ (400 MHz, d_6 -acetone) δ 7.98 (d, $J = 8.7$ Hz, 2H), 7.66 (d, $J = 8.7$ Hz, 2H), 7.36 (dd, $J = 8.3, 7.4$ Hz, 2H), 7.11-7.07 (m, 1H), 6.80 (dd, $J = 8.3, 1.3$ Hz, 2H), 2.24 (s, 3H).

(E)-N-(4-Methoxyphenyl)octan-2-imine (S25):^[47]

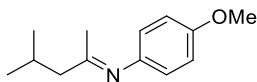


$^1\text{H NMR}$ (400 MHz, d_6 -acetone) δ 6.86 (d, $J = 8.9$ Hz, 2H), 6.59 (d, $J = 8.9$ Hz, 2H), 3.76 (s, 3H), 2.39-2.35 (m, 2H), 1.78 (s, 3H), 1.68-1.64 (m, 2H), 1.40-1.31 (m, 6H), 0.92-0.88 (m, 3H).

(E)-N-(4-Methoxyphenyl)-4-methylpentan-2-imine (S26):

Ratio: *E/Z* = 8:2

E: ¹H NMR (400 MHz, *d*₆-acetone) δ 6.86 (d, *J* = 8.8 Hz, 2H), 6.60 (d, *J* = 8.8 Hz, 2H), 3.76 (s, 3H), 2.26-2.24 (m, 2H), 2.19-2.11 (m, 1H), 1.77 (s, 3H), 0.98 (d, *J* = 6.5 Hz, 6H);



Z: ¹H NMR (400 MHz, *d*₆-acetone) δ 6.86 (d, *J* = 8.9 Hz, 2H), 6.54 (d, *J* = 8.9 Hz, 2H), 3.76 (s, 3H), 2.26-2.24 (m, 2H), 2.19-2.11 (m, 1H), 2.79 (s, 3H), 0.80 (d, *J* = 6.5 Hz, 6H).

2.6.4 Determination of the transfer hydrogenation Kinetics of imine S1

Abbreviations used: $R_{\text{sub},t}$ = fraction of unreacted substrate **S1** ($R_{\text{sub},0} = 1$); C_{cat} = catalyst concentration; $C_{0,\text{S1}}$ = initial substrate concentration.

Experimental parameters: $T = 373.15$ K; $C_{0,\text{S1}} = 0.25$ M; $C_{\text{cat}} = 12.5$ mM; solvent: *i*PrOH.

General procedure. Pre-catalyst **9d** (9.6 mg, 0.025 mmol, 0.05 eq.) and Me₃NO (3.8 mg, 0.05 mmol, 0.1 eq.) were weighted in a glass vessel and then, after purging with argon for 2 min, *i*PrOH (2 mL) was added followed by imine **S1** (112.6 mg, 0.5 mmol, 1 eq.). The vessel was sealed and put in an oil bath heated at 100 °C. Aliquots of the reaction mixture for GC analysis were taken every 15 min for the first 3 h of reaction and then every 30 min.

Note: time = 0 was marked when the reaction vessel was put in the oil bath. Pseudo-first order rate constants k_{app} and corresponding half-lives $t_{1/2}$ were determined from the slope of a linear least squares fit to the graph of $\ln(R_{\text{sub},t}) = -kt$. Second order constants k were calculated dividing k_{app} by C_{cat} (assumed to be constant).

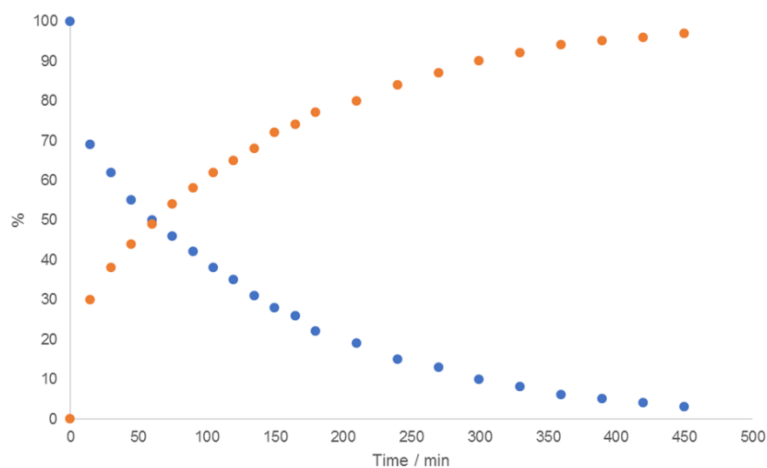


Figure 2.4. Kinetics of the CTH of **S1** promoted by complex **9d**: • Conversion to of **P1** (GC); • Percent of unreacted **S1**.

Conditions: **S1/9d**/Me₃NO = 100:5:10; solvent: *i*PrOH; C_{0,S1} = 0.25 M (0.5 mmol); T = 100 °C; C_{cat.} = 12.5 mM.

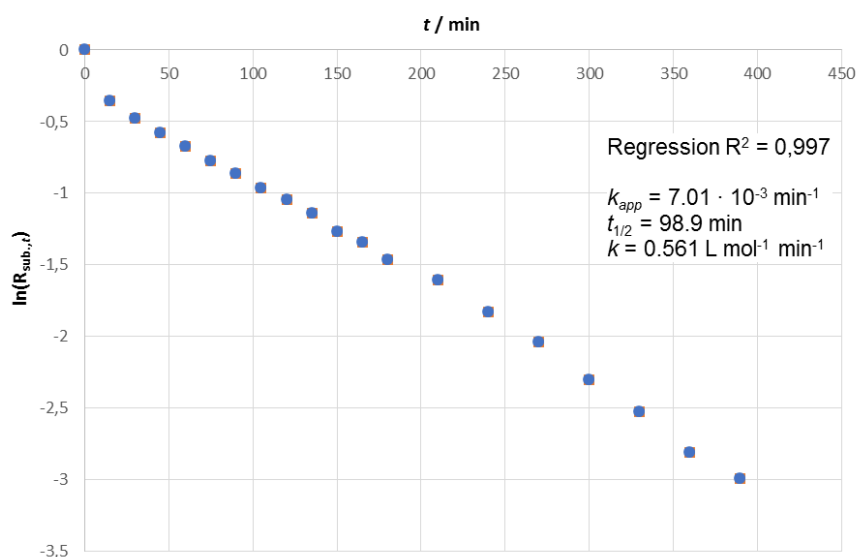


Figure 2.5. Least squares fit of $\ln(R_{\text{sub},t})$ vs t and calculated kinetic parameters.

2.6.5 Catalytic Tests – Transfer Hydrogenation of Imines – General Procedure

2.6.5.1 General Procedure for the CTH of pre-formed aldimines

Pre-catalyst **9d** (1.9 mg, 0.005 mmol, 0.01 eq.) and Me₃NO (0.8 mg, 0.010 mmol, 0.02 eq.) were dissolved in dry *i*PrOH (0.05 mL) under argon and the resulting solution, which gradually turned from yellow to dark red, was stirred for 20 minutes at r.t. The imine substrate (0.5 mmol, 1 eq.) was added, followed by dry *i*PrOH (1.95 mL). The reaction vessel was sealed and stirred in a pre-heated oil bath at 100 °C for 18 h. The volatiles were removed and the crude was purified by flash column chromatography (hexane/AcOEt).

2.6.5.2 General Procedure for the CTH of pre-formed ketimines

Pre-catalyst **9d** (3.8 mg, 0.010 mmol, 0.02 eq.) and Me₃NO (1.6 mg, 0.020 mmol, 0.04 eq.) were dissolved in dry *i*PrOH (0.1 mL) and the resulting solution, which gradually turned from yellow to dark red, was stirred for 20 minutes at r.t. The imine substrate (0.5 mmol, 1 eq.) was added, followed by dry *i*PrOH (1.9 mL). The reaction vessel was sealed and stirred in a pre-heated oil bath at 100 °C for 18 h. The volatiles were removed and the crude was purified by flash column chromatography (hexane/AcOEt).

2.6.5.3 General Procedure for the reductive amination of aldehydes

The aldehyde (0.5 mmol, 1 eq.) was added to a solution of amine (0.75 mmol, 1.5 eq.) in dry toluene (0.5 mL). The reaction mixture was added 3 Å MS (400 mg) and stirred at 100 °C for 1 h. Meanwhile, in another Schlenk tube, pre-catalyst **9d** (9.6 mg, 0.025 mmol, 0.05 eq.) and Me₃NO (1.9 mg, 0.025 mmol, 0.05 eq.) were dissolved in dry *i*PrOH (0.25 mL) and stirred at r.t. for 20 min. The activated catalyst solution was added into the vessel containing the imine, followed by dry *i*PrOH (1.2 mL). The reaction vessel was sealed and stirred in a pre-heated oil bath at 100 °C for 18 h. The volatiles were removed and the crude was purified by flash column chromatography (hexane/AcOEt).

2.6.5.4 General Procedure for the reductive amination of ketones

The ketone (0.5 mmol, 1 eq.) was added to a solution of amine (0.75 mmol, 1.5 eq.) in in dry toluene (final total volume: 0.5 mL). The resulting mixture were added 3 Å MS (400 mg) and TFA (4 µL, 0.05 mmol, 0.1 eq., dispensed as a stock solution in toluene) and stirred at 100 °C for 2 h. Meanwhile, in another vessel, pre-catalyst **9d** (9.6 mg, 0.025 mmol, 0.05 eq.) and Me₃NO (1.9 mg, 0.025 mmol, 0.05 eq.) were dissolved in dry *i*PrOH (0.25 mL) and stirred at r.t. for 20 min. After adding the freshly distilled DIPEA (13 µL, 0.075 mmol, 0.15 eq.), the activated catalyst solution was dispensed into the vessel containing the imine, followed by dry *i*PrOH (1.2 mL). The reaction vessel was sealed and stirred at 100 °C for 18 h. The volatiles were removed and the crude was purified by flash column chromatography (hexane/AcOEt).

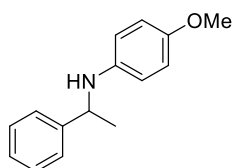
2.6.5.5 Characterization data of amines products

NMR conversions were calculated from the signal integrals (all the substrates and reduction products are known compounds, and our spectra are superimposable to those reported in the literature).

Amines (name, chemical formula)

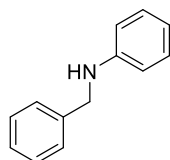
^1H NMR

4-Methoxy-*N*-(1-phenylethyl)aniline (P1): ^[48]



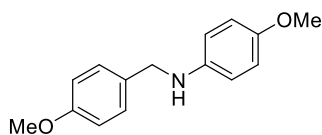
^1H NMR (400 MHz, CD_2Cl_2) δ 7.37-7.29 (m, 4H), 7.23-7.19 (m, 1H), 6.65 (d, $J = 8.9$ Hz, 2H), 6.45 (d, $J = 8.9$ Hz, 2H), 4.42 (q, $J = 6.7$ Hz, 1H), 3.88 (bs, 1H), 3.66 (s, 3H), 1.47 (d, $J = 6.7$ Hz, 3H).

***N*-Benzylaniline (P2):** ^[49]



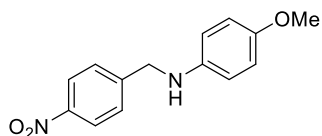
^1H NMR (400 MHz, CD_2Cl_2) δ 7.39-7.32 (m, 4H), 7.28-7.26 (m, 1H), 7.16-7.11 (m, 2H), 6.69-6.61 (m, 3H), 4.33 (s, 2H), 4.17 (s, 1H).

4-Methoxy-*N*-(4-methoxybenzyl)aniline (P3): ^[35]



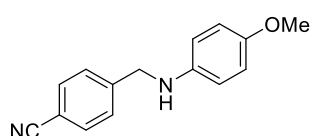
^1H NMR (400 MHz, d_6 -acetone) δ 7.30 (d, $J = 8.8$ Hz, 2H), 6.87 (d, $J = 8.8$ Hz, 2H), 6.70 (d, $J = 9.0$ Hz, 2H), 6.60 (d, $J = 9.0$ Hz, 2H), 4.93 (s, 1H), 4.21 (d, $J = 4.6$ Hz, 2H), 3.77 (s, 3H), 3.66 (s, 3H).

4-Methoxy-*N*-(4-nitrobenzyl)aniline (P4): ^[50]

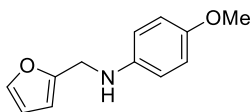


^1H NMR (400 MHz, CDCl_3) δ 8.20 (d, $J = 8.6$ Hz, 2H), 7.56 (d, $J = 8.6$ Hz, 2H), 6.79 (d, $J = 8.9$ Hz, 2H), 6.57 (d, $J = 8.9$ Hz, 2H), 4.45 (s, 2H), 3.76 (s, 3H).

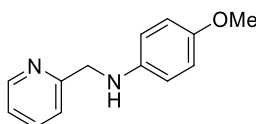
4-(((4-Methoxyphenyl)amino)methyl)benzonitrile (P5): ^[51]



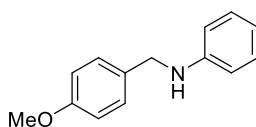
^1H NMR (400 MHz, CD_2Cl_2) δ 7.63 (d, $J = 8.3$ Hz, 2H), 7.45 (d, $J = 8.3$ Hz, 2H), 6.73 (d, $J = 8.9$ Hz, 2H), 6.54 (d, $J = 8.9$ Hz, 2H), 4.38 (s, 2H), 3.70 (s, 3H).

***N*-(Furan-2-ylmethyl)-4-methoxyaniline (P6):**^[35]

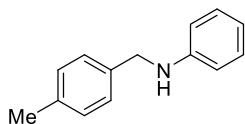
¹H NMR (400 MHz, *d*₆-acetone) δ 7.44 (dd, *J* = 1.9, 0.9 Hz, 1H), 6.73 (d, *J* = 9.0 Hz, 2H), 6.66 (d, *J* = 9.0 Hz, 2H), 6.33 (dd, *J* = 3.2, 1.9 Hz, 1H), 6.24 (dd, *J* = 3.2, 0.9 Hz, 1H), 4.88 (s, 1H), 4.26 (d, *J* = 5.7 Hz, 2H), 3.68 (s, 3H).

4-Methoxy-*N*-(pyridin-2-ylmethyl)aniline (P7):^[35]

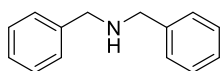
¹H NMR (400 MHz, *d*₆-acetone) δ 8.53 (ddd, *J* = 4.3, 1.9, 1.1 Hz, 1H), 7.70 (td, *J* = 7.9, 1.9 Hz, 1H), 7.41 (dt, *J* = 7.9, 1.1 Hz, 1H), 7.23-7.19 (m, 1H), 6.72 (d, *J* = 9.0 Hz, 2H), 6.62 (d, *J* = 9.0 Hz, 2H), 5.28 (s, 1H), 4.38 (s, 2H), 3.67 (s, 3H).

***N*-(4-Methoxybenzyl)aniline (P8):**^[49]

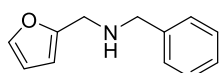
¹H NMR (400 MHz, *d*₆-acetone) δ 7.31 (d, *J* = 8.3 Hz, 2H), 7.08-7.04 (m, 2H), 6.87 (d, *J* = 8.6 Hz, 2H), 6.64 (d, *J* = 8.3 Hz, 2H), 6.56 (t, *J* = 7.3 Hz, 1H), 5.29 (s, 1H), 4.26 (d, *J* = 5.6 Hz, 2H), 3.77 (s, 3H).

***N*-(4-Methylbenzyl)aniline (P9):**^[52]

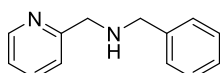
¹H NMR (400 MHz, *d*₆-acetone) δ 7.27 (d, *J* = 7.8 Hz, 2H), 7.12 (d, *J* = 7.8 Hz, 2H), 7.06 (dd, *J* = 8.6, 7.2 Hz, 2H), 6.64 (dd, *J* = 8.6, 1.1 Hz, 2H), 6.58-6.54 (m, 1H), 5.34 (s, 1H), 4.29 (d, *J* = 5.7 Hz, 2H), 2.29 (s, 3H).

Dibenzylamine (P10):^[53]

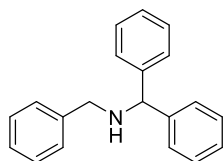
¹H NMR (400 MHz, CDCl₃) δ 7.37-7.27 (m, 10H), 3.85 (s, 4H).

***N*-Benzyl-1-(furan-2-yl)methanamine (P11):**^[54]

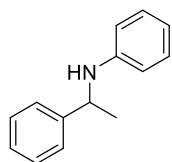
¹H NMR (400 MHz, *d*₆-acetone) δ 7.45 (dd, *J* = 1.9, 0.9 Hz, 1H), 7.28-7.20 (m, 5H), 6.35 (dd, *J* = 3.2, 1.9 Hz, 1H), 6.23 (dd, *J* = 3.2, 0.9 Hz, 1H), 3.77 (s, 2H), 3.73 (s, 2H).

***N*-Benzyl-1-(pyridin-2-yl)methanamine (P12):**^[55]

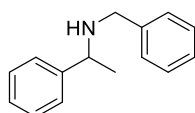
¹H NMR (400 MHz, *d*₆-acetone) δ 8.54-8.52 (m, 1H), 7.74 (td, *J* = 7.6, 1.8 Hz, 1H), 7.49-7.19 (m, 7H), 3.88 (s, 2H), 3.83 (s, 2H).

***N*-Benzyl-1,1-diphenylmethanamine (P13):**^[56]

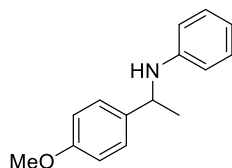
¹H NMR (400 MHz, CDCl₃) δ 7.45-7.42 (m, 4H), 7.34-7.20 (m, 11H), 4.87 (s, 1H), 3.76 (s, 2H).

***N*-(1-Phenylethyl)aniline (P14):**^[49]

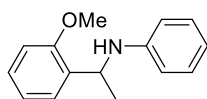
¹H NMR (400 MHz, CD₂Cl₂) δ 7.40-7.32 (m, 4H), 7.26-7.22 (m, 1H), 7.09-7.05 (m, 2H), 6.64-6.60 (m, 1H), 6.53-6.51 (m, 2H), 4.52-4.50 (m, 1H), 4.15 (s, 1H), 1.51 (d, *J* = 6.8 Hz, 3H).

***N*-Benzyl-1-phenylethan-1-amine (P15):**^[57]

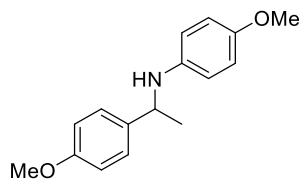
¹H NMR (400 MHz, CDCl₃) δ 7.38-7.22 (m, 10H), 3.82 (q, *J* = 6.6 Hz, 1H), 2.17 (s, 2H), 1.38 (d, *J* = 6.6 Hz, 3H).

***N*-(1-(4-Methoxyphenyl)ethyl)aniline (P16):**^[58]

¹H NMR (400 MHz, *d*₆-acetone) δ 7.32 (d, *J* = 8.5 Hz, 2H), 7.00-6.96 (m, 2H), 6.85 (d, *J* = 8.5 Hz, 2H), 6.54 (d, *J* = 8.0 Hz, 2H), 6.49 (t, *J* = 7.4 Hz, 1H), 5.27 (s, 1H), 4.48 (p, *J* = 6.6 Hz, 1H), 3.75 (s, 3H), 1.45 (d, *J* = 6.8 Hz, 3H).

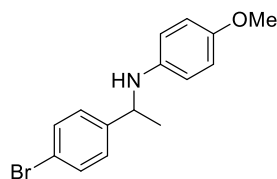
***N*-(1-(2-Methoxyphenyl)ethyl)aniline (P17):**

¹H NMR (400 MHz, *d*₆-acetone) δ 7.35 (dd, *J* = 7.7, 1.8 Hz, 1H), 7.16 (td, *J* = 7.8, 1.8 Hz, 1H), 6.97 (dd, *J* = 8.6, 7.3 Hz, 3H), 6.83 (td, *J* = 7.5, 1.1 Hz, 1H), 6.51-6.46 (m, 3H), 5.30 (s, 1H), 4.87 (p, *J* = 6.7 Hz, 1H), 3.92 (s, 3H), 1.42 (d, *J* = 6.7 Hz, 3H)

4-Methoxy-*N*-(1-(4-methoxyphenyl)ethyl)aniline (P18):^[59]

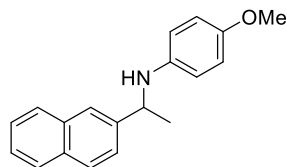
¹H NMR (400 MHz, CD₂Cl₂) δ 7.28 (d, *J* = 8.1 Hz, 2H), 6.87 (d, *J* = 8.1 Hz, 2H), 6.68 (d, *J* = 8.3 Hz, 2H), 6.48 (d, *J* = 8.3 Hz, 2H), 4.39 (q, *J* = 6.7 Hz, 1H), 3.78 (s, 3H), 3.68 (s, 3H), 1.46 (d, *J* = 6.7 Hz, 3H).

***N*-(1-(4-Bromophenyl)ethyl)-4-methoxyaniline (P19):**^[59]



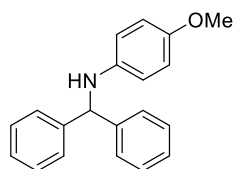
$^1\text{H NMR}$ (400 MHz, CD_2Cl_2) δ 7.45 (d, $J = 8.3$ Hz, 2H), 7.27 (d, $J = 8.3$ Hz, 2H), 6.67 (d, $J = 9.0$ Hz, 2H), 6.44 (d, $J = 9.0$ Hz, 2H), 4.39 (q, $J = 6.7$ Hz, 1H), 3.87 (s, 1H), 3.67 (s, 3H), 1.46 (d, $J = 6.7$ Hz, 3H).

4-Methoxy-*N*-(1-(naphthalen-2-yl)ethyl)aniline (P20):^[60]



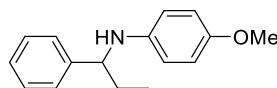
$^1\text{H NMR}$ (400 MHz, CD_2Cl_2) δ 7.85-7.81 (m, 4H), 7.52 (dd, $J = 8.5, 1.7$ Hz, 1H), 7.49-7.42 (m, 2H), 6.66 (d, $J = 8.9$ Hz, 2H), 6.52 (d, $J = 8.9$ Hz, 2H), 4.59 (q, $J = 6.7$ Hz, 1H), 3.99 (s, 1H), 3.65 (s, 3H), 1.57 (d, $J = 6.7$ Hz, 3H).

***N*-Benzhydryl-4-methoxyaniline (P21):**^[61]



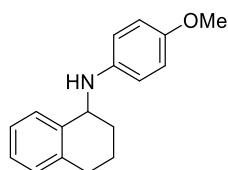
$^1\text{H NMR}$ (400 MHz, CD_2Cl_2) δ 7.40-7.31 (m, 8H), 7.27-7.23 (m, 2H), 6.68 (d, $J = 8.9$ Hz, 2H), 6.51 (d, $J = 8.9$ Hz, 2H), 5.44 (s, 1H), 4.15 (s, 1H), 3.67 (s, 3H).

4-Methoxy-*N*-(1-phenylpropyl)aniline (P22):^[62]



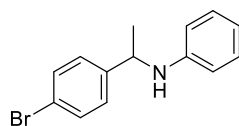
$^1\text{H NMR}$ (400 MHz, CDCl_3) δ 7.35-7.28 (m, 4H), 7.24-7.20 (m, 1H), 6.68 (d, $J = 8.9$ Hz, 2H), 6.47 (d, $J = 8.9$ Hz, 2H), 4.15 (t, $J = 6.7$ Hz, 1H), 3.69 (s, 3H), 1.86-1.76 (m, 2H), 0.94 (t, $J = 7.4$ Hz, 3H).

***N*-(4-Methoxyphenyl)-1,2,3,4-tetrahydronaphthalen-1-amine (P23):**^[63]



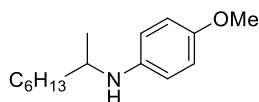
$^1\text{H NMR}$ (400 MHz, CD_2Cl_2) δ 7.44-7.41 (m, 1H), 7.22-7.14 (m, 3H), 6.82 (d, $J = 8.9$ Hz, 2H), 6.68 (d, $J = 8.9$ Hz, 2H), 4.54 (t, $J = 5.1$ Hz, 1H), 3.74 (s, 3H), 3.65 (s, 1H), 2.84-2.72 (m, 2H), 2.01-1.75 (m, 4H).

***N*-(1-(4-Bromophenyl)ethyl)aniline (P24):**^[64]



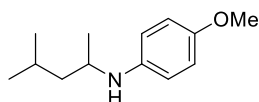
$^1\text{H NMR}$ (400 MHz, d_6 -acetone) δ 7.48 (d, $J = 8.5$ Hz, 2H), 7.40 (d, $J = 8.5$ Hz, 2H), 7.01 (7.48 (dd, $J = 8.7, 7.2$ Hz, 2H),), 6.56-6.51 (m, 3H), 5.42 (s, 1H), 4.58-4.51 (m, 1H), 1.49 (s, $J = 6.8$ Hz, 3H).

4-Methoxy-*N*-(octan-2-yl)aniline (P25):^[65]



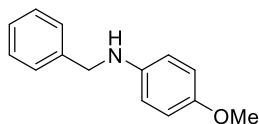
$^1\text{H NMR}$ (400 MHz, d_6 -acetone) δ 6.71 (d, $J = 9.0$ Hz, 2H), 6.56 (d, $J = 9.0$ Hz, 2H), 4.12 (s, 1H), 3.67 (s, 3H), 3.38 (q, $J = 6.0$ Hz, 1H), 1.57-1.28 (m, 10H), 1.12 (d, $J = 6.3$ Hz, 3H), 0.89-0.86 (m, 3H).

***N*-(4-Methylpentan-2-yl)aniline (P26):**^[66]



$^1\text{H NMR}$ (400 MHz, d_6 -acetone) δ 6.71 (d, $J = 9.0$ Hz, 2H), 6.57 (d, $J = 9.0$ Hz, 2H), 3.67 (s, 3H), 3.51-3.43 (m, 1H), 1.79 (dt, $J = 13.5, 6.7$ Hz, 1H), 1.47 (dt, $J = 13.5, 7.1$ Hz, 1H), 1.25-1.18 (m, 2H), 1.10 (d, $J = 6.2$ Hz, 3H), 0.91 (dd, $J = 12.1, 6.6$ Hz, 7H).

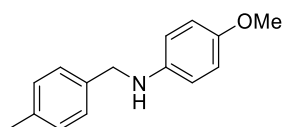
***N*-Benzyl-4-methoxyaniline (P27):**^[67]



$^1\text{H NMR}$ (400 MHz, CDCl_3) δ 7.53-7.20 (m, 6H), 6.90-6.77 (m, 2H), 6.74-6.63 (m, 2H), 4.32 (s, 2H), 3.77 (s, 3H).

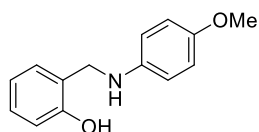
MC390

4-Methoxy-*N*-(4-methylbenzyl)aniline (P28):^[68]



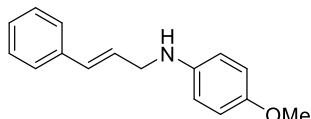
$^1\text{H NMR}$ (400 MHz, CDCl_3) δ 7.29 (d, $J = 7.7$ Hz, 2H), 7.18 (d, $J = 7.9$ Hz, 2H), 6.81 (d, $J = 8.9$ Hz, 2H), 6.67 (d, $J = 8.9$ Hz, 2H), 4.27 (s, 2H), 3.77 (s, 3H), 2.37 (s, 3H).

2-(((4-Methoxyphenyl)amino)methyl)phenol (P29):^[69]



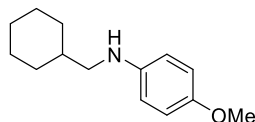
$^1\text{H NMR}$ (400 MHz, CDCl_3) δ 7.21 (td, $J = 7.8, 1.6$ Hz, 1H), 7.09 (d, $J = 7.3$ Hz, 1H), 6.93 (d, $J = 8.1$ Hz, 1H), 6.86-6.78 (m, 5H), 4.37 (s, 2H), 3.76 (s, 3H).

***N*-Cinnamyl-4-methoxyaniline (P30):**^[70]

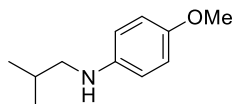


$^1\text{H NMR}$ (400 MHz, CDCl_3) δ 7.38-7.36 (m, 2H), 7.33-7.29 (m, 2H), 7.25-7.21 (m, 1H), 6.80 (d, $J = 9.0$ Hz, 2H), 6.38 (d, $J = 9.0$ Hz, 2H), 6.62 (dt, $J = 15.9, 1.6$ Hz, 1H), 6.37 (dt, $J = 15.9, 5.9$ Hz, 1H), 3.90 (dd, $J = 5.9, 1.6$ Hz, 2H), 3.76 (s, 3H).

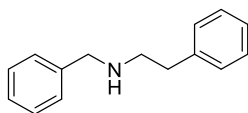
***N*-(Cyclohexylmethyl)-4-methoxyaniline (P31):**^[67]



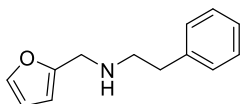
$^1\text{H NMR}$ (400 MHz, CDCl_3) δ 6.78 (d, $J = 8.9$ Hz, 2H), 6.68-6.65 (m, 2H), 3.75 (s, 3H), 2.92 (d, $J = 6.6$ Hz, 2H), 1.84-1.80 (m, 2H), 1.75-1.68 (m, 3H), 1.27-1.15 (m, 4H), 0.98 (qd, $J = 12.0, 3.4$ Hz, 2H).

***N*-Isobutyl-4-methoxyaniline (P32):**^[71]

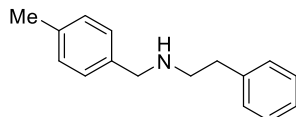
$^1\text{H NMR}$ (400 MHz, CDCl_3) δ 6.81 (d, $J = 8.9$ Hz, 2H), 6.70 (d, $J = 8.9$ Hz, 2H), 3.77 (s, 3H), 2.93 (d, $J = 6.8$ Hz, 2H), 1.91 (dq, $J = 13.5, 6.7$ Hz, 1H), 1.01 (d, $J = 6.7$ Hz, 6H).

***N*-Benzyl-2-phenylethan-1-amine (P34):**^[72]

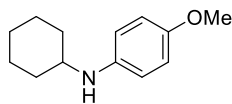
$^1\text{H NMR}$ (400 MHz, CDCl_3) δ 7.33-7.18 (m, 10H), 3.81 (s, 2H), 2.93-2.90 (m, 2H), 2.86-2.82 (m, 2H).

***N*-(Furan-2-ylmethyl)-2-phenylethan-1-amine (P35):**^[73]

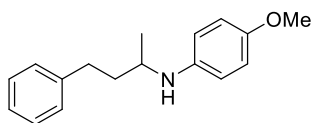
$^1\text{H NMR}$ (400 MHz, CDCl_3) δ 7.33 (dd, $J = 1.9, 0.8$ Hz, 1H), 7.31-7.27 (m, 2H), 7.22-7.18 (m, 3H), 6.30 (dd, $J = 3.1, 1.9$ Hz, 1H), 6.16 (d, $J = 3.1$ Hz, 1H), 3.81 (s, 2H), 2.93-2.89 (m, 2H), 2.85-2.81 (m, 2H).

***N*-(4-Methylbenzyl)-2-phenylethan-1-amine (P36):**^[74]

$^1\text{H NMR}$ (400 MHz, CDCl_3) δ 7.30-7.11 (m, 9H), 3.77 (s, 2H), 2.93-2.89 (m, 2H), 2.85-2.83 (m, 2H), 2.32 (s, 3H), 1.80 (s, 1H).

***N*-Cyclohexyl-4-methoxyaniline (P37):**^[68]

$^1\text{H NMR}$ (400 MHz, CDCl_3) δ 6.77 (d, $J = 8.9$ Hz, 2H), 6.58 (d, $J = 8.9$ Hz, 2H), 3.74 (s, 3H), 3.20-3.13 (m, 1H), 2.07-2.03 (m, 2H), 1.79-1.73 (m, 2H), 1.68-1.62 (m, 1H), 1.36-1.08 (m, 5H).

4-Methoxy-*N*-(4-phenylbutan-2-yl)aniline (P38):^[75]

$^1\text{H NMR}$ (400 MHz, CDCl_3) δ 7.29-7.26 (m, 2H), 7.20-7.16 (m, 3H), 6.76 (d, $J = 8.9$ Hz, 2H), 6.56 (d, $J = 7.8$ Hz, 2H), 3.75 (s, 3H), 3.40 (q, $J = 6.4$ Hz, 1H), 2.74-2.70 (m, 2H), 1.91-1.87 (m, 1H), 1.78-1.72 (m, 1H), 1.21 (d, $J = 6.2$ Hz, 3H).

References

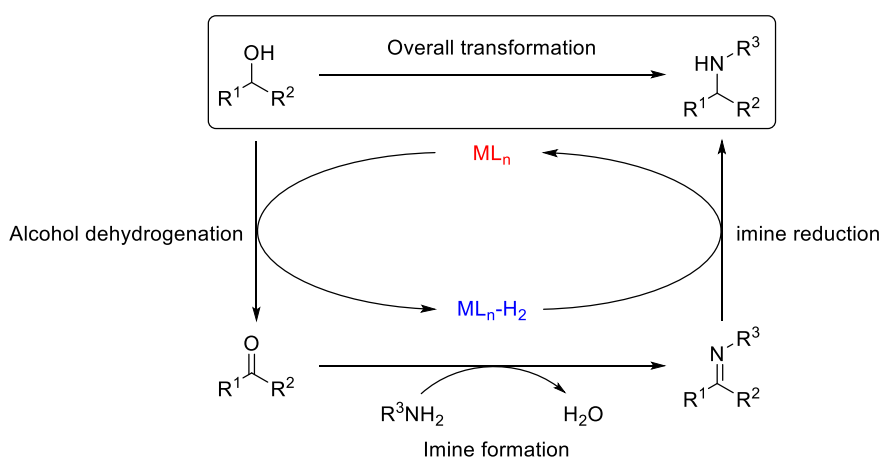
- [1] a) S. A. Lawrence, *Amines: Synthesis, Properties and Applications*, Cambridge University Press, Cambridge, **2006**; b) A. Ricci, *Amino Group Chemistry: From Synthesis to the Life Sciences*, Wiley-VCH, Weinheim, **2008**.
- [2] J. G. de Vries, C. J. Elsevier, *The handbook of homogeneous hydrogenation*, Wiley-VCH, **2007**.
- [3] D. Wang, D. Astruc, *Chem. Rev.* **2015**, *115*, 6621-6686.
- [4] For recent reviews, see: a) C. Claver, E. Fernández, in *Modern Reduction Methods*, Wiley-VCH Verlag GmbH & Co. KGaA, **2008**, pp. 235-269; b) P.-G. Echeverria, T. Ayad, P. Phansavath, V. Ratovelomanana-Vidal, *Synthesis* **2016**, *48*, 2523-2539.
- [5] For a recent reviews, see: D. B. Bagal, B. M. Bhanage, *Adv. Synth. Catal.* **2015**, *357*, 883-900.
- [6] For a recent reviews, see: A. Volkov, F. Tinnis, T. Slagbrand, P. Trillo, H. Adolfsson, *Chem. Soc. Rev.* **2016**, *45*, 6685-6697.
- [7] For a recent reviews, see: D. Amantini, F. Fringuelli, F. Pizza, L. Vaccaro, *Organic Preparations and Procedures International* **2002**, *34*, 109-147.
- [8] For a recent reviews, see: H. K. Kadam, S. G. Tilve, *RSC Adv.* **2015**, *5*, 83391-83407.
- [9] For a review in imine CTH, see: a) M. Wills, in *Modern Reduction Methods*, Wiley-VCH Verlag GmbH & Co. KGaA, **2008**, pp. 271-296. For recent examples of imine CTH promoted by precious metals, see: b) B. Václavíková Vilhanová, A. Budinská, J. Václavík, V. Matoušek, M. Kuzma, L. Červený, *Eur. J. Org. Chem.* **2017**, 5131-5134; c) S. Ibáñez, M. Poyatos, E. Peris, *ChemCatChem* **2016**, *8*, 3790-3795; d) V. S. Shende, S. K. Shingote, S. H. Deshpande, A. A. Kelkar, *ChemistrySelect* **2016**, *1*, 2221-2224; e) H.-J. Pan, Y. Zhang, C. Shan, Z. Yu, Y. Lan, Y. Zhao, *Angew. Chem., Int. Ed.* **2016**, *55*, 9615-9619.
- [10] For a recent reviews, see: Y.-Y. Li, S.-L. Yu, W.-Y. Shen, J.-X. Gao, *Acc. Chem. Res.* **2015**, *48*, 2587-2598.
- [11] For a recent reviews, see: I. Bauer, H.-J. Knölker, *Chem. Rev.* **2015**, *115*, 3170-3387
- [12] a) T.-T. Thai, D. S. Mérel, A. Poater, S. Gaillard, J.-L. Renaud, *Chem. Eur. J.* **2015**, *21*, 7066-7070; b) S. Moulin, H. Dentel, A. Pagnoux-Ozherelyeva, S. Gaillard, A. Poater, L. Cavallo, J.-F. Lohier, J.-L. Renaud, *Chem. Eur. J.* **2013**, *19*, 17881-17890; c) D. S. Mérel, M. Elie, J.-F. Lohier, S. Gaillard, J.-L. Renaud, *ChemCatChem* **2013**, *5*, 2939-2945; d) A. Pagnoux-Ozherelyeva, N. Pannetier, M. D. Mbaye, S. Gaillard, J.-L. Renaud, *Angew. Chem., Int. Ed.* **2012**, *51*, 4976-4980; e) S. Zhou, S. Fleischer, H. Jiao, K. Junge, M. Beller, *Adv. Synth. Catal.* **2014**, *356*, 3451-3455; f) S. Fleischer, S. Zhou, S. Werkmeister, K. Junge, M. Beller, *Chem. Eur. J.* **2013**, *19*, 4997-5003; g) S. Zhou, S. Fleischer, K. Junge, M. Beller, *Angew. Chem., Int. Ed.* **2011**, *50*, 5120-5124; h) D. Brenna, S. Rossi, F. Cozzi, M. Benaglia, *Org. Biomol. Chem.* **2017**, *15*, 5685-5688; i) P. O. Lagaditis, P. E. Sues, J. F. Sonnenberg, K. Y. Wan, A. J. Lough, R. H. Morris, *J. Am. Chem. Soc.* **2014**, *136*, 1367-1380. For a tandem nitro group reduction-imine hydrogenation, see: j) T. Stemmler, A.-E. Surkus, M.-M. Pohl, K. Junge, M. Beller, *ChemSusChem* **2014**, *7*, 3012-3016.
- [13] a) C. Bornschein, S. Werkmeister, B. Wendt, H. Jiao, E. Alberico, W. Baumann, H. Junge, K. Junge, M. Beller, *Nature Communications* **2014**, *5*, 4111; b) S. Lange, S. Elangovan, C. Cordes, A. Spannenberg, H. Jiao, H. Junge, S. Bachmann, M. Scalone, C. Topf, K. Junge, M. Beller, *Catal. Sci. Technol.* **2016**, *6*, 4768-4772.
- [14] a) S. Zhou, K. Junge, D. Addis, S. Das, M. Beller, *Angew. Chem., Int. Ed.* **2009**, *48*, 9507-9510; b) F. Schneck, M. Assmann, M. Balmer, K. Harms, R. Langer, *Organometallics* **2016**, *35*, 1931-1943; c) N. M. Rezayee, D. C. Samblanet, M. S. Sanford, *ACS Catal.* **2016**, *6*, 6377-6383; d) U. Jayarathne, Y. Zhang, N. Hazari, W. H. Bernskoetter, *Organometallics* **2017**, *36*, 409-416.
- [15] a) S. Zhou, S. Fleischer, K. Junge, S. Das, D. Addis, M. Beller, *Angew. Chem., Int. Ed.* **2010**, *49*, 8121-8125; b) W. Zuo, R. H. Morris, *Nature Protocols* **2015**, *10*, 241-257; c) W. Zuo, A. J. Lough, Y. F. Li, R. H. Morris, *Science* **2013**, *342*, 1080-1083; d) A. A. Mikhailine, M. I. Maishan, R. H. Morris, *Org. Lett.* **2012**, *14*, 4638-4641; e) H.-J. Pan, T. W. Ng, Y. Zhao, *Org. Biomol. Chem.* **2016**, *14*, 5490-5493; f) R. Bigler, R. Huber, A. Mezzetti, *Angew. Chem., Int. Ed.* **2015**, *54*, 5171-5174.
- [16] Mezzetti et al.,^[15f] Morris et al.,^[15b-d] and Beller et al.^[15a] developed chiral PNNP-Fe^{II} complexes (either preisolated or generated in situ) promoting the enantioselective CTH of pro-chiral C=N bonds. The scope of these methodologies is limited to activated *N*-(diphenylphosphinyl)- imines, while *N*-aryl and *N*-alkyl imines were apparently unreactive. Very recently, Zhao et al. reported that *N*-aryl and *N*-alkyl imines can be reduced by *i*PrOH in the presence of a (cyclopentadienone)iron complex, provided that a Lewis acid [e. g., 10 mol% Fe(acac)₃] is used as co-catalyst.^[15e]
- [17] a) T. J. Brown, M. Cumbes, L. J. Diorazio, G. J. Clarkson, M. Wills, *J. Org. Chem.* **2017**, *82*, 10489-10503; b) T.

- Yan, B. L. Feringa, K. Barta, *ACS Catal.* **2016**, *6*, 381-388; c) H.-J. Pan, T. W. Ng, Y. Zhao, *Chem. Commun.* **2015**, *51*, 11907-11910; d) A. J. Rawlings, L. J. Diorazio, M. Wills, *Org. Lett.* **2015**, *17*, 1086-1089; e) T. Yan, B. L. Feringa, K. Barta, *Nature Communications* **2014**, *5*, 5602. The scope of these methodologies is limited to primary alcohols, while secondary alcohols – which form a branched secondary amines – react only in the presence of large amounts of a Lewis acid co-catalysts (e. g., 40 mol% AgF).
- [18] For recent reviews on the ‘hydrogen borrowing’ approach, see: a) F. Huang, Z. Liu, Z. Yu, *Angew. Chem., Int. Ed.* **2016**, *55*, 862-875; b) A. Quintard, J. Rodriguez, *ChemSusChem* **2016**, *9*, 28-30; c) J. M. Ketcham, I. Shin, T. P. Montgomery, M. J. Krische, *Angew. Chem., Int. Ed.* **2014**, *53*, 9142-9150.
- [19] a) H.-J. Knölker, E. Baum, H. Goesmann, R. Klauss, *Angew. Chem., Int. Ed.* **1999**, *38*, 2064-2066; b) T. N. Plank, J. L. Drake, D. K. Kim, T. W. Funk, *Adv. Synth. Catal.* **2012**, *354*, 597-601.
- [20] C. P. Casey, H. Guan, *J. Am. Chem. Soc.* **2009**, *131*, 2499-2507.
- [21] S. Elangovan, S. Quintero-Duque, V. Dorcet, T. Roisnel, L. Norel, C. Darcel, J.-B. Sortais, *Organometallics* **2015**, *34*, 4521-4528.
- [22] a) A. Rosas-Hernández, P. G. Alsabeh, E. Barsch, H. Junge, R. Ludwig, M. Beller, *Chem. Commun.* **2016**, *52*, 8393-8396; b) R. Hodgkinson, A. Del Grosso, G. Clarkson, M. Wills, *Dalton Transactions* **2016**, *45*, 3992-4005; c) A. Berkessel, S. Reichau, A. von der Höh, N. Leconte, J.-M. Neudörfl, *Organometallics* **2011**, *30*, 3880-3887.
- [23] a) J. P. Hopewell, J. E. D. Martins, T. C. Johnson, J. Godfrey, M. Wills, *Org. Biomol. Chem.* **2012**, *10*, 134-145; b) P. Gajewski, M. Renom-Carrasco, S. Vailati Facchini, L. Pignataro, L. Lefort, J. G. de Vries, R. Ferraccioli, U. Piarulli, C. Gennari, *Eur. J. Org. Chem.* **2015**, 5526-5536; c) P. Gajewski, M. Renom-Carrasco, S. Vailati Facchini, L. Pignataro, L. Lefort, J. G. de Vries, R. Ferraccioli, A. Forni, U. Piarulli, C. Gennari, *Eur. J. Org. Chem.* **2015**, 1887-1893; d) T. W. Funk, A. R. Mahoney, R. A. Sponenburg, K. P. Zimmerman, D. K. Kim, E. E. Harrison, *Organometallics* **2018**, *37*, 1133-1140.
- [24] S. Vailati Facchini, J.-M. Neudörfl, L. Pignataro, M. Cettolin, C. Gennari, A. Berkessel, U. Piarulli, *ChemCatChem* **2017**, *9*, 1461-1468.
- [25] a) D. Fornals, M. A. Pericas, F. Serratos, J. Vinaixa, M. Font-Altaba, X. Solans, *J. Chem. Soc., Perkin Trans. 1* **1987**, 2749-2752; b) C. G. Krespan, *J. Org. Chem.* **1975**, *40*, 261-262; c) J. L. Boston, D. W. A. Sharp, G. Wilkinson, *J. Chem. Soc.* **1962**, 3488-3494; d) H.-J. Knölker, J. Heber, C. H. Mahler, *Synlett* **1992**, 1002-1004.
- [26] a) G. N. Schrauzer, *Chem. Ind. (London)* **1958**, 1403; b) G. N. Schrauzer, *Chem. Ind. (London)* **1958**, 1404; c) W. Hübel, E. H. Braye, *J. Inorg. Nucl. Chem.* **1959**, *10*, 250-268.
- [27] L. Brandsma, H. D. Verkruisje, *Synthesis* **1978**, *1978*, 290-290.
- [28] H. Kolshorn, H. Meier, E. Müller, *Tetrahedron Lett.* **1971**, *12*, 1469-1472.
- [29] Prepared from cyclododecanone according to a known procedure, K. M. Brummond, K. D. Gesenberg, J. L. Kent, A. D. Kerekes, *Tetrahedron Lett.* **1998**, *39*, 8613-8616.
- [30] P. Gajewski, A. Gonzalez-de-Castro, M. Renom-Carrasco, U. Piarulli, C. Gennari, J. G. de Vries, L. Lefort, L. Pignataro, *ChemCatChem* **2016**, *8*, 3431-3435.
- [31] W. C. Still, M. Kahn, A. Mitra, *J. Org. Chem.* **1978**, *43*, 2923-2925.
- [32] A. Hasegawa, Y. Naganawa, M. Fushimi, K. Ishihara, H. Yamamoto, *Org. Lett.* **2006**, *8*, 3175-3178.
- [33] Z. Wang, Q. Ding, X. He, J. Wu, *Org. Biomol. Chem.* **2009**, *7*, 863-865.
- [34] D.-J. Dong, H.-H. Li, S.-K. Tian, *J. Am. Chem. Soc.* **2010**, *132*, 5018-5020.
- [35] F. I. López, F. N. de la Cruz, J. López, J. M. Martínez, Y. Alcaraz, F. Delgado, A. Sánchez-Recillas, S. Estrada-Soto, M. A. Vázquez, *Med. Chem. Res.* **2017**, *26*, 1325-1335.
- [36] J. L. G. Ruano, J. Alemán, I. Alonso, A. Parra, V. Marcos, J. Aguirre, *Chemistry - A European Journal* **2007**, *13*, 6179-6195.
- [37] M. Hatano, Y. Hattori, Y. Furuya, K. Ishihara, *Org. Lett.* **2009**, *11*, 2321-2324.
- [38] F. Schaufelberger, L. Hu, O. Ramström, *Chem. Eur. J.* **2015**, *21*, 9776-9783.
- [39] R. M. Ceder, G. Muller, M. Ordinas, J. I. Ordinas, *Dalton Trans.* **2007**, 83-90.
- [40] N. Mršić, A. J. Minnaard, B. L. Feringa, J. G. de Vries, *J. Am. Chem. Soc.* **2009**, *131*, 8358-8359.
- [41] R. Sarma, D. Prajapati, *Chem. Commun.* **2011**, *47*, 9525-9527.
- [42] W. Li, G. Hou, M. Chang, X. Zhang, *Adv. Synth. Catal.* **2009**, *351*, 3123-3127.
- [43] F.-M. Gautier, S. Jones, S. J. Martin, *Org. Biomol. Chem.* **2009**, *7*, 229-231.
- [44] T. Kanemitsu, A. Umehara, R. Haneji, K. Nagata, T. Itoh, *Tetrahedron* **2012**, *68*, 3893-3898.

- [45] S. Liu, Y. Yu, L. S. Liebeskind, *Org. Lett.* **2007**, *9*, 1947-1950.
- [46] C. Moessner, C. Bolm, *Angew. Chem., Int. Ed.* **2005**, *44*, 7564-7567.
- [47] C. G. Hartung, A. Tillack, H. Trauthwein, M. Beller, *J. Org. Chem.* **2001**, *66*, 6339-6343.
- [48] D. J. Fisher, J. B. Shaum, C. L. Mills, J. Read de Alaniz, *Org. Lett.* **2016**, *18*, 5074-5077.
- [49] A. Bartoszewicz, R. Marcos, S. Sahoo, A. K. Inge, X. Zou, B. Martín-Matute, *Chem. Eur. J.* **2012**, *18*, 14510-14519.
- [50] O.-Y. Lee, K.-L. Law, D. Yang, *Org. Lett.* **2009**, *11*, 3302-3305.
- [51] T. Itoh, K. Nagata, M. Miyazaki, H. Ishikawa, A. Kurihara, A. Ohsawa, *Tetrahedron* **2004**, *60*, 6649-6655.
- [52] L. Li, Z. Niu, S. Cai, Y. Zhi, H. Li, H. Rong, L. Liu, L. Liu, W. He, Y. Li, *Chem. Commun.* **2013**, *49*, 6843-6845.
- [53] D. Wei, A. Bruneau-Voisine, D. A. Valyaev, N. Lugan, J.-B. Sortais, *Chem. Commun.* **2018**, *54*, 4302-4305.
- [54] L. Hizartzidis, M. Tarleton, C. P. Gordon, A. McCluskey, *RSC Adv.* **2014**, *4*, 9709-9722.
- [55] M. Carmona, R. Rodríguez, I. Méndez, V. Passarelli, F. J. Lahoz, P. García-Orduña, D. Carmona, *Dalton Trans.* **2017**, *46*, 7332-7350.
- [56] D. J. van As, T. U. Connell, M. Brzozowski, A. D. Scully, A. Polyzos, *Org. Lett.* **2018**, *20*, 905-908.
- [57] S. Guizzetti, M. Benaglia, G. Celentano, *Eur. J. Org. Chem.* **2009**, 3683-3687.
- [58] B. S. Takale, S. Tao, X. Yu, X. Feng, T. Jin, M. Bao, Y. Yamamoto, *Tetrahedron* **2015**, *71*, 7154-7158.
- [59] X. Zhu, H. Du, *Org. Biomol. Chem.* **2015**, *13*, 1013-1016.
- [60] P. Renzi, J. Hioe, R. M. Gschwind, *J. Am. Chem. Soc.* **2017**, *139*, 6752-6760.
- [61] W. Muramatsu, K. Nakano, C.-J. Li, *Org. Lett.* **2013**, *15*, 3650-3653.
- [62] R. Mamidala, V. Mukundam, K. Dhanunjayarao, K. Venkatasubbaiah, *Tetrahedron* **2017**, *73*, 2225-2233.
- [63] C. Wang, A. Pettman, J. Bacsá, J. Xiao, *Angew. Chem., Int. Ed.* **2010**, *49*, 7548-7552.
- [64] G. Wang, C. Chen, T. Du, W. Zhong, *Adv. Synth. Catal.* **2014**, *356*, 1747-1752.
- [65] J. Li, C. Wang, D. Xue, Y. Wei, J. Xiao, *Green Chem.* **2013**, *15*, 2685-2689.
- [66] V. M. Mokhov, Y. V. Popov, *Russ. J. Gen. Chem.* **2014**, *84*, 1921-1923.
- [67] C. Qin, T. Shen, C. Tang, N. Jiao, *Angew. Chem., Int. Ed.* **2012**, *51*, 6971-6975.
- [68] D. Gülcemal, S. Gülcemal, C. M. Robertson, J. Xiao, *Organometallics* **2015**, *34*, 4394-4400.
- [69] A. k. Shaikh, A. J. A. Cobb, G. Varvounis, *Org. Lett.* **2012**, *14*, 584-587.
- [70] B. Emayavaramban, M. Roy, B. Sundararaju, *Chem. Eur. J.* **2016**, *22*, 3952-3955.
- [71] P. Bachu, C. Zhu, T. Akiyama, *Tetrahedron Lett.* **2013**, *54*, 3977-3981.
- [72] Y.-H. Wang, J.-L. Ye, A.-E. Wang, P.-Q. Huang, *Org. Biomol. Chem.* **2012**, *10*, 6504-6511.
- [73] P. J. Rani, S. Thirumaran, *Eur. J. Med. Chem.* **2013**, *62*, 139-147.
- [74] M. Tomaszewski, J. Warkentin, N. Werstiuk, *Aust. J. Chem.* **1995**, *48*, 291-321.
- [75] Q. Lei, Y. Wei, D. Talwar, C. Wang, D. Xue, J. Xiao, *Chem. Eur. J.* **2013**, *19*, 4021-4029.

Chapter 3 - Applications of a highly active CIC to alcohol amination reactions

Alcohol amination is an attractive and atom-economic reaction which provides access to amines— a valuable class of fine chemicals^[1] – generating water as the sole byproduct. This transformation cannot occur via the S_N2 mechanism due to the poor leaving group ability of the OH^- ion. Although the transformation can be promoted by acid catalysis, very harsh reaction conditions are required.^[2] Alcohol amination could be effectively performed by catalytic processes involving the ‘hydrogen-borrowing’ (HB) mechanism (also known as ‘hydrogen autotransfer’), in which two H_2 transfer elementary steps occur without any net change in the oxidation state of the system. The HB amination proceeds through an alcohol dehydrogenation/imine formation/imine hydrogenation sequence (Scheme 3.1), without any net consumption or release of hydrogen. Upon alcohol dehydrogenation, the catalytic complex ML_n is temporarily converted into the species $\text{ML}_n\text{-H}_2$, which then reduces the imine or iminium ion intermediate formed by condensation of carbonyl compound with the amine substrate.



Scheme 3.1. General mechanism of HB amination of alcohols.

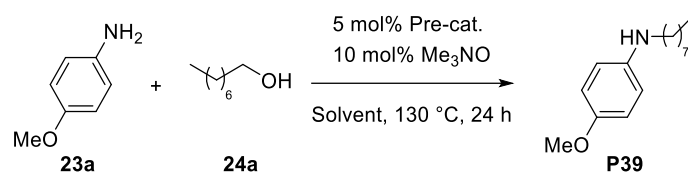
The first examples of HB alcohol amination were reported in the early 1980s using catalysts based on precious metals such as rhodium, ruthenium and iridium,^[3] and the latter two became the focus of the most recent studies.^[4] Use of cheaper metal catalysts such as copper,^[5] cobalt^[6] and iron^[7] complexes in the HB aminations remained quite limited until recent years, when homogeneous base metal catalysis started being increasingly studied.^[3a] In this context, Feringa, Barta *et al.* reported the application of a well-defined homogeneous iron catalysis for the HB amination of alcohols for the first time: the ‘Knölker complex’ **9aa** (already mentioned in Section 1.5), which is a highly stable and easy-to-handle pre-catalyst,^[8] was shown to promote the amination

of several primary alcohols and diols. Further investigation on the use of CICs for HB alcohol amination were carried out by different groups, as already discussed in Section 1.5. However, in these reactions, the substrate scope was limited to primary alcohols. As mentioned in Section 1.5, in 2015 Zhao and coworkers reported that the isolated HCIC **10aa** catalyzes the amination of different secondary alcohols with moderate to good yields (26-97%) in the presence of a co-catalysts (AgF, 40 mol%). Nevertheless, serious limitations still remained in this methodology. For example, the reaction requires a relatively high catalyst loading of the isolated HCIC **10aa**, which is sensitive to air and moisture and requires handling under glovebox. Moreover, large amounts of AgF (40 mol%) co-catalyst are necessary, thus overriding the advantages of using a cheap metal catalyst.

3.1 ‘Hydrogen-Borrowing’ amination of secondary alcohols

Building on our group’s expertise in the fields of CICs, an investigation on the use of (cyclopentadienone)iron complexes for the HB amination of secondary alcohols was undertaken. To this purpose, the highly active CIC **9d** was employed, which had shown remarkable catalytic activity in the CTH of imines and in the reductive amination of ketones involving a hydrogen transfer process (already discussed in Chapter 2). As the HB amination of alcohols shares the same elementary steps as these reactions, we surmised that pre-catalyst **9d** could be an effective catalyst and perhaps allow to expand the application scope to secondary alcohol substrates.

Table 3.1. Comparison between pre-catalysts **9aa** and **9d** in the HB amination of 1-octanol with *p*-anisidine.^[a]



#	Pre-cat.	Solvent	23a / 24a ratio	Yield (%) ^[a]
1 ^[b]	9aa	CPME	2	70
2 ^[c]	9aa	toluene	1.5	82
3 ^[c]	9d	toluene	1.5	> 95

[a] Isolated yield after column chromatography.

[b] Reaction conditions as described in the literature.^[8]

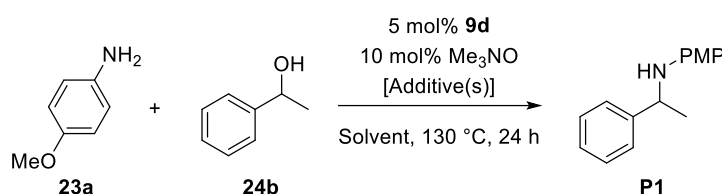
[c] Reaction conditions: **23a**/pre-cat./Me₃NO = 100:5:10. Catalyst activation: toluene, Me₃NO, r.t., 15 min, C_{0,catal.} = 0.1 M; HB amination: toluene, C_{0,sub.} = 0.25 M (0.5 mmol), T = 130 °C, 24 h.

CPME = cyclopentyl methyl ether

First, we compared the activity of CICs **9d** and **9aa** in the HB amination of a primary alcohol (1-octanol) with *p*-anisidine (Table 3.1). Complex **9aa** – activated *in situ* with Me₃NO – was tested in the conditions described

by Feringa, Barta *et al.*^[8] (Table 3.1, entry 1) and gave essentially the same yield reported by them (70% vs. 69%). Consistent with our expectations, under its optimized conditions (toluene instead of CPME as solvent) pre-catalyst **9d** showed higher activity than **9aa**, leading to the amination product **P39** in quantitative yield (Table 3.1, entry 3). CIC **9aa** was also tested under the same conditions used with pre-catalyst **9d** (Table 3.1, entry 2), giving an 82% yield. This result encouraged us to investigate whether complex **9d** could efficiently catalyze also the amination of secondary alcohols.

Table 3.2. HB amination of 1-phenylethanol with *p*-anisidine promoted by pre-catalyst **9d** - Optimization.^[a]



#	Solvent	Alcohol/ amine	MS [amount, mg]	Additives [mol%]	Conv. (%) ^[b]
1	toluene	1.5:1	-	-	17
2	toluene	1.5:1	3 Å [400]	-	48
3	toluene	3:1	3 Å [400]	-	42
4	toluene	4:1	3 Å [400]	-	76
5	toluene	6:1	3 Å [400]	-	46
6	toluene	10:1	3 Å [400]	-	0
7	toluene	1:1	3 Å [400]	-	58
8	toluene	1:1.5	3 Å [400]	-	35
9	toluene	1:4	3 Å [400]	-	34
10	toluene	4:1	3 Å [400]	TFA [1]	53
11	toluene	4:1	3 Å [400]	AcOH [1]	64
12	CPME	4:1	3 Å [400]	-	24
13	dioxane	4:1	3 Å [400]	-	22
14	DMF	4:1	3 Å [400]	-	0
15	DME	4:1	3 Å [400]	-	19
16	DCE	4:1	3 Å [400]	-	5
17 ^[c]	toluene	4:1	3 Å [400]	-	89

[a] Reaction conditions: **23a/9d/Me₃NO** = 100:5:10. Catalyst activation: solvent, Me₃NO, r.t., 15 min, $C_{0,cat.}$ = 0.1 M; HB amination: solvent, $C_{0,sub.}$ = 0.25 M (0.5 mmol), T = 130 °C, 24 h.

[b] Determined by ¹H NMR analysis of the reaction crude.

[c] Reaction run at 150 °C.

Thus, we tested pre-catalyst **9d** in the HB amination of *p*-anisidine with 1-phenylethanol under the same conditions used with 1-octanol, and we observed a poor conversion to the desired product **P1** (Table 3.2, entry 1). However, we found that the conversion was positively affected by the presence of 3 Å molecular sieves in

the reaction environment (Table 3.2, entry 2 vs. entry 1), which is likely to accelerate the imine formation step. We also found that the conversion is remarkably influenced by the reaction stoichiometry (Table 3.2, entries 3-9), 4:1 alcohol/amine ratio giving the best result (Table 3.2, entry 4). Moreover, the conversion was slightly reduced in the presence of TFA or AcOH (Table 3.2, entries 10 and 11 vs. entry 4), which were added to accelerate the imine formation step. Next, we screened several different aprotic solvents (Table 2, entries 12-16), but they generally resulted conversions lower than those obtained in toluene. Increasing the reaction temperature from 130 to 150 °C (Table 3.2, entry 17 vs. entry 4) led to improved conversion (89% vs. 76%).

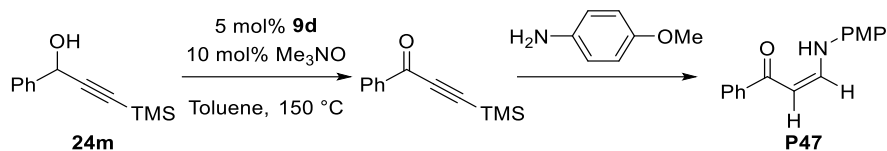
With the optimized conditions in hands, a series of secondary alcohols were screened in the reaction with *p*-anisidine (**23a**), giving the results shown in Table 3.3. Delightfully, excellent yields (84-99% range) were obtained with a number of alcohol substrates, thus demonstrating that our **9d**-based catalytic methodology is suitable for HB secondary alcohol amination.

From the analysis of the data shown in Table 3.3, the following general trends emerged:

- 1) For each type of substrate, the yield was roughly decreased with the increasing steric bulk surrounding the hydroxy group, i.e. along the series **24b** → **24c** → **24l** → **24n** for benzylic alcohols (Table 3.3, entries 1-2, 12 and 14), **24e** → **24g** → **24d** → **24h** → **24f** for aliphatic alcohols (Table 3.3, entries 3-7), and **24i** → **24j** → **24k** for allylic alcohols (Table 3.3, entries 9-11).
- 2) The yields of the reactions resulting incomplete after 24 h could be improved by extending the reaction time to 72 h (Table 3, entries 2, 5 and 7-14). Hence, it is evident that pre-catalyst **9d** underwent negligible or no decomposition, maintaining its catalytic activity for a long time. This is in agreement with other evidences previously reported by our group for the **9d**-catalyzed hydrogenation of ketones (see Section 1.4.1), that **9d** is more stable than 'Knölker complex' **9aa**, possibly due to the presence of bulky cyclooctane rings fused to the cyclopentadienone, capable of stabilizing the catalyst for longer time. In agreement with our interpretation, when the HB amination of cyclohexanol **24h** was carried out using pre-catalyst **9aa** under the same conditions used for **9d**, product **P37** was obtained in a much lower yield (Table 3.3, entry 8 vs. entry 7).

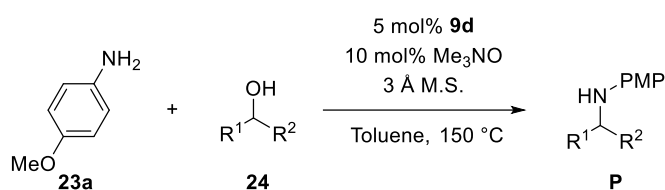
The HB amination of **24g** with **23a** was repeated on gram-scale with excellent yield (99%) under the same conditions (Table 3.3, entry 6). Surprisingly, the desired amine did not form in the amination of alcohol **24m** under optimized conditions. Instead, this reaction gave product **P47** (Table 3.3, entry 13), which derives from the conjugate addition of *p*-anisidine to an ynone intermediate, formed by alcohol dehydrogenation and alkyne deprotection (Scheme 3.2). The heterocyclic alcohol **24o**, possessing a tertiary amino group, was screened and

the corresponding secondary amine **P48** was obtained with a good yield (Table 3.3, entry 15). Other functionalized alcohols – α -hydroxyesters (e.g., methyl lactate, methyl mandelate, ethyl malate) – were also screened, but no formation of amination products was observed.



Scheme 3.2. Formation of product **P47** promoted by pre-catalyst **9d**.

Table 3.3. Alcohol scope evaluation in HB amination with *p*-anisidine promoted by pre-catalyst **9d**.^[a]



	Alcohol	Product	Yield (%) ^[b]	
			<i>t</i> = 24 h	<i>t</i> = 72 h
1			87	95
2			14	64
3			95	96
4			99	99
5			19	53
6			99 (99) ^[c]	99
7			89	95
8 ^[e]			32	63

9			10	31
10			6	28
11			40 (1:1) ^[d]	49 (1:1) ^[d]
12			16	27
13			6	29
14			10	30
15			84	82

[a] Reaction conditions: alcohol/**23a**/**9d**/Me₃NO = 400:100:5:10. Catalyst activation: toluene, Me₃NO, r.t., 15 min, C_{0,cat.} = 0.1 M; HB amination: toluene, C_{0,sub.} = 0.25 M (0.5 mmol), T = 150 °C.

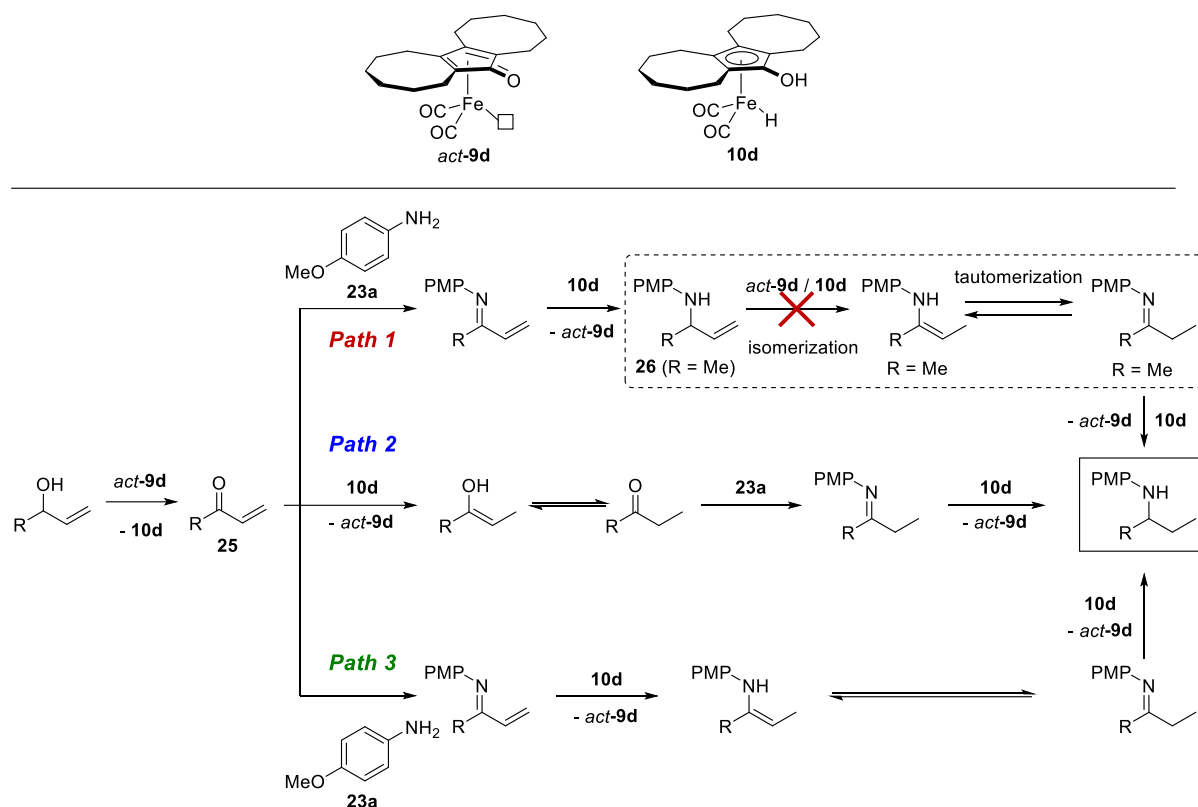
[b] Isolated yield after column chromatography.

[c] Yield of gram-scale experiment.

[d] Ratio **P37**:**P46**.

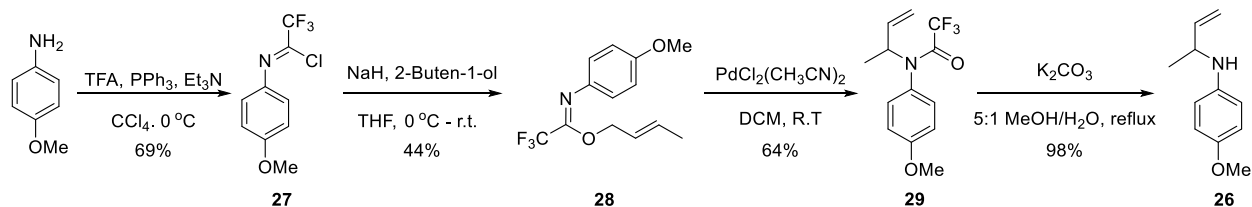
[e] Pre-catalyst **9d** was replaced by **9aa**

Interestingly, the HB amination of allylic alcohols was accompanied by partial (Table 3.3, entry 11) or full (Table 3.3, entries 9 and 10) reduction of the C=C bond. This outcome can be explained by the presence of excess alcohol, acting as terminal reductant. The activated catalyst *act-9d* dehydrogenates the allylic alcohol to α,β -unsaturated ketone **25**, then three possible pathways may be conceived (Scheme 3.3): Path 1 consists in a C=N reduction followed by C=C bond isomerization, enamine/imine tautomerization and another C=N reduction, whereas two consecutive conjugate reductions take place both Path 2 and 3.

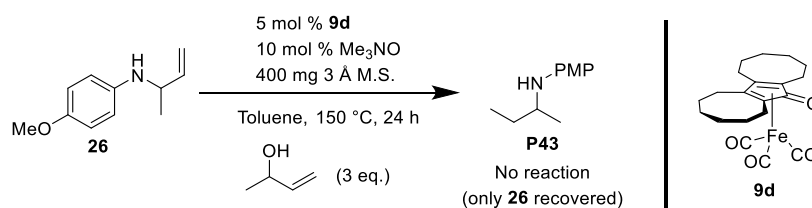


Scheme 3.3. Possible pathways for the amination of allylic alcohols with concomitant C=C bond reduction.

A, Synthesis of compound 31



B, Reduction of compound 31 promoted by pre-catalyst 9d



Scheme 3.4. A: Synthesis of intermediate **26**; **B:** reduction of **26** promoted by **9d**.

To investigate the mechanism of allylic alcohol amination accompanied with C=C double bonds reduction, a control experiment was carried out. Intermediate **26** was synthesized according to published procedures^[9] (Scheme 3.4 A) and then subjected to the same experimental conditions that led to the formation of product **P43** from 3-buten-2-ol (Scheme 3.4 B). As no formation of **P43** was observed, Path 1 could be ruled out, whereas both Path 2 and Path 3 are viable and probably operating.

Table 3.4. Screening of amine nucleophiles in the HB amination of 1-phenylethanol promoted by pre-catalyst **9d**.^[a]

#	Amine	Product	Yield [%] ^[b]	
			<i>t</i> = 24 h	<i>t</i> = 72 h
1			85	> 95
2			51	71
3			45	75
4			15	54
5			22	78
6			20	43

[a] Reaction conditions: **24b**/amine/**9d**/ Me_3NO = 400:100:5:10. Catalyst activation: toluene, Me_3NO , r.t., 15 min, $C_{0,\text{cat.}}$ = 0.1 M; HB amination: toluene, $C_{0,\text{sub.}}$ = 0.25 M (0.5 mmol), T = 150 °C.

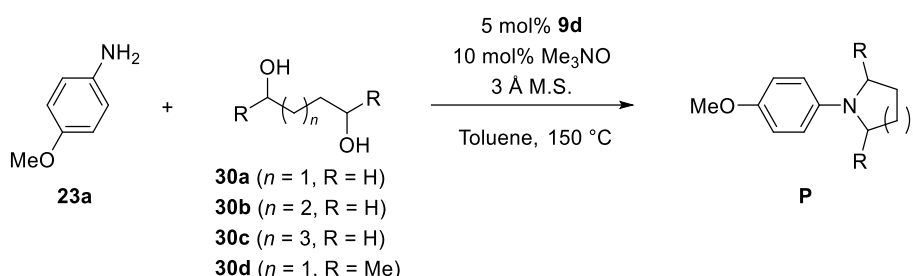
[b] Isolated yield after column chromatography.

Later on, the HB amination of 1-phenylethanol **24b** with different amine nucleophiles was performed under the optimized conditions (Table 3.4). The general trend observed in the alcohol screening (Table 3.3) – i.e., that increasing the steric bulk of the substrates leads to a drop of the yields – was observed also in the case of amines (Table 3.4): benzylamine (**23e**) gave higher yields (Table 3.4, entry 5 vs. entry 6) than *N*-methyl benzylamine (**23f**), and *p*-anisidine (**23a**) showed higher reactivity than **23b**, giving excellent yields (Table 3.4, entry 1 vs. entry 2). Although also in the amine screening, yields were improved by extending the reaction time (72 vs. 24 h), aliphatic (**23c,d**) and benzylic amines (**23e,f**) were found less reactive than anilines (**23a,b**), giving quite moderate yields.

Encouraged by the high activity displayed by pre-catalyst **9d**, we tested it in the reaction of primary amines with diols to afford saturated *N*-heterocycles. *p*-Anisidine (**23a**) reacted with primary diols (**30a-c**) to generate the corresponding five-, six- and seven-membered rings **P53-P55** in fair to good yields (Table 3.5, entries 1-3). In several cases (Table 3.5, entries 1-3), the yields were slightly higher after 24 h, rather than with 72 h, suggesting that the reaction products might undergo a partial decomposition under the reaction conditions.

The cyclization occurred also with the secondary diol **30d** forming 1-(4-methoxyphenyl)-2,5-dimethylpyrrolidine **P56**^[10] as a mixture of *cis* and *trans* isomers (Table 3.5, entry 4), and in this case an extended reaction time positively affected the yield.

Table 3.5. HB amination of *p*-anisidine with diols promoted by pre-catalyst **9d**.^[a]



#	Diol	Product	Yield [%] ^[b]	
			$t = 24$ h	$t = 72$ h
1	30a		55	44
2	30b		66	63
3	30c		40	25
4 ^[c]	30d		25 (57:43 <i>cis/trans</i>) ^[c]	71 (58:42 <i>cis/trans</i>)

[a] Reaction conditions: **30/23a/9d/Me₃NO** = 400:100:5:10. Catalyst activation: toluene, Me₃NO, r.t., 15 min, $C_{0,cat.} = 0.1$ M; HB amination: toluene, $C_{0,sub.} = 0.25$ M (0.5 mmol), $T = 150$ °C.

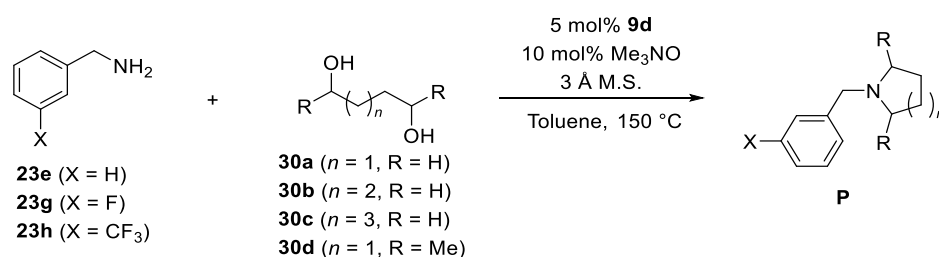
[b] Isolated yield after column chromatography.

[c] *Cis/trans* ratio determined by ¹H NMR of the reaction crude.^[10]

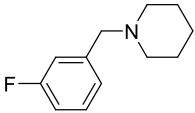
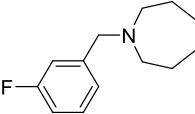
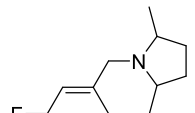
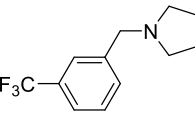
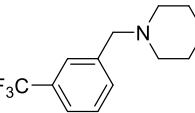
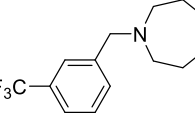
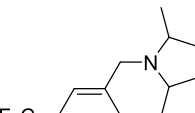
Further cyclization tests were carried out combining diols **30a-d** with benzylic amines **23e**, **23g** and **23h** under the optimized catalytic conditions (Table 3.6). The reaction of benzylamine **23e** with primary diols **30a-c** afforded the *N*-heterocycles **P57-59** in moderate yields (Table 3.6, entries 1-3). Consistent with the report by

Feringa, Barta *et al.*,^[8,11] the *meta*-substituted benzylamines bearing electron-withdrawing groups (**23g** and **23h**) were found slightly more reactive than **23e** in reactions forming six- and seven membered rings **P62-63** and **P66-67** (Table 3.6, entry 6, 10 vs. 2; entries 7, 11 vs. 3). However, amines **23e**, **23g** and **23h** gave similar yields in the formation of pyrrolidines **P57**, **P61** and **P65** from 1,4-butanediol **30a** (Table 3.6, entries 1, 5 and 9). Remarkably, the corresponding reactions with 2,5-hexanediol **30d** to form 2,5-dimethylpyrrolidines **P60**, **P64** and **P68** (as *cis/trans* diastereoisomer mixtures) gave higher yields (Table 3.6, entries 4 vs. 1, 8 vs. 5 and 12 vs. 9), thus further confirming the efficacy of pre-catalyst **9d** in the HB amination of secondary alcohols. To the best of our knowledge, the latter reactions and the corresponding reaction of *p*-anisidine **23a** (Table 3.5, entry 4) represent the first examples of secondary diol cyclization promoted by a (cyclopentadienone)iron complex.

Table 3.6. HB amination of benzylic amines with diols promoted by pre-catalyst **9d**.^[a]



#	Amine	Diol	Product	Yield [%] ^[b]	
				$t = 24$ h	$t = 72$ h
1	23e	30a		29	45
2	23e	30b		18	28
3	23e	30c		11	16
4	23e	30d		66 (79:21 <i>cis/trans</i>)	43 (79:21 <i>cis/trans</i>)
5	23g	30a		30	27

6	23g	30b		40	54
			P62		
7	23g	30c		51	61
			P63		
8	23g	30d		55 (76:24 <i>cis/trans</i>)	60 (79:21 <i>cis/trans</i>)
			P64		
9	23h	30a		8	29
			P65		
10	23h	30b		42	18
			P66		
11	23h	30c		64	68
			P67		
12	23h	30d		72 (73:27 <i>cis/trans</i>)	66 (76:24 <i>cis/trans</i>)
			P68		

[a] Reaction conditions: **30**/amine/**9d**/Me₃NO = 400:100:5:10. Catalyst activation: toluene, Me₃NO, r.t., 15 min, C_{0,catal.} = 0.1 M; HB amination: toluene, C_{0,sub.} = 0.25 M (0.5 mmol), T = 150 °C.

[b] Isolated yield after column chromatography.

[c] *Cis/trans* ratio determined by ¹H NMR of the reaction crude.^[10]

3.2 Conclusions on the **9d**-catalyzed HB amination of alcohols

CIC **9d** was successfully applied to the HB amination of alcohols, which allowed to remarkably expand the substrate scope to secondary alcohols without the need of semi-precious metal co-catalysts such as AgF. Thanks to the highly active CIC **9d**, a series of secondary alcohols were reacted with different amines (e.g., anilines, benzylamines and cyclic amines) giving moderate to excellent yields (28-99%). Pre-catalyst **9d** was also able to promote the reaction of diols with primary amines to form five-, six- and seven-membered *N*-

heterocycles in a fair to good yields. Notably, a secondary diol (2,5-hexanediol **30d**) was employed for the first time in the cyclization of diols to afford the corresponding 2,5-dimethylpyrrolidine products in good yields. These results certainly represent a step forward in the direction of replacing precious metals with cheap metals in an attractive atom-economic such as the HB amination of alcohols.

3.3 Experimental Section

3.3.1 General remarks

All reactions were carried out in flame-dried glassware with magnetic stirring under inert atmosphere (nitrogen or argon), unless otherwise stated. Solvents for reactions were distilled over the following drying agents and transferred under nitrogen: MeOH (CaH₂), toluene (Na/benzophenone). Dry ethanol (over molecular sieves in bottles with crown cap) were purchased from Sigma Aldrich and stored under nitrogen. The reactions were monitored by analytical thin-layer chromatography (TLC) using silica gel 60 F254 pre-coated glass plates (0.25 mm thickness). Visualization was accomplished by irradiation with a UV lamp and/or staining with a potassium permanganate alkaline solution or with a ninhydrin solution. Flash Column Chromatography was performed using silica gel (60 Å, particle size 40-64 µm) as stationary phase, following the procedure by Still and co-workers.^[12]

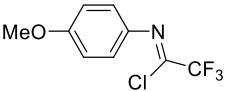
¹H NMR spectra were recorded on a spectrometer operating at 400.13 MHz. Proton chemical shifts are reported in ppm (δ) with the solvent reference relative to tetramethylsilane (TMS) employed as the internal standard (CDCl₃, δ = 7.26 ppm; CD₂Cl₂ δ = 5.32 ppm). The following abbreviations are used to describe spin multiplicity: s = singlet, d = doublet, t = triplet, q = quartet, m = multiplet, bs = broad signal, dd = doublet-doublet, td = triplet-doublet. ¹³C NMR spectra were recorded either on a 400 MHz spectrometer operating at 100 MHz or on a 600 MHz spectrometer operating at 150 MHz, with complete proton decoupling. Carbon chemical shifts are reported in ppm (δ) relative to TMS with the respective solvent resonance as the internal standard (CDCl₃ δ = 77.16 ppm; CD₂Cl₂ δ = 54.00 ppm). The coupling constant values are given in hertz (Hz). ¹⁹F NMR spectra were recorded on a 300 MHz spectrometer operating at 282 MHz, with complete proton decoupling. Fluorine chemical shifts are reported in ppm (δ) relative to external CFCl₃ at 0 ppm (positive values downfield). Infrared spectra were recorded on a standard FT/IR spectrophotometer. High resolution mass spectra (HRMS) were performed on a ESI QToF SYNAPT G2 Si mass spectrometer (Waters), available at the UNITECH-COSPECT laboratories (Università degli Studi di Milano).

Materials: alcohols and amines used in the substrate screening were purchased from commercial suppliers (TCI Chemicals, ACROS, Sigma Aldrich). The liquid amines were distilled before use, whereas the other reagents were used as received. Pre-catalyst **9d** was prepared as previously described in Chapter 2, Section 2.1. 3 Å MS were dried under high vacuum at 200 °C and then stored in an oven at 110 °C.

3.3.2 Control experiment for elucidating the mechanism of allylic alcohol amination with concomitant C=C reduction

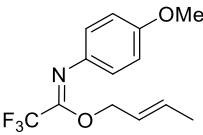
3.3.2.1 Synthesis of the putative intermediate **26**

2,2,2-Trifluoro-*N*-(4-methoxyphenyl)acetimidoyl chloride (**27**)^[9c]

 A mixture of triphenylphosphine (8.57 g, 132.0 mmol, 3 eq.), trifluoroacetic acid (1.24 g, 10.9 mmol, 1 eq.), Et₃N (1.82 mL, 13.1 mmol, 1.2 eq.) and carbon tetrachloride (10 mL) was magnetically stirred while cooled with an ice bath. After 10 min, 4-methoxyaniline (1.61 g, 13.1 mmol, 1.2 eq.) dissolved in carbon tetrachloride (10 mL) was added slowly (exothermic reaction). The ice bath was removed and the reaction mixture was stirred at reflux for 4 h. Upon cooling to r.t., the reaction mixture was washed with hexane (3 × 100 mL). Solvent was removed using a rotary evaporator to give an orange oil. Distillation gave 2.27 g of 2,2,2-trifluoro-*N*-(4-methoxyphenyl)acetimidoyl chloride **S1** as a light yellow liquid: b.p. 75-77 °C/0.3 mmHg (9.02 mmol, 69%).

¹H NMR (400 MHz, CDCl₃) δ 7.31 (d, *J* = 9.0 Hz, 2H), 6.96 (d, *J* = 9.0 Hz, 2H), 3.85 (s, 3H).

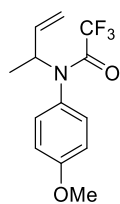
But-2-en-1-yl 2,2,2-trifluoro-*N*-(4-methoxyphenyl)acetimidate (**28**)^[9a]

 Sodium hydride (144 mg, 6 mmol, 1.2 eq.) was slurred in THF (8 mL) and cooled to 0 °C. 2-Buten-1-ol (433 mg, 6 mmol, 1.2 eq.) was added dropwise and the reaction was stirred at 0 °C for 30 min. The cooling bath was removed and the reaction was stirred for an additional 1.5 h at r.t. A solution of *N*-(4-methoxybenzyl)trifluoroacetimidoyl chloride **27** (1.26 g, 5 mmol, 1 eq.) and THF (8 mL) was added in one portion to the alkoxide solution. The reaction was maintained at r.t. for 18 h before concentrating. The residue was redissolved in hexanes, filtered through celite, and concentrated. The resulting residue was purified by flash chromatography (99:1 to 95:5 hexane/AcOEt) gave 601 mg of **28** as a pale-yellow oil (2.2 mmol, 44%).

¹H NMR (400 MHz, CDCl₃): δ 6.84 (d, *J* = 8.9, 2H), 6.76 (d, *J* = 8.9, 2H), 5.89-5.85 (m, 1H), 5.72-5.68 (m,

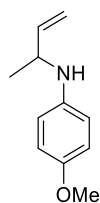
1H), 4.68 (s, br, 2H), 3.79 (s, 3H), 1.77 (d, $J = 6.3$ Hz, 3H).

***N*-(But-3-en-2-yl)-2,2,2-trifluoro-*N*-(4-methoxyphenyl)acetamide (**29**)**^[9a,b]



Bis(acetonitrile)-dichloropalladium(II) (69 mg, 0.183 mmol, 0.1 eq.) was dissolved in 3 mL of dry DCM at r.t., under Ar atmosphere. A solution of **28** (500 mg, 1.83 mmol, 1 eq.) in 3 mL of dry DCM was added one portion. The resulting mixture was stirred for 18 h at r.t. and filtered through a celite plug. The solvent was removed and the product was purified by flash chromatography (95:5 hexane/AcOEt) gave 320 mg of **29** as a pale-yellow oil (1.17 mmol, 64%). ¹H NMR (400 MHz, CDCl₃) δ 7.08-7.04 (m, 2H), 6.89-6.86 (m, 2H), 5.79-5.71 (m, 1H), 5.28-5.24 (m, 1H), 5.20-5.15 (m, 2H), 3.83 (s, 3H), 1.19 (d, $J = 6.9$ Hz, 3H).

***N*-(4-Methoxyphenyl)-3-amino-1-butene (**26**)**^[9a]



Potassium carbonate (380 mg, 2.75 mmol, 2.5 eq.) was added at r.t. to the solution of amide **29** (300 mg, 1.10 mmol, 1 eq.) in 5:1 MeOH/H₂O. The resulting solution was heated to reflux and stirred for 3 h. Upon cooling to r.t., the reaction mixture was washed with DCM (10 mL) and water (10 mL) and the phases were separated. The aqueous phase was extracted with DCM (3 × 20 mL) and the combined organic phases were washed with brine (20 mL), dried with Na₂SO₄ and concentrated. The crude was purified by flash chromatography (9:1 hexane/AcOEt) giving 191 mg of **26** (1.08 mmol, 98%). ¹H NMR (400 MHz, CDCl₃) δ 6.76 (d, $J = 8.9$, 2H), 6.58 (d, $J = 8.9$, 2H), 5.87-5.78 (m, 1H), 5.20 (dt, $J = 17.2$, 1.4 Hz, 1H), 5.07 (dt, $J = 10.4$, 1.4 Hz, 1H), 3.94-3.87 (m, 1H), 3.74 (s, 3H), 1.29 (d, $J = 6.6$ Hz, 3H).

3.3.2.2 Control experiment

Toluene (0.25 mL) was added to a mixture of pre-catalyst **9d** (9.6 mg, 0.025 mmol, 0.05 eq.) and Me₃NO (3.8 mg, 0.050 mmol, 0.1 eq.) under argon in a Schlenk vessel fitted with a Teflon screw cap. The resulting solution, which gradually turned from yellow to dark red, was stirred for 20 minutes at r.t. Compound **26** (0.5 mmol, 1 eq.) was added, followed by 3 Å M.S. (beads, 400 mg), alcohol (1.5 mmol, 3 eq.) and additional toluene (1.75 mL). The reaction vessel was sealed and stirred in a pre-heated oil bath at 150 °C for the 24 h. After cooling down, the mixture was filtered through celite (rinsing several times with AcOEt), and then the solvent was removed at rotavapor. NMR analysis revealed the exclusive presence of unreacted compound **26** in the reaction crude.

3.3.3 Catalytic Tests – ‘hydrogen-borrowing’ amination of secondary alcohols – General Procedure

3.3.3.1 General Procedure for the HB amination of alcohols

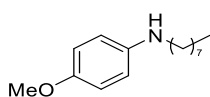
Pre-catalyst **9d** (9.6 mg, 0.025 mmol, 0.05 eq.) and Me₃NO (3.8 mg, 0.050 mmol, 0.1 eq.) were weighted in a Schlenk vessel fitted with a Teflon screw cap. The mixture was added dry toluene (0.25 mL) under argon and stirred for 20 minutes at r.t. The resulting solution gradually turned from yellow to dark red in this process. The amine substrate (0.5 mmol, 1 eq.), 3 Å M.S. (beads, 400 mg), alcohol (2.0 mmol, 4.0 eq.) and additional toluene (1.75 mL) were added successively. The reaction vessel was sealed and stirred in a pre-heated oil bath at 150 °C for the 24 h or 72 h. After cooling down to r.t., the resulting mixture was filtered through celite (rinsing several times with AcOEt), and then the solvent was removed under reduced pressure. The product was purified by flash chromatography (eluent: hexane/AcOEt mixtures, with 0.5-1% Et₃N additive in some cases)

3.3.3.2 Characterization data of amines products

The analytical data are in accordance with those reported in literature (see references in each case)

Amine (name, chemical formula)	Data
--------------------------------	------

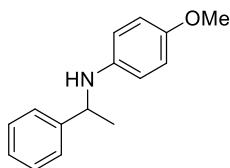
4-*N*-Octylamino-1-methoxybenzene (P39):^[8]



¹H NMR (400 MHz, CDCl₃): δ 6.78 (d, *J* = 8.9 Hz, 2H), 6.58 (d, *J* = 8.9 Hz, 2H), 3.75 (s, 3H), 3.06 (t, *J* = 7.1 Hz, 2H), 1.62-1.55 (m, 2H), 1.41-1.25 (m, 10H), 0.88 (t, *J* = 6.7 Hz, 3H).

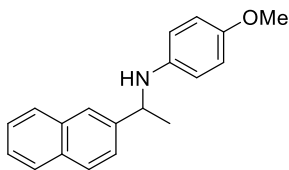
FCC eluent: hexane/AcOEt from 99:1 to 95:5 (+ 0.5% TEA).

4-Methoxy-*N*-(1-phenylethyl)aniline (P1):^[13]



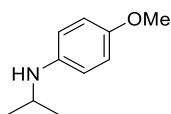
¹H NMR (400 MHz, CDCl₃): δ = 7.42–7.34 (m, 4 H), 7.29–7.25 (m, 1 H), 6.74 (d, *J* = 8.9 Hz, 2 H), 6.52 (d, *J* = 8.9 Hz, 2 H), 4.46 (q, *J* = 6.7 Hz, 1 H), 3.73 (s, 3 H), 1.54 (d, *J* = 6.7 Hz, 3 H).

FCC eluent: hexane/AcOEt 99: 1

4-Methoxy-*N*-(1-(naphthalen-2-yl)ethyl)aniline (P20):^[14]

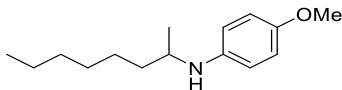
¹H NMR (400 MHz, CDCl₃): δ = 7.83–7.79 (m, 4 H), 7.52 (dd, *J* = 8.5, 1.7 Hz, 1 H), 7.48–7.41 (m, 2 H), 6.68 (d, *J* = 9.0 Hz, 2 H), 6.55 (d, *J* = 9.0 Hz, 2 H), 4.58 (q, *J* = 6.7 Hz, 1 H), 3.68 (s, 3 H), 1.60 (d, *J* = 6.7 Hz, 3 H).

FCC eluent: hexane/AcOEt 95: 1

4-(Isopropilamino)anisole (P40):^[8]

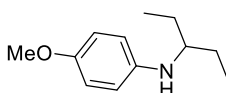
¹H NMR (400 MHz, CDCl₃): δ 6.78 (d, *J* = 8.8 Hz, 2H), 6.60 (d, *J* = 8.8 Hz, 2H), 3.75 (s, 3H), 3.59-3.50 (m, 1H), 1.19 (d, *J* = 6.3 Hz, 6H).

FCC eluent: hexane/AcOEt 95:5.

4-Methoxy-*N*-(octan-2-yl)aniline (P25):^[15]

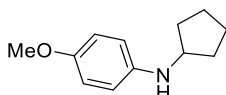
¹H NMR (400 MHz, CDCl₃) δ 6.77 (d, *J* = 8.9 Hz, 2H), 6.62-6.59 (m, 2H), 3.75 (s, 3H), 3.36-3.33 (m, 1H), 1.43-1.27 (m, 10H), 1.16 (d, *J* = 6.3 Hz, 3H), 0.88 (t, *J* = 6.9 Hz, 3H).

FCC eluent: hexane/AcOEt 99: 1

4-Methoxy-*N*-(3-pentyl)aniline (P41):^[16]

¹H NMR (400 MHz, CDCl₃): δ 6.77 (d, *J* = 8.9 Hz, 2H), 6.55 (d, *J* = 8.9 Hz, 2H), 3.74 (s, 3H), 3.14 (pent, *J* = 5.9 Hz, 1H), 1.62-1.42 (m, 4H), 0.93 (t, *J* = 7.4 Hz, 6H).

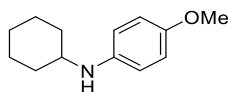
FCC eluent: hexane/AcOEt 99:1.

***N*-Cyclopentyl-4-methoxyaniline (P42):**^[17]

¹H NMR (400 MHz, CDCl₃): δ 6.77 (d, *J* = 8.9 Hz, 2H), 6.58 (d, *J* = 8.9 Hz, 2H), 3.74 (s, 3H), 3.73-3.71 (m, 1H), 2.05-1.96 (m, 2H), 1.74-1.69 (m, 2H), 1.63-1.58 (m, 2H), 1.49-1.41 (m, 2H).

FCC eluent: hexane/AcOEt 70:30.

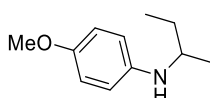
***N*-Cyclohexyl-4-methoxyaniline (P37):**^[8]



^1H NMR (400 MHz, CDCl_3) δ 6.76 (d, $J = 8.9$ Hz, 2H), 6.57 (d, $J = 8.9$ Hz, 2H), 3.74 (s, 3H), 3.20-3.12 (m, 1H), 2.06-2.02 (m, 2H), 1.78-1.72 (m, 2H), 1.67-1.63 (m, 1H), 1.40-1.10 (m, 5H).

FCC eluent: hexane/AcOEt 99: 1

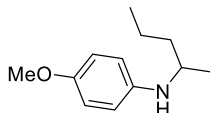
***N*-(*sec*-Butyl)-4-methoxyaniline (P43)^[17]**



^1H NMR (400 MHz, CDCl_3): δ 6.77 (d, $J = 8.9$ Hz, 2H), 6.55 (d, $J = 8.9$ Hz, 2H), 3.74 (s, 3H), 3.33-3.29 (m, 1H), 1.61-1.57 (m, 1H), 1.49-1.38 (m, 1H), 1.15 (d, $J = 6.3$ Hz, 3H), 0.94 (t, $J = 7.4$ Hz, 3H).

FCC eluent: hexane/AcOEt 95:5.

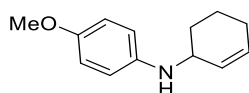
4-Methoxy-*N*-(pentan-2-yl)aniline (P44):^[17]



^1H NMR (400 MHz, CDCl_3): δ 6.77 (d, $J = 8.9$ Hz, 2H), 6.59 (d, $J = 8.9$ Hz, 2H), 3.75 (s, 3H), 3.41-3.34 (m, 1H), 1.60-1.52 (m, 1H), 1.45-1.36 (m, 3H), 1.15 (d, $J = 6.3$ Hz, 3H), 0.92 (t, $J = 7.1$ Hz, 3H).

FCC eluent: hexane/AcOEt 95:5.

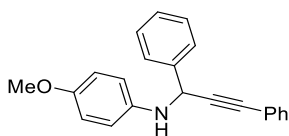
***N*-(Cyclohex-2-en-1-yl)-4-methoxyaniline (P45):^[18]**



^1H NMR (400 MHz, CDCl_3): δ 6.78 (d, $J = 8.9$ Hz, 2H), 6.61 (d, $J = 8.8$ Hz, 2H), 5.86-5.74 (m, 2H), 3.91 (br s, 1H), 3.75 (s, 3H), 2.06-2.00 (m, 2H), 1.94-1.87 (m, 1H), 1.77-1.55 (m, 3H).

FCC eluent: hexane/AcOEt 98:2.

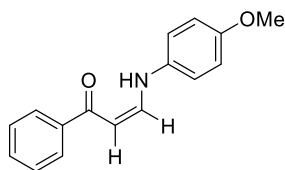
***N*-(1,3-Diphenylprop-2-yn-1-yl)-4-methoxyaniline (P46):^[19]**



^1H NMR (400 MHz, CDCl_3): δ 7.67-7.65 (m, 2H), 7.43-7.38 (m, 4H), 7.36-7.27 (m, 4H), 6.82-6.75 (m, 4H), 5.41 (s, 1H), 3.88 (bs, 1H), 3.76 (s, 3H).

FCC eluent: hexane/AcOEt 98:2.

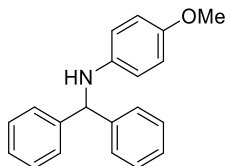
4-Methoxy-*N*-(1-phenylprop-2-yn-1-yl)aniline (P47):^[20]



$^1\text{H NMR}$ (400 MHz, CDCl_3): δ 12.19 (d, $J = 12.4$ Hz, 1 H), 7.93 (d, $J = 6.5$ Hz, 2 H), 7.51–7.42 (m, 4 H), 6.06 (d, $J = 8.9$ Hz, 2 H), 6.90 (d, $J = 8.9$ Hz, 2 H), 5.98 (d, $J = 7.7$ Hz, 1 H), 3.81 (s, 3 H).

FCC eluent: hexane/AcOEt 98:2.

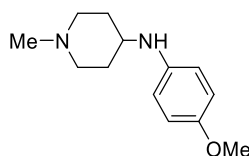
***N*-Benzhydryl-4-methoxyaniline (P21):**^[21]



$^1\text{H NMR}$ (400 MHz, CD_2Cl_2) δ 7.39–7.30 (m, 8 H), 7.27–7.22 (m, 2 H), 6.68 (d, $J = 8.9$ Hz, 2 H), 6.50 (d, $J = 8.9$ Hz, 2 H), 5.44 (s, 1 H), 4.12 (br s, 1 H), 3.67 (s, 3 H).

FCC eluent: hexane/AcOEt 98:2.

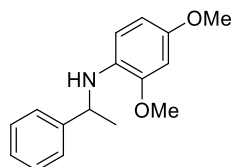
***N*-(4-Methoxyphenyl)-1-methylpiperidin-4-amine (P48)**^[22]



$^1\text{H NMR}$ (400 MHz, CDCl_3): $\delta =$ 6.77 (d, $J = 8.9$ Hz, 2H), 6.58 (d, $J = 8.9$ Hz, 2H), 3.74 (s, 3H), 3.24-3.17 (m, 1H), 2.85-2.82 (m, 2H), 2.31 (s, 3H), 2.17-2.03 (m, 4H), 1.53-1.44 (m, 2H).

FCC eluent: DCM/MeOH 9:1 + 0.5% Et_3N

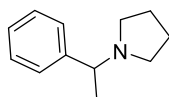
2,4-Dimethoxy-*N*-(1-phenylethyl)aniline (P49):^[23]



$^1\text{H NMR}$ (400 MHz, CDCl_3): δ 7.37-7.29 (m, 4H), 7.23-7.19 (m, 1H), 6.44 (t, $J = 1.4$ Hz, 1H), 6.24-6.23 (m, 2H), 4.40 (q, $J = 6.7$ Hz, 1H), 4.29 (bs, 1H), 3.86 (s, 3H), 3.69 (s, 3H), 1.53 (d, $J = 6.7$ Hz, 3H).

FCC eluent: hexane/AcOEt from 99:1 to 90:10.

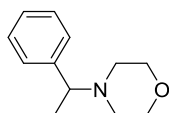
1-(1-Phenylethyl)pyrrolidine (P50):^[24]



$^1\text{H NMR}$ (400 MHz, CDCl_3): δ 7.37-7.23 (m, 5H), 3.21 (q, $J = 6.6$ Hz, 1H), 2.61-2.55 (m, 2H), 2.43-2.35 (m, 2H), 1.82-1.75 (m, 4H), 1.43 (d, $J = 6.6$ Hz, 3H).

FCC eluent: hexane/AcOEt from 95:5 to 70:30.

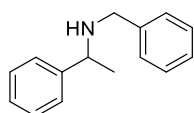
4-(1-Phenylethyl)morpholine (P51):^[25]



^1H NMR (400 MHz, CDCl_3) δ 7.34–7.33 (m, 4 H), 7.29–7.23 (m, 1 H), 3.71 (t, $J = 4.7$ Hz, 4 H), 3.32 (q, $J = 6.7$ Hz, 1 H), 2.56–2.47 (m, 2 H), 2.42–2.32 (m, 2 H), 1.38 (d, $J = 6.7$ Hz, 3 H).

FCC eluent: hexane/AcOEt 80:20 (+ 0.5% TEA).

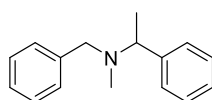
***N*-Benzyl-1-phenylethylamine (P15):^[26]**



^1H NMR (400 MHz, CDCl_3): δ 7.36–7.24 (m, 10 H), 3.82 (q, $J = 6.8$ Hz, 1 H), 3.67 (d, $J = 13.1$ Hz, 1 H), 3.60 (d, $J = 13.1$ Hz, 1 H), 1.37 (d, $J = 6.6$ Hz, 3 H)

FCC eluent: hexane/AcOEt 95:5.

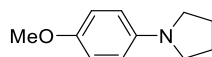
***N*-Benzyl-*N*-methyl-1-phenylethylamine (P52):^[27]**



^1H NMR (400 MHz, CDCl_3): δ 7.42–7.23 (m, 10H), 3.64 (q, $J = 6.8$ Hz, 1H), 3.58 (d, $J = 13.3$ Hz, 1H), 3.31 (d, $J = 13.3$ Hz, 1H), 2.14 (s, 3H), 1.43 (d, $J = 6.7$ Hz, 3H).

FCC eluent: hexane/AcOEt 95: 5.

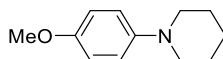
1-(4-Methoxyphenyl)pyrrolidine (P53):^[28]



^1H NMR (400 MHz, CDCl_3): δ 6.87 (d, $J = 9.0$ Hz, 2H) , 6.56 (d, $J = 9.0$ Hz, 2H), 3.78 (s, 3H), 3.27–3.24 (m, 4H), 2.03–1.99 (m, 4H).

FCC eluent: hexane/AcOEt from 98: 2 to 95: 5.

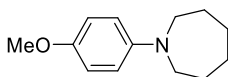
1-(4-Methoxyphenyl)piperidine (P54):^[28]



^1H NMR (400 MHz, CDCl_3): δ 6.92 (d, $J = 9.1$ Hz, 2H), 6.83 (d, $J = 9.1$ Hz, 2H), 3.77 (s, 3H), 3.04–3.01 (m, 4H), 1.75–1.69 (m, 4H), 1.57–1.51 (m, 2H).

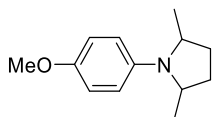
FCC eluent: hexane/AcOEt from 97: 3 to 97: 3.

1-(4-Methoxyphenyl)azepane (P55):^[28]



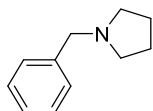
^1H NMR (400 MHz, CDCl_3): δ 6.82 (d, $J = 9.1$ Hz, 2H), 6.63 (d, $J = 9.1$ Hz, 2H), 3.75 (s, 3H), 3.42–3.39 (m, 4H), 1.80–1.74 (m, 4H), 1.55–1.52 (m, 4H).

FCC eluent: hexane/AcOEt from 98:2 to 92:8.

1-(4-Methoxyphenyl)-2,5-dimethylpyrrolidine (P56) (mixture of diastereomers):^[10]

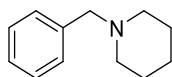
¹H NMR (400 MHz, CDCl₃): δ 6.85-6.82 (m, 2 H), 6.62 (d, *J* = 9.0 Hz, 2 H, *cis*-isomer), 6.55 (d, *J* = 9.0 Hz, 2 H, *trans*-isomer), 3.96-3.93 (m, 2 H, *trans*-isomer), 3.76 (s, 3 H), 3.66-3.62 (m, 2 H, *cis*-isomer), 2.24-2.20 (m, 2 H, *trans*-isomer), 2.07-1.99 (m, 2 H, *cis*-isomer), 1.71-1.69 (m, 2 H, *cis*-isomer), 1.63-1.60 (m, 2 H, *trans*-isomer), 1.25 (d, *J* = 6.1 Hz, 6 H, *cis*-isomer) 1.07 (d, *J* = 6.1 Hz, 6 H, *trans* isomer).

FCC eluent: hexane/AcOEt from 99:1 to 90:10.

N-Benzylpyrrolidine (P57):^[4p]

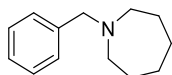
¹H NMR (400 MHz, CDCl₃): δ 7.39-7.26 (m, 5H), 3.70 (s, 2H), 2.63-2.60 (m, 4H), 1.85-1.82 (s, 4H).

FCC eluent: hexane/AcOEt from 75:25 (+ 0.1% TEA).

N-Benzylpiperidine (P58):^[4p]

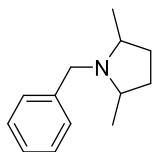
¹H NMR (400 MHz, CDCl₃): δ 7.36-7.25 (m, 5H), 3.52 (d, *J* = 1.8 Hz, 2H), 2.44-2.40 (m, 4H), 1.64-1.58 (m, 4H), 1.47-1.41 (m, 2H).

FCC eluent: hexane/AcOEt from 75:25 (+ 0.1% TEA).

N-Benzylazepane (P59):^[4p]

¹H NMR (400 MHz, CDCl₃): δ 7.36-7.23 (m, 5H), 3.64 (s, 2H), 2.62 (t, *J* = 5.0 Hz, 4H), 1.66-1.60 (m, 8H).

FCC eluent: hexane/AcOEt from 75:25 (+ 0.1% TEA).

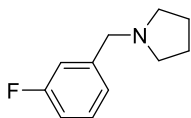
1-Benzyl-2,5-dimethylpyrrolidine (P60), mixture of diastereomers):^[10]

¹H NMR (400 MHz, CDCl₃): δ 7.38-7.25 (m, 4 H), 7.24-7.20 (m, 1 H), 3.83 (d, *J* = 13.8 Hz, 1 H, *trans*-isomer), 3.74 (s, 2 H, *cis*-isomer), 3.52 (d, *J* = 13.8 Hz, 1 H, *trans*-isomer), 3.04-3.00 (m, 2 H, *trans*-isomer), 2.61-2.53 (m, 2 H, *cis*-isomer), 2.05-1.97 (m, 2 H, *trans*-isomer), 1.81-1.74 (m, 2 H, *cis*-isomer), 1.40-1.34 (m, 2 H, *cis*- and *trans*-isomer), 1.05 (d, *J* = 6.0 Hz, 6 H,

cis-isomer), 0.97 (d, $J = 6.0$ Hz, 6 H, *trans*-isomer).

FCC eluent: DCM/MeOH from 98: 2 to 92: 8.

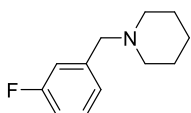
1-(3-Fluorobenzyl)pyrrolidine (P61):^[8]



¹H NMR (400 MHz, CD₂Cl₂): δ 7.27 (td, $J = 7.9, 6.0$ Hz, 1H), 7.12-7.06 (m, 2H), 6.96-6.91 (m, 1H), 3.60 (s, 2H), 2.50-2.47 (m, 4H), 1.78-1.75 (m, 4H).

FCC eluent: DCM/MeOH from 99: 1 to 98: 2(+ 0.5% TEA).

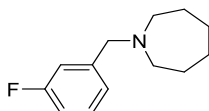
1-(3-Fluorobenzyl)piperidine (P62):^[8]



¹H NMR (400 MHz, CD₂Cl₂): δ 7.26 (td, $J = 8.0, 6.1$ Hz, 1H), 7.10-7.05 (m, 2H), 6.95-6.90 (m, 1H), 3.43 (s, 2H), 2.37-2.32 (m, 4H), 1.58-1.53 (m, 4H), 1.46-1.41 (m, 2H).

FCC eluent: DCM/MeOH from 98: 2 to 97: 3 (+ 0.1% TEA).

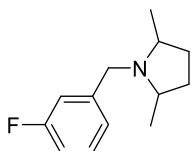
1-(3-Fluorobenzyl)azepane (P63):^[8]



¹H NMR (400 MHz, CDCl₃): δ 7.25 (dt, $J = 7.7, 6.1$ Hz, 1H), 7.12-7.09 (m, 2H), 6.95-6.89 (m, 1H), 3.64 (s, 2H), 2.62 (t, $J = 5.0$ Hz, 4H), 1.66-1.63 (m, 8H).

FCC eluent: hexane/AcOEt from 90:10 (+ 0.1% TEA).

1-(3-Fluorobenzyl)-2,5-dimethylpyrrolidine (P64, mixture of diastereomers)



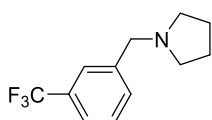
¹H NMR (400 MHz, CD₂Cl₂): 7.27-7.23 (m, 1 H), 7.15-7.10 (m, 2 H), 6.94-6.88 (m, 1 H), 3.82 (d, $J = 14.4$ Hz, 1 H, *trans*-isomer), 3.69 (s, 2 H, *cis*-isomer), 3.58 (d, $J = 14.4$ Hz, 1 H, *trans*-isomer), 3.08-3.02 (m, 2 H, *trans*-isomer), 2.65-2.58 (m, 2 H, *cis*-isomer), 2.06-1.98 (m, 2 H, *trans*-isomer), 1.87-1.76 (m, 2 H, *cis*-isomer), 1.46-1.32 (m, 2 H), 1.00 (d, $J = 6.1$ Hz, 6 H, *cis*-isomer), 0.97 (d, $J = 6.3$ Hz, 6 H, *trans*-isomer); ¹³C NMR (100MHz, CD₂Cl₂): δ 163.6 (d, $J_{C,F} = 242.4$ Hz, *trans* isomer), 163.4 (d, $J_{C,F} = 242.5$ Hz, *cis* isomer), 144.8 (d, $J_{C,F} = 9.2$ Hz), 130.0 (d, $J_{C,F} = 9$ Hz, *trans* isomer), 129.8 (d, $J_{C,F} = 8.3$ Hz, *cis* isomer), 124.8 (d, $J_{C,F} = 2.6$ Hz, *cis* isomer), 124.5 (d, $J_{C,F} = 2.6$ Hz, *trans* isomer), 116.0 (d, $J = 21.1$ Hz, *cis* isomer), 115.6 (d,

$J = 21.2$ Hz, *trans* isomer), 113.7 (d, $J_{C,F} = 21.1$ Hz, *trans* isomer), 113.7 (d, $J = 21.1$ Hz, *cis* isomer), 61.6 (*cis* isomer), 56.4 (*cis* isomer), 55.6 (*trans* isomer), 51.6 (*trans* isomer), 32.1 (*cis* isomer), 31.6 (*trans*-isomer), 21.4 (*cis* isomer), 17.5 (*trans* isomer); ^{19}F NMR (282 MHz, CD_2Cl_2): $\delta = -115.15$; IR (neat) 2962.13, 2927.41, 2870.52, 2802.06, 1616.06, 1590.99, 1485.88, 1450.21, 1373.07, 1350.89, 1328.71, 1254.47, 1203.36, 1130.08, 1073.19, 992.20, 944.95, 926.63, 871.67, 783.92, 745.35, 686.53 cm^{-1}

HRMS (ESI+): m/z 208.1501 $[\text{M}+\text{H}]^+$ (calcd. for $\text{C}_{13}\text{H}_{19}\text{FN}$: 208.1502).

FCC eluent: DCM/MeOH 97: 3.

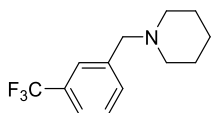
1-(3-(Trifluoromethyl)benzyl)pyrrolidine (P65):^[29]



^1H NMR (400 MHz, CDCl_3): δ 7.60-7.59 (m, 1H), 7.54-7.49 (m, 2H), 7.42 (t, $J = 7.7$ Hz, 1H), 3.67 (s, 2H), 2.54-2.51 (m, 4H), 1.82-1.79 (m, 4H).

FCC eluent: hexane/AcOEt from 7:3 to 3: 2 (+ 0.1% TEA).

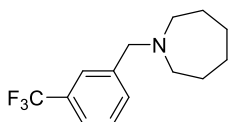
1-(3-(Trifluoromethyl)benzyl)piperidine (P66):^[29]



^1H NMR (400 MHz, CDCl_3): δ 7.58 (s, 1H), 7.50 (t, $J = 8.3$ Hz, 2H), 7.41 (t, $J = 7.7$ Hz, 1H), 3.51 (s, 2H), 2.37 (t, $J = 5.2$ Hz, 4H), 1.61-1.55 (m, 4H), 1.47-1.42 (m, 2H).

FCC eluent: hexane/AcOEt from 7: 3.

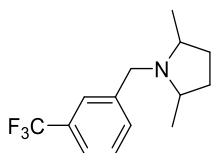
1-(3-(Trifluoromethyl)benzyl)azepane (P67):^[8]



^1H NMR (400 MHz, CDCl_3): δ 7.63 (s, 1H), 7.55 (d, $J = 7.6$ Hz, 1H), 7.50-7.48 (m, 1H), 7.41 (t, $J = 7.7$ Hz, 1H), 3.69 (s, 2H), 2.63 (t, $J = 4.8$ Hz, 4H), 1.66-1.63 (m, 8H).

FCC eluent: hexane/AcOEt from 90:10 (+ 0.1% TEA).

2,5-Dimethyl-1-(3-(trifluoromethyl)benzyl)pyrrolidine (P68, mixture of diastereomers)



^1H NMR (400 MHz, CDCl_3): δ 7.64 (s, 1H, *trans*-isomer), 7.59 (s, 1H, *cis*-isomer), 7.56 (d, $J = 7.6$ Hz, 1H, *trans*-isomer), 7.52 (d, $J = 7.8$ Hz, 1H, *cis*-isomer), 7.47 (d, $J = 8.0$ Hz, 1H), 7.39 (t, $J = 7.6$ Hz, 1H), 3.85 (d, $J = 14.4$

Hz, 1 H, *trans*-isomer), 3.75 (s, 2 H, *cis*-isomer), 3.60 (d, $J = 14.4$ Hz, 1 H, *trans*-isomer), 3.04–3.00 (m, 2 H, *trans*-isomer), 2.61–2.56 (m, 2 H, *cis*-isomer), 2.04–1.98 (m, 2 H, *trans*-isomer), 1.85–1.79 (m, 2 H, *cis*-isomer), 1.43–1.35 (m, 2 H), 1.00 (d, $J = 6.0$ Hz, 6 H, *cis*-isomer), 0.96 (d, $J = 6.4$ Hz, 6 H, *trans*-isomer). ^{13}C NMR (100MHz, CDCl_3): δ 142.2 (*trans* isomer), 141.9 (*cis* isomer), 132.2 (q, $J_{\text{C,F}} = 2.6$ Hz, *cis* isomer), 131.8 (q, $J_{\text{C,F}} = 2.5$ Hz, *trans* isomer), 130.5 (q, $J_{\text{C,F}} = 31.7$ Hz, *trans* isomer), 130.4 (q, $J_{\text{C,F}} = 31.7$ Hz, *cis* isomer), 128.5 (*trans* isomer), 128.4 (*cis* isomer), 125.5 (q, $J_{\text{C,F}} = 7.6$ Hz, *cis* isomer), 125.1 (q, $J_{\text{C,F}} = 7.5$ Hz, *trans* isomer), 124.5 (d, $J_{\text{C,F}} = 270.5$ Hz, *trans* isomer), 124.5 (d, $J_{\text{C,F}} = 270.4$ Hz, *cis* isomer), 123.5 (q, $J_{\text{C,F}} = 7.7$ Hz), 60.9 (*cis* isomer), 55.9 (*cis* isomer), 55.1 (*trans* isomer), 51.4 (*trans* isomer), 31.5 (*cis* isomer), 31.1 (*trans* isomer), 21.0 (*cis* isomer), 17.3 (*trans* isomer); ^{19}F NMR (282 MHz, CDCl_3): $\delta = -62.46$; IR (neat) 2964.05, 2928.38, 2871.49, 2803.03, 2611.14, 1676.80, 1615.09, 1597.73, 1491.67, 1451.17, 1374.03, 1329.68, 1256.40, 1199.51, 1163.83, 1126.22, 1091.51, 1073.19, 948.81, 920.84, 889.99, 799.35, 750.17, 702.93, 660.50 cm^{-1} ; HRMS (ESI+): m/z 258.1472 $[\text{M}+\text{H}]^+$ (calcd. for $\text{C}_{14}\text{H}_{19}\text{F}_3\text{N}$: 258.1470).

FCC eluent: hexane/AcOEt from 85: 15 to 4: 1 (+0.1% TEA).

References

- [1] For the importance of amines as fine chemistry intermediates, see: (a) S. A. Lawerence, *Amine: Synthesis Properties and Applications*; Cambridge University Press: Cambridge, **2004**; (b) B. R. Brown, *The Organic chemistry of Aliphatic Nitrogen Compounds*; Cambridge University: Cambridge, **2004**.
- [2] a) F. Valot, F. Fache, R. Jacquot, M. Spagnol, M. Lemaire, *Tetrahedron Lett.* **1999**, *40*, 3689-3692; b) S. Narayanan, K. Deshpande, *Appl. Catal., A* **2000**, *199*, 1-31.
- [3] a) S.-I. Murahashi, K. Kondo, T. Hakata, *Tetrahedron Lett.* **1982**, *23*, 229-232; b) R. Grigg, T. R. B. Mitchell, S. Sutthivaiyakit, N. Tongpenyai, *J. Chem. Soc., Chem. Commun.* **1981**, 611-612; c) Y. Watanabe, Y. Tsuji, Y. Ohsugi, *Tetrahedron Lett.* **1981**, *22*, 2667-2670.
- [4] For ruthenium, see: a) K. O. Marichev, J. M. Takacs, *ACS Catal.* **2016**, *6*, 2205-2210; b) V. R. Jumde, L. Gonsalvi, A. Guerriero, M. Peruzzini, M. Taddei, *Eur. J. Org. Chem.* **2015**, 1829-1833; c) V. R. Jumde, E. Cini, A. Porcheddu, M. Taddei, *Eur. J. Org. Chem.* **2015**, 1068-1074; d) E. Balaraman, D. Srimani, Y. Diskin-Posner, D. Milstein, *Catal. Lett.* **2015**, *145*, 139-144; e) S. P. Shan, X. Xiaoke, B. Gnanaprakasam, T. T. Dang, B. Ramalingam, H. V. Huynh, A. M. Seayad, *RSC Adv.* **2015**, *5*, 4434-4442; f) N. J. Oldenhuis, V. M. Dong, Z. Guan, *J. Am. Chem. Soc.* **2014**, *136*, 12548-12551; g) A. B. Enyong, B. Moasser, *J. Org. Chem.* **2014**, *79*, 7553-7563; h) M. Chen, M. Zhang, F. Xie, X. Wang, H. Jiang, *ChemCatChem* **2014**, *6*, 2993-2997; i) S. Demir, F. Coşkun, İ. Özdemir, *J. Organomet. Chem.* **2014**, *755*, 134-140; j) M. H. S. A. Hamid, C. L. Allen, G. W. Lamb, A. C. Maxwell, H. C. Maytum, A. J. A. Watson, J. M. J. Williams, *J. Am. Chem. Soc.* **2009**, *131*, 1766-1774. For iridium, see: k) S. Wöckel, P. Plessow, M. Schelwies, M. K. Brinks, F. Rominger, P. Hofmann, M. Limbach, *ACS Catal.* **2014**, *4*, 152-161; l) Y. Zhang, C.-S. Lim, D. S. B. Sim, H.-J. Pan, Y. Zhao, *Angew. Chem., Int. Ed.* **2014**, *53*, 1399-1403; m) S. Ruch, T. Irrgang, R. Kempe, *Chem. Eur. J.* **2014**, *20*, 13279-13285; n) P. Qu, C. Sun, J. Ma, F. Li, *Adv. Synth. Catal.* **2014**, *356*, 447-459; o) Y.-H. Chang, Y. Nakajima, F. Ozawa, *Organometallics* **2013**, *32*, 2210-2215; p) K.-i. Fujita, T. Fujii, R. Yamaguchi, *Org. Lett.* **2004**, *6*, 3525-3528.
- [5] a) A. Martínez-Asencio, D. J. Ramón, M. Yus, *Tetrahedron Lett.* **2010**, *51*, 325-327; b) F. Shi, M. K. Tse, X. Cui, D. Gördes, D. Michalik, K. Thurow, Y. Deng, M. Beller, *Angew. Chem., Int. Ed.* **2009**, *48*, 5912-5915.
- [6] S. Rösler, M. Ertl, T. Irrgang, R. Kempe, *Angew. Chem., Int. Ed.* **2015**, *54*, 15046-15050.
- [7] a) M. Bala, P. K. Verma, U. Sharma, N. Kumar, B. Singh, *Green Chem.* **2013**, *15*, 1687-1693; b) X. Cui, F. Shi, Y. Zhang, Y. Deng, *Tetrahedron Lett.* **2010**, *51*, 2048-2051; c) U. Jana, S. Maiti, S. Biswas, *Tetrahedron Lett.* **2008**, *49*, 858-862.
- [8] T. Yan, B. L. Feringa, K. Barta, *Nat. Commun.* **2014**, *5*, 5602.
- [9] a) L. E. Overman, C. E. Owen, M. M. Pavan, C. J. Richards, *Org. Lett.* **2003**, *5*, 1809-1812; b) L. E. Overman, *Angew. Chem., Int. Ed.* **1984**, *23*, 579-586; c) K. Tamura, H. Mizukami, K. Maeda, H. Watanabe, K. Uneyama, *J. Org. Chem.* **1993**, *58*, 32-35.
- [10] C. Boga, F. Manescalchi, D. Savoia, *Tetrahedron* **1994**, *50*, 4709-4722.
- [11] T. Yan, B. L. Feringa, K. Barta, *ACS Catal.* **2016**, *6*, 381-388.
- [12] W. C. Still, M. Kahn, A. Mitra, *J. Org. Chem.* **1978**, *43*, 2923-2925.
- [13] D. J. Fisher, J. B. Shaum, C. L. Mills, J. Read de Alaniz, *Org. Lett.* **2016**, *18*, 5074-5077.
- [14] P. Renzi, J. Hioe, R. M. Gschwind, *J. Am. Chem. Soc.* **2017**, *139*, 6752-6760.
- [15] J. Li, C. Wang, D. Xue, Y. Wei, J. Xiao, *Green Chem.* **2013**, *15*, 2685-2689.
- [16] B. Li, J.B. Sortais, C. Darcel, P. H. Dixneuf, *ChemSusChem* **2012**, *5*, 396-399.
- [17] D. Gülcemal, S. Gülcemal, C. M. Robertson, J. Xiao, *Organometallics* **2015**, *34*, 4394-4400.
- [18] S. Silva, P. Rodrigues, I. Bento, C. D. Maycock, *J. Org. Chem.* **2015**, *80*, 3067-3074.
- [19] X. Liu, B. Lin, Z. Zhang, H. Lei, Y. Li, *RSC Adv.* **2016**, *6*, 94399-94407.
- [20] R. J. Detz, Z. Abiri, R. le Griel, H. Hiemstra, J. H. van Maarseveen, *Chem. Eur. J.* **2011**, *17*, 5921-5930.
- [21] T. Iwai, T. Harada, H. Shimada, K. Asano, M. Sawamura, *ACS Catal.* **2017**, *7*, 1681-1692.
- [22] E. Perissutti, F. Fiorino, C. Renner, B. Severino, F. Roviezzo, L. Sautebin, A. Rossi, G. Cirino, V. Santagada, G. Caliendo, *Journal of Medicinal Chemistry* **2006**, *49*, 7774-7780.
- [23] S. D. L. Marin, T. Martens, C. Mioskowski, J. Royer, *J. Org. Chem.* **2005**, *70*, 10592-10595.
- [24] E. Kuchuk, K. Muratov, D. S. Perekalin, D. Chusov, *Org. Biomol. Chem.* **2019**, *17*, 83-87.
- [25] Y. Otake, J. D. Williams, J. A. Rincón, O. D. Frutos, C. Mateos, C. Oliver Kappe, *Org. Biomol. Chem.* **2019**, *17*,

1384-1388.

- [26] R. R. R. Prasad, D. M. Dawson, P. A. Cox, S. E. Ashbrook, P. A. Wright, M. L. Clarke, *Chem. Eur. J.* **2018**, *24*, 15309-15318.
- [27] N. Sakai, N. Takahashi, Y. Ogiwara, *Eur. J. Org. Chem.* **2014**, 5078-5082.
- [28] C. Deldaele, G. Evano, *ChemCatChem* **2016**, *8*, 1319-1328.
- [29] N. Choudhary, U. Gupta, O. D. Gupta, *Int.J. ChemTech Res.* **2014**, *6*, 5687-5691.

Chapter 4 - Chiral complexes for enantioselective applications

As discussed in Chapter 1, CICs have recently become the object of a blossoming interest among researchers active in the field of hydrogen transfer reactions. Nevertheless, applications of these complexes in enantioselective catalysis are still very limited, with the exception of the dual catalysis approach reported by Beller *et al.* in 2011, in which a chiral Brønsted acid co-catalyst was combined with an achiral HCIC **10aa**.^[1] In order to expand the catalytic application of CICs to enantioselective catalysis, the development of chiral complexes is an ineludible challenge, which has been tackled – so far with limited success – following two alternative strategies (see Section 1.6.1): 1) replacing one of the CO groups with a chiral ligand (Figure 4.1 A);^[2] 2) using a chiral cyclopentadienone ligand (Figure 4.1 B).^[3] Although several chiral CICs have been developed, only poor to moderate enantioselectivity was obtained in the reduction of ketones and ketimines (Figure 4.1 A and B). A possible explanation of these modest results is that, in these chiral complexes, the stereogenic group(s) sit far away from the substrate in the pericyclic reduction TS (see Figure 4.2).

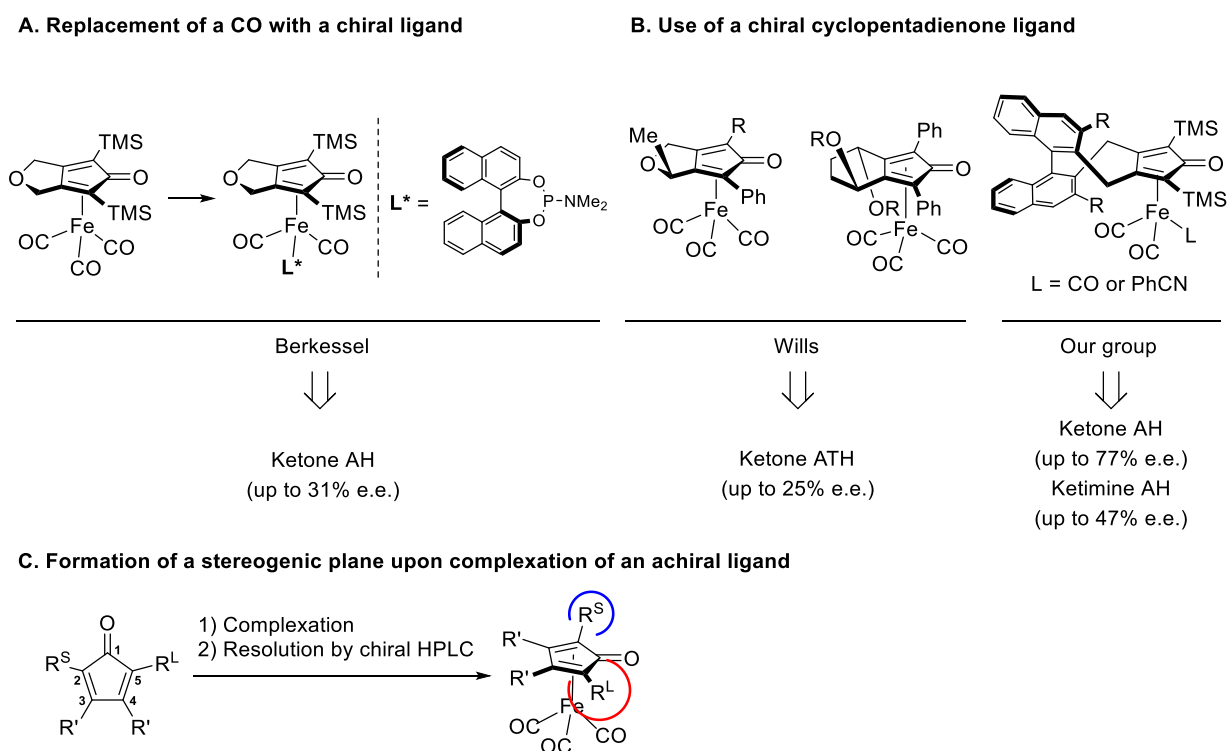


Figure 4.1. Main strategies for synthesis of chiral CICs. AH = asymmetric hydrogenation; ATH = asymmetric transfer hydrogenation.

A third possible strategy is the synthesis of chiral iron complexes possessing a stereogenic plane by employing achiral cyclopentadienones bearing different substituents on the two sides of the C=O group. This strategy has been already applied by Hayashi and co-workers to the synthesis of chiral Shvo-type ruthenium complexes in

2016 (Figure 4.1 C).^[4] We envisaged that chiral complexes featuring substituents of different sizes at the 2,5-positions of the cyclopentadienone ring could ensure a more efficient transfer of the stereochemical information. Moreover, during my PhD work I also contributed to the development of a new class of chiral CICs, in which the Fe-complex is incorporated into a macrocycle.

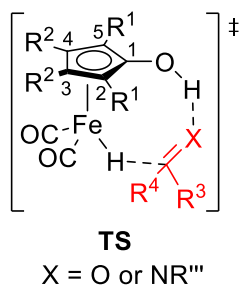


Figure 4.2. TS of the reactions involving transfer of hydrogen promoted by CICs.

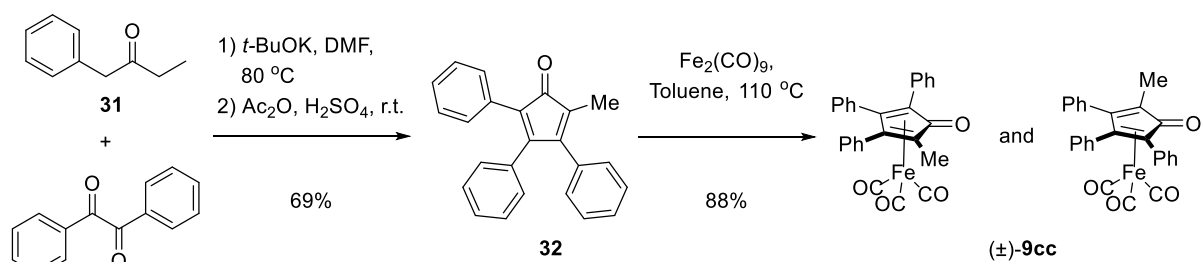
4.1 Chiral CICs featuring a stereogenic plane

As a starting point, the preparation of a small library of racemic complexes and the evaluation of their catalytic activity in ketone and imine hydrogenation was performed. This initial screening aimed at selecting one or two complexes to be subjected to enantiomer separation by semipreparative chiral HPLC (in collaboration with the group of Prof. Pierini and Prof. Gasparri at the Sapienza University of Rome) and then tested in asymmetric hydrogenation.

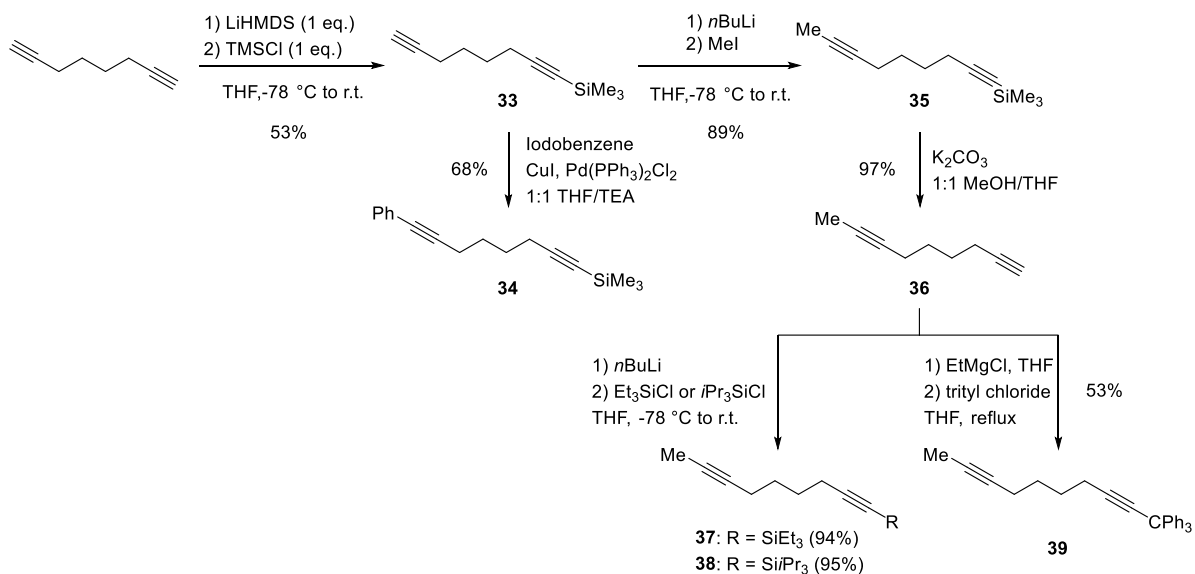
4.1.1 Synthesis of chiral CICs with stereogenic plane in racemic form and test of their catalytic activity

Considering the pericyclic Transition State (TS) typical of the reductions promoted by CICs, we expected that best enantioselectivity should be displayed by those chiral complexes whose substituents at C2 and C5 (see Figure 4.2) are largely different in terms of steric and/or stereoelectronic properties. Indeed, comparing with 3,4 position, the substituents at 2,5 position are relatively close to the approaching substrate.

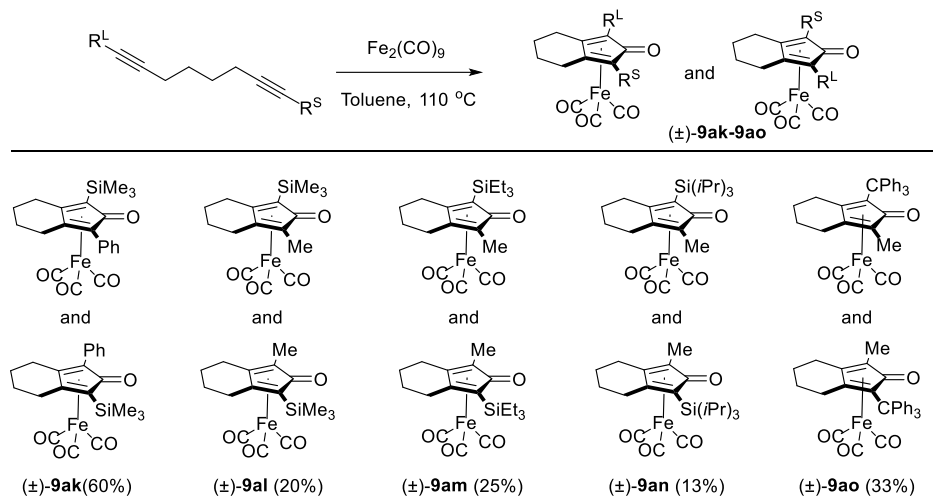
Starting from the new chiral CIC (\pm)-**9cc**, bearing the same cyclopentadienone ligand as one of the Ru-complexes reported by Hayashi,^[4] we prepared a series of chiral iron complexes in racemic form. The commercially available benzil reacted with 1-phenyl-2-butanone (**31**) through condensation followed by dehydration to afford cyclopentadienone **32** with good yield as described in the literature.^[4,5] Then, CIC (\pm)-**9cc** was synthesized by complexation of **32** with $\text{Fe}_2(\text{CO})_9$,^[4] as shown in Scheme 4.1.

Scheme 4.1. Synthesis of the racemic CIC (±)-**9cc**.

A. Synthesis of the asymmetric diyne precursors



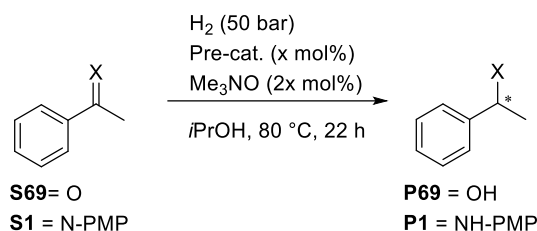
B. Synthesis of the (cyclopentadienone)iron complexes

Scheme 4.2. A: Synthesis of the unsymmetricac diynes **33-39**. B: Synthesis of the racemic CICs (±)-**9ak-9ao**

Subsequently, the commercially available 1,7-octadiyne was employed as a common precursor to synthesize five racemic CICs bearing different substituents at 2,5 positions (Scheme 4.2). The mono-TMS-functionalized diyne **33** was easily synthesized from 1,7-octadiyne upon deprotonation with LiHMDS followed by reaction with trimethylsilyl chloride (TMSCl).^[6] The other C-terminus of compound **33** was functionalized in two

different ways: i) with a methyl group, forming the unsymmetrical diyne **35** by nucleophilic reaction; ii) with a phenyl group, synthesizing the unsymmetrical diyne **34**^[7] through Sonogashira coupling reaction. The former was either de-silylated with K_2CO_3 to provide diyne **36**^[8] or used directly for the synthesis of CIC **9al**. The terminal alkyne group of diyne **36** was either functionalized with a triethylsilyl (TES) or a triisopropylsilyl (TIPS), synthesizing diynes **37**, **38** respectively.^[6] Additionally, the unsymmetrical diyne **39** was prepared by functionalizing diyne **36** in the presence of a Grignard reagent ($EtMgCl$).^[9] After finishing the synthesis of diynes **34-35** and **37-39**, all compounds were treated with $Fe_2(CO)_9$ in toluene at 110 °C, and the racemic CICs (\pm)-**9ak-9ao** were obtained with yields in the 13-60% range.^[10]

Table 4.1. Test of the activity of the racemic complexes (\pm)-**9cc** and (\pm)-**9ak-9ao** in C=O and C=N hydrogenation.^[a]



#	Pre-cat.	Loading (mol%)	Conv. S69 [%] ^[b]	Conv. S1 [%] ^[b]
1	(\pm)- 9cc	2	> 99	> 99
2	(\pm)- 9ak	2	> 99	89
3	(\pm)- 9al	2	> 99	69
4	(\pm)- 9am	2	> 99	4
5	(\pm)- 9an	2	73	8
6	(\pm)- 9ao	2	0	12
7	(\pm)- 9cc	5	> 99	> 99
8	(\pm)- 9ak	5	> 99	> 99
9	(\pm)- 9al	5	> 99	82
10	(\pm)- 9am	5	> 99	92
11	(\pm)- 9an	5	76	62
12	(\pm)- 9ao	5	35	18

[a] Reaction conditions: Pre-cat./ Me_3NO = 1:2, T = 80 °C, P_{H_2} = 50 bar, 22 h. $C_{0,sub.}$ = 0.5 M.

[b] Determined by 1H NMR.

The activity of complexes (\pm)-**9ak-9ao** and (\pm)-**9cc**, activated *in situ* with Me_3NO , was tested in the hydrogenation of acetophenone (**S69**) and (*E*)-*N*-(4-methoxyphenyl)-1-phenylethan-1-imine (**S1**) (Table 4.1).

Excellent conversions of **S69** and **S1** at both 5 mol% and 2 mol% catalyst loading were obtained with pre-catalysts (\pm)-**9cc** and (\pm)-**9ak** (Table 4.1, entries 1-2 and 7-8). A general trend – conversions roughly decrease with the increasing size of the “large” substituent R^L (Table 4.1, entries 3-6 and 9-12) – was clearly found: pre-catalysts (\pm)-**9al** ($R^L = \text{TMS}$) and (\pm)-**9am** ($R^L = \text{TES}$) gave full conversion of **S69** and acceptable conversions of **S1** (entries 9-10), whereas the activity of (\pm)-**9an** ($R^L = \text{TIPS}$) and (\pm)-**9ao** ($R^L = \text{CPh}_3$), possessing bulkier “large” groups, decreased dramatically (Table 4.1 entries 5-6 and 11-12).

Finally, complex (\pm)-**9am** was selected for the enantioselectivity screening, due to its optimal equilibrium between the large size of the R^L substituent and the catalytic activity, and the (\pm)-**9am** racemate was submitted for enantiomer separation. Moreover, the two enantiomers of complex (\pm)-**9cc** were also separated, not only due its superior activity within the catalyst series, but also to establish a comparison with the corresponding ruthenium complex developed by Hayashi and co-workers.^[4]

4.1.2 Resolution of complexes (\pm)-**9cc** and (\pm)-**9am** by semipreparative enantioselective HPLC and determination of the absolute configuration of the enantiomerically pure complexes

The enantiomer separation of complexes (\pm)-**9cc** and (\pm)-**9am** was performed by enantioselective HPLC in the group of Prof. Pierini and Prof. Gasparri at Sapienza University of Rome. In the former case, the enantiomers were resolved on the (*R,R*)-DACH-DNB chiral stationary phase (CSP) under normal phase conditions (mobile phase: *n*-hexane/DCM 80:20 + 2% MeOH *v/v*), using both UV and ECD detection ($k'_1 = 2.36$; $\alpha = 1.27$; $T = 25$ °C, see Figure 4.3 A).

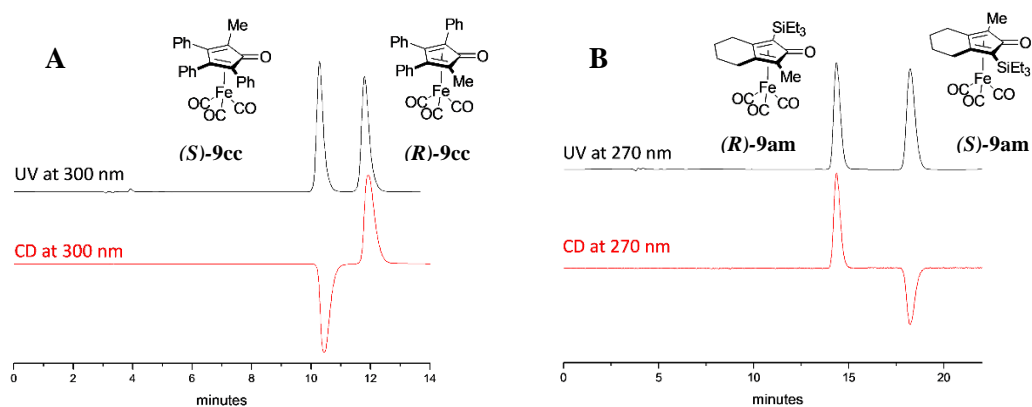


Figure 4.3. Analytical separation of racemic mixtures (\pm)-**9cc** (A) and (\pm)-**9am** (B) by enantioselective HPLC. A) column: (*R,R*)-DACH-DNB 5 μm (250 mm \times 4.6 mm L. \times I.D.); eluent: *n*-hexane/DCM 80:20 + 2% MeOH *v/v*; flow rate 1.0

mL/min at 25 °C. B) column: Chiralpak IC 5 μm (250 mm \times 4.6 mm L. \times I.D.); eluent: *n*-hexane/IPA 95:5 v/v; flow rate 1.0 mL/min at 25 °C.

Once the optimal settings for purification were identified, the separation was scaled-up to semipreparative conditions. The replicate separations (2 mg of sample injected in each run) were carried out on a 1.0 cm internal diameter (*R,R*)-DACH-DNB column. The two enantiomers were obtained in an overall recovery of 80%. The e.e. values of the first and second eluted enantiomer were determined by analytical HPLC with UV and ECD detection at 300 nm, which were 99% and 98%, respectively.

The enantiomer separation of racemic complexes (\pm)-**9am** was carried out on a different Chiralpak IC CSP column (mobile phase: *n*-hexane/IPA 95:5 v/v), and an α value of 1.37 was achieved ($k'_1 = 2.84$, Figure 4.3 B). Each enantiomer (70 mg, process yield = 79%) obtained in the semipreparative scale-up stage has a high enantiomeric excess value (up to 99%), as measured by analytical HPLC with UV and CD detection at 270 nm.

With the enantiopure **9cc** and **9am** complexes in hands, the assignment of the absolute configuration (AC) of the separated enantiomers was carried out.^[11] The X-ray diffraction (XRD) analysis may be considered as the first-choice method for AC assignment if configurationally known reference compounds which can be correlated to the chiral analyte is scarce or absent.^[12] Suitable crystals of the first-eluted enantiomer of complex **9cc** for XRD were obtained by vapor diffusion of pentane into a DCM solution of the complex, followed by cooling (-18 °C). Diffractometric analysis of a single crystal – performed by Dr. Valentina Colombo, Università degli Studi di Milano – showed that the absolute configuration of this enantiomer is *S* (Figure 4.4), which was assigned according to the extended CIP rules.^[13]

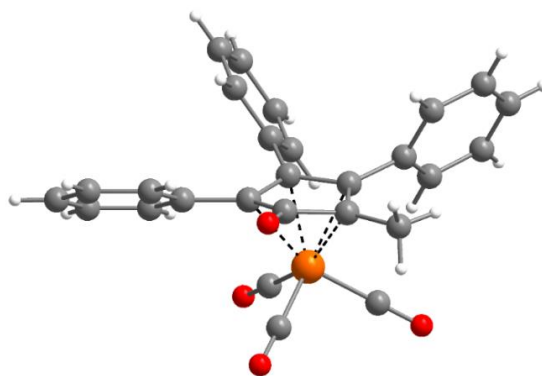


Figure 4.4. X-Ray crystal structure of the first-eluted enantiomer (*S*) of complex **9cc**. Color codes: Fe, orange; O, red; C, gray; H, white. Selected bond distances: Fe-C1B, 1.802(2); Fe-C1A, 1.804(2); Fe-C1C, 1.804(2); Fe-C4, 2.0721(16); Fe-C3, 2.0830(16); Fe-C5, 2.1222(18); Fe-C2, 2.1389(17).

As any attempts to obtain suitable crystals of complex **9am** failed, the AC of the enantiomerically pure **9am**

were assigned by a spectroscopic/computational procedure.^[14] For each enantiomer, electronic circular dichroism (ECD) and optical rotation dispersion (ORD) spectra were registered, and the *R* enantiomer was assigned by similarity with simulated spectra, obtained by DFT calculations. The superimposed spectra are shown in Figure 4.5.

Comparing the ECD and ORD spectra of the first-eluted enantiomer with the calculated, *R* absolute configuration was assigned to the first-eluted enantiomer of **9am**, and *S* configuration to the second eluted.

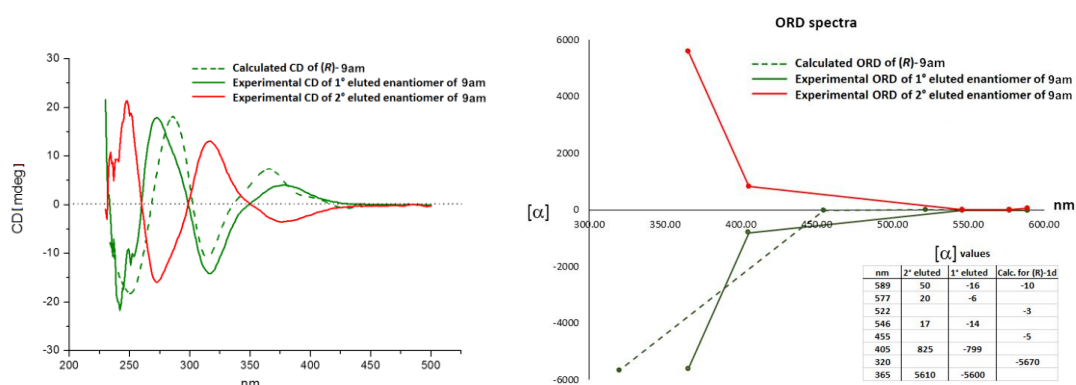
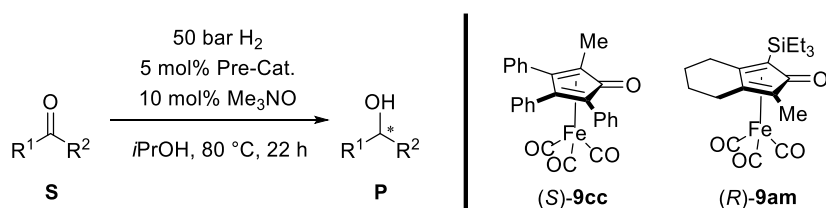


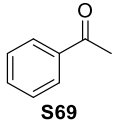
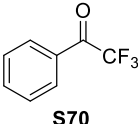
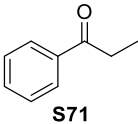
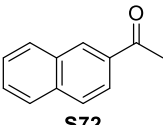
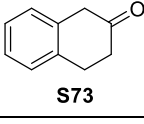
Figure 4.5. ECD and ORD experimental spectra of the resolved enantiomers of **9am** superimposed to the equivalent ones simulated through DFT calculations for the *R* enantiomer.

4.1.3 Asymmetric hydrogenation of C=O and C=N polar bonds with chiral iron complexes

Both enantiomerically pure complexes (*S*)-**9cc** and (*R*)-**9am** were tested in the AH of ketones. Several ketones were reduced to the corresponding alcohols with excellent yields in the presence of pre-catalyst (*R*)-**9am** (Table 4.2). The complex (*S*)-**9cc** showed lower activity than (*R*)-**9am**, affording excellent yields in only three cases (Table 4.2, entries 1-2 and 5). Unfortunately, both pre-catalysts gave low enantioselectivity with substrates **S69**, **S71-73** (Table 4.2, entries 1, 3-5), and only moderate e.e. values were obtained with 2,2,2-trifluoro-1-phenylethan-1-one **S70** (Table 4.2, entries 2). Notably, in most cases (*S*)-**9cc** and (*R*)-**9am** showed opposite stereochemical preference, in line with their opposite configurations.

Table 4.2. AH of ketones promoted by the chiral pre-catalysts (*S*)-**9cc** and (*R*)-**9am**.^[a]



#	Substrate	Pre-catalyst (<i>S</i>)- 9cc		Pre-catalyst (<i>R</i>)- 9am	
		Conv. (%) ^[b]	e.e. (%) ^[b]	Conv. (%) ^[b]	e.e. (%) ^[b]
1 ^[c]	 S69	> 99 (99)	3, <i>R</i>	> 99 (99)	9, <i>R</i>
2 ^[c]	 S70	> 99 (98)	45, <i>R</i>	> 99 (98)	41, <i>S</i>
3 ^[c]	 S71	36 (33)	9, <i>S</i>	> 99 (99)	9, <i>R</i>
4 ^[c]	 S72	73 (72)	13, <i>S</i>	> 99 (99)	18, <i>R</i>
5 ^[d]	 S73	> 99 (85)	14, <i>S</i>	> 99 (99)	18, <i>S</i>

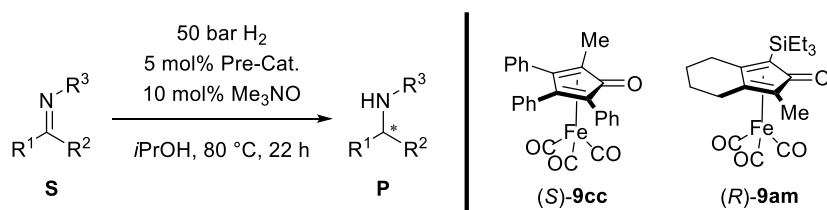
[a] Reaction conditions: Substrate/Me₃NO/Pre-cat. = 100:10:5, *T* = 80 °C, *P*_{H₂} = 50 bar, 22 h. *C*_{0,sub.} = 0.5 M.

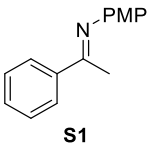
[b] Determined by GC analysis with a chiral capillary column; isolated yield shown in parenthesis.

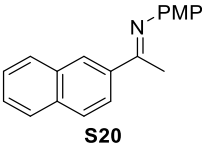
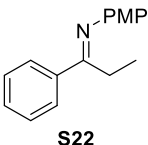
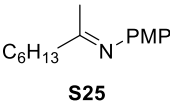
[c] Absolute configuration of the product assigned by comparing the order of elution with literature data (see the experimental section).

[d] Absolute configuration of the product assigned by comparing the sign of optical rotation with literature data (see the experimental section).

Table 4.3. AH of ketimines promoted by the chiral pre-catalysts (*S*)-**9cc** and (*R*)-**9am**.^[a]



#	Substrate	Pre-catalyst (<i>S</i>)- 9cc		Pre-catalyst (<i>R</i>)- 9am	
		Conv. (%) ^[b]	e.e. (%) ^[c]	Conv. (%) ^[b]	e.e. (%) ^[c]
1 ^[d]	 S1	> 99 (98)	40, <i>R</i>	96 (96)	39, <i>S</i>

2 ^[e]		97 (91)	29, <i>R</i>	91 (78)	6, <i>S</i>
3 ^[e]		> 99 (76)	54, <i>R</i>	65 (41)	40, <i>S</i>
4 ^[e]		76 (57)	18, <i>S</i>	73 (48)	6, <i>R</i>

[a] Reaction conditions: Substrate/Me₃NO/Pre-cat. = 100:10:5, *T* = 80 °C, *P*_{H₂} = 50 bar, 22 h. *C*_{0,sub.} = 0.5 M.

[b] Determined by ¹H NMR; isolated yield shown in parenthesis.

[c] Determined by enantioselective HPLC.

[d] Absolute configuration of the product assigned by comparing the sign of optical rotation with literature data (see the experimental section).

[e] Absolute configuration assigned by comparing the order of elution with literature data (see the experimental section).

The chiral iron complexes (*S*)-**9cc** and (*R*)-**9am** were also tested in the AH of several *N*-PMP ketimines prepared in Chapter 2. As shown in Table 4.3, with the exception of few moderate yields (entry 3 with (*R*)-**9am** and entry 4), high conversions were obtained in all cases (>90%).

As for the enantioselectivity, moderate e.e. values were achieved with the acetophenone- and the propiophenone-derived imines **S1** and **S22** (Table 3, entries 1 and 3), (*S*)-**9cc** being slightly more enantioselective than (*R*)-**9am**. Imines **S20** and **S25** were hydrogenated with a low level of stereoselectivity, slightly higher with (*S*)-**9cc** than with (*R*)-**9am** (Table 3, entries 2 and 4). With all ketimines, the two pre-catalysts showed opposite stereochemical preferences.

4.2 Chiral macrocyclic CICs

New strategy for the synthesis of chiral CICs was designed to obtain effective chiral CICs for enantioselective catalysis, consisting in the incorporation of the (cyclopentadienone)iron tricarbonyl group into a chiral cavity, as shown in Figure 4.6.

Two main advantages were expected from this approach: i) the stability of CICs would be enhanced by incorporation into a macrocycle; ii) the enantioselectivity should be granted by chiral residue(s), such as aminoacid or chiral diamines, which would be close to the substrate in the pericyclic TS of reductions (Figure

4.2).

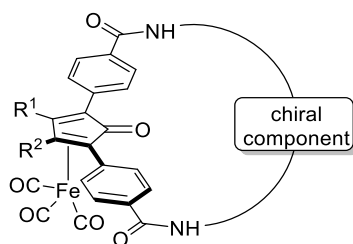
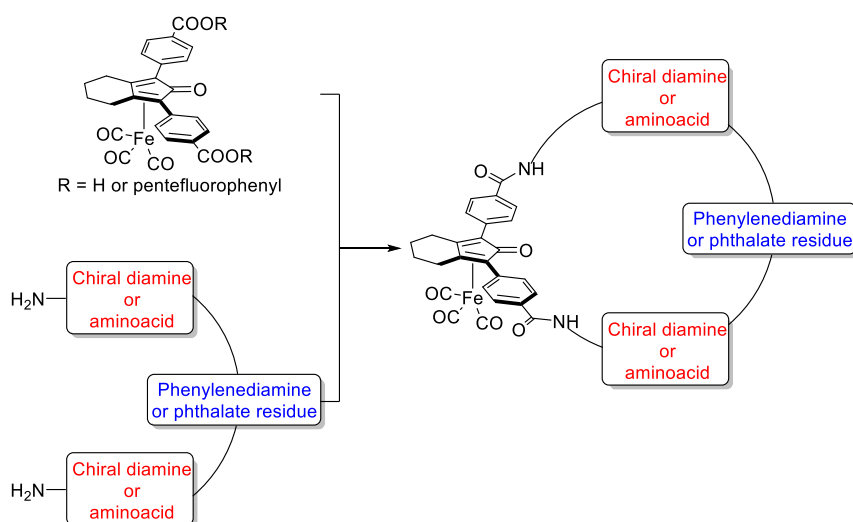


Figure 4.6. Chiral macrocyclic complexes incorporating the (cyclopentadienone)iron group into a chiral cavity.



Scheme 4.3. Synthetic plan of chiral macrocyclic complexes.

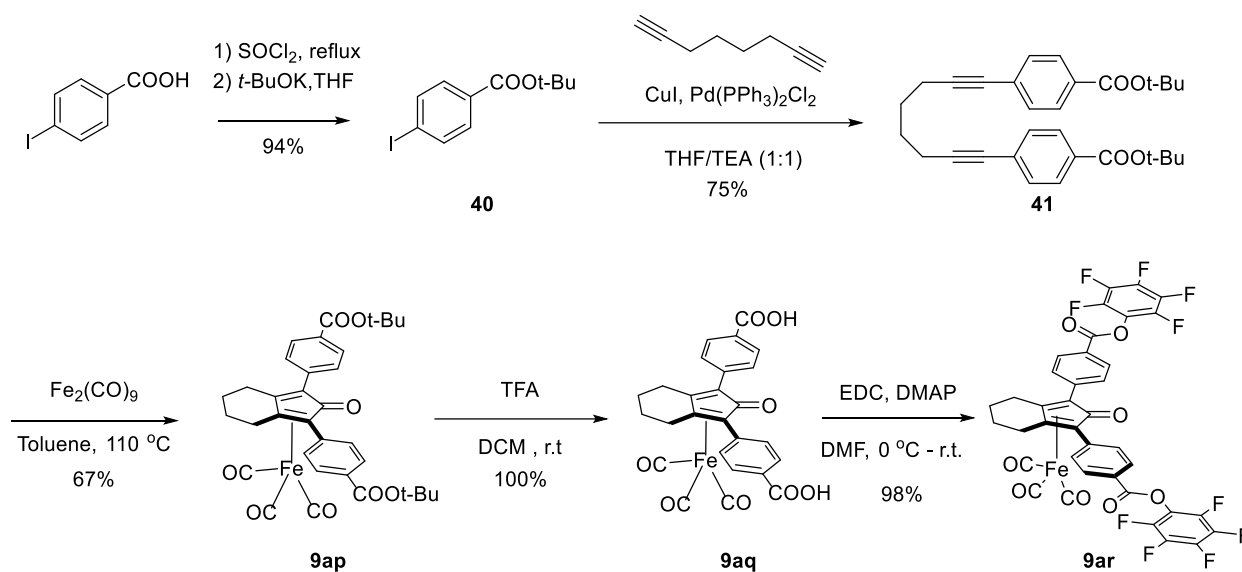
Thus, we elaborated the synthetic plan shown in Scheme 4.3. The activated ester containing the framework of CICs or the easily synthesized CICs with two carboxyl groups could react with chiral diamines containing amino acid or chiral diamine residues connected by phenylenediamine or phthalate residue.

4.2.1 Synthesis of chiral macrocyclic iron complexes

4.2.1.1 Synthesis of CICs featuring two carboxyl groups or ester groups

Starting from commercially available 4-iodobenzoic acid, the ester **40** was formed in high yield (94%) by esterification of 4-iodobenzoyl chloride, formed by chlorination in the presence of thionyl chloride following a known literature procedure (Scheme 4.4).^[7] Compound **40** was then reacted with 1,7-octadiyne under Sonogashira coupling conditions (CuI and Pd(PPh₃)₂Cl₂ as catalyst),^[15] to form diyne **41** in good yield (75%). Complex **9ap** was then obtained in good yields by carbonylative cyclization of diyne **41** in the presence of Fe₂(CO)₉ in good yield (Scheme 4.4).^[10] The CIC featuring two free carboxy groups was obtained upon

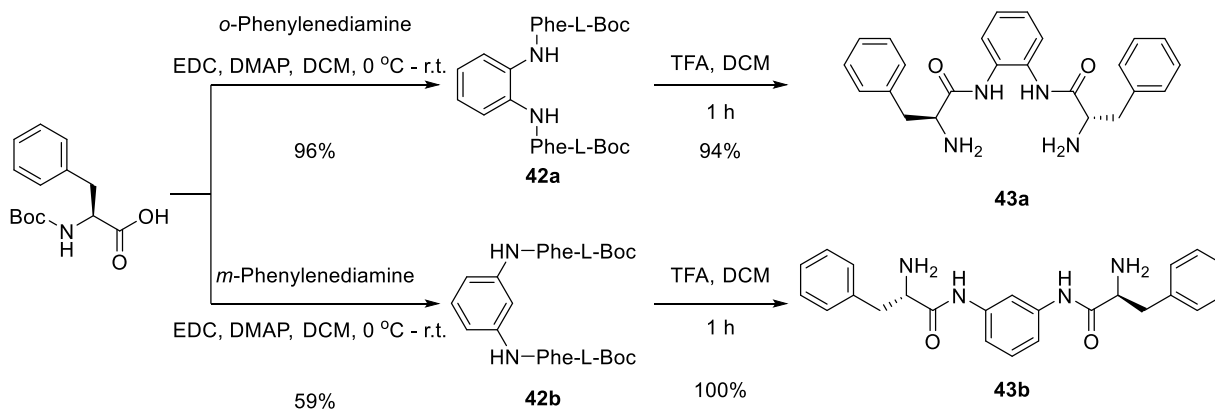
deprotection of both *t*-butyl groups with TFA. The activated ester **9ar** was finally obtained in excellent yields (98%) by esterification of **9aq** with pentafluorophenol.^[16]



Scheme 4.4. Synthesis of CICs featuring two carboxyl groups or ester groups.

4.2.1.2 Synthesis of chiral diamines

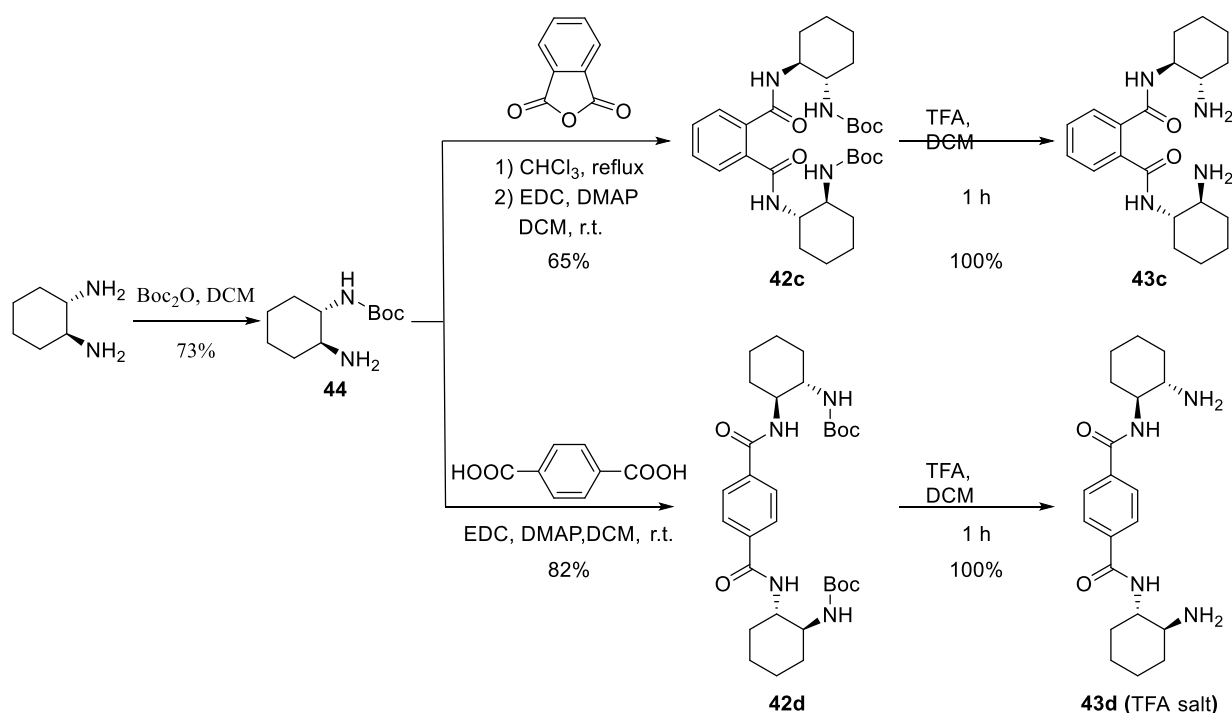
N-Boc-*L*-phenylalanine was reacted, respectively, with *o*-phenylenediamine or *m*-phenylenediamine in the presence of EDC and DMAP, giving the corresponding Boc-protected diamines **42a** and **42b**, respectively (Scheme 4.5). Diamines **43a** and **43b** were then obtained by deprotection with trifluoroacetic acid (TFA).



Scheme 4.5. Synthesis of the chiral diamines **43a** and **43b**.

Meanwhile, the preparation of chiral diamines **43c** and **43d** from (1*S*,2*S*)-(+)-1,2-diaminocyclohexane was carried out. The monoprotected diamine **44** was obtained in good yields (73%) by reacting (1*S*,2*S*)-(+)-1,2-diaminocyclohexane with Boc anhydride, following a known procedure.^[17] As for the synthesis of the Boc-protected diamine **42c**, being aware that the coupling of the amine **44** with phthalic acid would have favored

the formation of an undesired imide by intramolecular amidation, we prepared diamine **43c** by reacting **44** with phthalic anhydride, followed by coupling of the resulting phthalic acid monoamide with another equivalent of **44** in the presence of EDC and DMAP (Scheme 4.6).^[17,18] Terephthalic acid was directly employed for the synthesis of the Boc-protected diamine **42d**, as no intramolecular amidation of the mono-amide intermediate can occur in this case. With this procedure, compound **42d** was obtained in good yield (82%). Upon Boc deprotection with a known procedure, diamine **43c** was easily obtained in excellent yield. However, due to its poor solubility in conventional extraction solvents such as DCM and AcOEt, diamine **43d** proved difficult to be extracted and could only be obtained as TFA salt in quantitative yield.

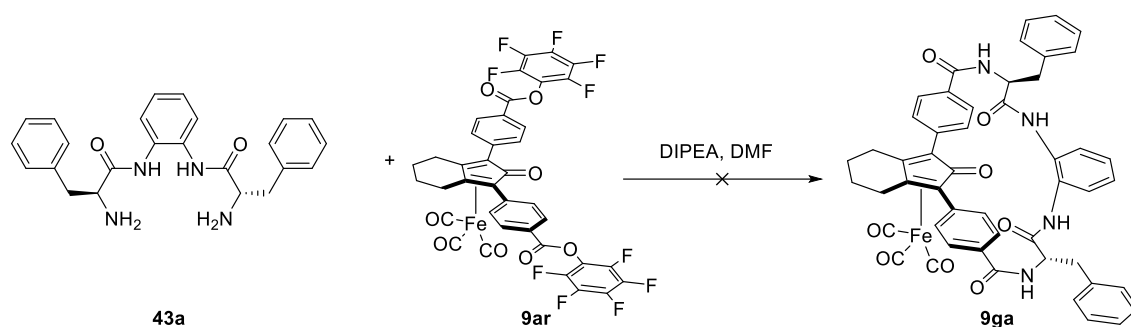


Scheme 4.6. Synthesis of chiral diamines **43c** and **43d**.

4.2.1.3 Synthesis of chiral macrocyclic iron complexes

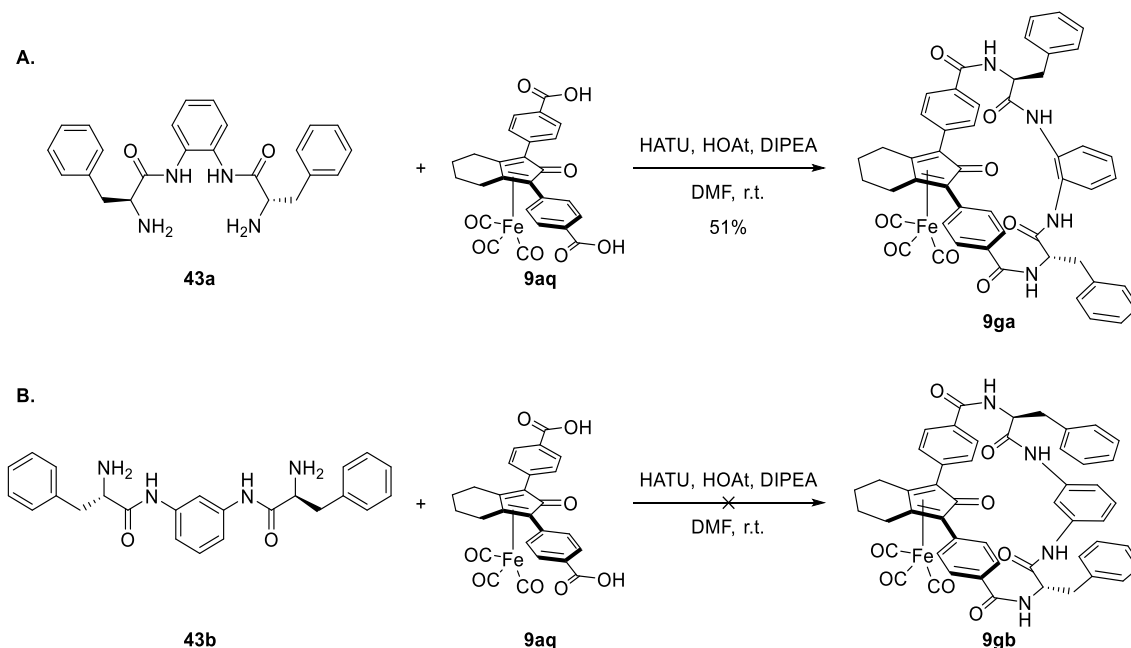
We planned the synthesis of chiral macrocyclic iron complexes by double-coupling of a diamine with a diacid through formation of two amide bonds. The latter type of reaction has been widely investigated and successfully achieved, especially for the preparation of peptide and peptidomimetic compounds of biochemical/pharmaceutical interest.^[19] As a first option, we chose to react the activated ester **9ar** with diamine **43a** in the presence of *N,N*-diisopropylethylamine (DIPEA), as shown in Scheme 4.7. Unfortunately, even extending the reaction time and varying the temperature, the synthesis of complex **9ga** always proved

unsuccessful. For this reason, we switched to a one-pot method in which the dicarboxylic acid component is activated *in situ* as acyl ester by using HATU and HOAt, and then reacted with the selected diamine.^[20]



Scheme 4.7. Synthesis of chiral macrocyclic iron complexes **9ga** with activated ester **9ar**.

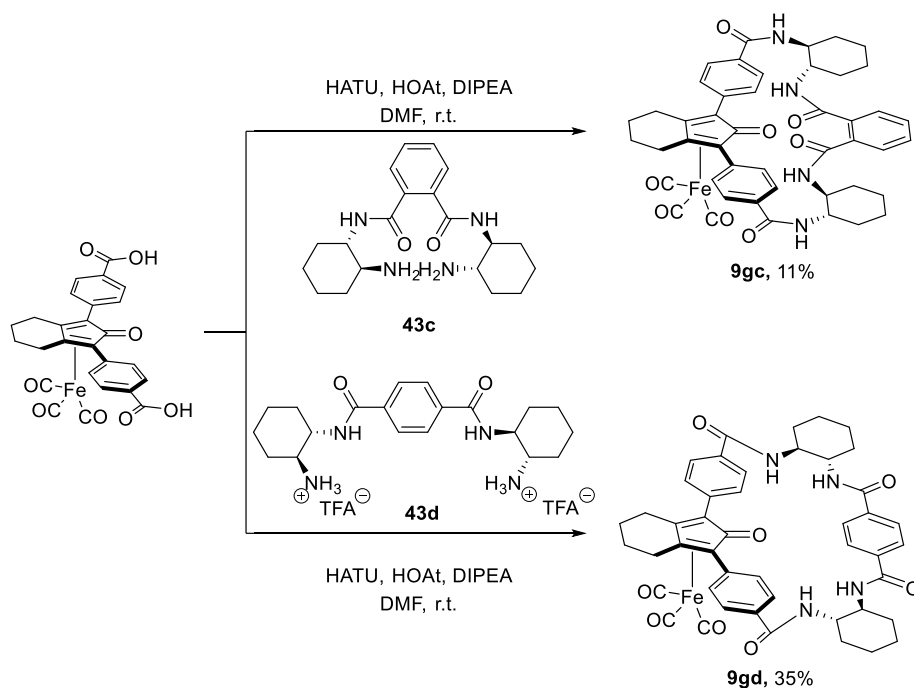
Starting from the diamine **43a** and the diacid **9aq**, we prepared the chiral macrocyclic complex **9ga** using HATU and HOAt as coupling reagents, obtaining the product in 51% yield (Scheme 4.8 A). The reaction was performed under high dilution conditions ($C_{0,\text{sub.}} = 5 \text{ mM}$), to prevent the possible formation of oligomers. However, when the diamine **43b** was reacted with iron complex **9aq** under the same conditions we could not obtain the desired product **9gb** (Scheme 4.8 B), and we addressed this outcome to the poor solubility of diamine **43b**.



Scheme 4.8. Synthesis of chiral macrocyclic iron complexes **9ga**.

Next, we used the same high dilution conditions to synthesize chiral complexes **9gc** and **9gd**, which were uneventfully obtained, although in lower yields compared to **9ga** (Scheme 4.9). Due to the low solubility of diamine **43d** in organic solvents, we used its TFA salt for the synthesis of complex **9gd** in the presence of an

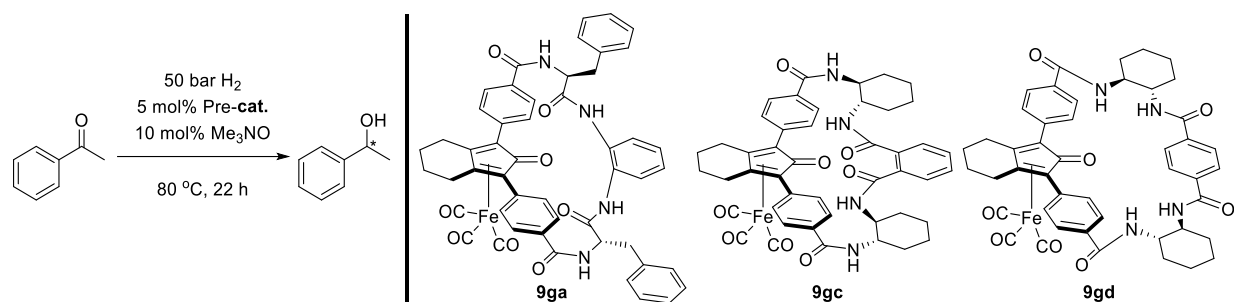
excess of DIPEA (2 eq.), obtaining the product in a moderate yield (35%).



4.2.2 Asymmetric hydrogenation of C=O double bonds with chiral macrocyclic iron complexes

The first chiral macrocyclic CICs **9ga** and **9gc-9gd** were tested in the AH of acetophenone, and the results obtained are shown in Table 4.4.

Complex **9ga** showed poor catalytic reactivity in the model reaction, giving a very low conversion (Table 4.4, entry 1). We addressed such poor reactivity to the small size of macrocycle **9ga**, seemingly too small to accommodate the reaction substrate. Consistent with this hypothesis, a positive correlation between macrocycle size and the experimental catalytic activity emerged: indeed, the conversion remarkably grew switching from 23-membered **9ga** (Table 4.4, entry 1) to 25-membered **9gc** (entry 2) and then to 27-membered **9gd** (entry 3), which allowed to obtain the product with quantitative conversion. Unfortunately, only poor e.e. values were obtained with these first representatives. Even so, chiral complex **9gd** showed slightly higher enantioselectivity than the chiral iron complexes with a stereogenic plane (Section 4.1). The highly modular structure of this class of chiral macrocyclic CICs will allow to quickly prepare a number of representatives, which will be screened in the enantioselective reduction of C=O and C=N bonds.

Table 4.4. AH of acetophenone promoted by chiral pre-catalysts **9ga**, **9gc** and **9gd**.^[a]

#	Catalyst	Solvents	Conversion (%) ^[b]	e.e. (%) ^[c]
1	9ga	DCM/ <i>i</i> PrOH (1:7)	8	0
2	9gc	<i>i</i> PrOH/H ₂ O (5:2)	17	5, <i>R</i>
3	9gd	<i>i</i> PrOH/H ₂ O (5:2)	99	11, <i>R</i>

[a] Reaction conditions: Substrate/Me₃NO/Pre-cat. = 100:10:5, *T* = 80 °C, *P*_{H₂} = 50 bar, 22 h. *C*_{0,sub.} = 1 M.

[b] Determined by GC analysis with a chiral capillary column.

[c] Absolute configuration of the product assigned by comparing the order of elution with literature data (see the experimental section).

4.3 Conclusions on chiral iron complexes

In the attempt to achieve highly enantioselective CIC-catalyzed C=O and C=N reductions, we synthesized in racemic form six chiral CICs ((±)-**9cc** and (±)-**9ak**-(±)-**9ao**) possessing a stereogenic plane and carried out catalytic tests to evaluate their activity. The largest possible difference – in terms of sterics and stereoelectronics – between the substituents at positions 2 and 5 of the cyclopentadienone ring was taken as requisite to achieve high enantioselectivity. However, the catalytic activity of the racemic complexes decreased with the increasing size of the ‘large’ substituent, thus limiting the possibility to exploit the different size of the 2,5-substituents. Complexes (±)-**9cc** and (±)-**9am** represented the best compromise between catalytic activity and substituents size, and thus were selected for enantiomer separation by chiral HPLC. According to XRD analysis, *S* configuration was assigned to first-eluted enantiomer of complex **9cc**, while the configuration of complex **9am** [first-eluted enantiomer = (*R*)-product] was assigned by comparing the ORD and ECD spectra of the separated enantiomers to computationally simulated spectra. The enantiomerically pure complex (*S*)-**9cc** showed similar enantioselectivities to those reported by Hayashi and co-workers using ruthenium analog, giving low to moderate e.e. values.

Furthermore, the development of a new class of chiral complexes was started, in which the CIC is incorporated

into a chiral macrocycle with modular structure: the first three chiral macrocyclic CICs (**9ga**, **9gc** and **9gd**) were synthesized by combining chiral diamines (**43a** and **43c-d**) with CIC **9aq** possessing two carboxyl groups for enantioselective reduction. Catalytic tests carried out with these chiral macrocyclic complexes revealed that catalytic activity is strongly affected by the size of macrocycle, which should be larger than 25 members. Further preparation and screening of macrocyclic complexes is currently underway in our group.

In general, these results confirm that developing an effective chiral CICs for enantioselective applications is still a challenging goal, although the results described in this Chapter will provide useful indication for future work.

4.4 Experimental Section

4.4.1 General remarks

All reactions were carried out in flame-dried glassware with magnetic stirring under inert atmosphere (nitrogen or argon), unless otherwise stated. Solvents for reactions were distilled over the following drying agents and transferred under nitrogen: THF (Na), toluene (Na). Dry *N,N*-dimethylformamide (DMF, over molecular sieves in bottles with crown cap) was purchased from Sigma Aldrich and stored under nitrogen. All reagents were used without purification. Imines were prepared in Chapter 2. Reactions were monitored by analytical thin-layer chromatography (TLC) using silica gel 60 F254 pre-coated glass plates (0.25 mm thickness). Visualization was accomplished by irradiation with a UV lamp and/or staining with a potassium permanganate alkaline solution or with a ninhydrin solution. Flash Column Chromatography (FCC) was performed using silica gel (60 Å, particle size 40-64 µm) as stationary phase, following the procedure by Still and co-workers.^[21] Optical rotations were measured with a Jasco-P-2000 digital polarimeter at 20 or 22 °C, and concentrations (*c*) are given in g/100 mL.

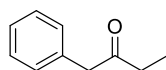
¹H-NMR spectra were recorded on a spectrometer operating at 400.13 MHz. Proton chemical shifts are reported in ppm (δ) with the solvent reference relative to tetramethylsilane (TMS) employed as the internal standard (CDCl₃, δ = 7.26 ppm; CD₂Cl₂ δ = 5.32 ppm; *d*₆-DMSO δ = 2.50 ppm; CD₃OD δ = 3.34 ppm). The following abbreviations are used to describe spin multiplicity: s = singlet, d = doublet, dd = doublet-doublet, ddd = doublet-doublet-doublet, t = triplet, td = triplet-doublet, q = quartet, pen = pentad, m = multiplet. ¹³C-NMR spectra were recorded on a 400 MHz spectrometer operating at 100.56 MHz, with complete proton decoupling. Carbon chemical shifts are reported in ppm (δ) relative to TMS with the respective solvent

resonance as the internal standard (CDCl_3 $\delta = 77.16$ ppm; CD_2Cl_2 $\delta = 54.00$ ppm; d_6 -DMSO $\delta = 40.45$ ppm; CD_3OD $\delta = 49.86$ ppm). The coupling constant values are given in Hz. Infrared spectra were recorded on a standard FT/IR spectrometer. Melting points were recorded with a standard melting-point apparatus. High resolution mass spectra (HRMS) were performed on a ESI QToF SYNAPT G2 Si mass spectrometer (Waters), equipped with ESI source, available at the UNITECH-COSPECT laboratories (Università degli Studi di Milano). Elemental analyses were performed on a Perkin Elmer Series II CHNS/O Analyzer 2000. X-ray intensity data were collected with a Bruker AXS APEXII CCD area detector by using graphite monochromated Mo-K α radiation.

4.4.2 Synthesis of chiral iron complexes with stereogenic plane

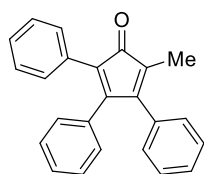
4.4.2.1 Preparation of 2-methyl-3,4,5-triphenylcyclopenta-2,4-dien-1-one (32)

1-phenylbutan-2-one (31)^[5a]



To an ice-cooled solution of phenylacetyl chloride (2 mL, 12.8 mmol) and CuI (185 mg, 1 mmol) in anhydrous THF (40 mL) was added dropwise a solution of EtMgBr (1 M in THF, 12.8 mL, 12.8 mmol). The mixture was stirred for 1 h at 0 °C. After completion of the reaction (TLC), the reaction was quenched by addition of saturated aqueous NH_4Cl . The mixture was extracted with diethyl ether (3 \times 100 mL). The combined organic layers was washed with brine (2 \times 100 mL) and water (2 \times 100 mL), dried over MgSO_4 , filtered, and concentrated under reduced pressure. The crude compound was purified by flash chromatography (silica gel, 4: 96 AcOEt/hexane). Yield: 1.05 g (56%). Spectroscopic data are in agreement with those reported in the literature.^[5a] $^1\text{H-NMR}$ (400 MHz, CDCl_3): δ 7.35-7.30 (m, 2H), 7.28-7.24 (m, 1H), 7.22-7.20 (m, 2H), 3.69 (s, 2H), 2.47 (q, $J = 7.3$ Hz, 2H), 1.03 (t, $J = 7.3$ Hz, 3H).

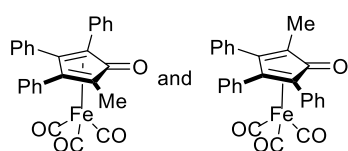
2-methyl-3,4,5-triphenylcyclopenta-2,4-dien-1-one (32)^[4]



A solution of 1-phenyl-2-butanone **31** (359 mg, 2.422 mmol) and benzil (509 mg, 2.422 mmol) in dry DMF (7 mL) was heated at 80 °C and stirred for 1 hour, then a 0.1 M solution of *t*BuOK in DMF (4.8 mL, 0.484 mmol) was added dropwise. The resulting mixture was stirred overnight at 80 °C. The solvent was evaporated and water was added, and the mixture was extracted with AcOEt (3 \times 40 mL). The combined organic extract was dried over Na_2SO_4 , filtered and concentrated. The unpurified residue was dissolved in Ac_2O (10 mL), and a few drops of concentrated

H₂SO₄ were added (a deep purple color instantaneously developed). The mixture was stirred at r.t. for 1 h. Water (100 mL) was added to dilute the reaction and a purple solid precipitated, which was collected by filtration. The crude product was then recrystallized from a DCM/hexane mixture. Yield: 541.9 mg (89%). Spectroscopic data are in agreement with those reported in the literature.^[4] ¹H-NMR (400 MHz, CD₂Cl₂): δ 7.29-7.14 (m, 11H), 7.01-6.98 (m, 2H), 6.94-6.91 (m, 2H), 1.89(s, 3H); ¹³C-NMR (100 MHz, CD₂Cl₂): δ 202.35, 155.34, 153.91, 134.10, 133.82, 131.94, 130.46, 129.77, 129.45, 128.98, 128.76, 128.49, 128.44, 128.34, 127.77, 126.16, 124.45, 9.01; FT-IR: ν = 2920.7, 1703.8, 1491.7, 1440.6, 1349.0, 1300.8, 1071.3, 1005.7, 903.5, 800.3, 782.0, 765.6, 709.7, 396.1 cm⁻¹; elemental analysis (%): C 88.64, H 6.03, (calcd. for C₂₄H₁₈O: C 89.41, H 5.63).

4.4.2.2 Preparation of complex (±)-9cc

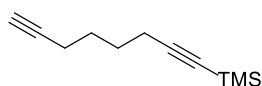


In a Schlenk tube fitted with a Teflon-topped screw cap, Fe₂(CO)₉ (1.1284 g, 3.102 mmol, 2 eq.) was added to a stirred solution of cyclopentadienone **32** (500 mg, 1.551 mmol, 1 eq.) in toluene (10 mL) under N₂. The reaction mixture

was heated to 110°C and stirred for 16 hours. The reaction mixture was cooled down to r.t. and filtered through celite (rinsing with AcOEt). After removal of the solvent under reduced pressure, the residue was purified by flash column chromatograph (9:1 hexane/AcOEt) to afford the product as a light yellow solid. Yield: 628 mg (88%). M.p. = 199.1 °C; ¹H-NMR (400 MHz, CD₂Cl₂) δ 7.52-7.49 (m, 2H), 7.41-7.33 (m, 5H), 7.28-7.23 (m, 4H), 7.16-7.15 (m, 4H), 1.94(s, 3H); ¹³C-NMR (100 MHz, CD₂Cl₂) δ 209.52, 171.68, 132.28, 132.02, 131.93, 130.96, 130.66, 130.49, 129.39, 129.18, 128.79, 128.55, 128.49, 128.44, 128.33, 105.35, 104.93, 83.63, 80.60, 10.81; IR (film): ν = 3058.6, 2922.6, 2855.1, 2062.5, 1991.1, 1641.1, 1577.5, 1499.4, 1445.4, 1390.4, 1171.5, 1073.2, 1029.8, 1003.8, 927.6, 853.3, 769.5, 757.9, 853.3, 769.5, 757.9, 736.7, 698.1, 666.3, 645.1, 613.3 cm⁻¹; HRMS (ESI⁺): *m/z* 463.0631 [M+H]⁺ (calcd. for C₃₂H₂₇FeO₄: 463.0633).

4.4.2.3 Preparation of the diyne intermediates 33-39

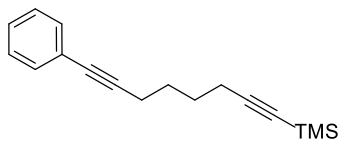
Trimethyl(octa-1,7-diyne-1-yl)silane (**33**)^[6]



A solution of LiHMDS was prepared by dropwise addition of *n*-BuLi (1.6 M in hexanes, 94.2 mL, 150.7 mmol, 1 eq.) to a stirred solution of hexamethyldisilazane

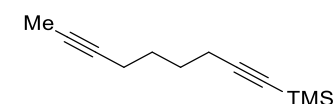
(31.42 mL, 150.7 mmol, 1 eq.) in THF (78 mL) at -78 °C. Once the addition was complete, the mixture was allowed to reach 0 °C and stirred for 30 min before use. The LiHMDS solution was cooled to -78 °C before and then added to a solution of 1,7-octadiyne (20 mL, 150.7 mmol, 1 eq.) in THF (210 mL) kept at -78 °C. After stirring the resulting mixture for 0.5 hours at -78 °C, chlorotrimethylsilane (19.1 mL, 150.7 mmol, 1 eq.) was added dropwise. The mixture was stirred for 10 min at -78 °C and then it was allowed to reach r.t. After stirring for 2 h, the reaction was quenched with water (400 mL). The mixture was extracted with hexane (3 × 400 mL) and the combined organic extracts were then washed with 1 M aq. HCl (400 mL), water (400 mL) and brine (400 mL), before being dried over Na₂SO₄ and concentrated. Distillation of the crude product (Vigreux column, b.p. = 50-55 °C at 1 mbar) gave the title compound as a colorless oil. Yield: 14.23 g (53%). Spectroscopic data are in agreement with those reported in the literature.^[6] ¹H NMR (400 MHz, CDCl₃): δ 2.20-2.17 (m, 4H), 1.90 (t, *J* = 2.68 Hz, 1H), 1.61-1.57 (m, 4H), 0.10 (s, 9H); ¹³C NMR (100 MHz, CDCl₃): δ 106.92, 84.80, 84.07, 68.62, 27.61, 27.57, 19.44, 18.02, 0.23; FT-IR: *ν* = 3308.3, 2950.6, 2865.7, 2360.4, 2175.3, 2118.42, 1457.9, 1431.9, 1326.8, 1249.7, 1046.2, 992.2, 936.3, 902.5, 842.7, 759.8, 699.1, 638.3 cm⁻¹; elemental analysis (%): C 70.44, H 9.90, (calcd. for C₁₁H₁₈Si: C 74.08, H 10.17).

Trimethyl(8-phenylocta-1,7-diyn-1-yl)silane (34)



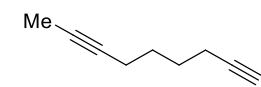
A solution of iodobenzene (2.288 g, 11.21 mmol, 1 eq.) and diyne **33** (2 g, 11.21 mmol, 1 eq.) in THF (30 mL) and NEt₃ (30 mL) was added dichlorobis(triphenylphosphine) palladium (323 mg, 0.46 mmol, 0.041 eq.) and CuI (87.6 mg, 0.46 mmol, 0.041 eq.) under N₂. The reaction mixture was heated to 60 °C and stirred for 16 hours under inert atmosphere. The mixture was diluted with DCM and then washed with sat. aq. NH₄Cl and water. After removing the solvent under reduced pressure, the resulting crude product was purified by column chromatography (99.5:0.5 hexane/AcOEt) to afford the pure product as a light yellow oil. Yield: 1.94 g (68%). Spectroscopic data are in agreement with those reported in the literature.^[22] ¹H-NMR (400 MHz, CD₂Cl₂): δ 7.40-7.38 (m, 2H), 7.30-7.28 (m, 3H), 2.46 (t, *J* = 6.68 Hz, 2H), 2.29 (t, *J* = 6.76 Hz, 2H), 1.72-1.68 (m, 4H), 0.14 (s, 9H); ¹³C-NMR (100 MHz, CD₂Cl₂): δ 132.02, 128.81, 128.12, 124.62, 107.63, 90.50, 85.04, 81.20, 28.41, 28.41, 19.92, 19.45, 0.45; FT-IR: *ν* = 3584.1, 2946.7, 2862.8, 2173.4, 1598.7, 1489.7, 1442.5, 1327.8, 1248.7, 1046.2, 912.2, 841.8, 756.0, 691.4 cm⁻¹; elemental analysis (%): C 80.79, H 8.61, (calcd. for C₁₇H₂₂Si: C 80.25, H 8.72).

Trimethyl(nona-1,7-diyn-1-yl)silane (35)^[6]



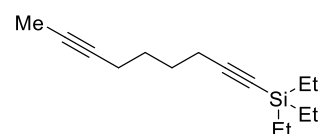
A solution of *n*-BuLi (2.5 M in hexanes, 26.4 mL, 66.05 mmol, 1.5 eq.) was added dropwise to a solution of compound **33** (7.8532 g, 44.03 mmol, 1.0 eq.) in THF (206 mL) at -78 °C. After stirring for 1 h, iodomethane (5.48 mL, 88.06 mmol) was slowly introduced, the mixture was allowed to warm to ambient temperature while stirring was continued for 2 h. The reaction was cooled at 0 °C, quenched with water and then extracted with hexane (3 × 200 mL). The combined organic extracts were washed with water and brine, dried over Na₂SO₄, and concentrated. The crude product was purified by distillation (b.p. = 119-125 °C at 20 mbar) to give the title compound as a colorless oil. Yield: 7.53 g (89%). Spectroscopic data are in agreement with those reported in the literature.^[6] ¹H-NMR (400 MHz, CD₂Cl₂): δ 2.22 (t, *J* = 6.92 Hz, 2H), 2.14-2.12 (m, 2H), 1.75 (t, *J* = 2.60 Hz, 1H), 1.61-1.55 (m, 4H), 0.13 (s, 9H); ¹³C NMR (100 MHz, CD₂Cl₂): δ 107.81, 84.98, 79.25, 76.14, 28.88, 28.50, 20.02, 18.89, 3.78, 0.55; FT-IR: ν = 2947.7, 2920.6, 2861.8, 2174.4, 1431.9, 1328.7, 1249.7, 1046.2, 932.4, 841.8, 759.8, 698.1, 639.3, cm⁻¹; elemental analysis (%): C 73.13, H 10.18, (calcd. for C₁₂H₂₀Si: C 74.92, H 10.48).

Nona-1,7-diyne (**36**)



K₂CO₃ (7.03 g, 50.87 mmol, 1.1 eq.) was added to a solution of compound **35** (8.8956 g, 46.24 mmol, 1.0 eq.) in 1:1 THF/MeOH (142 mL) at r.t. The mixture was stirred overnight at r.t., then water was added and the aqueous phase was extracted with hexane (3 × 200 mL). The combined organic phases were washed with sat. aq. NaCl and dried over Na₂SO₄, then the solvent was removed.. The crude product was purified by distillation (b.p. = 119-125 °C at 20 mbar) to give the title compound as a colorless oil. Yield: 5.4 g (97%). Spectroscopic data are in agreement with those reported in the literature.^[23] ¹H NMR (400 MHz, CDCl₃): δ 2.22-2.19 (m, 2H), 2.17-2.14 (m, 2H), 1.94 (t, *J* = 2.68 Hz, 3H), 1.1.77 (t, *J* = 2.56 Hz, 1H), 1.63-1.59 (m, 4H); ¹³C NMR (100 MHz, CDCl₃): δ 84.19, 78.67, 75.73, 68.43, 28.03, 27.60, 18.25, 17.99, 3.38; FT-IR: ν = 3584.1, 3295.8, 2944.8, 2920.7, 2861.82359.5, 2117.5, 1629.6, 1432.9, 1330.6, 1033.7, 630.6 cm⁻¹; elemental analysis (%): C 83.61, H 9.48, (calcd. for C₉H₁₂: C 89.94, H 10.06).

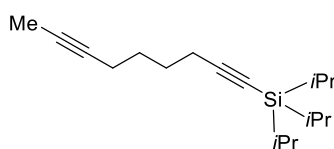
Triethyl(nona-1,7-diyn-1-yl)silane (**37**)



n-BuLi (1.6 M in hexanes, 2.29 mL, 3.66 mmol, 1 eq.) was added dropwise to a stirred solution of diyne **36** (400 mg, 3.33 mmol) in THF (22 mL) at -78 °C. After stirring for 1 hour at -78 °C, Chlorotriethylsilane (601.9 mg, 3.9936 mmol) was added and the mixture was stirred at -78 °C for 1 h before being allowed to warm to r.t. overnight. The reaction

was quenched using saturated sat. aq. NH_4Cl (25 mL) and extracted with Et_2O (3×25 mL). The combined organic extracts were dried over MgSO_4 and the solvent was removed in vacuo. The residue was purified by flash column chromatograph (98:2 hexane/AcOEt) to afford the pure product as a light yellow oil. Yield: 733 mg (94%). $^1\text{H-NMR}$ (400 MHz, CDCl_3): δ 2.25 (t, $J = 6.80$ Hz, 2H), 2.15-2.12 (m, 2H), 1.76 (t, $J = 2.56$ Hz, 3H), 1.61-1.57 (m, 4H), 0.97 (t, $J = 7.96$ Hz, 9H), 0.59 (q, $J = 15.80, 7.84$ Hz, 6H); $^{13}\text{C-NMR}$ (100 MHz, CDCl_3): δ 108.38, 81.80, 78.92, 75.77, 28.18, 27.99, 19.57, 18.37, 7.58, 4.69, 3.55; IR (film): $\nu = 3585.0, 2953.5, 2916.8, 2874.4, 2733.6, 2172.4, 1655.6, 1458.9, 1414.5, 1377.9, 1326.8, 1260.3, 1236.2, 1096.3, 1017.3, 973.9, 930.5, 842.7, 806.1, 736.7, 726.1$ cm^{-1} ; MS (ESI+) m/z 257.51 $[\text{M} + \text{Na}]^+$ (calcd. for $\text{C}_{15}\text{H}_{26}\text{SiNa}$: 257.17); elemental analysis (%): C 75.60, H 11.01, (calcd. for $\text{C}_{15}\text{H}_{26}\text{Si}$: C 76.84, H 11.18).

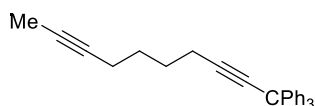
Triisopropyl(nona-1,7-diyn-1-yl)silane (38)



$n\text{-BuLi}$ (1.6 M in hexanes, 2.29 mL, 3.661 mmol) was added dropwise to a stirred solution of diyne **36** (400 mg, 3.328 mmol) in THF (22 mL) at -78 $^\circ\text{C}$. After stirring for 1 hour at -78 $^\circ\text{C}$, Triisopropylsilyl chloride (770 mg, 3.9936

mmol) was added and the mixture was stirred at -78 $^\circ\text{C}$ for 1 h before being allowed to warm to r.t. overnight. The reaction was quenched using saturated sat. aq. NH_4Cl (25 mL) and extracted with Et_2O (3×25 mL). The combined organic extracts were dried over MgSO_4 and the solvent was removed in vacuo. The residue was purified by flash column chromatograph (98:2 hexane/AcOEt) to afford the pure product as a light yellow oil. Yield: 1.167 g (95%). $^1\text{H-NMR}$ (400MHz, CDCl_3): δ 2.28-2.24 (m, 2H), 2.15-2.13 (m, 2H), 1.76 (t, $J = 2.60$ Hz 3H), 1.62-1.60 (m, 4H), 1.07-1.02 (m, 21H); $^{13}\text{C-NMR}$ (100 MHz, CDCl_3): δ 108.89, 80.41, 78.92, 75.75, 28.13, 28.06, 19.53, 18.75, 18.34, 11.45, 3.55; IR (film): $\nu = 3584.1, 2942.8, 2892.7, 2865.7, 2724.0, 2171.5, 1639.2, 1462.7, 1383.7, 1366.3, 1326.8, 1242.9, 1071.3, 1016.3, 995.1, 919.9, 883.2, 702.0, 676.9, 660.5, 621.0$ cm^{-1} ; elemental analysis (%): C 71.21, H 11.05, (calcd. for $\text{C}_{18}\text{H}_{32}\text{Si}$: C 78.18, H 11.66).

Deca-2,8-diyne-1,1,1-triyltribenzene (39)



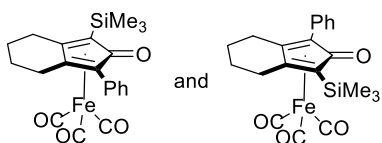
In a Schlenk tube at 0 $^\circ\text{C}$, a solution of ethylmagnesium bromide (2 M in THF, 4.1 mL, 8.33 mmol, 1.0 eq.) was added dropwise to a stirred solution of compound **36** (1g, 8.33 mmol, 1.0 eq.) and THF (11 mL). The resulting mixture was heated to reflux and stirred for 1 h. After cooling down to r.t., trityl chloride (2.322 g, 8.33 mmol, 1.0 eq.) was added. The resulting mixture was heated to reflux and stirred overnight. After cooling down to r.t., the reaction was quenched with sat. aq. NH_4Cl (15 mL), and the obtained aqueous phase was extracted with AcOEt

(3 × 30 mL). The organic layer was washed with water (25 mL) and brine (25 mL), dried over Na₂SO₄ and concentrated in vacuo. The crude product was purified by column chromatography on silica gel (9:1 hexane/AcOEt) to give the product as a white solid. Yield: 1.61 g (53%). M.p. = 85.2 °C; ¹H-NMR (400MHz, CD₂Cl₂): δ 7.31-7.25 (m, 15H), 2.41 (t, *J* = 6.72 Hz, 2H), 2.20-2.15 (m, 2H), 1.77 (t, *J* = 2.56 Hz, 3H), 1.72-1.63 (m, 4H); ¹³C-NMR (100MHz, CD₂Cl₂): δ 146.48, 129.65, 128.44, 127.21, 86.73, 86.17, 79.25, 76.07, 56.17, 28.94, 28.59, 19.10, 18.78, 3.73; IR (film): ν = 3584.1, 3083.6, 3058.6, 3021.9, 2939.0, 2859.0, 1951.6, 1595.8, 1489.7, 1445.4, 1328.7, 1182.2, 1077.1, 1032.7, 1001.8, 891.0, 746.3, 689.1, 638.3, 618.1 cm⁻¹; MS (ESI +) *m/z* 363.52 [M + H]⁺ (calcd. for C₂₈H₂₆: 363.52); elemental analysis (%): C 92.77, H 7.22, (calcd. for C₂₈H₂₆: C 92.77, H 7.23).

4.4.2.4 General procedure for the synthesis of complexes (±)-**9ak-9ao**

In a Schlenk tube fitted with a Teflon-topped screw cap, distilled toluene (6 mL) was added to a mixture of the diyne (0.853 mmol, 1.0 eq.) and Fe₂(CO)₉ (621 mg, 1.706 mmol, 2.0 eq.) under N₂. The mixture was heated to 110 °C and stirred overnight. After cooling down to r.t., the resulting mixture was concentrated under reduced pressure. The products were purified by column chromatography (4:1 hexane/AcOEt) to afford the pure iron complexes.

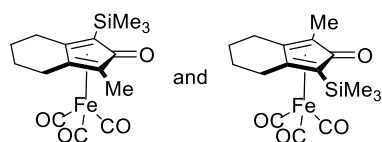
CIC (±)-**9ak**



Prepared from diyne **34** according to the General procedure. Yield: 216 mg (60%). M.p. = 117.8 °C; ¹H-NMR (400 MHz, CD₂Cl₂): δ 7.65-7.62 (m, 2H), 7.38-7.31 (m, 3H), 2.71-2.68 (m, 2H), 2.65-2.55 (m, 2H), 1.91-1.84

(m, 4H), 0.32 (s, 9H); ¹³C-NMR (100 MHz, CD₂Cl₂): δ 209.86, 175.84, 132.51, 130.19, 128.76, 128.20, 107.37, 106.12, 85.16, 68.79, 60.05, 24.87, 24.85, 22.88, 22.82, 0.01; IR (film): ν = 2949.6, 2852.2, 2057.7, 1998.9, 1632.5, 1501.3, 1442.5, 1403.0, 1247.7, 1181.2, 1152.3, 1017.3, 892.0, 838.9, 757.9, 695.2, 617.1 cm⁻¹; HRMS (ESI+): *m/z* 423.0708 [M+H]⁺ (calcd. for C₃₂H₂₇FeO₄: 423.0715).

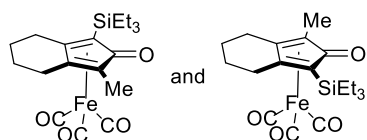
CIC (±)-**9al**



Prepared from diyne **35** according to the General procedure. Yield: 61.4 mg (25%). M.p. = 74.4 °C; ¹H-NMR (400 MHz, CD₂Cl₂): δ 2.57-2.43 (m, 4H), 1.84-1.81 (m, 4H), 1.68 (s, 3H), 0.26 (s, 9H); ¹³C-NMR (100 MHz,

CD₂Cl₂): δ 210.10, 176.89, 107.04, 81.98, 68.47, 24.81, 23.07, 22.59, 22.43, 8.87, 0.04; IR (film): ν = 2950.6, 2056.7, 1996.0, 1635.3, 1447.3, 1247.7, 1087.7, 845.6, 761.7, 698.1, 654.7, 618.1 cm⁻¹; HRMS (ESI⁺): m/z 361.0552 [M+H]⁺ (calcd. for C₃₂H₂₇FeO₄: 361.0559).

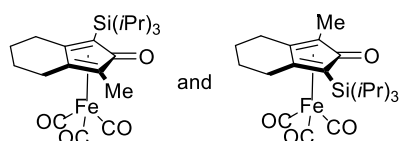
CIC (±)-**9am**



Prepared from diyne **37** according to the General procedure. Yield: 90.7 mg (25%). M.p. = 58.5 °C; ¹H-NMR (400 MHz, CD₂Cl₂): δ 2.52-2.47 (m, 4H), 1.84-1.79 (m, 4H), 1.64 (s, 3H), 1.01 (t, J = 7.84 Hz, 9H), 0.88-0.81 (m, 6H);

¹³C-NMR (100 MHz, CD₂Cl₂): δ 210.10, 176.82, 107.28, 107.17, 82.08, 67.19, 25.36, 23.15, 22.54, 22.43, 8.91, 7.91, 4.36; IR (film): ν = 2951.5, 2874.4, 2056.7, 1996.0, 1979.6, 1636.3, 1446.4, 1293.0, 1240.0, 1143.6, 1004.7, 784.9, 732.8, 699.1, 617.1 cm⁻¹; HRMS (ESI⁺): m/z 403.1018 [M+H]⁺ (calcd. for C₃₂H₂₇FeO₄: 403.1028).

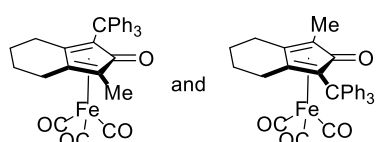
CIC (±)-**9an**



Prepared from diyne **38** according to the General procedure. Yield: 49.3 mg (13%). M.p. = 86.4 °C; ¹H-NMR (400 MHz, CD₂Cl₂): δ 2.60-2.52 (m, 4H), 1.88-1.78 (m, 4H), 1.64 (s, 3H), 1.49-1.41 (m, 3H), 1.16 (t, J = 7.88

Hz, 18H); ¹³C-NMR (100 MHz, CD₂Cl₂): δ 210.12, 176.55, 107.96, 106.46, 81.60, 69.92, 26.28, 23.43, 22.42, 22.40, 19.85, 19.82, 18.99, 13.10, 8.96; IR (film): ν = 2945.7, 2865.7, 2057.7, 1997.9, 1980.5, 1632.5, 1446.4, 1385.6, 1365.4, 1289.2, 1254.5, 1139.7, 1070.3, 1021.1, 881.3, 729.0, 687.5, 665.3, 618.1 cm⁻¹; HRMS (ESI⁺): HRMS (ESI⁺): m/z 445.1493 [M+H]⁺ (calcd. for C₃₂H₂₇FeO₄: 445.1498).

CIC (±)-**9ao**



Prepared from diyne **39** according to the General procedure. Yield: 149.3 mg (33%). M.p. = 90.8 °C; ¹H-NMR (400 MHz, CD₂Cl₂): δ 7.25-7.16 (m, 15H), 2.60-2.51 (m, 2H), 1.81-1.70 (m, 2H), 1.63 (s, 3H), 1.56-1.46 (m, 2H),

1.30-1.19 (m, 2H); ¹³C-NMR (100 MHz, CD₂Cl₂): δ 210.39, 174.29, 146.61, 131.80, 127.83, 127.10, 104.03, 101.74, 95.58, 78.84, 60.61, 24.21, 23.75, 22.67, 21.86, 8.94; IR (film): ν = 3057.6, 2932.2, 2054.8, 1994.0, 1647.9, 1491.7, 1445.4, 1034.6, 854.3, 755.0, 736.7, 699.1, 613.3 cm⁻¹; HRMS (ESI⁺): m/z 531.1254 [M+H]⁺ (calcd. for C₃₂H₂₇FeO₄: 531.1259).

4.4.2.5 Resolution of complexes **9cc** and **9am** by chiral semipreparative HPLC and ECD spectra registration (performed by the group of Prof. Pierini and Prof. Gasparrini, Sapienza University of Rome)

The analytical liquid chromatography was performed on an HPLC equipped with a Rheodyne model 7725i 20 μL loop injector, a PU-1580-CO₂ and PU-980 Jasco HPLC pumps, a UV detector Jasco-975, and a circular dichroism detector Jasco 995-CD. Chromatographic data were collected and processed using Borwin software (Jasco Europe, Italy). The semipreparative liquid chromatography was performed on a Waters chromatograph (WatersAssociates) equipped with a 200 μL loop injector, a UV SpectroMonitor 4100 spectrophotometer, and a refractive index detector. Racemic complex (\pm)-**9cc** were resolved by semipreparative HPLC, using a (*R,R*)-DACH-DNB column (250 mm \times 10 mm L. \times I.D.), a mixture of *n*-hexane/DCM 80:20 + 2% MeOH v/v was employed as eluent (flow rate 4.0 mL/min and $T_{\text{col.}} = 25\text{ }^{\circ}\text{C}$). The sample of (\pm)-**9cc** was dissolved in the mobile phase ($c = 20\text{ mg/mL}$); each injection was 100 μL (process yield 80%). The enantiomeric excess, the UV, and ECD at 300 nm were determined by analytical HPLC with use of a Regis (*R,R*)-DACH-DNB column (250 mm \times 4.6 mm L. \times I.D.) under the same conditions employed for semipreparative HPLC, excepting the flow rate (1.0 mL/min). Concerning the racemic (\pm)-**9am**, the enantiomers were resolved by using a Chiralpak IC column (250 mm \times 10 mm L. \times I.D.) in semipreparative HPLC conditions, mobile phase consisted in a mixture of *n*-hexane/IPA 95:5 v/v (flow rate 5.0 mL/min and $T_{\text{col.}} = 25\text{ }^{\circ}\text{C}$). The racemic (\pm)-**9am** was dissolved in the mobile phase ($c = 60\text{ mg/mL}$); each injection was 100 μL (process yield 79%). The enantiomeric excess, the UV, and ECD at 270 nm were determined by analytical HPLC with use of a Chiralpak IC column (250 mm \times 4.6 mm L. \times I.D.) with a flow rate of 1.0 mL/min. The ECD spectra of chromatographically resolved (*R*)-**9am** and (*S*)-**9am** were recorded with the circular dichroism detector Jasco J710 CD spectrometer, using 2.1×10^{-5} M solutions in CHCl_3 .

Complex (*S*)-**9cc**

$$[\alpha]_{\text{D}}^{22} = -20.82 \quad (c = 0.061 \text{ in } \text{CHCl}_3).$$

Complex (*R*)-**9am**

$$[\alpha]_{\text{D}}^{20} = -16.22 \quad (c = 0.018 \text{ in } \text{CHCl}_3).$$

4.4.2.6 Peak purity checks of **9cc** and **9am** enantiomers collected after semipreparative enantioselective HPLC

The peak purity of the pooled fractions, containing enantiomers of **9cc** and **9am** complexes, after semipreparative enantioselective HPLC was checked. (*S*)-**9cc** (e.e. 99%), (*R*)-**9cc** (e.e. 98%) were checked by using analytical enantioselective HPLC column (*R,R*)-DACH-DNB [5 μ m (250 mm \times 4.6 mm L. \times I.D.)]; the eluent was *n*-hexane/DCM 80:20 + 2% MeOH v/v; flow rate 1.0 mL/min at 25 $^{\circ}$ C. (*R*)-**9am** (e.e. 99.7%) and (*S*)-**9am** (e.e. 99.6%) were checked on an analytical column Chiralpak IC [5 μ m (250 mm \times 4.6 mm L. \times I.D.)]; eluent: *n*-hexane/IPA 95:5 v/v; flow rate 1.0 mL/min at 25 $^{\circ}$ C.

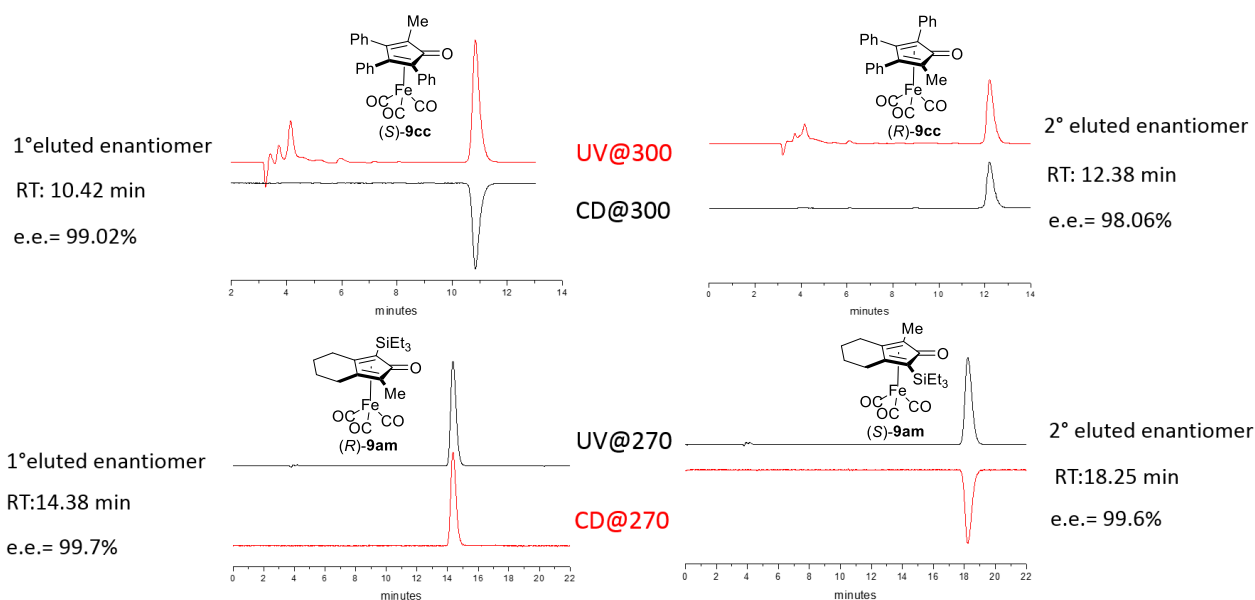


Figure 4.7. Enantiomeric excess evaluation of fraction collected after semipreparative enantioselective HPLC.

4.4.2.7 Single crystal XRD analysis of compound (*S*)-**9cc** (performed by Dr. Valentina Colombo, Università degli Studi di Milano)

The chiral CIC **9cc**, possessing a stereogenic plane, exists in the two enantiomeric forms (*R*)-**9cc** and (*S*)-**9cc**. To unambiguously assign the absolute configuration of this iron complex, single-crystal X-ray diffraction analysis was performed on one of the enantiomers of **9cc** (the first fraction obtained by semipreparative enantioselective HPLC). The absolute configuration, assigned according to the extended CIP rules,^[13] was found to be *S*. The correctness of this absolute configuration is secured by the presence of an iron anomalous scattering in the tile compound: the Flack parameter refined to 0.003(3).^[24]

X-ray quality sample obtained by vapor diffusion of pentane in DCM followed by cooling at -18 $^{\circ}$ C was

selected at the optical microscope, resulting in pale-yellow prisms with dimensions of about $0.15 \times 0.10 \times 0.10$ mm (Figure 4.8 A). A crystal of (*S*)-**9cc** was mounted on a Bruker AXS APEXII CCD area-detector diffractometer, at r.t., for the unit cell determination and data collection. Graphite-monochromatized MoK α ($\lambda = 0.71073$ Å) radiation was used with the generator working at 50 kV and 30 mA. Orientation matrixes were initially obtained from least-squares refinement on ca. 300 reflections measured in three different ω regions, in the range $0^\circ < \theta < 23^\circ$; cell parameters were optimized on the position, determined after integration, of ca. 7000 reflections. The intensity data were retrieved in the full sphere, within the θ limits reported in the crystal data section, from 1080 frames collected with a sample–detector distance fixed at 5.0 cm (50 s frame $^{-1}$; ω scan method, $\Delta\omega = 0.5^\circ$). An empirical absorption correction was applied (SADABS).^[25] Crystal structure was solved by direct methods using SHELXT2017 and refined with SHELXL-2017/1^[26] within the Wingx suite of programs.^[27] The compound crystallizes in the chiral space group $P2_12_12_1$ with one molecule in general position. No significant HB donors are present, thus no significant intermolecular interactions are observed in the crystal packing. Hydrogen atoms were riding on their carbon atoms. Anisotropic temperature factors were assigned to all non-hydrogen atoms. Refinement parameters are listed in the cif files.

CCDC number 1885148 contains the full supplementary crystallographic data for this work. The latter can be obtained free of charge from the Cambridge Crystallographic Data Centre via www.ccdc.cam.ac.uk/data_request/cif.

Crystal data for compound (*S*)-**9cc**: $C_{27}H_{18}FeO_4$, $f_w = 462.26$ g mol $^{-1}$, orthorhombic $P2_12_12_1$ (No. 19), $a = 9.1937(5)$, $b = 12.5845(6)$ and $c = 19.2348(10)$ Å; $V = 2225.4(2)$ Å 3 ; $Z = 4$; Mo-K α $\lambda = 0.71073$ Å; T (K) $293(2)$; $\rho_{\text{calc}} = 1.38$ g cm $^{-3}$, $\mu(\text{Mo-K}\alpha) = 0.708$ mm $^{-1}$; θ range 1.934 – 31.685° ; Limiting indices $-13 \leq h \leq 13$, $-18 \leq k \leq 18$, $-28 \leq l \leq 27$; data (unique), 6992 (6191); restraints, 0; parameters, 289; Goodness-of-Fit on F^2 , 1.015; R_1 and wR_2 ($I > 2\sigma(I)$), 0.0279 and 0.0676; R_1 and wR_2 (all data), 0.0349 and 0.071; Flack parameter, 0.003(3); Largest Diff. Peak and Hole (e Å $^{-3}$), 0.261 and -0.212.

An ORTEP^[28] view of the molecules with the full numbering scheme is given in Figure 4.8 B. Selected distances of bond lengths (Å) and angles ($^\circ$) are given in Table 4.4, while atomic coordinates and displacement parameters are listed in the corresponding cif file.

A:



B:

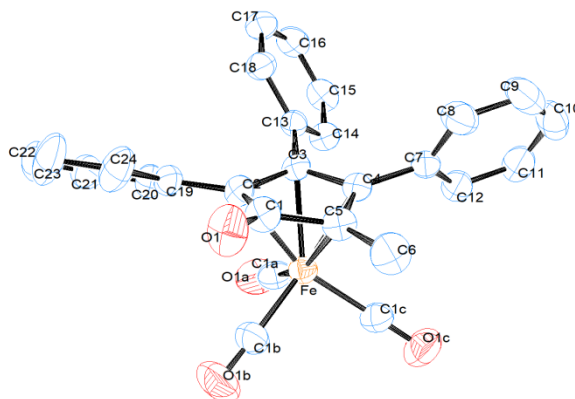


Figure 4.8. A: Diffraction quality pale-yellow crystal used for this analysis. B: ORTEP view of the Iron complex, (*S*)-**9cc**. Ellipsoids are drawn at 50% probability. Color code: O, red; C, blue; Fe, orange. H atoms are omitted for clarity.

As highlighted in Figure 4.9, a top-view of the iron complex shows that the position of the metal with respect to the center of the cyclopentadienone ring is, as expected, slightly shifted in the direction of the basis of the penta-atomic ring, as a consequence of its η^4 coordination to the two C=C double bonds of the cyclopentadienone ligand.

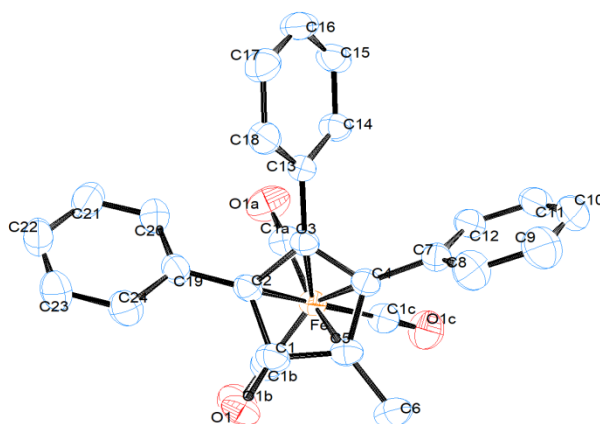


Figure 4.9. Top view of the iron complex (*S*)-**9cc**. Ellipsoids are drawn at 50% probability. Color code: O, red; C, blue; Fe, orange. H atoms are omitted for clarity.

Table 4.5. Selected bond distances (Å) and angles (°) for (*S*)-**9cc**.

Atom Names	Distance (Å)	Atoms Names	Angle (°)	Atoms Names	Angle (°)
Fe-C1B	1.802(2)	C1B-Fe-C1A	97.17(10)	C8-C7-C12	118.46(18)
Fe-C1A	1.804(2)	C1B-Fe-C1C	96.88(9)	C8-C7-C4	117.48(17)
Fe-C1C	1.804(2)	C1A-Fe-C1C	95.83(9)	C12-C7-C4	124.05(16)
Fe-C4	2.0721(16)	C1B-Fe-C4	139.50(8)	C5-C4-C3	107.71(15)
Fe-C3	2.0830(16)	C1A-Fe-C4	121.04(8)	C5-C4-C7	124.50(15)
Fe-C5	2.1222(18)	C1C-Fe-C4	92.37(8)	C3-C4-C7	126.80(14)
Fe-C2	2.1389(17)	C1B-Fe-C3	135.00(8)	C5-C4-Fe	71.92(10)

Fe-C1	2.4132(19)	C1A-Fe-C3	92.08(7)	C3-C4-Fe	70.11(9)
C13-C18	1.390(2)	C1C-Fe-C3	125.92(8)	C7-C4-Fe	132.29(12)
C13-C14	1.397(2)	C4 -Fe-C3	40.59(7)	C17-C18-C13	120.98(18)
C13-C3	1.481(2)	C1B-Fe-C5	99.89(9)	C20-C19-C24	117.69(19)
O1-C1	1.227(2)	C1A-Fe-C5	158.86(8)	C20-C19-C2	123.39(16)
O1A-C1A	1.131(2)	C1C-Fe-C5	94.42(8)	C24-C19-C2	118.91(19)
O1C-C1C	1.125(3)	C4 -Fe-C5	39.93(6)	O1-C1-C5	126.33(18)
C3-C2	1.438(2)	C3-Fe-C5	66.99(7)	O1-C1-C2	129.73(19)
C3-C4	1.441(2)	C1B-Fe-C2	95.20(8)	C5-C1-C2	103.62(14)
O1B-C1B	1.134(2)	C1A-Fe-C2	99.85(8)	O1-C1-Fe	137.05(17)
C14-C15	1.389(2)	C1C-Fe-C2	158.83(8)	C5-C1-Fe	60.60(9)
C7-C8	1.388(3)	C4-Fe-C2	67.35(7)	C2-C1-Fe	61.15(9)
C7-C12	1.389(3)	C3-Fe-C2	39.81(6)	C16-C15-C14	121.03(18)
C7-C4	1.486(2)	C5-Fe-C2	66.33(7)	C4-C5-C1	108.91(15)
C4-C5	1.433(2)	C1B-Fe-C1	80.60(9)	C4-C5-C6	126.81(17)
C18-C17	1.382(3)	C1A-Fe-C1	135.93(8)	C1-C5-C6	122.24(16)
C19-C20	1.382(3)	C1C-Fe-C1	128.23(8)	C4-C5-Fe	68.15(9)
C19-C24	1.394(3)	C4-Fe-C1	63.10(7)	C1-C5-Fe	82.18(11)
C19-C2	1.483(3)	C3-Fe-C1	62.99(6)	C6-C5-Fe	128.98(15)
C1-C5	1.473(3)	C5-Fe-C1	37.22(7)	O1C-C1C-Fe	177.17(19)
C1-C2	1.492(2)	C2-Fe-C1	37.67(6)	C3-C2-C19	126.56(15)
C15-C16	1.370(3)	C18-C13-C14	118.63(16)	C3-C2-C1	107.63(15)
C5-C6	1.495(3)	C18-C13-C3	118.56(15)	C19-C2 C1	124.30(15)
C20-C21	1.386(3)	C14-C13-C3	122.75(15)	C3-C2-Fe	68.00(9)
C11-C10	1.361(4)	C2-C3-C4	108.40(14)	C19-C2-Fe	127.52(13)
C11-C12	1.394(3)	C2-C3-C13	126.04(15)	C1-C2-Fe	81.18(11)
C17-C16	1.386(3)	C4-C3-C13	124.64(14)	C19-C20-C21	121.7(2)
C21-C22	1.376(4)	C2-C3-Fe	72.19(10)	O1A-C1A-Fe	177.88(19)
C8-C9	1.382(3)	C4-C3-Fe	69.30(9)	C10-C11-C12	120.4(2)
C10-C9	1.376(4)	C13-C3-Fe	132.86(11)	C7-C12-C11	120.4(2)
C24-C23	1.390(4)	C15-C14-C13	119.77(17)	C18-C17-C16	119.93(19)

4.4.2.8 Simulation of ORD and CD spectra for the (*R*) enantiomer of **9am** (performed by Prof. Pierini, Sapienza University of Rome).

The chiroptical properties of the enantiomers of **9am** were estimated by molecular modelling calculations performed in two steps. In the first step the structure of the (*R*)-**9am** enantiomer was optimized at the B3LYP/6-31G* level of theory using the computer program SPARTAN 10v1.1.0 (Wavefunction Inc., 18401 Von Karman Avenue, Suite 370, Irvine, CA 92612, USA). In the second step, by resorting to the Amsterdam Density Functional (ADF) package v. 2007.01, the optimized structure of (*R*)-**9am** was subjected to assessment

of chiroptical properties, represented by the Optical Rotatory Dispersion (ORD) and the Electronic Circular Dichroism (ECD) spectra. Optical Rotation values $[\alpha]_n$ at four different wavelengths n , in the range 320-589 nm, were assessed using the BLYP method, employing the QZ4P large core basis set, as implemented in ADF. Always starting from the same optimized (*R*)-**9am** geometry, and again resorting to the ADF program, further calculations were also performed in order to simulate the relevant ECD spectrum. To this end, the set options were: single point calculation at the BLYP level of theory, employing the QZ4P large core basis set; 40 singlet and triplet excitations; diagonalization method: Davidson; velocity representation; scaling factor 1.00; peak width 31.0. It was found that, from comparison with the relevant experimental ECD and ORD spectra, the first-eluted enantiomer of **9am** under the CSP/mobile phase conditions explored in the study had the *R* configuration. As a consequence, *S* configuration was assigned to the second-eluted enantiomer.

4.4.3 General Procedure for the AH of ketones and ketimines

Under argon atmosphere, the pre-catalyst (0.01 mmol, 0.05 eq.) was dispensed as DCM solution into oven-dried glass tubes fitted in an aluminum block inside a Schlenk tube. After removing DCM under vacuum, a 0.2 M solution of Me₃NO in *i*PrOH (0.1 mL, 0.02 mmol, 0.1 eq.) was dispensed. The resulting mixture was stirred at r.t. for 20 min, during which a deep orange color gradually developed. *i*PrOH (0.3 mL) and the substrate (0.2 mmol, 1 eq.) were added in each vial. Each vial was capped with a Teflon septum pierced by a needle, the block was transferred into the autoclave, and stirring was started. After purging four times with hydrogen, the reaction was pressurized at 50 bar and heating was started (80 °C). The reactions were stirred for 22 h under hydrogen pressure at 80 °C. After cooling down to r.t., the mixtures were filtered through a short part of celite and then analyzed for conversion and e.e. determination. When needed, product purification was carried out by flash column chromatography (hexane/AcOEt eluent mixtures).

4.4.3.1 Analysis of ketone AH products

The reaction mixtures were analyzed either by GC with a chiral column or by ¹H NMR/enantioselective HPLC to measure conversion and enantiomeric excess. Absolute configurations were determined by comparing the elution order with previous data obtained with the same column, unless otherwise stated.

1-Phenylethanol (**P69**)

Conversion and e.e. were determined by chiral GC.^[3c,d]

Capillary column: MEGA-DEX DAC Beta, diacetyl-*tert*-butylsilyl- β -cyclodextrin, 0.25 μ m; diameter = 0.25 mm; length = 25 m; carrier: hydrogen; inlet pressure: 1 bar; oven temperature: 95 °C for 20 min: $t_{\text{sub.}}$ = 4.76 min; t_R = 10.36 min; t_S = 12.39 min.

2,2,2-Trifluoro-1-phenylethan-1-ol (**P70**)^[4]

Conversion was determined by ¹H NMR, the product was purified by flash chromatography (hexane/ethyl acetate = 9/1) and then analyzed by enantioselective HPLC.^[4]

HPLC conditions of e.e. determination: column: Chiralcel OD-H, 0.8 mL/min, 95:5 hexane/*i*PrOH, λ = 210 nm, t_S = 12.7 min, t_R = 21.5 min.

GC conditions for determining conversion and e.e. were also established. Capillary column: MEGA-DEX DAC Beta, diacetyl-*tert*-butylsilyl- β -cyclodextrin, 0.25 μ m; diameter = 0.25 mm; length = 25 m; carrier: hydrogen; inlet pressure: 1 bar; oven temperature: 100 °C for 20 min: $t_{\text{sub.}}$ = 1.38 min; t_S = 8.97 min, t_R = 10.23 min;

1-Phenylpropan-1-ol (**P71**)

Conversion and e.e. were determined by chiral GC.^[3c,d]

Capillary column: MEGA-DEX DAC Beta, diacetyl-*tert*-butylsilyl- β -cyclodextrin, 0.25 μ m; diameter = 0.25 mm; length = 25 m; carrier: hydrogen; inlet pressure: 1 bar; oven temperature: 120 °C for 15 min: $t_{\text{sub.}}$ = 2.91 min; t_R = 3.45 min; t_S = 3.58 min.

1-(Naphthalen-2-yl)ethan-1-one (**P72**)

Conversion and e.e. were determined by chiral GC.^[3c,d]

Capillary column: MEGA-DEX DAC Beta, diacetyl-*tert*-butylsilyl- β -cyclodextrin, 0.25 μ m; diameter = 0.25 mm; length = 25 m; carrier: hydrogen; inlet pressure: 1 bar; oven temperature: 150 °C for 20 min: $t_{\text{sub.}}$ = 9.23 min; t_R = 14.89 min; t_S = 16.07 min.

3,4-Dihydronaphthalen-2(1*H*)-one (**P73**)

Conversion and e.e. were determined by chiral GC. Capillary column: MEGA-DEX DAC Beta, diacetyl-*tert*-butylsilyl- β -cyclodextrin, 0.25 μ m; diameter = 0.25 mm; length = 25 m; carrier: hydrogen; inlet pressure: 1 bar; oven temperature: 110 °C for 40 min: t_R = 18.74 min; t_S = 19.43 min; $t_{\text{sub.}}$ = 26.03 min. Absolute

configurations were assigned by comparing the sign of optical rotation with literature data ($[\alpha]_{\text{D}}^{23} = -51.4$, c 0.70 in CHCl_3 , 82% e.e., S).^[29]

4.4.3.2 Analysis of ketimine AH products

Conversions were determined by ^1H NMR analysis of the crude reaction mixtures. After purification by flash chromatography (hexane/ethyl acetate/triethylamine, 89.6/10/0.4), the enantiomeric excesses were determined by HPLC analysis with a chiral column.

4-Methoxy-*N*-(1-phenylethyl)aniline (**P1**)

Column: Chiralpak AD-H, 0.8 mL/min, 97:3 hexane/*i*PrOH, $\lambda = 210$ nm, $t_{\text{R}} = 11.79$ min, $t_{\text{S}} = 13.40$ min. Absolute configuration was determined by comparison of the sign of optical rotation with literature data ($[\alpha]_{\text{D}}^{15} = +8.5$, c 0.9 in CHCl_3 , 98% e.e., R).^[30]

4-Methoxy-*N*-(1-(naphthalen-2-yl)ethyl)aniline (**P20**)

Column: Chiralcel OD-H, 0.5 mL/min, 9:1 hexane/*i*PrOH, $\lambda = 210$ nm, $t_{\text{R}} = 15.70$ min, $t_{\text{S}} = 17.73$ min. Absolute configuration was determined by comparing the elution order with previous data obtained with the same column.^[30a]

4-Methoxy-*N*-(1-phenylpropyl)aniline (**P22**)

Column: Chiralcel OD-H, 0.8 mL/min, 98:2 hexane/*i*PrOH, $\lambda = 210$ nm, $t_{\text{R}} = 10.66$ min, $t_{\text{S}} = 11.90$ min. Absolute configuration was determined by comparing the elution order with previous data obtained with the same column.^[30a]

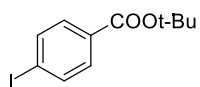
4-Methoxy-*N*-(octan-2-yl)aniline (**P25**)

Column: Phenomenex Cellulose 3 (5 μm), 0.5 mL/min, 100:1 hexane/*i*PrOH, $\lambda = 210$ nm, $t_{\text{R}} = 14.93$ min, $t_{\text{S}} = 15.57$ min. Absolute configuration was determined by comparing the elution order with previous data obtained with the same column.^[30a]

4.4.4 Synthesis of chiral macrocyclic complexes

4.4.4.1 Synthesis of CICs 9aq and 9ar

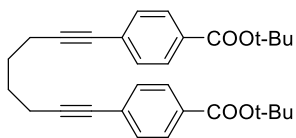
tert-Butyl 4-iodobenzoate (**40**)^[7]



Three drops of DMF were added to a suspension of 4-iodobenzoic acid (4.8616 g, 19.6 mmol, 1 eq.) in thionyl chloride (35.6 mL). The mixture was heated to reflux and stirred for 1 hour, during which time it became a clean pale green solution. After completion of

the reaction, the excess of thionyl chloride was removed under reduced pressure. The residual yellowish solid was dissolved in dry THF (48 mL) and cooled down to 0 °C. To this solution was added slowly, over the period of 1 hour and under constant stirring, a solution of potassium *tert*-butylate (4.84 g, 43.12 mmol, 2.2 eq.) in dry THF (72 mL). During the addition the temperature was not allowed to exceed 5 °C. The suspension was stirred for 1 hour at 0 °C and carefully quenched with water (5 mL). The resulting solution was concentrated under reduced pressure, and additional water (100 mL) was added. The mixture was extracted with diethyl ether (3 × 100 mL). Combined organic phase was washed with 5% NaOH solution (100 mL) and with brine (2 × 100 mL), then dried over MgSO₄ and evaporated to give the pure product as a light yellow oil. Yield: 5.6 g (94%). ¹H-NMR (400 MHz, CDCl₃): δ 7.77 (d, *J* = 8.6 Hz, 2H), 7.69 (d, *J* = 8.6 Hz, 2H), 1.58 (s, 9H).

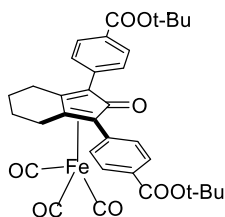
Di-*tert*-butyl 4,4'-(octa-1,7-diyne-1,8-diyl)dibenzoate (**41**)



In Schlenk tube fitted with a Teflon cap, dichlorobis(triphenylphosphine) palladium (4.1 %, 207.3 mg, 0.2954 mmol) and CuI (4.1 %, 56.3 mg, 0.2954 mmol) were added to a solution of compound **40** (4.38 g, 14.41 mmol, 2 eq.) and 1,7-

octadiyne (765 mg, 7.2 mmol, 1.0 eq.) in dry 1:1 THF/TEA (154 mL) at r.t. under N₂. The reactor was sealed and the stirred mixture heated to 60 °C under 16 hours. The resulting mixture was concentrated under reduced pressure. The residue was dissolved in DCM (100 mL) and washed with sat. aq. NH₄Cl (50 mL) and brine (2 × 50 mL). The organic phase was dried over MgSO₄ and evaporated to give the crude product. The residue was purified by flash column chromatograph (98:2 hexane/AcOEt) to afford the pure product as a pale yellow solid. Yield: 2.48 g (75%). M.p. = 114.8 °C; ¹H-NMR (400 MHz, CDCl₃): δ 7.89 (d, *J* = 8.4 Hz, 4H), 7.42 (d, *J* = 8.4 Hz, 4H), 2.52-2.49 (m, 4H), 1.80 (pen, *J* = 3.5 Hz, 4H), 1.59(s, 18H); IR (film): ν = 3650.6, 3403.7, 2977.6, 2932.2, 2864.7, 2229.3, 1934.3, 1711.5, 1605.5, 1550.1, 1506.1, 1478.2, 1457.0, 1428.0, 1403.9, 1392.4, 1368.3, 1305.5, 1294.0, 1280.5, 1256.4, 1163.8, 1116.6, 1096.3, 1017.3, 858.2, 848.5 cm⁻¹; ESI-MS (+): *m/z* 481.54 [M+Na]⁺ (calcd. for C₃₀H₃₄NaO₄: 481.24).

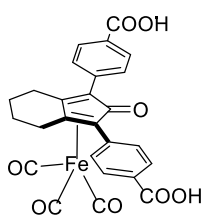
CIC **9ap**



In a Schlenk tube fitted with a Teflon-topped screw cap, distilled toluene (44 mL) was added to a mixture of the diyne **41** (2 g, 4.36 mmol, 1.0 eq.) and $\text{Fe}_2(\text{CO})_9$ (3.17 g, 8.72 mmol, 2.0 eq.) under N_2 . The mixture was heated to 110 °C and stirred overnight. After cooling down to r.t., the products were purified by column chromatography (5:1 hexane/AcOEt) to afford the pure iron complexes. Yield: 1.83 g (67%). M.p. = 90.8 °C;

$^1\text{H-NMR}$ (400 MHz, CD_2Cl_2): δ 8.00 (d, $J = 8.5$ Hz, 4H), 7.80 (d, $J = 8.5$ Hz, 4H), 2.82-2.72 (m, 4H), 1.95 (pen, $J = 3.2$ Hz, 4H), 1.59 (s, 18H); $^{13}\text{C-NMR}$ (100 MHz, CD_2Cl_2): δ 209.2, 169.8, 165.6, 136.7, 129.9, 129.8, 101.6, 81.5, 80.7, 28.5, 24.3, 22.7; IR (film): $\nu = 2925.5, 2854.1, 2062.5, 2006.6, 1711.5, 1642.1, 1607.4, 1456.0, 1392.4, 1368.3, 1295.0, 1257.4, 1167.7, 1111.8, 108.23, 848.5, 797.7, 773.3, 720.3, 700.0, 657.6, 635.4, 618.1\text{cm}^{-1}$; ESI-MS (+): m/z 649.32 $[\text{M}+\text{Na}]^+$ (calcd. for $\text{C}_{34}\text{H}_{34}\text{FeNaO}_8$: 649.15).

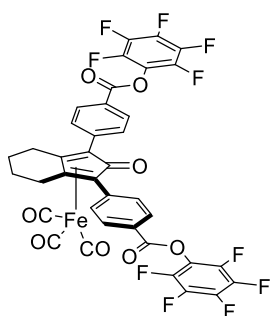
CIC **9aq**



To a solution of **9ap** (1.8 mg, 2.87 mmol, 1.0 eq.) in dry DCM (19 mL) was added 2, 2, 2-trifluoroacetic acid (8.54 mL) at 0 °C under N_2 . The reaction mixture was stirred at r.t. for 3h. Thin layer chromatography showed that starting material was consumed completely. The suspension was diluted with dichloromethane and filtered, and the

collected yellow solid was washed with DCM and dried under reduced pressure to give product. Yield: 1.48 g (100%). M.p.: 207 °C; $^1\text{H-NMR}$ (400 MHz, d_6 -DMSO): δ 7.99 (d, $J = 8.5$ Hz, 4H), 7.83 (d, $J = 8.5$ Hz, 4H), 2.84 (dt, $J = 16.7, 5.2$ Hz, 2H), 2.68-2.61 (m, 2H), 1.94-1.83 (m, 4H); $^{13}\text{C-NMR}$ (100 MHz, d_6 -DMSO): δ 208.8, 168.4, 166.9, 136.4, 129.9, 129.6, 129.2, 101.2, 79.5, 23.0, 21.5; IR (film): $\nu = 3612.02, 3582.13, 2934.16, 2076.96, 2007.53, 1719.23, 1666.2, 1610.27, 1535.06, 1404.89, 1245.79, 665.32\text{cm}^{-1}$; ESI-MS (+): m/z 537.68 $[\text{M}+\text{Na}]^+$ (calcd. for $\text{C}_{26}\text{H}_{18}\text{FeNaO}_8$: 537.02).

CIC **9ar**



To a solution of **9aq** (400 mg, 0.78 mmol, 1.0 eq.) and pentafluorophenol (315 mg, 1.71 mmol, 2.2 eq.) in DMF (4 mL) at 0 °C were added EDC (447.3 mg, 2.33 mmol, 3.0 eq.) and DMAP (38 mg, 0.31 mmol, 0.4 eq.) under N_2 . The reaction mixture was stirred at r.t. for 16 h followed by addition of saturated solution of NH_4Cl (15 mL). The mixture was extracted with DCM (3 \times 20 mL), and the combined organic extracts were washed with brine, dried over MgSO_4 , filtered, and concentrated under reduced

pressure. The crude products were purified by column chromatography (DCM) to afford the pure iron

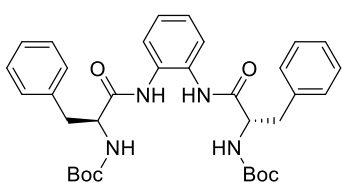
complexes as a yellow solid. Yield: 645 mg (98%). M.p. = 218.2°C; ¹H-NMR (400 MHz, CD₂Cl₂): δ 8.24 (d, *J* = 8.6 Hz, 4H), 8.00 (d, *J* = 8.6 Hz, 4H), 2.90-2.79 (m, 4H), 2.0 (pen, *J* = 3.3 Hz, 4H); ¹³C-NMR (100 MHz, CD₂Cl₂): δ 208.8, 169.7, 162.8, 139.5, 131.2, 130.5, 126.7, 101.8, 80.0, 24.5, 22.7; IR (film): *ν* = 3249.5, 1947.7, 2069.3, 2014.3, 1759.7, 1643.1, 1607.4, 1520.6, 1472.4, 1450.2, 1402.0, 1321.0, 1251.6, 1187.0, 1146.5, 1049.1, 1014.4, 996.1, 978.7, 898.7, 858.2, 791.6, 764.6, 739.6, 718.3, 692.3, 678.8 cm⁻¹; ESI-MS (+): *m/z* 868.95 [M+Na]⁺ (calcd. for C₃₈H₁₆F₁₀FeNaO₈: 868.99).

4.4.4.2 Synthesis of diamines 43a-d

4.4.4.2.1 General produce for the synthesis of Boc-protected diamines 42a-d

To a stirred solution of Boc-protected amino acid or amine (2 mmol, 2.0 eq.) and phenylenediamine or terephthalic acid (1 mmol, 1.0 eq.), respectively, in DCM was added EDC (3 mmol, 3.0 eq.) and DMAP (0.4 mmol, 0.4 eq.) at 0 °C. The mixture was stirred at r.t. for 4 h followed by addition of saturated solution of NH₄Cl. The reaction mixture was extracted with DCM, and the combined organic phases were washed with brine, dried over Na₂SO₄, filtered, and concentrated under reduced pressure. The residue was purified by column chromatography (7:3 hexane/AcOEt or 95:5 DCM/MeOH) to afford the pure product.

Di-tert-butyl ((2*S*,2'*S*)-(1,2-phenylenebis(azanediyl))bis(1-oxo-3-phenylpropane-1,2-diyl))dicarbamate (42a)

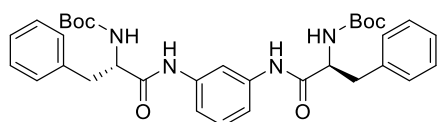


Prepared from Boc-L-phenylalanine according to the General procedure.

White solid; Yield: 578.2 mg (96%). M.p. = 112.5 °C; ¹H-NMR (400 MHz, CD₂Cl₂): δ 8.23 (s, 2H), 7.37-7.18 (m, 14H), 5.22 (bs, 2H), 4.45-4.40 (m, 2 H), 3.26 (dd, *J* = 14.0, 6.0 Hz, 2H), 3.06-3.01 (m, 2H), 1.4 (s, 18H); ¹³C-NMR (100

MHz, CD₂Cl₂): δ 171.0, 155.7, 137.0, 130.5, 129.5, 128.5, 126.9, 126.3, 125.3, 80.1, 56.4, 38.2; IR (film): *ν* = 3736.4, 3650.6, 3310.2, 3027.7, 2975.6, 2931.3, 2842.6, 2363.3, 1671.0, 1599.7, 1509.0, 1451.2, 1390.4, 1365.4, 1248.7, 1161.9, 1050.1, 1031.7, 1019.2, 918.9, 852.4, 752.1, 699.1 cm⁻¹; ESI-MS (+): *m/z* 625.41 [M+Na]⁺ (calcd. for C₃₄H₄₂N₄NaO₆: 625.30).

Di-tert-butyl ((2*S*,2'*S*)-(1,3-phenylenebis(azanediyl))bis(1-oxo-3-phenylpropane-1,2-diyl))dicarbamate (42b)



Prepared from Boc-L-phenylalanine according to the General procedure. White solid; Yield: 710.7 mg (59%). M.p.= 123.8 °C; ¹H-

NMR (400 MHz, CD₂Cl₂): δ 8.99 (s, 2H), 7.69 (d, *J* = 2.1 Hz, 1H),

7.29-7.16(m, 10H), 6.96 (m, 3H), 5.62 (d, *J* = 8.2 Hz, 2H), 4.78-4.74 (m, 2 H), 3.20 (dd, *J* = 14.0, 5.6 Hz, 2H),

3.00-2.94 (m, 2H), 1.43 (s, 18H); ¹³C-NMR (100 MHz, CD₂Cl₂): δ 170.8, 157.0, 138.9, 137.5, 129.8, 129.1,

127.3, 115.5, 111.8, 81.0, 57.1, 39.0, 28.7; IR (film): ν = 3686.3, 3673.7, 3667.0, 3646.7, 3626.5, 3616.8,

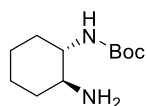
3606.2, 2976.6, 2945.7, 2832.9, 2516.7, 2220.6, 2038.4, 1694.2, 1681.6, 1614.1, 1565.0, 1556.3, 1538.9,

1504.2, 1494.6, 1486.9, 1454.1, 1428.0, 1392.4, 1367.3, 1288.2, 1252.5, 1167.7, 1113.7, 1081.9, 1031.7, 918.0,

857.2, 783.0, 741.5, 699.0 cm⁻¹; ESI-MS (+): *m/z* 625.70 [M+Na]⁺ (calcd. for C₃₄H₄₂N₄NaO₆: 625.30).

***tert*-Butyl ((1*S*,2*S*)-2-aminocyclohexyl)carbamate (**44**)^[17]**

(1*S*,2*S*)-Cyclohexane-1,2-diamine (1 g, 8.76 mmol, 3.0 eq.) was dissolved in CH₂Cl₂ (32.7 mL)



followed by dropwise addition of a solution of (Boc)₂O (637.1 mg, 2.92 mmol, 1.0 eq.) in 15

mL of DCM at r.t. After addition the reaction was stirred for 7 h at r.t. The reaction mixture was

washed with H₂O (3 × 18 mL), the organic phase was dried over MgSO₄, and concentrated under reduced

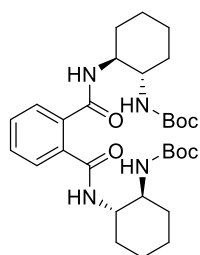
pressure. The residue was purified by column to give light yellow solid. Yield: 710.7 mg (59%). ¹H-NMR (400

MHz, CD₂Cl₂): δ 4.5 (s, 1H), 3.12 (d, *J* = 10.9 Hz, 1H), 2.31 (td, *J* = 10.3, 4.0 Hz, 1H), 2.01-1.93 (m, 2H),

1.69 (dt, *J* = 12.1, 2.7 Hz, 2H), 1.44 (s, 9H), 1.32-1.06 (m, 4H); ¹³C-NMR (100 MHz, CD₂Cl₂): δ 156.2, 79.2,

57.7, 55.7, 35.3, 32.9, 28.5, 25.3, 25.1.

Di-*tert*-butyl ((1*S*,1'*S*,2*S*,2'*S*)-(phthaloylbis(azanediyl))bis(cyclohexane-2,1-diyl))dicarbamate (42c**)**



The compound **44** (150 mg, 0.70 mmol, 1.0 eq.) was added to a stirring solution of phthalic anhydride (103.7 mg, 0.70 mmol, 1.0 eq.) in CHCl₃ (7.5 mL); a white precipitate was form.

The mixture was heated to reflux and stirred for 3 h, then it was cooled down to r.t. and concentrated under reduced pressure. The crude product was used directly for next step.

To a stirred solution of compound **44** (150 mg, 0.70 mmol, 1.0 eq.) and the crude product (0.47 mmol) in DCM (6 mL) was added EDC (201.3 mg, 1.05 mmol, 1.5 eq.) and DMAP (17.1 mg, 0.14 mmol,

0.2 eq.) at 0 °C. The resulting mixture was stirred at r.t. for 5 h. The mixture was concentrated under reduced

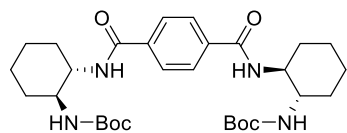
pressure and purified by column chromatography (97:3 DCM/MeOH) to afford the pure product as a white

solid. Yield: 254.2 mg (65%). M.p. = 210.7 °C; ¹H-NMR (400 MHz, CD₂Cl₂): δ 7.51-7.30 (m, 4H), 7.01 (s,

2H), 4.98 (s, 2H), 3.76-3.68 (m, 2H), 3.40 (d, *J* = 10.2 Hz, 2H), 2.13-2.03 (m, 4H), 1.77-1.73 (m, 4H), 1.39 (s,

18H), 1.35-1.23 (m, 8H); ^{13}C -NMR (100 MHz, CD_2Cl_2): δ 169.4, 157.0, 135.9, 130.4, 128.6, 79.7, 33.3, 32.8, 28.7, 25.5, 25.3; IR (film): $\nu = 3353.6, 2977.6, 2932.2, 2858.0, 1688.4, 1645.0, 1595.8, 1520.6, 1452.1, 1391.4, 1365.4, 1321.0, 1301.7, 1254.5, 1237.1, 1172.5, 1052.9, 1013.4, 956.5, 870.7, 783.0, 737.6, 694.2, 640.3 \text{ cm}^{-1}$; ESI-MS (+): m/z 581.59 $[\text{M}+\text{Na}]^+$ (calcd. for $\text{C}_{30}\text{H}_{46}\text{N}_4\text{NaO}_6$: 581.33).

Di-tert-butyl ((1S,1'S,2S,2'S)-(terephthaloylbis(azanediy))bis(cyclohexane-2,1-diyl))dicarbamate (42d)



Prepared from compound **44** according to the General procedure. White solid;

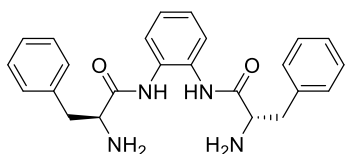
Yield: 320.7 mg (82%). ^1H -NMR (400 MHz, 4:1 $\text{CD}_2\text{Cl}_2/\text{CD}_3\text{OD}$): δ 7.83 (s, 4H), 7.78 (d, $J = 8.0$ Hz, 2H), 5.66 (d, $J = 8.9$ Hz, 2H), 3.69 (q, $J = 9.8, 8.9$ Hz,

2H), 3.42 (d, $J = 8.9$ Hz, 2H), 2.09 (q, $J = 5.3, 4.4$ Hz, 2H), 1.95 (d, $J = 8.6$ Hz, 2H), 1.77-1.73 (m, 4H), 1.33-1.28 (m, 8H) 1.28 (s, 18H); ^{13}C -NMR (100 MHz, 4:1 $\text{CD}_2\text{Cl}_2/\text{CD}_3\text{OD}$): δ 167.9, 158.0, 137.6, 127.8, 80.1, 56.3, 54.1, 33.0, 32.7, 28.6, 25.7, 25.2; IR (film): $\nu = 3583.1, 3349.8, 3304.4, 2921.6, 2856.1, 2487.7, 1684.5, 1632.5, 1544.7, 1525.4, 1502.3, 1421.3, 1365.4, 1323.9, 1288.2, 1240.0, 1173.5, 1082.8, 1017.3, 854.3, 656.6 \text{ cm}^{-1}$; ESI-MS (+): m/z 582.68 $[\text{M}+\text{Na}]^+$ (calcd. for $\text{C}_{30}\text{H}_{46}\text{N}_4\text{NaO}_6$: 581.33).

4.4.4.2.2 General produce for the synthesis of diamines 43a-d

Boc-protected diamines (1 mmol, 1.0 eq.) was added to a stirred solution of CF_3COOH (4.2 mL) in dichloromethane (8.5 mL) at r.t. The mixture was stirred at r.t. for 30 min, diluted with dichloromethane (10 mL), basified with aq 0.5 N NaOH. The organic layer was separated, dried over anhydrous MgSO_4 and evaporated to give the desired diamine.

(2S,2'S)-N,N'-(1,2-Phenylene)bis(2-amino-3-phenylpropanamide) (43a)

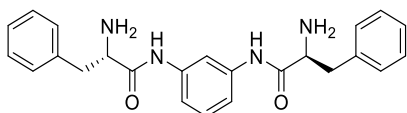


Prepared from Boc-protected diamine **43a** according to the General procedure.

White solid; Yield: 313.9 mg (94%). M.p. = 109.7 °C; ^1H -NMR (400 MHz, CD_2Cl_2): δ 9.45 (s, 2H), 7.63 (dd, $J = 6.0, 3.5$ Hz, 2H), 7.35-7.20 (m, 12H),

3.71 (dd, $J = 9.2, 4.2$ Hz, 2H), 3.30 (dd, $J = 13.8, 4.2$ Hz, 2H), 2.78 (dd, $J = 13.8, 9.2$ Hz, 2H); ^{13}C -NMR (100 MHz, CD_2Cl_2): δ 173.6, 138.5, 130.7, 129.9, 129.2, 127.3, 126.2, 124.9, 57.5, 41.4; IR (film): $\nu = 3383.5, 3296.7, 3059.5, 3026.7, 2924.5, 2852.2, 1673.0, 1597.7, 1518.7, 1496.5, 1454.1, 1303.6, 1265.1, 1180.2, 1103.1, 1074.2, 1030.8, 918.9, 845.6, 754.0, 701.0 \text{ cm}^{-1}$; ESI-MS (+): m/z 403.11 $[\text{M}+\text{H}]^+$ (calcd. for $\text{C}_{24}\text{H}_{27}\text{N}_4\text{O}_2$: 403.21).

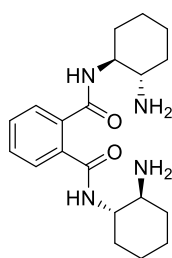
(2S,2'S)-N,N'-(1,3-Phenylene)bis(2-amino-3-phenylpropanamide) (43b)



Prepared from Boc-protected diamine **42b** according to the General procedure. White solid; Yield: 467.5 mg (100%). M.p. = 80.8 °C; ¹H-NMR (400 MHz, CD₂Cl₂): δ 7.76 (t, *J* = 2.0 Hz, 1H), 7.30-7.18 (m, 13H), 3.68

(t, *J* = 6.9 Hz, 2H), 3.08 (dd, *J* = 13.3, 6.5 Hz, 2H), 2.89 (dd, *J* = 13.3, 7.2 Hz, 2H); ¹³C-NMR (100 MHz, CD₂Cl₂): δ 175.1, 139.7, 138.7, 130.4, 129.6, 127.8, 127.8, 117.3, 113.5, 58.3, 42.6; IR (film): ν = 3297.7, 3059.5, 3027.7, 2925.5, 2851.2, 1680.7, 1607.4, 1530.2, 1493.6, 1453.1, 1422.2, 1303.6, 1264.1, 1208.2, 1164.8, 1094.4, 1029.8, 878.4, 786.8, 737.6, 701.0, 643.1 cm⁻¹; ESI-MS (+): *m/z* 425.27 [M+Na]⁺ (calcd. for C₂₄H₂₆N₄NaO₂: 425.20).

***N*¹,*N*²-Bis((1*S*,2*S*)-2-aminocyclohexyl)phthalamide (43c)**

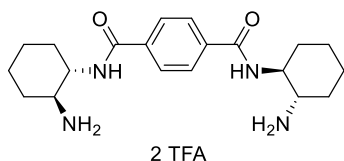


Prepared from Boc-protected diamine **42c** according to the General procedure. White solid;

Yield: 467.5 mg (100%). M.p. = 213.2 °C; ¹H-NMR (400 MHz, CD₂Cl₂): δ 7.53 (dd, *J* = 5.7, 3.4 Hz, 2H), 7.45 (dd, *J* = 5.7, 3.4 Hz, 2H), 6.68 (s, 2H), 3.58 (ddd, *J* = 13.1, 10.7, 6.6 Hz, 2H), 2.44 (td, *J* = 10.3, 4.0 Hz, 2H), 2.02 (dt, *J* = 9.4, 2.9 Hz, 2H), 1.92-1.87 (m, 2H), 1.76-1.71 (m, 4H), 1.37-1.17 (m, 8H); ¹³C-NMR (100 MHz, 9:1 CD₂Cl₂/CD₃OD): δ 170.5, 136.5,

130.4, 127.9, 56.8, 34.7, 32.6, 25.7, 25.5; IR (film): ν = 3414.4, 2932.2, 2858.0, 2362.4, 1635.3, 1592.9, 1545.6, 1449.2, 1387.5, 1333.5, 1165.8, 1114.7 cm⁻¹; ESI-MS (+): *m/z* 359.26 [M+H]⁺ (calcd. for C₂₀H₃₁N₄O₂: 359.24).

***N*¹,*N*⁴-Bis((1*S*,2*S*)-2-aminocyclohexyl)terephthalamide (TFA salts, 43d)**



Prepared from Boc-protected diamine **42d** according to the General procedure

without treatment. Yield: 296.5 mg (100%). M.p. = 259.5 °C; ¹H-NMR (400 MHz, CD₃OD): δ 9.55 (s, 4H), 5.61 (td, *J* = 11.2, 4.3 Hz, 2H), 4.72 (td, *J* = 11.2, 4.3 Hz, 2H), 3.73-3.69 (m, 2H), 3.62-3.56 (m, 2H), 3.45-3.41 (m, 4H),

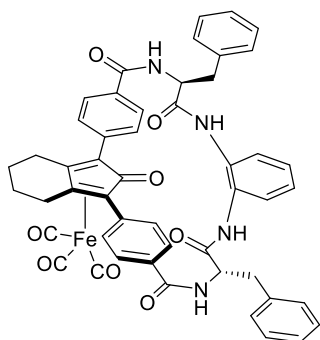
3.18-2.94 (m, 8H); ¹³C-NMR (100 MHz, CD₃OD): δ 169.8, 138.1, 128.8, 55.8, 53.0, 32.5, 31.2, 25.6, 25.0; IR (film): ν = 3310.2, 2932.2, 1677.8, 1630.5, 1535.1, 1331.6, 1206.3, 648.9 cm⁻¹; ESI-MS (+): *m/z* 359.32 [M+Na]⁺ (calcd. for C₂₀H₃₁N₄O₂: 359.24).

4.4.4.3 General produce for the synthesis of iron complexes 9ga, 9gc and 9gd

To a solution of CIC **9aq** (0.2 mmol, 1.0 eq.) in dry DMF (20 mL), HATU (0.48 mmol, 2.4 eq.), HOAt (0.48 mmol, 2.4 eq.) and DIPEA (2.4 mmol, 12 eq.) was added at 0 °C under N₂. After 15 min, a solution of chiral

diamine (0.24 mmol, 1.2 eq.) in DMF (20 mL) was added dropwise and the resulting mixture was stirred overnight at r.t. The mixture was concentrated under reduced pressure. The residue was dissolved in DCM. The resulting solution was washed with a 1 M aqueous solution of KHSO_4 and a sat. solution of NaHCO_3 , dried over Na_2SO_4 and concentrated. The products were purified by column chromatography (95:5 DCM/MeOH) to afford the pure product.

CIC 9ga

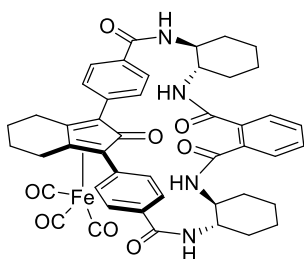


Prepared from CIC 9aq and chiral diamine according to the General procedure.

Yield: 43.6 mg (51%).

$^1\text{H-NMR}$ (400 MHz, CD_2Cl_2): δ 8.72-8.53 (m, 2H), 7.59-7.04 (m, 22H), 5.01-4.87 (m, 2H), 3.44-3.26 (m, 4H), 2.52-2.30 (m, 4H), 1.80-1.75 (m, 4H); ESI-MS (+): m/z 903.16 $[\text{M}+\text{Na}]^+$ (calcd. for $\text{C}_{50}\text{H}_{40}\text{FeN}_4\text{NaO}_8$: 903.21).

CIC 9gc

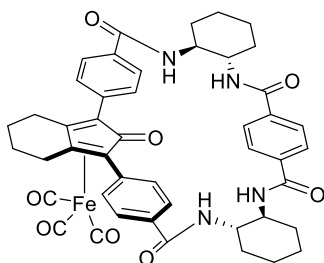


Prepared from CIC 9aq and chiral diamine according to the General procedure.

Yield: 5.7 mg (11%).

$^1\text{H-NMR}$ (400 MHz, CD_2Cl_2): δ 8.13-7.19 (m, 12H), 3.78-3.74 (m, 2H), 3.08-2.39 (m, 2H), 2.22-0.84 (m, 24H); ESI-MS (+): m/z 860.17 $[\text{M}+\text{Na}]^+$ (calcd. for $\text{C}_{46}\text{H}_{44}\text{FeN}_4\text{NaO}_8$: 859.24).

CIC 9gd



Prepared from CIC 9aq and chiral diamine according to the General procedure.

Yield: 41.2 mg (35%).

$^1\text{H-NMR}$ (400 MHz, CD_2Cl_2): δ 7.73-7.64 (m, 12H), 3.94-3.93 (m, 4H), 3.44-3.40 (m, 4H), 2.70-2.60 (m, 4H), 2.10 (s, 4H), 1.81 (s, 8H), 1.40-1.15 (m, 8H); ESI-MS (+): m/z 859.42 $[\text{M}+\text{Na}]^+$ (calcd. for $\text{C}_{46}\text{H}_{44}\text{FeN}_4\text{NaO}_8$: 859.24).

4.4.5 Catalytic tests with chiral macrocyclic iron complexes **9ga**, **9gc**, and **9gd**

Under argon atmosphere, the pre-catalyst (0.005 mmol) was dispensed into oven-dried glass tubes fitted in an aluminum block inside a Schlenk tube. The solvent *i*PrOH (0.071 mL) was added in each tube. A 0.345 M solution of Me₃NO in water (0.029 mL, 0.01 mmol) was dispensed. The resulting mixture was stirred at r.t. for 20 min, during which a deep orange color gradually developed. The substrate (0.1 mmol) were added in each vial. Each vial was capped with a Teflon septum pierced by a needle, the block was transferred into the autoclave, and stirring was started. After purging four times with hydrogen, the reaction was pressurized at 50 bar and heating was started (80 °C). The reactions were stirred for 22 h under hydrogen pressure at 80 °C. After cooling down to r.t., the mixtures were filtered through a short part of celite and then analyzed for conversion and e.e. determination.

Analysis of acetophenone AH products

The reaction mixtures were analyzed by GC with a chiral column to measure conversion and enantiomeric excess. Absolute configurations were determined by comparing the elution order with previous data obtained with the same column.

1-Phenylethanol (**P69**)

Conversion and e.e. were determined by chiral GC.^[3c,d]

Capillary column: MEGA-DEX DAC Beta, diacetyl-*tert*-butylsilyl- β -cyclodextrin, 0.25 μ m; diameter = 0.25 mm; length = 25 m; carrier: hydrogen; inlet pressure: 1 bar; oven temperature: 95 °C for 20 min: $t_{\text{sub.}}$ = 4.76 min; t_R = 10.36 min; t_S = 12.39 min.

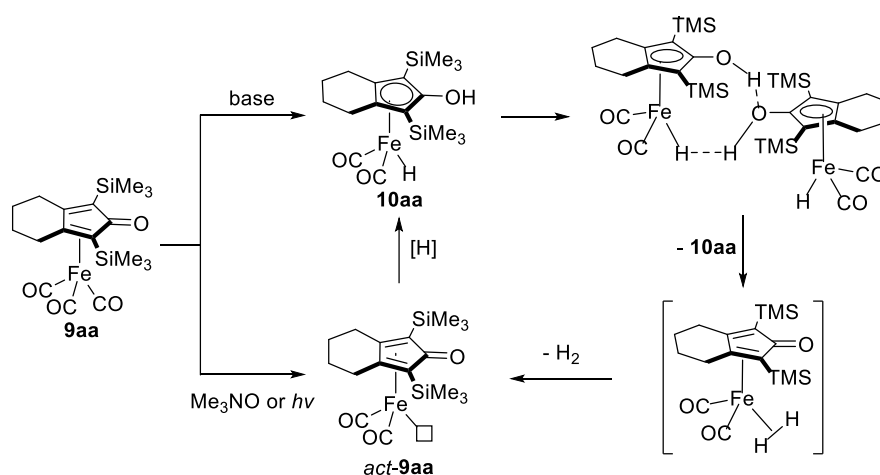
References

- [1] a) S. Zhou, S. Fleischer, K. Junge, M. Beller, *Angew. Chem., Int. Ed.* **2011**, *50*, 5120-5124; b) S. Fleischer, S. Zhou, S. Werkmeister, K. Junge, M. Beller, *Chem. Eur. J.* **2013**, *19*, 4997-5003; c) S. Zhou, S. Fleischer, H. Jiao, K. Junge, M. Beller, *Adv. Synth. Catal.* **2014**, *356*, 3451-3455.
- [2] A. Berkessel, S. Reichau, A. von der Höh, N. Leconte, J.-M. Neudörfl, *Organometallics* **2011**, *30*, 3880-3887.
- [3] a) R. Hodgkinson, A. Del Grosso, G. Clarkson, M. Wills, *Dalton Trans.* **2016**, *45*, 3992-4005; b) J. P. Hopewell, J. E. D. Martins, T. C. Johnson, J. Godfrey, M. Wills, *Org. Biomol. Chem.* **2012**, *10*, 134-145; c) P. Gajewski, M. Renom-Carrasco, S. Vailati Facchini, L. Pignataro, L. Lefort, J. G. de Vries, R. Ferraccioli, A. Forni, U. Piarulli, C. Gennari, *Eur. J. Org. Chem.* **2015**, 1887-1893; d) P. Gajewski, M. Renom-Carrasco, S. Vailati Facchini, L. Pignataro, L. Lefort, J. G. de Vries, R. Ferraccioli, U. Piarulli, C. Gennari, *Eur. J. Org. Chem.* **2015**, 5526-5536.
- [4] X. Dou, T. Hayashi, *Adv. Synth. Catal.* **2016**, *358*, 1054-1058.
- [5] a) T. V. Chciuk, W. R. Anderson, R. A. Flowers II, *Organometallics* **2017**, *36*, 4579-4583; b) Z. B. Lim, K. S. Tan, A. V. Lunchev, H. Li, S. J. Cho, A. C. Grimsdale, R. Yazami, *Synthetic Metals* **2015**, *200*, 85-90; c) C. F. H. Allen, J. A. VanAllan, *J. Am. Chem. Soc.* **1950**, *72*, 5165-5167; d) J. E. Moore, M. York, J. P. A. Harrity, *Synlett* **2005**, 0860-0862.
- [6] L. Hoffmeister, T. Fukuda, G. Pototschnig, A. Fürstner, *Chem. Eur. J.* **2015**, *21*, 4529-4533.
- [7] S. Kolodych, O. Koniev, Z. Baatarkhuu, J.-Y. Bonnefoy, F. Debaene, S. Cianférani, A. Van Dorsselaer, A. Wagner, *Bioconjugate Chem.* **2015**, *26*, 197-200.
- [8] A. Molina-Ontoria, G. Fernández, M. Wielopolski, C. Atienza, L. Sánchez, A. Gouloumis, T. Clark, N. Martín, D. M. Guldi, *J. Am. Chem. Soc.* **2009**, *131*, 12218-12229.
- [9] a) J. M. Smith, T. Qin, R. R. Merchant, J. T. Edwards, L. R. Malins, Z. Liu, G. Che, Z. Shen, S. A. Shaw, M. D. Eastgate, P. S. Baran, *Angew. Chem., Int. Ed.* **2017**, *56*, 11906-11910; b) M. Shi, K. Shouki, Y. Okamoto, S. Takamuku, *J. Chem. Soc., Perkin Trans. 1* **1990**, 2443-2450.
- [10] T.-T. Thai, D. S. Mérel, A. Poater, S. Gaillard, J.-L. Renaud, *Chem. Eur. J.* **2015**, *21*, 7066-7070.
- [11] The articulated relationship between 3D-geometry and the electronic configuration of transition metals located in a chiral environment makes the assignment of the absolute configuration (AC) of chiral metal complexes become to be an arduous task. Indeed, except d-type orbitals and higher angular momentum orbital, the spin-polarized must be also considered in some cases. Comparing to chiral organic molecules only involving s and p orbitals, these parameters make the the theoretical description of the metal-ligand interactions become to be more complicated. For a recent review on this topic, see: T. Wu, X.-Z. You, P. Bouř, *Coord. Chem. Rev.* **2015**, *284*, 1-18.
- [12] a) H. D. Flack, G. Bernardinelli, *Chirality* **2008**, *20*, 681-690; b) S. Parsons, *Tetrahedron: Asymmetry* **2017**, *28*, 1304-1313.
- [13] a) J.-P. Djukic, A. Hijazi, H. D. Flack, G. Bernardinelli, *Chem. Soc. Rev.* **2008**, *37*, 406-425; b) T. E. Sloan, in *Topics in Stereochemistry, Vol. 12* (Ed.: G. L. Geoffroy), Wiley, **1981**, pp. 1-36; c) K. Schlägl, in *Topics in Stereochemistry, Vol. 1* (Eds.: N. L. Allinger, E. L. Eliel), Wiley, **1967**, pp. 39-91; d) R. S. Cahn, C. Ingold, V. Prelog, *Angew. Chem., Int. Ed.* **1966**, *5*, 385-415.
- [14] First, the spectroscopic measurements based on chiroptical methods, such as electronic circular dichroism (ECD), vibrational circular dichroism (VCD), or optical rotation (OR), were carried out with the enantiomerically pure sample. Second, the spectra of one or more of the possible stereoisomers was simulated by quantum chemical calculations and compared to that of spectra acquired by spectroscopic measurements. Third, the absolute configuration was provided by a good match between the compared spectra, see: S. Superchi, P. Scafato, M. Gorecki, G. Pescitelli, *Curr. Med. Chem.* **2018**, *25*, 287-320.
- [15] K. Sonogashira, *J. Organomet. Chem.* **2002**, *653*, 46-49.
- [16] S. Specklin, J. Cossy, *J. Org. Chem.* **2015**, *80*, 3302-3308.
- [17] L. Yan, G. Huang, H. Wang, F. Xiong, H. Peng, F. Chen, *Eur. J. Org. Chem.* **2018**, 99-103.
- [18] L. Pignataro, M. Boghi, M. Civera, S. Carboni, U. Piarulli, C. Gennari, *Chem. Eur. J.* **2012**, *18*, 1383-1400.
- [19] See a review: C. A. G. N. Montalbetti, V. Falque, *Tetrahedron* **2005**, *61*, 10827-10852.
- [20] a) L. A. Carpino, *J. Am. Chem. Soc.* **1993**, *115*, 4397-4398; b) L. A. Carpino, A. El-Faham, F. Albericio, *Tetrahedron Lett.* **1994**, *35*, 2279-2282.
- [21] W. C. Still, M. Kahn, A. Mitra, *J. Org. Chem.* **1978**, *43*, 2923-2925.

- [22] H. Urabe, F. Sato, *J. Am. Chem. Soc.* **1999**, *121*, 1245-1255.
- [23] D.-A. Roşca, K. Radkowski, L. M. Wolf, M. Wagh, R. Goddard, W. Thiel, A. Fürstner, *J. Am. Chem. Soc.* **2017**, *139*, 2443-2455.
- [24] S. Parsons, H. D. Flack, T. Wagner, *Acta Crystallogr., Sect. B: Struct. Sci.* **2013**, *69*, 249-259.
- [25] G. M. Sheldrick, *SADABS*, Program for Empirical Absorption Correction of Area Detector Data, University of Göttingen, Göttingen, Germany, **1996**.
- [26] a) G. Sheldrick, *Acta Crystallogr., Sect. A: Found. Crystallogr.* **2008**, *64*, 112-122; b) G. Sheldrick, *Acta Crystallogr., Sect. C: Cryst. Struct. Commun.* **2015**, *71*, 3-8.
- [27] L. Farrugia, *J. Appl. Crystallogr.* **2012**, *45*, 849-854.
- [28] L. Farrugia, *J. Appl. Crystallogr.* **1997**, *30*, 565.
- [29] R. Soni, J.-M. Collinson, G. C. Clarkson, M. Wills, *Org. Lett.* **2011**, *13*, 4304-4307.
- [30] a) K. Saito, H. Miyashita, T. Akiyama, *Org. Lett.* **2014**, *16*, 5312-5315; b) C. Zhu, T. Akiyama, *Org. Lett.* **2009**, *11*, 4180-4183.

Chapter 5 - MOF-supported CICs

As discussed in the previous chapters, even though CICs possess interesting catalytic properties,^[1] their activated forms suffer from stability issues, as they are believed to undergo deactivation through dimerization pathways (Scheme 5.1).^[2]



Scheme 5.1. Commonly accepted pathway for the deactivation of CICs and HCICs.^[2]

To overcome this limitation, a possible approach is the introduction of steric bulk into the CICs structure to prevent the dimerization. In particular, pre-catalyst **9d** – featuring bulky cyclooctane rings fused to the cyclopentadienone ring – represents a successful example in this sense (see Chapter 2). An alternative strategy is represented by complex heterogenization, which may lead to the following general advantages: i) increased stability of the active complex, due to site isolation; ii) substrate selectivity based on shape and size of the catalyst's pores; iii) general intrinsic advantages of heterogeneous catalysts, i.e. easy manipulation, separation from the reaction product and re-use.

This chapter describes the efforts I made towards incorporating CICs into metal-organic frameworks (MOFs), in collaboration with the research group of Dr. Marco Ranocchiari (Paul Scherrer Institute, Villigen, Switzerland), specialized in the synthesis and characterization of these fascinating materials. MOFs are porous crystalline solids formed by multi-functionalized organic molecules and inorganic units (metal or metal clusters) with a regular – and in some cases predictable – geometry.^[3] These porous coordination polymers have a strong potential in catalytic transformations due to their unique features,^[4] such as presence of multiple active sites, tunable porosity, and possibility to adjust structure and environment of the active site, whereas their applications are still quite limited. MOFs for catalytic applications may be obtained in different ways: 1) by direct synthesis, employing either inorganic nodes^[5] or linkers^[6] possessing catalytic activity. An example

of this approach is the replacement of the terephthalate linkers of MOF-5 (Figure 5.1 A) with the corresponding amino-functionalized linkers (Figure 5.1 B).^[6e] 2) Encapsulating catalysts into the MOF cavities, whose size may be modulated by varying the size of linkers and inorganic units (Figure 5.1 C).^[7] 3) By post-synthetic modification of an existing MOF, in which catalytically active sites may be introduced by metal exchange, linker exchange or by grafting a catalytic complex to functional groups present on the linkers.^[8]

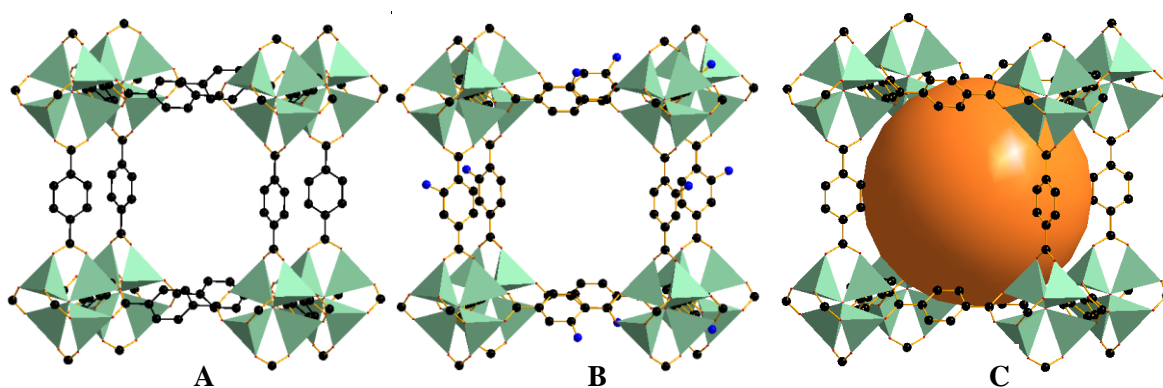


Figure 5.1. A: MOF-5; B: IRMOF-3 containing amino groups (blue); C: MOF-5 cage (green/black) with encapsulated catalyst (orange).

5.1 Preparation of MOF-supported CICs

Our original plan to prepare MOF-supported CIC-pre-catalysts consisted in a direct synthesis performed combining suitable CIC- and cyclopentadienone-linkers in the presence of a suitable metal. Based on our expertise in the field of CICs and their catalytic applications,^[9] the synthesis of new CICs and new cyclopentadienones to be used for the incorporation into MOFs were carried out.

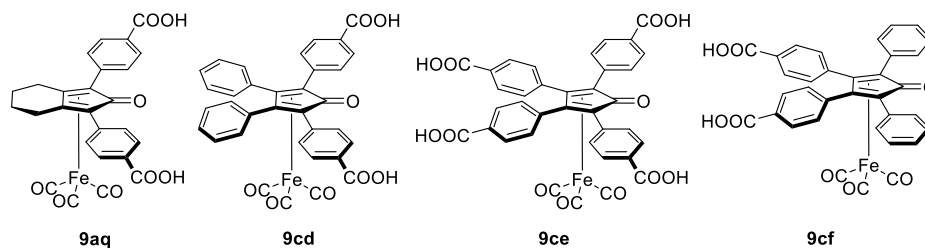
5.1.1 Synthesis of CICs and cyclopentadienones as linkers or active site

We designed and synthesized a series of new carboxy-substituted CICs (**9aq** and **9cd-9cf** in Figure 5.2) and cyclopentadienones (**48a-d** in Figure 5.2) as linkers for the direct preparation of new MOFs.

As shown in Scheme 5.2, starting from suitable 1,3-diphenylacetone derivatives (**45**) and benzil derivatives (**46**), we synthesized cyclopentadienones **47a-c** by condensation. Although the starting materials **45b** and **46b** are commercially available, the 1,3-diphenylacetone derivative **45a** and the benzil derivative **46a** were synthesized. According to literature reports,^[10] compound **45a** could be easily prepared from *p*-toluic acid through esterification, bromination and then reaction with $\text{Fe}(\text{CO})_5$ and NaOH under phase-transfer conditions

(Scheme 5.3 A). Following again known procedures,^[11] we also synthesized compound **46a** in four steps from methyl 4-formylbenzoate (Scheme 5.3 B).

A. Carboxy-substituted (cyclopentadiene)iron complexes



B. Carboxy-substituted cyclopentadienones

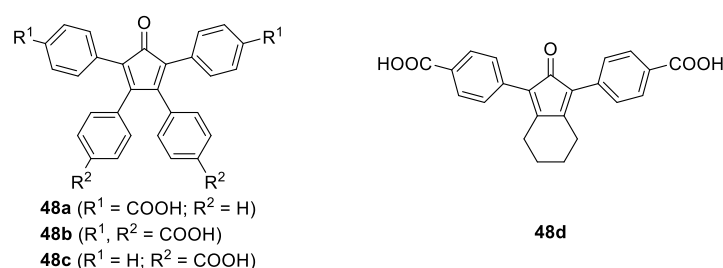
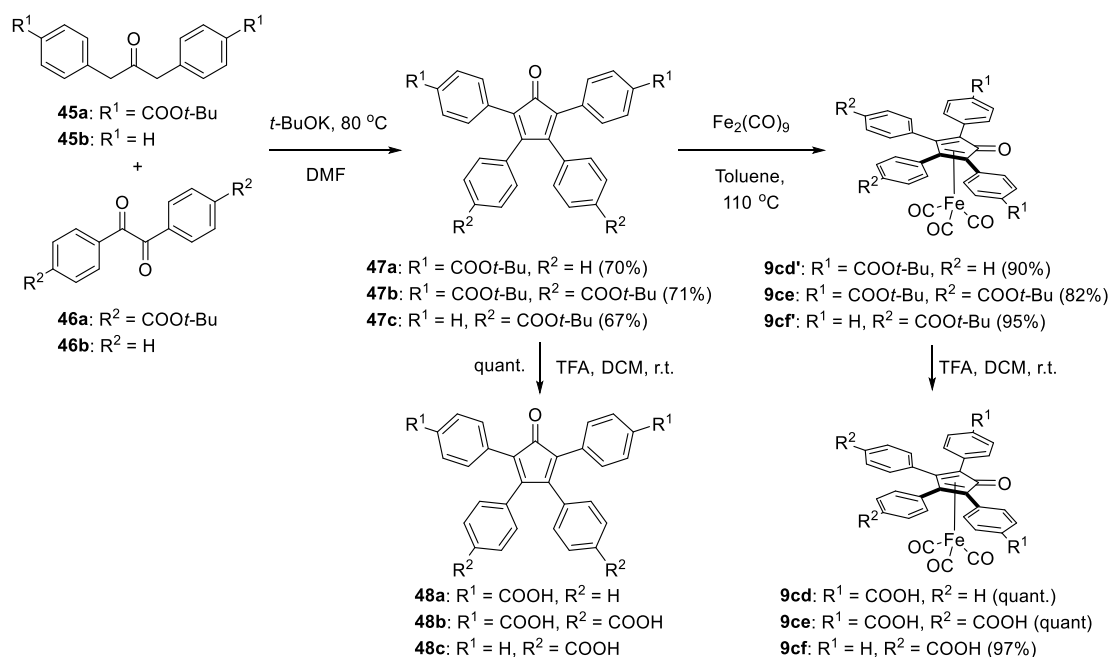
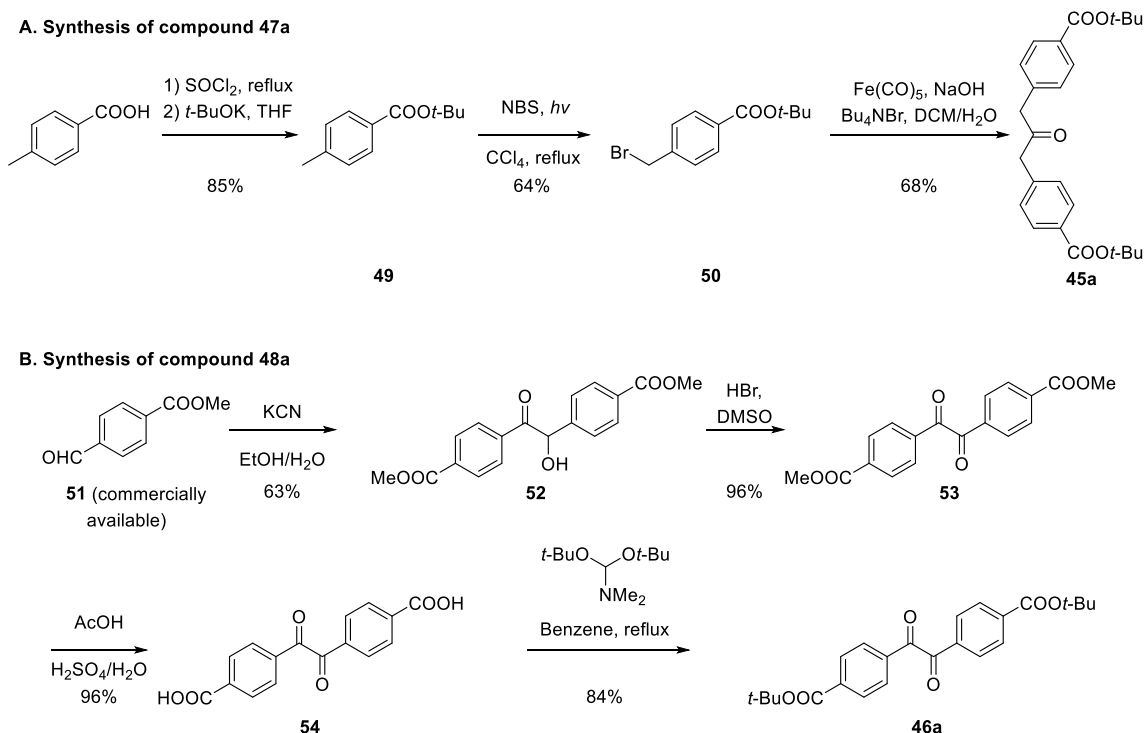
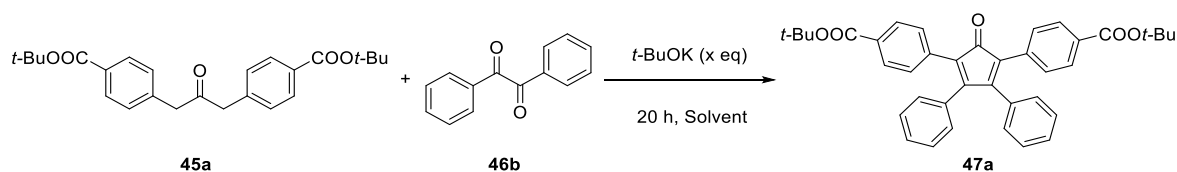


Figure 5.2. Carboxy-substituted CICs (A) and cyclopentadienones (B).



Scheme 5.2. Synthesis of CICs **9cd-9cf** and cyclopentadienones **48a-c**.

The synthesis of cyclopentadienone **47a** was initially carried out adopting literature conditions (KOH in EtOH),^[12] which led to the final product in only in low yield (18%). For this reason, different reaction conditions were screened on a model reaction (Table 5.1), to identify a general protocol for the condensation of diphenylacetones (**45**) with benzil derivatives (**46**).

Scheme 5.3. Synthesis of compound **45a** and **46a**.Table 5.1. Optimization for the reaction conditions for the synthesis of cyclopentadienones.^[a]

#	Solvent	<i>t</i> -BuOK (eq)	<i>T</i> (°C)	Yield (%) ^[b]
1	THF	0.1	40	0
2	THF	0.1	70	40
3	Dioxane	0.1	100	44
4	DMF	0.05	80	18
5	DMF	0.1	80	57
6	DMF	0.2	80	70
7	DMF	0.3	80	56
8	DMF	0.5	80	41

[a] Reaction conditions: **45a/46b** = 1:1, 20 h. $C_{0,\text{sub.}} = 0.122 \text{ M}$ (0.122 mmol).

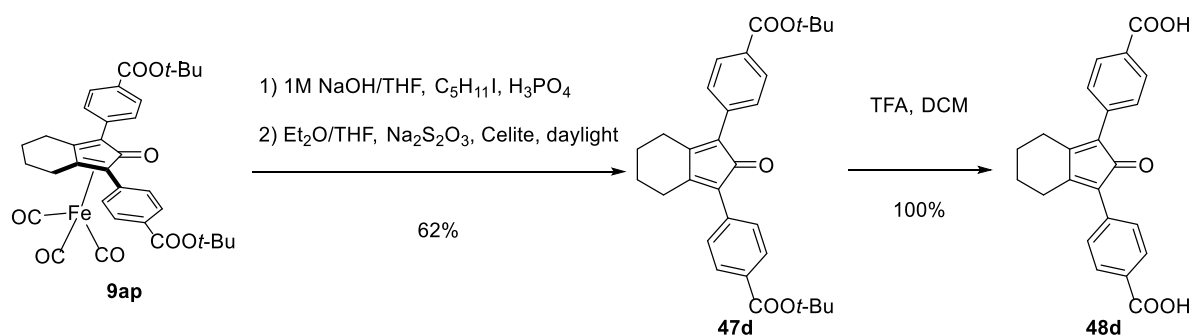
[b] Isolated yield.

To improve the yields, we decided to use a non-nucleophilic base (*t*-BuOK) and a polar aprotic solvents. No product was obtained at low temperature (40 °C) in THF (Table 5.1, entry 1), but the yield could be improved by increasing the temperature to 70 °C (Table 5.1, entry 2). However, a further increase of temperature (to 100 °C, reaction performed in dioxane) produced only a slight improvement in terms of yield (Table 5.1, entry 3 vs. entry 2). Higher yields were obtained running the reaction in DMF at 80 °C (Table 5.1, entry 5 vs. entry

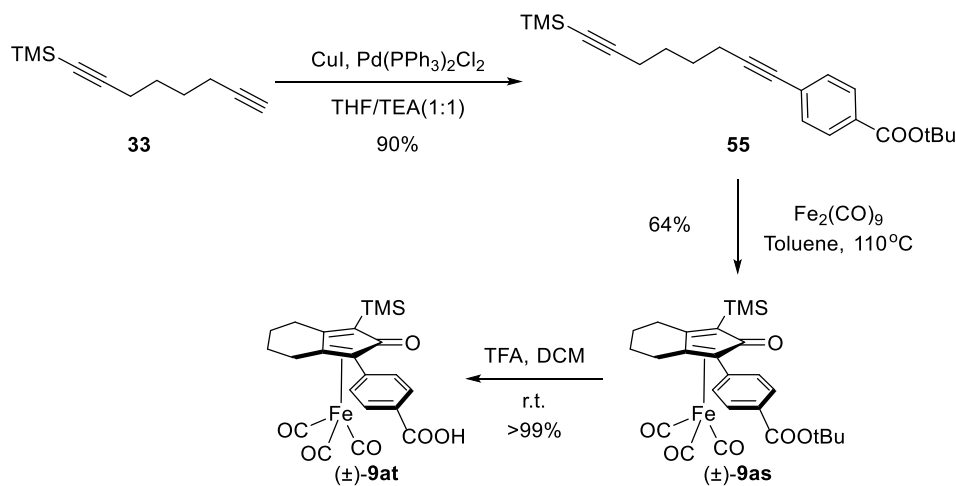
2). Test reactions with different amounts of base were performed in DMF at 80 °C (Table 5.1, entries 4-8), and the best yield (70%) was obtained using 0.2 equivalents of *t*BuOK (Table 5.1, entry 6). With the optimized conditions (1 eq. of **45**, 1 eq. of **46**, 0.2 eq. of *t*-BuOK, DMF, 80 °C, 20 h) in hand, we synthesized compounds **47b** and **47c** in good yields (see Schem 5.2). Next, linkers **48a-c** were obtained in quantitative yields by deprotection in the presence of TFA.

As shown in Scheme 5.2, iron complexes **9cd'-9cf'** were successfully prepared by complexation of cyclopentadienones with $\text{Fe}_2(\text{CO})_9$, then linkers **9cd-9cf** were then obtained by treatment of the corresponding *t*-butyl-protected complexes with TFA in DCM.

Under the above-mentioned conditions, use of 1,2-cyclohexanedione and compound **45a** to synthesize the corresponding cyclopentadienone **47d** failed. Therefore, a different synthetic strategy was designed for the synthesis of cyclopentadienone **47d** (Scheme 5.4), which was prepared by demetalation of complex **9ap** (prepared as described in Chapter 4, Section 4.3.1.1) in good yield under the conditions described by Knölker *et al.*^[13] Finally, compounds **47d** was fully deprotected in the presence of TFA, affording diacid **48d**.



Scheme 5.4. Synthesis of cyclopentadienone **48d**.

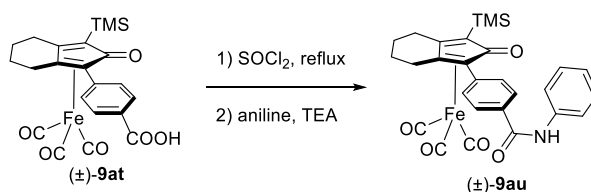


Scheme 5.5. Synthesis of CIC (±)-**9at**.

In order to explore different approaches for the preparation of MOF-supported CICs, we prepared the iron complex (\pm)-**9at**, bearing a single carboxy group (Scheme 5.5). It should be noted that complex (\pm)-**9at** is chiral, possessing a stereogenic plane. As at this stage achieving enantioselectivity was not a priority, we did not separate the two enantiomeric forms and we used the complex as a racemate. In particular, this design would allow the MOF grafting with the complex by formation of an amide bond between the carboxylate of (\pm)-**9at** and suitable amino groups on the MOF's structure. Starting from diyne **33** (already prepared in Chapter 4, Section 4.1.1.1), compound **55** was synthesized by Sonogashira reaction in excellent yield. Subsequently, iron complex (\pm)-**9as** was prepared by carbonylative cyclization in the presence of $\text{Fe}_2(\text{CO})_9$ in toluene at 110 °C in 64% yield. Finally, the desired CIC (\pm)-**9at** was obtained by deprotection with TFA in DCM.

With the aim to find suitable conditions for the grafting reaction with the MOF's aromatic amino groups, a preliminary optimization was carried out on the model reaction of complex (\pm)-**9at** with aniline. The carboxylic acid was initially converted in the corresponding acyl chloride by reaction with SOCl_2 , and then reacted with aniline in the presence of base and DMAP, affording amide (\pm)-**9au**. Optimization of reaction conditions was carried out on this model reaction, as shown in Table 5.2: several reaction parameters were varied but, unfortunately, the yield could not be brought above 64%.

Table 5.2. Optimization for the reaction conditions for the synthesis of (\pm)-**9au**.

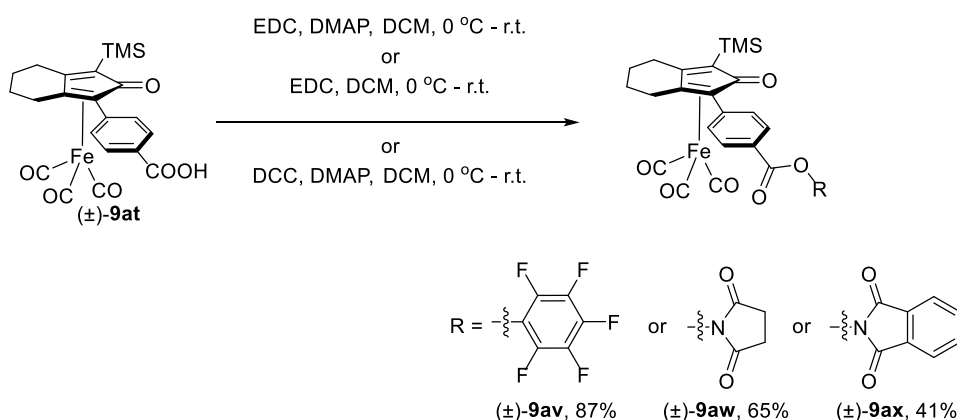


#	Solvent	DMAP (mol %)	T (°C)	TEA (eq.)	Yield (%) ^[a]
1	DCM	5	r.t.	1.5	64
2	DCM	0	r.t.	1.5	29
3	THF	5	60	1.5	33
4	DCM	5	r.t.	3	43

[a] isolated yield

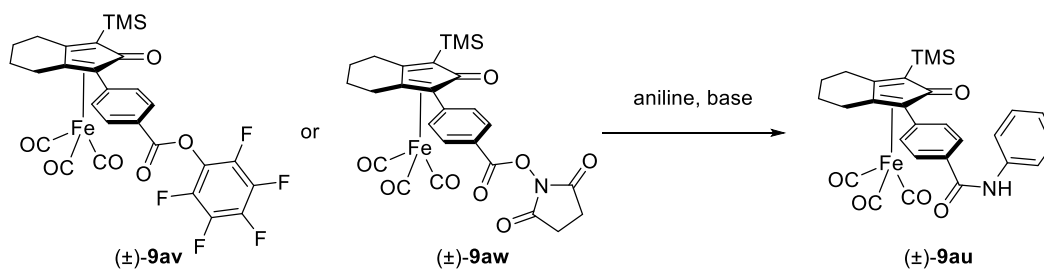
To enhance the yield of amide bond formation, three different activated esters ((\pm)-**9av**, (\pm)-**9aw** and (\pm)-**9ax**) were prepared (according to published procedures,^[14] Scheme 5.6), which may be used for direct amide bond formation in the absence of coupling reagents. Complex (\pm)-**9at** was reacted with pentafluorophenol, *N*-hydroxysuccinimide and *N*-hydroxyphthalimide, respectively, in the presence of DCC or EDC, to give the corresponding esters in moderate to good yields. The activated esters (\pm)-**9av** and (\pm)-**9aw**, which were obtained in good yields, were chosen for optimization of amide bond formation.

The activated esters were screened as shown in Table 5.3: condensation of complex (\pm)-**9av** with aniline in the presence of triethylamine gave better yield in the absence of DMAP (Table 5.3 entry 1 vs. entry 2). In addition, the yield decreased when the temperature was lowered from 100 °C to 50 °C (Table 5.3 entry 4 vs. entry 3). The yield could not be improved when the reaction was carried out in dioxane rather than in DMF (Table 5.3 entry 5). While the activated ester (\pm)-**9aw** led to the amide bond with similar efficacy to (\pm)-**9av** (Table 5.3 entry 6 vs. entries 1 and 4-5), the better reaction yields for the preparation of the latter starting from acid (\pm)-**9at** prompted us to use the pentafluorophenol ester (\pm)-**9av** for the MOF grafting.



Scheme 5.6. Synthesis of activated esters.

Table 5.3. Optimization for the reaction conditions for the synthesis of (\pm)-**9au**.



#	Substrate	Aniline (eq.)	Base (eq.)	Solvent	Tem. (°C)	Time (h)	Yield (%) ^[a]
1	(\pm)- 9av	1.2	TEA (1.5)	DMF	100	16	73
2	(\pm)- 9av	1.2	TEA(1.5), DMAP (0.05)	DMF	100	16	62
3	(\pm)- 9av	0.83	DIPEA (1.7)	DMF	50	20	55
4	(\pm)- 9av	0.83	DIPEA (1.7)	DMF	100	20	77
5	(\pm)- 9av	1.8	DMAP (1.2)	Dioxane	100	48	70
6	(\pm)- 9aw	4	-	AcOEt	70	20	73

[a] isolated yield

5.1.2 Synthesis of MOF-supported CICs

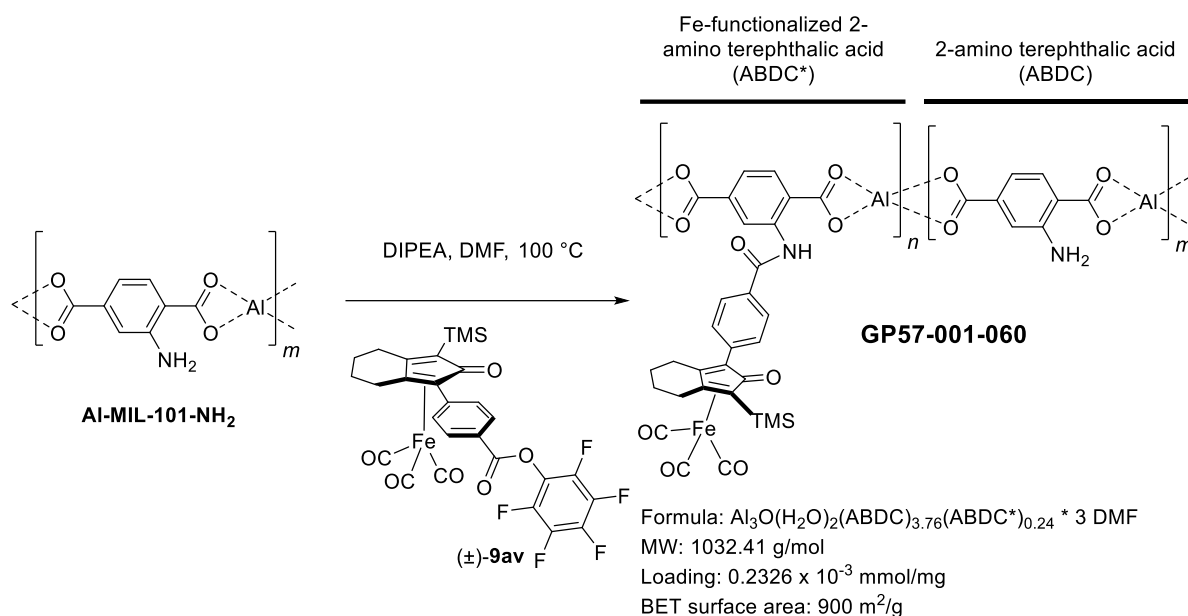
MOF synthesis, post-synthetic modification and characterization were carried out by the group of Dr. Marco

Ranocchiari at the Paul Scherrer Institute (Villigen, Switzerland). The direct synthesis of functionalized MOFs using mixtures of a CIC linker (**9aq**) and a cyclopentadienone linker (**48d**) was initially attempted but gave no results, as no stable MOF could be obtained. It was then decided to attempt to incorporate the iron complexes **9aq** and **9cd-9cf** within an existing, known MOF structure. As they possess fairly similar geometry to **9aq**, several copper MOFs built from benzene-1,3,5-tribenzoate (**btb**) linkers – i.e. HKUST-1,^[15] MOF-14 (Cu_3btb_2)^[16] and DUT-34^[17] – were deemed suitable for post-synthetic insertion of complex **9aq** by linker exchange. Several synthetic methods to include **9aq** within MOF-14 and DUT-34 structures were tried. After several attempts to synthesize defective copper MOFs, IR spectroscopic analysis quickly showed that the linker had been never included in the structure under any of the experimental conditions adopted (concentration, solvent and additive).

For this reason, it was decided to adopt a different approach, consisting in the synthesis of MOFs with new topologies using the free linkers **48a-d**, followed by introduction of the iron complexes **9aq** and **9cd-9cf**. The bidentate linkers **48a** and **48c-d** were tested in the synthesis of Zr MOFs, which are known for their high thermal and chemical stability.^[18] No fully crystalline materials could be produced with **48a** and **48d**, whereas the linker **48c** led to a partially crystalline MOF, whose structure had a BET surface area of around 170 m²/g, not very high but a very good starting point to start including the Fe complex for preliminary catalytic and characterization tests. The tetradentate linker **48b** also showed promising results in the synthesis of corresponding MOF. Although the structure is mostly amorphous and does not show long range order, the surface area of 90 m²/g was found encouraging for further tests. Thus, incorporation of the CIC catalytic moiety in these two MOFs was attempted both by post-synthetic ligand exchange with CICs **9ce** and **9cf** and by reaction with $\text{Fe}_2(\text{CO})_9$, in the attempt to convert some of cyclopentadienone linkers **48a** and **48d** into the corresponding CIC linkers. Unfortunately, even these attempts did not lead to incorporation of the $\text{Fe}(\text{CO})_3$ group into the MOF, as measured by IR spectroscopy.

It was then decided to quit the idea to produce MOFs containing CIC linkers and to graft, instead, a CIC complex to a *known MOF* possessing a suitable functional group. To this end, the MOF Al-MIL-101-NH₂ – firstly reported by Gascon *et al.*^[19] and largely available in Villigen – was chosen, which possesses free aromatic amino groups suitable for grafting carboxy-functionalized CIC complexes by formation of amide bonds. The grafting reaction was performed using the activated ester (\pm)-**9av** under the optimized conditions devised on a model reaction with aniline (see Section 5.1.1), in the presence of DIPEA in DMF. The MOF-supported CIC **GP57-001-060** was successfully obtained and characterized by NMR, IR, BET surface area

and powder XRD (most important parameters are shown in Scheme 5.7). The new MOF showed a very good surface area ($900 \text{ m}^2/\text{g}$), although the iron loading was fairly low ($0.2326 \text{ } \mu\text{mol}/\text{mg}$).



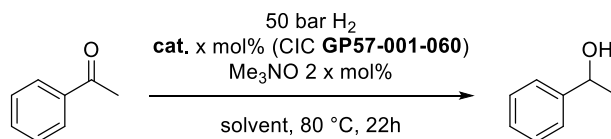
Scheme 5.7. Synthesis of the MOF-supported CIC **GP57-001-060**.

5.2 Hydrogenation of C=O double bonds with MOF-supported CICs

I performed a series of preliminary tests of the MOF-supported CIC **GP57-001-060** in the hydrogenation of acetophenone, and the results obtained are shown in Table 5.4. Several parameters such as solvent, temperature for activation, reaction time and concentration of starting substrates and activator, were screened. Poor conversion were obtained in *i*PrOH/ H_2O due to the poor stability of our MOF in water (Table 5.4 entries 1-3), which was later confirmed by experiments run in Villigen. Poor conversion was obtained in the solvent mixtures 3:1 toluene/DCM and 3:1 toluene/DCE (Table 5.4 entries 4-5). No benefit could be achieved by performing the activation stage at 60°C (Table 5.4 entry 4 vs. entry 5 and entry 2 vs. entry 3). Slightly increased conversions were achieved when DCM was used for the catalyst activation stage and then removed under vacuum and replaced by toluene (Table 5.4 entries 6-8). Increasing the substrate concentration also positively affected the conversion (Table 5.4 entry 8 vs. entry 7). Poor conversion was obtained when pure toluene was employed as solvent (Table 5.4 entry 14), although use of *i*PrOH for catalyst activation allowed to slightly increase the conversion in toluene (Table 5.4 entry 15). The conversion was improved using pure *i*PrOH as solvent, and was found to be affected by the concentration of Me_3NO during the activation stage (optimum: $C_{\text{act.}} = 0.16 \text{ M}$, see Table 5.4 entries 9-10). Slightly improved conversions were obtained by increasing catalyst

loading to 5 mol% (Table 5.4 entry 12 vs. entry 10) or extending reaction time to 72 h (Table 5.4 entry 14).

Table 5.4. Preliminary test and optimization of the obtained MOF-supported CICs in hydrogenation of acetophenone.^[a]



#	Solvent	Catalyst (mol %)	Activation conditions	$C_{0, \text{sub}}$ (M)	Conversion (%) ^[b]
1	<i>i</i> PrOH/H ₂ O (5:2)	5	20 min, r.t. ($C_{\text{act.}} = 0.1$ M)	1	7
2	<i>i</i> PrOH/ H ₂ O (5:2)	2	20 min, r.t. ($C_{\text{act.}} = 0.04$ M)	1	3
3	<i>i</i> PrOH/ H ₂ O (5:2)	2	1 h, 60 °C ($C_{\text{act.}} = 0.04$ M)	1	1
4	Toluene/DCM (3:1)	2	20 min, r.t. in DCM ($C_{\text{act.}} = 0.08$ M)	0.5	9
5	Toluene/DCE (3:1)	2	1 h, 60 °C in DCE ($C_{\text{act.}} = 0.08$ M)	0.5	4
6	Toluene	5	20 min, r.t. in DCM ($C_{\text{act.}} = 0.08$ M), then vac. down and add toluene	0.5	18
7	Toluene	2	20 min, r.t. in DCM ($C_{\text{act.}} = 0.08$ M), then vac. down and add toluene	0.5	12
8	Toluene	2	20 min, r.t. in DCM ($C_{\text{act.}} = 0.08$ M), then vac. down and add toluene	1	15
9	<i>i</i> PrOH	2	20 min, r.t. ($C_{\text{act.}} = 0.08$ M)	1	24
10 ^[d]	<i>i</i> PrOH	2	20 min, r.t. ($C_{\text{act.}} = 0.16$ M)	1	28
11 ^[e]	<i>i</i> PrOH	2	20 min, r.t. ($C_{\text{act.}} = 0.24$ M)	1	20
12 ^[d]	<i>i</i> PrOH	5	20 min, r.t. ($C_{\text{act.}} = 0.16$ M)	1	35
13 ^[c,d]	<i>i</i> PrOH	2	20 min, r.t. ($C_{\text{act.}} = 0.16$ M)	1	31
14 ^[d]	Toluene	5	20 min, r.t. ($C_{\text{act.}} = 0.16$ M)	1	6
15 ^[d]	Toluene	2	20 min, r.t. in <i>i</i> PrOH ($C_{\text{act.}} = 0.16$ M)	1	13

[a] Reaction conditions: acetophenone (0.1 mmol), Me₃NO/Pre-cat. = 2:1, $T = 80$ °C, $P_{\text{H}_2} = 50$ bar, 22 h.

[b] Determined by GC analysis.

[c] Reaction time is 72 h.

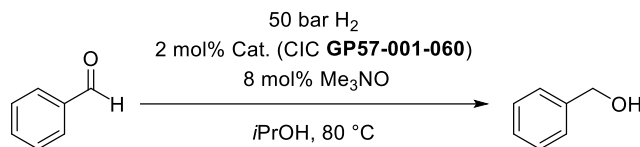
[d] Me₃NO/Pre-cat. = 4:1.

[e] Me₃NO/Pre-cat. = 6:1

Under the best conditions for ketone hydrogenation, we also carried out a preliminary test in aldehyde hydrogenation promoted by MOF **GP57-001-060** (results were shown in Table 5.5). Delightfully, our functionalized MOFs was found very efficient in the hydrogenation of benzaldehyde, giving an excellent conversion (Table 5.5 entry 1). To exclude aldehyde dimerization mechanisms, two control experiments were run on the reactions in the absence of catalyst and of both catalyst and Me₃NO (Table 5.5 entries 2-3). As no conversion was obtained in the latter experiments, we concluded the new MOF **GP57-001-060** is efficient in aldehyde hydrogenation, excluding the occurrence of dimerization pathways. Tests on catalyst recyclability are in progress in Milan, whereas the possibility to employ MOF **GP57-001-060** in flow conditions will be

studied in Villigen.

Table 5.5. Preliminary test of the functionalized MOF in hydrogenation of benzaldehyde and control experiments.^[a]



#	Loading (mol%)	Me ₃ NO (mol%)	Conversion (%) ^[b]
1	2	8	99
2	-	8	1
3	-	-	1

[a] Reaction conditions: acetophenone (0.1 mmol)/Me₃NO/Pre-cat. = 100:8:2, *T* = 80 °C, *P*_{H₂} = 50 bar, 22 h

[b] Determined by GC analysis.

5.3 Conclusions on MOF-supported CICs

To directly synthesize MOF-supported CICs, four carboxy-substituted CICs and four carboxy-substituted cyclopentadioneones were synthesized in good yields in Milan and shipped to the Paul Scherrer Institute (Villigen, Switzerland), where MOF synthesis and characterization was carried out in the group of Dr. Marco Ranocchiari. As the synthesis of MOFs bearing carboxy-functionalized CICs as linkers proved unsuccessful, it was decided to graft the activated ester (±)-**9av** (synthesized in Milan) onto the known MOF Al-MIL-101-NH₂, possessing primary amino groups. A first MOF-supported CIC, **GP57-001-060**, was obtained and characterized by NMR, IR, BET surface area and powder XRD. The MOF-supported CIC was tested in Milan in the hydrogenation of ketones and aldehydes, giving excellent conversion with the latter substrates. Studies on the recyclability of compound **GP57-001-060** and the development of improved second-generation pre-catalysts are currently underway.

5.4 Experimental Section

This section contains details of the experiments which were carried out by myself in Milan, namely the synthesis of CIC and cyclopentadienone linkers and the catalytic tests of the MOF-supported CIC **GP57-001-060** in ketone and aldehyde hydrogenation. No details on the MOF synthesis and characterization carried out in Villigen are provided.

5.4.1 General remarks

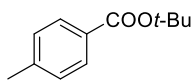
All reactions were carried out in flame-dried glassware with magnetic stirring under inert atmosphere (nitrogen or argon), unless otherwise stated. Solvents for reactions were distilled over the following drying agents and transferred under nitrogen: THF (Na), toluene (Na). Dry *N,N*-dimethylformamide (DMF, over molecular sieves in bottles with crown cap) was purchased from Sigma Aldrich and stored under nitrogen. All reagents were used without purification. Imines were prepared in Chapter 2. Reactions were monitored by analytical thin-layer chromatography (TLC) using silica gel 60 F254 pre-coated glass plates (0.25 mm thickness). Visualization was accomplished by irradiation with a UV lamp and/or staining with a potassium permanganate alkaline solution or with a ninhydrin solution. Flash Column Chromatography (FCC) was performed using silica gel (60 Å, particle size 40-64 µm) as stationary phase, following the procedure by Still and co-workers.^[20]

¹H-NMR spectra were recorded on a spectrometer operating at 400.13 MHz. Proton chemical shifts are reported in ppm (δ) with the solvent reference relative to tetramethylsilane (TMS) employed as the internal standard (CDCl₃, δ = 7.26 ppm; CD₂Cl₂ δ = 5.32 ppm; *d*₆-DMSO δ = 2.50 ppm; CD₃OD δ = 3.34 ppm). The following abbreviations are used to describe spin multiplicity: s = singlet, d = doublet, dd = doublet-doublet, t = triplet, q = quartet, m = multiplet. ¹³C-NMR spectra were recorded on a 400 MHz spectrometer operating at 100.56 MHz, with complete proton decoupling. Carbon chemical shifts are reported in ppm (δ) relative to TMS with the respective solvent resonance as the internal standard (CDCl₃ δ = 77.16 ppm; CD₂Cl₂ δ = 54.00 ppm; *d*₆-DMSO δ = 40.45 ppm; CD₃OD δ = 49.86 ppm). The coupling constant values are given in Hz. Infrared spectra were recorded on a standard FT/IR spectrometer. Melting points were recorded with a standard melting-point apparatus.

5.4.2 Synthesis of CICs as linkers or active site

5.4.2.1 Synthesis of 1,3-diphenylacetone derivative 45a

tert-Butyl 4-methylbenzoate (49)^[21]

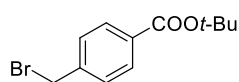


SOCl₂ (74.7 mL, 1.03 mol, 25 eq.) was added to *p*-toluic acid (5.61 g, 41.2 mmol, 1 eq.) at r.t. Three drops of DMF were added and the suspension was heated to reflux and stirred for

1 hour. After completion of the reaction, the excess of thionyl chloride was removed *in vacuo*. The residual yellowish solid was dissolved in dry THF (56 mL) and cooled down to 0 °C. A solution of potassium *tert*-

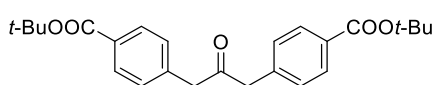
butylate (10.17 g, 90.65 mmol, 2.2 eq.) in dry THF (84 mL) was added dropwise over the period of 1 hour. During the addition, the temperature must be kept under 5 °C. After addition of *t*BuOK, the suspension was warmed up to r.t. and stirred for 1 hour. The reaction mixture was carefully quenched with water (2 mL). The resulting solution was concentrated under reduced pressure and the residue was dissolved in diethyl ether (50 mL) and diluted with water (50 mL). The aqueous phase was extracted with diethyl ether (2 × 50 mL). The combined organic phase was washed with 5% NaOH solution and brine, then dried over Na₂SO₄ and evaporated to give the product. Yield: 6.73 g (85%). ¹H-NMR (400 MHz, CDCl₃) δ 7.87 (d, *J* = 8.0 Hz, 2H), 7.21 (d, *J* = 7.9 Hz, 2H), 2.40 (s, 3H), 1.59 (s, 9H).

***tert*-Butyl 4-(bromomethyl)benzoate (50)**^[22]



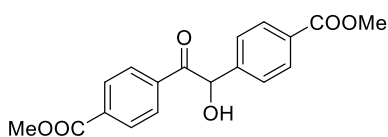
To a stirred solution of compound **49** (6.73 g, 35.0 mmol, 1 eq.) in tetrachloromethane (6.7 mL), NBS (6.23 g, 35.0 mmol, 1 eq.) and benzoyl peroxide (0.85 g, 3.5 mmol, 0.1 eq.) were added. The mixture was heated under reflux for 5 h under light irradiation. After completion of the reaction (TLC), the reaction was cooled down to r.t. and concentrated under reduced pressure. The mixture was dissolved in AcOEt and extracted (3 × 100 mL). The combined organic layers was washed with water (2 × 100 mL) and brine (2 × 100 mL), dried over MgSO₄, filtered, and concentrated under reduced pressure. The crude compound was purified by flash chromatography (silica gel, 0.5: 99.5 AcOEt/hexane). Yield: 6.07 g (64%). ¹H-NMR (400 MHz, CDCl₃) δ 7.96 (d, *J* = 8.3 Hz, 2H), 7.43 (d, *J* = 8.3 Hz, 2H), 4.50 (s, 2H), 1.59 (s, 9H).

Di-*tert*-butyl 4,4'-(2-oxopropane-1,3-diyl)dibenzoate (45a)

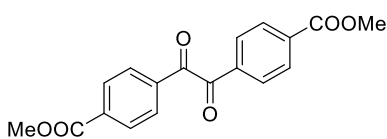


A mixture of compound **50** (6.07 g, 22.4 mmol, 1 eq.), Fe(CO)₅ (4.39 g, 22.4 mmol, 1 eq.), 40% aqueous NaOH (60 mL), and tetrabutylammonium bromide [Bu₄NBr] (0.89 g, 2.69 mmol, 0.12 eq.) in 62.5 mL of benzene was stirred for 3h at r.t. under N₂. The resulting mixture was poured onto I₂-benzene solution and stirred for 0.5h. The mixture was washed successively with aqueous Na₂S₂O₃, 10% HCl, and water. The benzene solution was dried (Na₂SO₄) and evaporated, and the residue was purified by flash chromatography (silica gel, 5: 95 AcOEt/hexane). Yield: 3.13 g (68%). ¹H-NMR (400 MHz, CDCl₃) δ 7.94 (d, *J* = 8.3 Hz, 4H), 7.19 (d, *J* = 8.3 Hz, 4H), 3.77 (s, 4H), 1.59 (s, 18H).

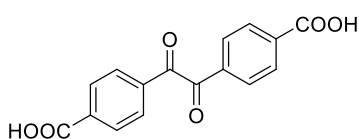
5.4.2.2 Synthesis of benzil derivative 46a

Dimethyl 4,4'-(1-hydroxy-2-oxoethane-1,2-diyl)dibenzoate (52)^[11a]

To a solution of methyl 4-formylbenzoate (**51**) (8.21 g, 50 mmol, 1 eq.) stirred in 99% ethanol (35 mL) and water (9 mL) sodium cyanide (0.735 g, 15 mmol, 0.3 eq.) was added at r.t. The resulting mixture was stirred at 30 °C for 15 min. After completion of the reaction (TLC), the crude mixture was concentrated under reduced pressure. The resulting mixture was extracted with AcOEt, and the combined organic solution was washed with water, dried over Na₂SO₄ and concentrated under reduced pressure. The product was recrystallized from ethanol to give pale yellow needles. Yield: 5.17g (63%). ¹H-NMR (400 MHz, CDCl₃) δ 8.05 (d, *J* = 8.5 Hz, 2H), 7.99 (d, *J* = 8.4 Hz, 2H), 7.93 (d, *J* = 8.5 Hz, 2H), 7.40 (d, *J* = 8.4 Hz, 2H), 6.01 (d, *J* = 5.9 Hz, 1H), 4.52 (d, *J* = 5.9 Hz, 1H), 3.92 (s, 3H), 3.88 (s, 3H).

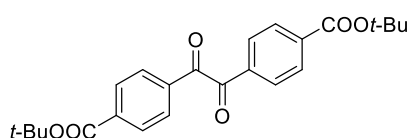
Dimethyl 4,4'-oxalyldibenzoate (53)^[11a]

48% Aqueous hydrobromic acid (18 ml) was added slowly to a stirred solution of compound **52** (5.17g, 15.75 mmol, 1 eq.) in DMSO (72 mL). The solution was heated to 55 °C for 24 h followed by addition of water (48 mL). The mixture was extracted with AcOEt (3 × 100 mL), and combined organic phase was washed with water and dried over MgSO₄ and concentrated under reduced pressure. Yield: 4.93 g (96%). ¹H-NMR (400 MHz, ¹H-NMR (400 MHz, *d*₆-DMSO) δ 8.17 (d, *J* = 8.5 Hz, 4H), 8.11 (d, *J* = 8.5 Hz, 4H), 3.91 (s, 6H).

4,4'-Oxalyldibenzoic acid (54)^[11a]

A solution of compound **53** (3.91g, 12 mmol, 1 eq.) in acetic acid (290 mL) was added to a solution of 4:1 H₂SO₄/H₂O (133 mL). The mixture was refluxed and stirred for 10 h. Water (200 mL) was added and the mixture solution was cooled on ice and then filtered on a Buchner funnel. The solid product on filter was washed with water, and dried at 70 °C *in vacuo* to give a pale yellow solid. Yield: 3.44 g (96%). ¹H-NMR (400 MHz, *d*₆-DMSO) δ 13.52 (s, 2H), 8.15 (d, *J* = 8.5 Hz, 4H), 8.08 (d, *J* = 8.5 Hz, 4H).

Di-*tert*-butyl 4,4'-oxalyldibenzoate (46a)



1,1-Di-*tert*-butoxy-*N,N*-dimethylmethanamine (9.35 g, 46 mmol, 4 eq.)

was added to a solution of acid **54** (3.44 g, 11.5 mmol, 1 eq.) in refluxing

benzene (115 mL, 0.50 M) over a period of 1 h. After refluxing for 30 min,

the reaction mixture was cooled to r.t. diluted with water (100 mL). The resulting mixture was extracted with

benzene (2 × 100 mL). The combined organic layers was washed with saturated sodium bicarbonate (2 × 100

mL) and brine (2 × 100 mL), dried over Na₂SO₄, filtered and concentrated under reduced pressure. The crude

product was purified by flash chromatography (silica gel, 2: 98 AcOEt/hexane). Yield: 3.96 g (84%). ¹H-NMR

(400 MHz, CDCl₃) δ 8.11 (d, *J* = 8.6 Hz, 4H), 8.01 (d, *J* = 8.6 Hz, 4H), 1.61 (s, 18H).

5.4.2.3 General procedure for the synthesis of cyclopentadienones **47a-c**

Diphenylacetone derivatives **45** (1 mmol, 1 eq.) and benzil derivatives **46** (1 mmol, 1 eq.) were added to a two-

necked round-bottom flask containing 6.2 mL of dry DMF and equipped with a stirring bar under N₂. The

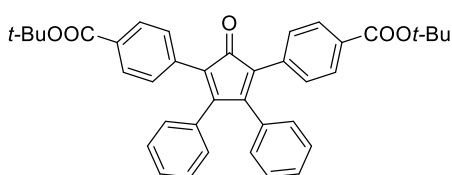
solution was heated to 80 °C for 1 h, then a solution of *t*-BuOK (0.2 eq., 0.1 mol/mL) in dry DMF was added

drop-wise to the warm solution. The mixture was stirred for 24 h at 80 °C. After removing the solvent under

reduced pressure, the crude product was purified by flash chromatography (silica gel, 5: 95 AcOEt/hexane) to

give the desired products.

Di-*tert*-butyl 4,4'-(2-oxo-4,5-diphenylcyclopenta-3,5-diene-1,3-diyl)dibenzoate (**47a**)



Prepared from diphenylacetone **45a** and benzyl **46b** according to the

General procedure. Yield: 1.34 mg (70%). M.p. = 213 °C; ¹H-NMR

(400 MHz, CD₂Cl₂) δ 7.84 (d, *J* = 8.5 Hz, 4H), 7.29-7.26 (m, 6H),

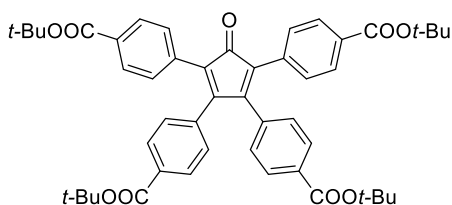
7.22-7.18 (m, 4H), 6.94-6.92 (m, 4H), 1.56 (s, 18H); ¹³C-NMR (100

MHz, CD₂Cl₂) δ 199.7, 165.8, 156.7, 135.5, 133.2, 131.5, 130.4, 129.7, 129.5, 129.4, 128.7, 125.6, 81.4, 28.4;

IR (film): ν = 3370.0, 2973.7, 2919.7, 1711.5, 1605.5, 1367.3, 1295.9, 1164.8, 1108.9, 1024.0 cm⁻¹; ESI-MS

(+): *m/z* 607.01 [M+Na]⁺ (calcd. for C₃₉H₃₆NaO₅: 607.25).

Tetra-*tert*-butyl 4,4',4'',4'''-(5-oxocyclopenta-1,3-diene-1,2,3,4-tetrayl)tetrabenzoate (**47b**)



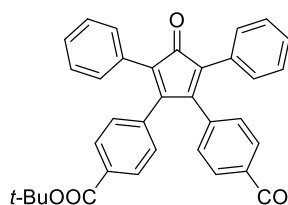
Prepared from diphenylacetone **45a** and benzyl **46a** according to the

General procedure. Yield: 2.23 g (71%). M.p. = 241 °C; ¹H-NMR (400

MHz, CD₂Cl₂) δ 7.85 (d, *J* = 8.8 Hz, 4H), 7.80 (d, *J* = 8.7 Hz, 4H), 7.25

(d, $J = 8.8$ Hz, 4H), 6.99 (d, $J = 8.7$ Hz, 4H), 1.56 (s, 36H); $^{13}\text{C-NMR}$ (100 MHz, CD_2Cl_2) δ 199.1, 165.7, 165.4, 155.3, 137.1, 134.8, 133.0, 131.9, 130.4, 129.8, 129.6, 129.6, 126.5, 81.9, 81.5, 28.4, 28.4; IR (film): $\nu = 3612.0$, 3582.1, 2976.59, 2934.2, 1713.4, 1606.4, 1368.3, 1295.0, 1253.5, 1165.8, 1116.6, 1017.3, 848.5, 665.3 cm^{-1} ; ESI-MS (+): m/z 807.18 $[\text{M}+\text{Na}]^+$ (calcd. for $\text{C}_{49}\text{H}_{52}\text{NaO}_9$: 807.35).

Di-*tert*-butyl 4,4'-(4-oxo-3,5-diphenylcyclopenta-2,5-diene-1,2-diyl)dibenzoate (47c)



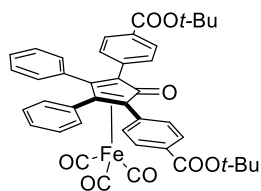
Prepared from diphenylacetone **45b** and benzyl **46a** according to the General procedure. Yield: 1.72 g (67%). M.p. = 219.3 °C; $^1\text{H-NMR}$ (400 MHz, CD_2Cl_2)

δ 7.80 (d, $J = 8.4$ Hz, 4H), 7.28-7.25 (m, 6H), 7.22-7.19 (m, 4H), 7.01 (d, $J = 8.4$ Hz, 4H), 1.56 (s, 18H); $^{13}\text{C-NMR}$ (100 MHz, CD_2Cl_2) δ 200.2, 165.5, 154.0, 137.7, 132.7, 131.0, 130.7, 129.6, 128.7, 128.4, 126.9, 81.8, 28.4; IR (film): $\nu = 2975.6$, 2360.4 2342.1, 1714.4, 1457.0, 1394.3, 1368.3, 1295.0, 1164.8, 1117.6, 1017.3, 866.8, 806.1, 756.0, 723.2, 695.2, 658.2 cm^{-1} ; ESI-MS (+): m/z 607.28 $[\text{M}+\text{Na}]^+$ (calcd. for $\text{C}_{39}\text{H}_{36}\text{NaO}_5$: 607.25).

5.4.2.4 General procedure for the synthesis of CICs **9cd'**-**9cf'**

In a dried Schlenk tube fitted with a Teflon-topped screw cap, the cyclopentadienone **47** (1 mmol, 1 eq.) and $\text{Fe}_2(\text{CO})_9$ (2 mmol, 2 eq.) were introduced in freshly distilled toluene (11.5 mL) under N_2 . The reaction mixture was stirred at 110 °C for 20 hours. The resulting mixture was cooling down to r.t. and filtered through celite (rinsing with AcOEt). After removal of the solvent, the residue was purified by flash column chromatograph (9:1 hexane/ AcOEt) to afford the product as a light yellow solid.

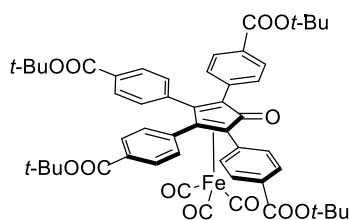
CIC **9cd'**



Prepared from compound **47a** according to the General procedure. Yield: 589.3 mg (90%). M.p. = 218 °C; $^1\text{H-NMR}$ (400 MHz, CD_2Cl_2) δ 7.84 (d, $J = 8.5$ Hz, 4H), 7.64 (d, $J = 8.5$ Hz, 4H), 7.30-7.17 (m, 10H), 1.56 (s, 18H); $^{13}\text{C-NMR}$ (100 MHz, CD_2Cl_2) δ 208.8, 170.3, 165.6, 136.3, 132.3, 131.9, 130.5, 130.2, 129.5, 129.5, 128.8, 105.4,

81.6, 28.4; IR (film): $\nu = 2922.6$, 2842.6, 2299.7, 2070.2, 2023.0, 1709.6, 1653.7, 1053.6 cm^{-1} ; ESI-MS (+): m/z 725.15 $[\text{M}+\text{H}]^+$ (calcd. for $\text{C}_{42}\text{H}_{37}\text{FeO}_8$: 725.18).

CIC **9ce'**

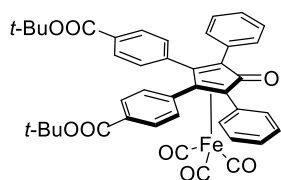


Prepared from compound **47b** according to the General procedure. Yield:

694.6 mg (82%). M.p. = 188.5 °C; ¹H-NMR (400 MHz, CD₂Cl₂) δ 7.85 (d, *J* = 8.7 Hz, 4H), 7.79 (d, *J* = 8.5 Hz, 4H), 7.60 (d, *J* = 8.7 Hz, 4H), 7.22 (d, *J* = 8.5 Hz, 4H), 1.56 (s, 18H), 1.54 (s, 18H); ¹³C-NMR (100 MHz, CD₂Cl₂) δ 208.4, 170.2, 165.6, 165.1, 135.7, 134.3, 133.3, 132.2, 130.4, 129.8, 129.6,

104.3, 82.1, 81.7, 81.5, 28.4, 28.4; IR (film): ν = 3608.2, 3582.1, 2977.6, 2934.2, 2071.2, 2020.1, 2002.7, 1714.4, 2653.7, 1608.3, 1457.0, 1393.3, 1368.3, 1296.9, 1253.5, 1167.7, 1119.5, 1018.2848.5, 767.5, 665.3 cm⁻¹; ESI-MS (+): *m/z* 925.26 [M+H]⁺ (calcd. for C₅₂H₅₃FeO₁₂: 925.29).

CIC 9cf'



Prepared from compound **47c** according to the General procedure. Yield: 555.3 mg

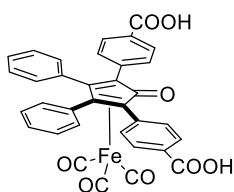
(95%). M.p. = 155 °C; ¹H-NMR (400 MHz, CD₂Cl₂) δ 7.77 (d, *J* = 8.4 Hz, 4H), 7.51 (dd, *J* = 7.6, 2.0 Hz, 4H), 7.31-7.26 (m, 6H), 7.21 (d, *J* = 8.4 Hz, 4H), 1.54 (s, 18H); ¹³C-NMR (100 MHz, CD₂Cl₂) δ 209.0, 170.6, 165.2, 134.8, 133.0, 132.3, 131.2,

130.9, 129.6, 128.8, 128.7, 100.6, 83.3, 82.0, 28.4; IR (film): ν = 3582.1, 3074.0, 3058.6, 2978.5, 2933.2, 2068.3, 2015.3, 2000.8, 1714.4, 1648.8, 1498.4, 1448.3, 1393.3, 1368.3, 1296.9, 1165.8, 1125.3, 1018.2, 835.0, 762.7, 733.8, 695.2, 665.3, 614.2 cm⁻¹; ESI-MS (+): *m/z* 747.25 [M+Na]⁺ (calcd. for C₄₂H₃₆FeNaO₈: 747.17).

5.4.2.5 General procedure for the synthesis of CICs 9cd-9cf

2, 2, 2-Trifluoroacetic acid (90mmol, 90 eq.) was added to a solution of acid (1mmol, 1 eq.) in dry DCM (11.6 mL) at 0 °C under N₂. The reaction mixture was stirred at r.t. for 3h. After completion of the reaction (monitored by TLC), the suspension was diluted with dichloromethane and filtered. The collected yellow solid was washed with DCM and dried under reduced pressure to give product.

CIC 9cd

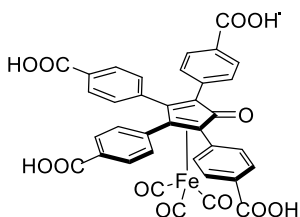


Prepared from CIC **9cd'** according to the General procedure. Yield: 498.0 mg (100%).

M.p. = 286 °C; ¹H-NMR (400 MHz, *d*₆-DMSO) δ 7.82 (d, *J* = 8.5 Hz, 4H), 7.63 (d, *J* = 8.5 Hz, 4H), 7.32-7.21 (m, 10H); ¹³C-NMR (100 MHz, *d*₆-DMSO) δ 208.4, 169.4, 166.8, 136.3, 131.7, 129.7, 129.7, 129.3, 128.8, 128.8, 128.1, 104.5, 79.7; IR (film): ν = 3582.1,

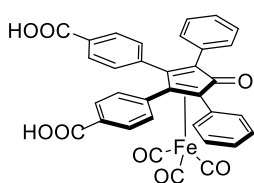
3418.2, 2076.0, 2014.3, 1643.1, 1542.8, 1388.5, 665.3 cm⁻¹; ESI-MS (+): *m/z* 613.13 [M+H]⁺ (calcd. for C₃₄H₂₁FeO₈: 613.6).

CIC 9ce



Prepared from CIC 9ce' according to the General procedure. Yield: 526.1 mg (100%). M.p. = 218 °C; ¹H-NMR (400 MHz, *d*₆-DMSO) δ 7.84 (d, *J* = 8.2 Hz, 4H), 7.77 (d, *J* = 8.1 Hz, 4H), 7.64 (d, *J* = 8.2 Hz, 4H), 7.48 (d, *J* = 8.1 Hz, 4H); ¹³C-NMR (100 MHz, *d*₆-DMSO) δ 208.0, 169.3, 166.8, 166.5, 135.8, 134.0, 132.0, 131.0, 129.9, 129.6, 128.9, 128.9, 104.6, 79.4; IR (film): ν = 3582.1, 3416.3, 2077.0, 2021.0, 1633.4, 1388.5, 1273.8, 665.3 cm⁻¹; ESI-MS (+): *m/z* 722.95 [M+Na]⁺ (calcd. for C₃₆H₂₀FeNaO₁₂: 723.02).

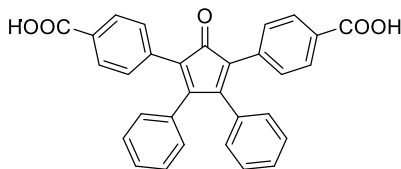
CIC 9cf



Prepared from CIC 9cf' according to the General procedure. Yield: 455.2 mg (97%). M.p. = 155 °C; ¹H-NMR (400 MHz, *d*₆-DMSO) δ 7.77 (d, *J* = 8.4 Hz, 4H), 7.51 (dd, *J* = 7.6, 2.0 Hz, 4H), 7.31-7.26 (m, 6H), 7.21 (d, *J* = 8.4 Hz, 4H), 1.54 (s, 18H); ¹³C-NMR (100 MHz, *d*₆-DMSO) δ 209.0, 170.6, 165.2, 134.8, 133.0, 132.3, 131.2, 130.9, 129.6, 128.8, 128.7, 100.6, 83.3, 82.0, 28.4; IR (film): ν = 3582.1, 3074.0, 3058.6, 2978.5, 2933.2, 2068.3, 2015.3, 2000.8, 1714.4, 1648.8, 1498.4, 1448.3, 1393.3, 1368.3, 1296.9, 1165.8, 1125.3, 1018.2, 835.0, 762.7, 733.8, 695.2, 665.3, 614.2 cm⁻¹; ESI-MS (+): *m/z* 634.87 [M+Na]⁺ (calcd. for C₃₄H₂₀FeNaO₈: 635.04).

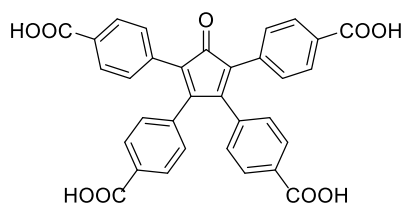
5.4.2.6 Synthesis of cyclopentadienone 48

4,4'-(2-Oxo-4,5-Diphenylcyclopenta-3,5-diene-1,3-diyl)dibenzoic acid (48a)



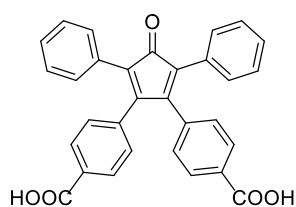
Prepared from compound 47a according to the General procedure (already mentioned in Section 5.4.2.5). Yield: 605 mg (100%). M.p. = 327 °C; ¹H-NMR (400 MHz, *d*₆-DMSO) δ 12.95 (s, 2H), 7.83 (d, *J* = 8.3 Hz, 4H), 7.32-7.22 (m, 10H), 6.97 (d, *J* = 8.3 Hz, 4H); ¹³C-NMR (100 MHz, *d*₆-DMSO) δ 198.5, 167.0, 156.1, 134.8, 132.2, 129.9, 129.6, 129.0, 128.9, 128.8, 128.2, 124.5; IR (film): ν = 3328.5, 2917.8, 2846.4, 1713.4, 1686.4, 1606.4, 1424.2, 1313.3, 1297.9, 1070.3, 866.8 cm⁻¹; ESI-MS (+): *m/z* 967.96 [2M+Na]⁺ (calcd. for C₆₂H₄₀NaO₁₀: 967.25).

4,4',4'',4'''-(5-Oxocyclopenta-1,3-diene-1,2,3,4-tetrayl)tetrabenzoic acid (48b)



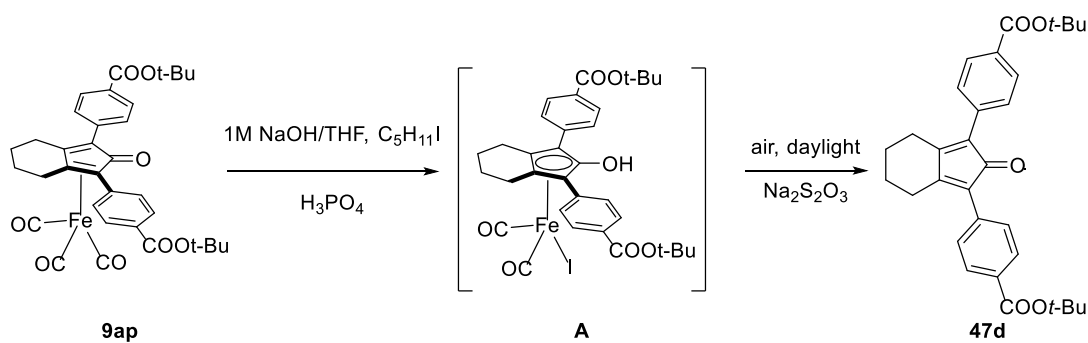
Prepared from compound **47b** according to the General procedure (already mentioned in Section 5.4.2.5). Yield: 1.10 g (100%). M.p. = 274.1 °C; ¹H-NMR (400 MHz, *d*₆-DMSO) δ 13.03 (s, 4H), 7.85 (d, *J* = 8.4 Hz, 4H), 7.80 (d, *J* = 8.4 Hz, 4H), 7.29 (d, *J* = 8.4 Hz, 4H), 7.11 (d, *J* = 8.4 Hz, 4H); ¹³C-NMR (100 MHz, *d*₆-DMSO) δ 198.0, 166.9, 166.8, 154.8, 136.6, 134.4, 131.0, 130.0, 129.9, 129.2, 129.1, 129.1, 125.3; IR (film): ν = 3608.2, 3582.1, 3413.4, 2838.7, 1694.2, 1606.4, 1408.8, 1279.5, 1182.2, 1016.3, 665.3 cm⁻¹; ESI-MS (-): *m/z* 559.38 [M-H]⁻ (calcd. for C₃₃H₁₉O₉: 559.10).

4,4'-(4-Oxo-3,5-Diphenylcyclopenta-2,5-diene-1,2-diyl)dibenzoic acid (**48c**)

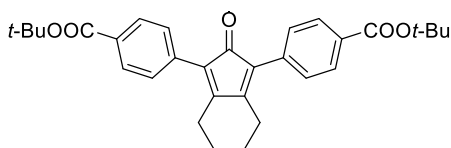


Prepared from compound **47c** according to the General procedure (already mentioned in Section 5.4.2.5). Yield: 1.05 g (100%). M.p. = 334.2 °C ¹H-NMR (400 MHz, CD₃OD) δ 7.84 (d, *J* = 8.4 Hz, 4H), 7.25-7.18 (m, 10H), 7.06 (d, *J* = 8.4 Hz, 4H); ¹³C-NMR (100 MHz, CD₃OD) δ 200.9, 169.1, 154.8, 139.1, 132.0, 131.6, 131.3, 130.5, 130.5, 129.1, 129.0, 127.5; IR (film): ν = 3855.0, 3839.6, 3752.8, 3735.4, 3691.1, 3650.6, 3630.3, 3568.6, 3402.8, 2366.2, 1654.6, 1490.7, 1404.9, 1268.0, 1110.8, 866.8, 751.1, 727.0, 396.2 cm⁻¹; ESI-MS (-): *m/z* 471.27 [M-H]⁻ (calcd. for C₃₁H₁₉O₅: 471.12).

Di-*tert*-butyl 4,4'-(2-oxo-4,5,6,7-tetrahydro-2H-indene-1,3-diyl)dibenzoate (**47d**)^[13]



Scheme 5.8. Demetalation of CIC **9ap**

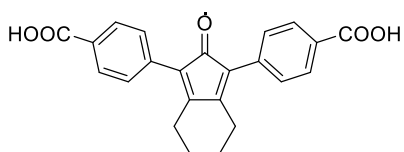


A 1 M aqueous solution of NaOH (17.65 mL) was added to a solution of CIC **9ap** (1.32 g, 2.11 mmol, 1 eq.) in THF (35.6 mL) at r.t., and the resulting mixture was stirred for 2.5 h under N₂. 1-Iodopentane (1.1 g, 5.06 mmol, 2.4 eq.) was added and the solution turned from yellow to brown. The resulting

1-Iodopentane (1.1 g, 5.06 mmol, 2.4 eq.) was added and the solution turned from yellow to brown. The resulting

mixture was stirred at r.t. for an additional 15 min under N₂, followed by addition of H₃PO₄ (664 μL, C ≥ 85%). Then the organic layer was separated, and the aqueous layer was extracted with dichloromethane (2 × 100 mL). The combined organic layers were dried over Na₂SO₄, filtered and concentrated under reduced pressure. The crude product was purified by chromatography to get the intermediate product **A**. The latter was dissolved in dichloromethane (100 mL) followed by addition of Na₂S₂O₃ (1.3 g) and stirred slowly in the air for 10 h in the presence of daylight. The mixture was filtrated through a short path of celite and concentrated under reduced pressure. The residue was purified by flash column chromatograph (9:1 hexane/AcOEt) to afford the product as a purple solid. Yield: 636.1 mg (62%). M.p. = 219 °C; ¹H-NMR (400 MHz, CD₂Cl₂) δ 7.99 (d, *J* = 8.5 Hz, 4H), 7.52 (d, *J* = 8.5 Hz, 4H), 2.90-2.87 (m, 4H), 1.78-1.75 (m, 4H), 1.59 (s, 18H); ¹³C-NMR (100 MHz, CD₂Cl₂) δ 200.3, 165.9, 156.1, 136.0, 131.1, 129.6, 129.5, 122.7, 81.4, 28.5, 27.4, 23.1; IR (film): ν = 3608.2, 3582.1, 2976.6, 2934.2, 2866.7, 1765.5, 1708.6, 1604.5, 1367.3, 1292.1, 1253.5, 1166.7, 1111.8, 1017.3, 848.5, 665.3 cm⁻¹; ESI-MS (+): *m/z* 509.14 [M+Na]⁺ (calcd. for C₃₁H₃₄NaO₅: 509.23).

4,4'-(2-Oxo-4,5,6,7-Tetrahydro-2H-indene-1,3-diyl)dibenzoic acid (**48d**)

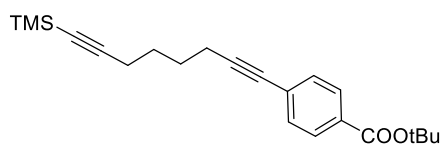


Prepared from **47d** according to the General procedure (already mentioned in Section 5.4.2.5). Yield: 489.8 mg (100%). M.p. = 257 °C;

¹H-NMR (400 MHz, *d*₆-DMSO) δ 12.95 (s, 2H), 7.98 (d, *J* = 8.5 Hz, 4H), 7.58 (d, *J* = 8.5 Hz, 4H), 2.91-2.89 (m, 4H), 1.70 (pen, 4H); ¹³C-NMR (100 MHz, *d*₆-DMSO) δ 199.2, 167.1, 156.3, 135.2, 129.1, 129.0, 129.0, 121.2, 26.2, 21.8; IR (film): ν = 3608.2, 3582.1, 1996, 1673.9, 1598.7, 1403.0, 1274.7, 1187.0, 862.0, 750.2, 665.3 cm⁻¹; ESI-MS (-): *m/z* 373.4 [M-H]⁻ (calcd. for C₂₃H₁₇O₅: 373.11).

5.4.2.7 Synthesis of CIC **9aw**

tert-Butyl 4-(8-(trimethylsilyl)octa-1,7-diyn-1-yl)benzoate (**55**)

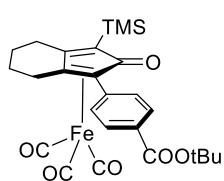


In a dried Schlenk tube fitted with a Teflon-topped screw cap, dichlorobis(triphenylphosphine) palladium (86 mg, 0.123 mmol, 0.041 eq.) and CuI (23 mg, 0.123 mmol, 0.041 eq.) were added to a

solution of compound **40** (0.91 g, 3 mmol, 1 eq.) and diyne **33** (0.54 g, 3 mmol, 1 eq.) in dry 1:1 THF/TEA (154 mL) at r.t. under N₂. The reactor was sealed and the stirred mixture heated to 60 °C under 16 hours. The resulting mixture was concentrated under reduced pressure. The residue was dissolved in DCM (100 mL) and washed with sat. aq. NH₄Cl (50 mL) and brine (2 × 50 mL). The organic phase was dried over Na₂SO₄ and

evaporated to give the crude product. The residue was purified by flash column chromatography (99:1 hexane/AcOEt) to afford the pure product as a yellow oil. Yield: 0.96 g (90%). M.p. = 39.9 °C; $^1\text{H-NMR}$ (400 MHz, CDCl_3) δ 7.89 (d, $J = 8.5$ Hz, 2H), 7.41 (d, $J = 8.5$ Hz, 2H), 2.47-2.44 (m, 2H), 2.30-2.27 (m, 2H), 1.74-1.66 (m, 4H), 1.58 (s, 9H), 0.14 (s, 9H); $^{13}\text{C-NMR}$ (400 MHz, CDCl_3) δ 165.4, 131.4, 130.9, 129.3, 128.3, 107.0, 93.0, 84.9, 81.2, 80.6, 28.3, 27.9, 27.8, 19.6, 19.2, 0.3; IR (film): $\nu = 2954.4, 2854.7, 2228.3, 2174.4, 1713.4, 1606.4, 1478.2, 1457.0, 1428.0, 1403.9, 1392.4, 1368.3, 1305.6, 1293.0, 1279.5, 1249.7, 1163.8, 1116.6, 1045.2, 1017.3, 843.7, 770.4, 759.8, 696.2, 640.3$ cm^{-1} ; ESI-MS (+): m/z 377.13 $[\text{M}+\text{Na}]^+$ (calcd. for $\text{C}_{22}\text{H}_{30}\text{NaO}_2\text{Si}$: 377.19).

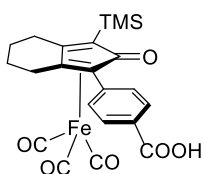
CIC (\pm)-**9as**



Prepared from diyne **55** according to the General procedure (already used for the synthesis of complex **9ap** in Chapter 4, Section 4.4.4.1). Yield: 0.9 g (64%). M.p. = 146.9 °C; $^1\text{H-NMR}$ (400 MHz, CD_2Cl_2) δ 7.95 (d, $J = 8.7$ Hz, 2H), 7.75 (d, $J = 8.7$ Hz, 2H), 2.74-2.71 (m, 2H), 2.64-2.56 (m, 2H), 1.93-1.82 (m, 4H), 1.58 (s, 9H), 0.33 (s, 9H);

$^{13}\text{C-NMR}$ (400 MHz, CD_2Cl_2) δ 209.6, 175.7, 165.8, 137.3, 131.7, 129.7, 129.7, 107.9, 105.7, 83.2, 81.5, 69.2, 28.5, 25.0, 24.9, 22.9, 22.8, 0.0; IR (film): $\nu = 3585.0, 2951.5, 2050.6, 2002.7, 1711.5, 1633.4, 1514.8, 1478.2, 1445.4, 1393.3, 1368.3, 1293.0, 1248.7, 1166.7, 1116.6, 1015.3, 949.8, 896.7, 848.5, 779.1, 765.6, 735.7, 704.9, 619.0$ cm^{-1} ; ESI-MS (+): m/z 522.98 $[\text{M}+\text{H}]^+$ (calcd. for $\text{C}_{26}\text{H}_{31}\text{FeO}_6\text{Si}$: 523.12).

CIC (\pm)-**9at**

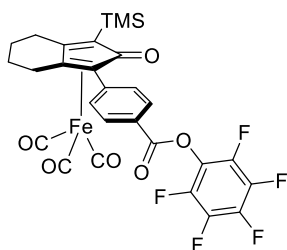


2, 2, 2-Trifluoroacetic acid (90 mmol, 90 eq.) was added to a solution of CIC (\pm)-**9as** (1 mmol, 1 eq.) in dry DCM (11.6 mL) at 0 °C under N_2 . The reaction mixture was stirred at r.t. for 3h. After completion of the reaction (monitored by TLC), the resulting mixture was concentrated under reduced pressure. The residue was dissolved in DCM and diluted with

n-hexane. The suspension was filtered. The collected yellow solid was washed with DCM/*n*-hexane (1:1, v/v) and dried under reduced pressure to give product. Yield: 0.8 g (100%). M.p. = 225.5 °C; $^1\text{H-NMR}$ (400 MHz, CD_2Cl_2) δ 10.46 (s, 2H), 8.05 (d, $J = 8.0$ Hz, 2H), 7.61 (d, $J = 8.0$ Hz, 2H), 2.71-2.46 (m, 4H), 1.96-1.69 (m, 4H), 0.37 (s, 9H); $^{13}\text{C-NMR}$ (400 MHz, CD_2Cl_2) δ 208.2, 172.2, 171.0, 136.2, 131.2, 130.7, 129.9, 108.6, 106.9, 86.4, 69.9, 24.3, 24.3, 22.7, 22.5, 0.0; IR (film): $\nu = 3439.4, 2953.5, 2530.2, 2069.3, 2005.6, 1780.9, 1717.3, 1693.2, 1612.2, 1567.8, 1401.0, 1250.6, 1178.3, 1016.3, 896.7, 844.7, 780.1, 760.8, 736.7, 703.9, 619.0$ cm^{-1} ; ESI-MS (+): m/z 489.04 $[\text{M}+\text{Na}]^+$ (calcd. for $\text{C}_{22}\text{H}_{22}\text{FeNaO}_6\text{Si}$: 489.04).

5.4.3 Synthesis of activated esters featuring CICs

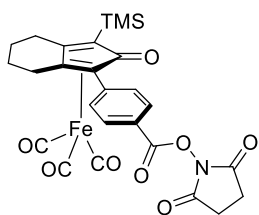
Activated ester (\pm)-**9av**



In a dried Schlenk tube fitted with a Teflon-topped screw cap, EDC (783.1 mg, 4.085 mmol, 1.5 eq.) and DMAP (66.5 mg, 0.54466 mmol, 0.2 eq.) were added to a solution of complex (\pm)-**9at** (1.27 g, 2.7233 mmol, 1 eq.) and pentafluorophenol (551.4 mg, 2.9957 mmol, 1.1 eq.) in DCM (12.7 mL) at 0 °C under N₂. The reaction mixture was stirred at r.t. for 3 h followed by addition of saturated aqueous NH₄Cl.

The resulting mixture was extracted with AcOEt, and the combined organic extracts were dried over Na₂SO₄, filtered, and concentrated under reduced pressure to afford the crude product. The crude product was purified by flash column chromatography (9:1 hexane/ AcOEt t) to afford the pure product as a yellow solid. Yield: 1.5 g (87%). M.p. = 167.1 °C; ¹H-NMR (400 MHz, CD₂Cl₂) δ 8.18 (d, *J* = 8.5 Hz, 2H), 7.94 (d, *J* = 8.5 Hz, 2H), 2.84-2.69 (m, 2H), 2.65-2.57 (m, 2H), 1.93-1.84 (m, 4H), 0.35 (s, 9H); ¹³C-NMR (400 MHz, CD₂Cl₂) δ 209.4, 175.6, 162.8, 140.4, 131.0, 130.2, 126.2, 108.3, 105.4, 81.9, 69.6, 25.1, 25.0, 22.9, 22.8, 0.0; IR (film): ν = 3667.0, 3645.8, 3626.5, 3584.1, 3441.4, 2952.5, 2866.7, 2054.4, 2007.5, 1759.7, 1632.5, 1607.4, 1521.6, 1472.4, 1447.3, 1398.1, 1321.0, 1304.6, 1250.6, 1187.9, 1145.5, 1049.1, 1012.5, 996.1, 978.7, 895.8, 843.7 cm⁻¹; ESI-MS (+): *m/z* 655.46 [M+Na]⁺ (calcd. for C₂₈H₂₁F₅FeNaO₆Si: 655.03).

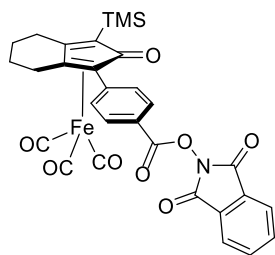
Activated ester (\pm)-**9aw**



In a dried Schlenk tube fitted with a Teflon-topped screw cap, *N*-hydroxysuccinimide (19.7 mg, 0.1716 mmol) and EDC (32.9 mg, 0.1716 mmol) were added to a stirred solution of complex (\pm)-**9at** (0.10722 mmol) in CH₂Cl₂ (0.16 mL) under N₂. After 3 h, the reaction mixture was diluted with CH₂Cl₂ (4 mL). The organic layer was washed

with saturated aqueous NaHCO₃ (2 mL) and brine (2 × 2 mL), dried over Na₂SO₄, filtered and concentrated to afford the crude product. The crude product was purified by flash column chromatography (1:1 hexane/AcOEt) to afford the pure product as a yellow solid. Yield: 39.2 mg (65%). ¹H-NMR (400 MHz, CD₂Cl₂) δ 8.11 (d, *J* = 8.6 Hz, 2H), 7.92 (d, *J* = 8.6 Hz, 2H), 2.88 (s, 4H), 2.77-2.74 (m, 2H), 2.65-2.61 (m, 2H), 1.93-1.83 (m, 4H), 0.34 (s, 9H); ¹³C-NMR (400 MHz, CD₂Cl₂) δ 209.3, 175.5, 169.8, 162.2, 140.7, 130.7, 130.1, 124.3, 108.3, 105.3, 81.6, 69.5, 26.3, 25.1, 25.0, 22.8, 22.7, 0.1.

Activated ester (\pm)-**9ax**



In a dried Schlenk tube fitted with a Teflon-topped screw cap, *N,N'*-dicyclohexylcarbodiimide (26.5 mg, 0.129 mmol, 1.20 eq.) and 4-dimethylaminopyridine (1.3 mg, 0.011 mmol, 0.10 eq.) were added to a solution of complex (±)-**9at** (50 mg, 0.107 mmol, 1 eq.) in dry THF (1.5 mL) under N_2 . After stirring for one minute at r.t., *N*-hydroxyphthalimide (19.2 mg, 0.118 mmol, 1.1 eq.) was added and the reaction mixture was stirred for 24 h at r.t. The precipitating dicyclohexyl urea was filtered off and the solution was concentrated under reduced pressure. The crude product was purified by flash column chromatography (1:1 hexane/ AcOEt) to afford the pure product as a yellow solid. Yield: 26.8 mg (41%). 1H -NMR (400 MHz, CD_2Cl_2) δ 8.16 (d, $J = 8.2$ Hz, 2H), 7.96-7.92 (m, 4H), 7.86-7.83 (m, 2H), 2.84-2.72 (m, 2H), 2.69-2.58 (m, 2H), 1.93-1.86 (m, 4H), 0.35 (s, 9H); ^{13}C -NMR (400 MHz, CD_2Cl_2) δ 209.3, 175.5, 163.1, 162.6, 140.7, 135.5, 130.8, 130.2, 129.5, 124.5, 124.4, 108.3, 105.4, 81.7, 69.6, 25.1, 25.0, 22.9, 22.7, 0.0.

5.4.4 Synthesis of CICs (±)-**9au**

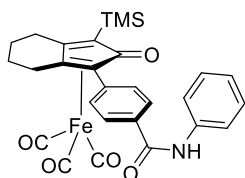
General procedure A: DMF (3 drops) was added to a solution of acid (±)-**9at** (30 mg, 0.064 mmol, 1.1 eq.) in thionyl chloride (124 mg, 1.04 mmol, 18 eq.), and the reaction mixture was heated to reflux for 4 h under N_2 . The excess thionyl chloride was removed under reduced pressure. The residual yellowish solid was dissolved in dichloromethane or THF (0.1 mL) and cooled to 0 °C. A solution of *N,N*-dimethyl-4-aminopyridine (0.05 or 0 eq.), aniline (5.45 mg, 0.059 mmol, 1 eq.) and Et_3N (1.5 or 3 eq.) in dichloromethane (0.12 mL) was added dropwise at 0 °C. The reaction mixture was stirred at r.t. or 60 °C for 12 h, and then quenched with water and extracted with CH_2Cl_2 (2 \times 2 mL). The combined organic layer was dried over Na_2SO_4 and concentrated. The resulting residue was purified by flash column chromatography (4:1 hexane/ AcOEt) to afford the pure product as a yellow solid.

General procedure B: To a solution of activated ester (±)-**9av** (50 mg, 0.0791 mmol, 1 eq.) in DMF or dioxane (0.8 mL) were added aniline (given amount) and base (given amount) at r.t. The reaction mixture was heated to 100 °C or 50 °C, and monitored by TLC. After reaction completion, the reaction mixture was concentrated under reduced pressure. The residue was purified by flash column chromatography (4:1 hexane/ AcOEt) to afford the pure product as a yellow solid.

General procedure C: Aniline (26 mg, 0.2784 mmol, 4 eq.) was added to a solution of activated ester (±)-

9aw (39.2 mg, 0.0696 mmol, 1 eq.) in AcOEt (0.7 mL). The reaction mixture was stirred at 70 °C for 20 h. After reaction completion, the solvent was removed under reduced pressure and the residue was purified by flash column chromatography (4:1 hexane/ AcOEt) to afford the pure product as a yellow solid.

CIC (±)-**9au**



M.p. = 119.7 °C; ¹H-NMR (400 MHz, CD₂Cl₂) δ 7.98 (s, 1H), 7.85-7.80 (m, 4H), 7.67-

7.65 (m, 2H), 7.38 (dd, *J* = 8.5, 7.4 Hz, 2H), 7.18-7.14 (m, 1H), 2.74 (t, *J* = 5.8 Hz, 2H),

2.69-2.57 (m, 2H), 1.91-1.85 (m, 4H), 0.34 (s, 9H); ¹³C-NMR (400 MHz, CD₂Cl₂) δ

209.4, 175.7, 165.8, 139.4, 135.4, 134.7, 130.4, 129.3, 127.8, 124.6, 121.0, 107.9, 106.4,

85.0, 69.1, 24.7, 24.6, 22.8, 22.7, 0.0; IR (film): ν = 3851.2, 3646.7, 3297.7, 3136.7, 3056.6, 2926.5, 2854.1,

2347.9, 2053.5, 2002.7, 1746.2, 1671.0, 1599.7, 1539.9, 1512.9, 1499.4, 1440.6, 1409.7, 1322.0, 1249.7,

1183.1, 1076.0, 1015.3, 891.0, 843.7, 756.9, 693.3 cm⁻¹; ESI-MS (+): *m/z* 542.21 [M+H]⁺ (calcd. for

C₂₈H₂₈FeNO₅Si: 542.11).

5.4.5 Hydrogenation of C=O double bonds with MOF-supported CICs

Under argon atmosphere, the catalytic MOFs (8.6 mg, 0.002 mmol) was dispensed into oven-dried glass tubes fitted in an aluminum block inside a Schlenk tube. A solution of Me₃NO (0.05 mL, 0.16 M or given concentration) in *i*PrOH (or other given solvent) was dispensed. The resulting mixture was stirred at r.t. for 20 min (or at 60 °C for 1 h), during which a deep orange color gradually developed. The substrate (0.1 mmol) and other *i*PrOH (0.05 mL, or other given solvent) were added in each vial. Each vial was capped with a Teflon septum pierced by a needle, the block was transferred into the autoclave, and stirring was started. After purging four times with hydrogen, the reaction was pressurized at 50 bar and heating was started (80 °C). The reactions were stirred for 22 h under hydrogen pressure at 80 °C. After cooling down to r.t., the mixtures were filtered through a short part of celite and then analyzed for conversion determination.

Analysis of acetophenone AH products

The reaction mixtures were analyzed either by GC with a chiral column to measure conversion and enantiomeric excess. Absolute configurations were determined by comparing the elution order with previous data obtained with the same column.

1-Phenylethanol (**P69**)^[23]

Conversion and e.e. were determined by chiral GC.

Capillary column: MEGA-DEX DAC Beta, diacetyl-*tert*-butylsilyl- β -cyclodextrin, 0.25 μ m; diameter = 0.25 mm; length = 25 m; carrier: hydrogen; inlet pressure: 1 bar; oven temperature: 95 °C for 20 min: $t_{\text{sub.}}$ = 4.76 min; t_{R} = 10.36 min; t_{S} = 12.39 min.

Benzenemethanol (**P74**)

Capillary column: MEGA-DEX DAC Beta, diacetyl-*tert*-butylsilyl- β -cyclodextrin, 0.25 μ m; diameter = 0.25 mm; length = 25 m; carrier: hydrogen; inlet pressure: 1 bar; oven temperature: 95 °C for 20 min: $t_{\text{sub.}}$ = 3.64 min; t_{P} = 8.82 min.

References

- [1] a) A. Quintard, J. Rodriguez, *Angew. Chem., Int. Ed.* **2014**, *53*, 4044-4055; b) U. Piarulli, S. Vailati Facchini, L. Pignataro, *CHIMIA International Journal for Chemistry* **2017**, *71*, 580-585.
- [2] a) M. G. Coleman, A. N. Brown, B. A. Bolton, H. Guan, *Adv. Synth. Catal.* **2010**, *352*, 967-970; b) S. Moulin, H. Dentel, A. Pagnoux-Ozherelyeva, S. Gaillard, A. Poater, L. Cavallo, J.-F. Lohier, J.-L. Renaud, *Chem. Eur. J.* **2013**, *19*, 17881-17890.
- [3] a) G. Férey, *Chem. Soc. Rev.* **2008**, *37*, 191-214; b) O. M. Yaghi, M. O'Keeffe, N. W. Ockwig, H. K. Chae, M. Eddaoudi, J. Kim, *Nature* **2003**, *423*, 705-714; c) S. Kitagawa, R. Kitaura, S.-i. Noro, *Angew. Chem., Int. Ed.* **2004**, *43*, 2334-2375; d) J. L. C. Rowsell, O. M. Yaghi, *Microporous Mesoporous Mater.* **2004**, *73*, 3-14; e) Y. Cui, Y. Yue, G. Qian, B. Chen, *Chem. Rev.* **2012**, *112*, 1126-1162; f) M. O'Keeffe, O. M. Yaghi, *Chem. Rev.* **2012**, *112*, 675-702; g) M. Li, D. Li, M. O'Keeffe, O. M. Yaghi, *Chem. Rev.* **2014**, *114*, 1343-1370; h) A. J. Howarth, P. Li, O. K. Farha, M. O'Keeffe, *Cryst. Growth Des.* **2018**, *18*, 449-455; i) V. Bon, I. Senkowska, S. Kaskel, in *Nanoporous Materials for Gas Storage* (Eds.: K. Kaneko, F. Rodríguez-Reinoso), Springer Singapore, Singapore, **2019**, pp. 137-172; j) O. M. Yaghi, M. J. Kalmutzki, C. S. Diercks, *Introduction to Reticular Chemistry: Metal-Organic Frameworks and Covalent Organic Frameworks*, Wiley, **2019**.
- [4] For application of MOFs, see following reviews: a) M. Ranocchiari, J. A. van Bokhoven, *Phys. Chem. Chem. Phys.*

- 2011, 13, 6388-6396; b) A. Corma, H. García, F. X. Llabrés i Xamena, *Chem. Rev.* **2010**, 110, 4606-4655; c) Z. Wang, G. Chen, K. Ding, *Chem. Rev.* **2009**, 109, 322-359; d) D. Farrusseng, S. Aguado, C. Pinel, *Angew. Chem., Int. Ed.* **2009**, 48, 7502-7513; e) L. Ma, C. Abney, W. Lin, *Chem. Soc. Rev.* **2009**, 38, 1248-1256; f) J. Lee, O. K. Farha, J. Roberts, K. A. Scheidt, S. T. Nguyen, J. T. Hupp, *Chem. Soc. Rev.* **2009**, 38, 1450-1459; g) H. Furukawa, K. E. Cordova, M. O'Keeffe, O. M. Yaghi, *Science* **2013**, 341, 1230444.
- [5] For activity at the inorganic nodes, see: a) M. Fujita, Y. J. Kwon, S. Washizu, K. Ogura, *J. Am. Chem. Soc.* **1994**, 116, 1151-1152; b) K. Schlichte, T. Kratzke, S. Kaskel, *Microporous Mesoporous Mater.* **2004**, 73, 81-88; c) Y. K. Hwang, D.-Y. Hong, J.-S. Chang, S. H. Jhung, Y.-K. Seo, J. Kim, A. Vimont, M. Daturi, C. Serre, G. Férey, *Angew. Chem., Int. Ed.* **2008**, 47, 4144-4148; d) P. Horcajada, S. Surblé, C. Serre, D.-Y. Hong, Y.-K. Seo, J.-S. Chang, J.-M. Grenèche, I. Margiolaki, G. Férey, *Chem. Commun.* **2007**, 2820-2822; e) F. X. Llabrés i Xamena, A. Abad, A. Corma, H. Garcia, *J. Catal.* **2007**, 250, 294-298.
- [6] For activity at the linkers, see: a) K. S. Suslick, P. Bhyrappa, J. H. Chou, M. E. Kosal, S. Nakagaki, D. W. Smithenry, S. R. Wilson, *Acc. Chem. Res.* **2005**, 38, 283-291; b) A. M. Shultz, O. K. Farha, J. T. Hupp, S. T. Nguyen, *J. Am. Chem. Soc.* **2009**, 131, 4204-4205; c) J. Gascon, U. Aktay, M. D. Hernandez-Alonso, G. P. M. van Klink, F. Kapteijn, *J. Catal.* **2009**, 261, 75-87; d) G. A. Morris, S. T. Nguyen, J. T. Hupp, *J. Mol. Catal. A: Chem.* **2001**, 174, 15-20, e) M. Eddaoudi, J. Kim, N. Rosi, D. Vodak, J. Wachter, M. O'Keeffe, O. M. Yaghi, *Science* **2002**, 295, 469-472.
- [7] a) S. Hermes, M.-K. Schröter, R. Schmid, L. Khodeir, M. Muhler, A. Tissler, R. W. Fischer, R. A. Fischer, *Angew. Chem., Int. Ed.* **2005**, 44, 6237-6241; b) U. Mueller, O. Metelkina, H. Junicke, T. Butz and O. M. Yaghi, *US Patent*, 2004/081611 (A1), **2004**; c) N. V. Maksimchuk, K. A. Kovalenko, S. S. Arzumanov, Y. A. Chesalov, M. S. Melgunov, A. G. Stepanov, V. P. Fedin, O. A. Kholdeeva, *Inorg. Chem.* **2010**, 49, 2920-2930.
- [8] a) M. J. Ingleson, J. Perez Barrio, J.-B. Guilhaud, Y. Z. Khimiyak, M. J. Rosseinsky, *Chem. Commun.* **2008**, 2680-2682; b) X. Zhang, F. X. Llabrés i Xamena, A. Corma, *J. Catal.* **2009**, 265, 155-160; c) C.-D. Wu, A. Hu, L. Zhang, W. Lin, *J. Am. Chem. Soc.* **2005**, 127, 8940-8941.
- [9] a) S. Vailati Facchini, J.-M. Neudörfl, L. Pignataro, M. Cettolin, C. Gennari, A. Berkessel, U. Piarulli, *ChemCatChem* **2017**, 9, 1461-1468; b) P. Gajewski, A. Gonzalez-de-Castro, M. Renom-Carrasco, U. Piarulli, C. Gennari, J. G. de Vries, L. Lefort, L. Pignataro, *ChemCatChem* **2016**, 8, 3431-3435; c) P. Gajewski, M. Renom-Carrasco, S. Vailati Facchini, L. Pignataro, L. Lefort, J. G. de Vries, R. Ferraccioli, U. Piarulli, C. Gennari, *Eur. J. Org. Chem.* **2015**, 5526-5536; d) P. Gajewski, M. Renom-Carrasco, S. Vailati Facchini, L. Pignataro, L. Lefort, J. G. de Vries, R. Ferraccioli, A. Forni, U. Piarulli, C. Gennari, *Eur. J. Org. Chem.* **2015**, 1887-1893.
- [10] a) K. Yoshikazu, T. Yoshiro, N. Saburo, O. Yoshio, *Chem. Lett.* **1979**, 8, 321-324; b) S. Kolodych, O. Koniev, Z. Baatarkhuu, J.-Y. Bonnefoy, F. Debaene, S. Cianférani, A. Van Dorsselaer, A. Wagner, *Bioconjugate Chem.* **2015**, 26, 197-200; c) M. Dong, J. Zhang, X. Peng, H. Lu, L. Yun, S. Jiang, Q. Dai, *Eur. J. Med. Chem.* **2010**, 45, 4096-4103.
- [11] a) Q. Miao, J. Gao, Z. Wang, H. Yu, Y. Luo, T. Ma, *Inorganica Chimica Acta* **2011**, 376, 619-627; b) S. S. Zimmerman, A. Khatri, E. C. Garnier-Amblard, P. Mullasseril, N. L. Kurtkaya, S. Gyoneva, K. B. Hansen, S. F. Traynelis, D. C. Liotta, *J. Med. Chem.* **2014**, 57, 2334-2356.
- [12] Z. B. Lim, K. S. Tan, A. V. Lunchev, H. Li, S. J. Cho, A. C. Grimsdale, R. Yazami, *Synth. Met.* **2015**, 200, 85-90.
- [13] H.-J. Knölker, E. Baum, H. Goesmann, R. Klaus, *Angew. Chem., Int. Ed.* **1999**, 38, 2064-2066.
- [14] a) S. Specklin, J. Cossy, *J. Org. Chem.* **2015**, 80, 3302-3308; b) S. F. Andrade, B. G. Oliveira, L. C. Pereira, J. P. Ramos, A. R. Joaquim, M. Steppe, E. M. Souza-Fagundes, R. J. Alves, *Eur. J. Med. Chem.* **2017**, 138, 13-25; c) L. M. Kammer, A. Rahman, T. Opatz, *Molecules* **2018**, 23, 764.
- [15] Z. Fang, J. P. Dürholt, M. Kauer, W. Zhang, C. Lochenie, B. Jee, B. Albada, N. Metzler-Nolte, A. Pöpl, B. Weber, M. Muhler, Y. Wang, R. Schmid, R. A. Fischer, *J. Am. Chem. Soc.* **2014**, 136, 9627-9636.
- [16] B. Chen, M. Eddaoudi, S. T. Hyde, M. O'Keeffe, O. M. Yaghi, *Science* **2001**, 291, 1021-1023.
- [17] N. Klein, I. Senkovska, I. A. Baburin, R. Grunker, U. Stoeck, M. Schlichtenmayer, B. Streppel, U. Mueller, S. Leoni, M. Hirscher, S. Kaskel, *Chem. Eur. J.* **2011**, 17, 13007-13016.
- [18] J. H. Cavka, S. Jakobsen, U. Olsbye, N. Guillou, C. Lamberti, S. Bordiga, K. P. Lillerud, *J. Am. Chem. Soc.* **2008**, 130, 13850-13851.
- [19] P. Serra-Crespo, E. V. Ramos-Fernandez, J. Gascon, F. Kapteijn, *Chem. Mater.* **2011**, 23, 2565-2572.
- [20] W. C. Still, M. Kahn, A. Mitra, *J. Org. Chem.* **1978**, 43, 2923-2925.
- [21] S. Pramanik, R. R. Reddy, P. Ghorai, *Org. Lett.* **2015**, 17, 1393-1396.

[22] T. Chen, M. Ning, Y. Ye, K. Wang, Y. Leng, J. Shen, *Eur. J. Med. Chem.* **2018**, *152*, 175-194.

[23] a) P. Gajewski, M. Renom-Carrasco, S. Vailati Facchini, L. Pignataro, L. Lefort, J. G. de Vries, R. Ferraccioli, A. Forni, U. Piarulli, C. Gennari, *Eur. J. Org. Chem.* **2015**, 1887-1893; b) P. Gajewski, M. Renom-Carrasco, S. Vailati Facchini, L. Pignataro, L. Lefort, J. G. de Vries, R. Ferraccioli, U. Piarulli, C. Gennari, *Eur. J. Org. Chem.* **2015**, 5526-5536.

Conclusions

This work of thesis has been aimed at addressing some general limitations of (cyclopentadienone)iron complexes (CICs) when applied to promote reactions involving hydrogen transfer (RIHTs): #1 the rather low catalytic activity, which restricts the application scope of CICs; #2 the limited stability of the activated forms of these complexes, which is also an important reason of the modest observed activity; #3 the lack of effective chiral complexes for applications in enantioselective catalysis.

The state of the art in homogenous iron-catalyzed RIHTs is introduced in Chapter 1, with a special focus on CICs and their applications. In my thesis work, the above-mentioned issues #1 and #2 have been tackled exploiting the peculiar catalytic properties of CIC **9d** (previously developed by our group), which exhibits higher catalytic activity than most other derivatives of its class and thus was found able to promote reactions previously unreported using CICs in the absence of co-catalysts: the catalytic transfer hydrogenation of ketimines (Chapter 2), the reductive amination of ketones (Chapter 2) and the ‘hydrogen borrowing’ amination of secondary alcohols and diols (Chapter 3). CIC heterogenization into metal-organic frameworks (MOFs) was also investigated as a possible way to overcome issue #2, taking advantage of site isolation (which prevents complex dimerization) and of protection of the catalytic units located inside the MOF pores (Chapter 5). Issue #3 was faced developing two new classes of chiral CICs (Chapter 4): i) complexes possessing a stereogenic plane with two different substituents at the 2,5-positions of the cyclopentadienone system; ii) macrocyclic complexes with modular structure derived from readily available chiral compounds.

I believe that the work carried out in this thesis has significantly expanded the application scope of CICs in RIHTs, and its results will provide useful directions for the development of more effective derivatives of this class of pre-catalysts.

List of Abbreviations

Å	1 Angstrom (10^{-10} m)
acac	Acetylacetonate
AcOEt	Ethyl acetate
ADF	Amsterdam Density Functional
ARA	Asymmetric reductive amination
ATH	Asymmetric Transfer Hydrogenation
AH	Asymmetric Hydrogenation
BINOL	1,1'-Bi-2-naphthol
Bn	Benzyl-
Bu	Butyl-
CD	Circular Dichroism
CH	Catalytic Hydrogenation
CICs	(Cyclopentadienone)iron complexes
CIC	(Cyclopentadienone)iron complex
CPME	Cyclopentyl methyl ether
CSP	Chiral stationary phase
CTH	Catalytic Transfer Hydrogenation
CV	Cyclic voltammetry
Cy	Cyclohexyl-
DCE	1,2-dichloroethane
DCC	<i>N,N'</i> -Dicyclohexylcarbodiimide
DCM	Dichloromethane
DFT	Density Functional Theory
DIC	<i>N,N'</i> -Diisopropylcarbodiimide
DMAP	4-Dimethylaminopyridine
DME	Dimethoxyethane
DMF	<i>N,N</i> -dimethylformamide
DIPEA	<i>N,N</i> -diisopropylethylamine
δ	Chemical shift
ECD	Electronic Circular Dichroism
EDC	(3-Dimethylaminopropyl)- <i>N</i> -ethylcarbodiimide hydrochloride
eq.	Equivalent
ESI	Electrospray-ionization
Et	Ethyl-
FCC	Flash Column Chromatography
FTIR	Fourier-transform infrared spectroscopy
GC	Gas chromatography
HATU	(1-[Bis(dimethylamino)methylene]-1H-1,2,3-triazolo[4,5-b]pyridinium 3-oxide hexafluorophosphate
HB	Hydrogen borrowing
HCICs	hydroxycyclopentadienyl iron complexes
hex	Hexyl-
HMDS	Hexamethyldisilazane

List of abbreviations

HMTA	Hexamethylenetetraamine (urotropine)
HOAt	1-Hydroxy-7-azabenzotriazole
HPLC	High-performance liquid chromatography
HRMS	High resolution mass spectrometry
Hz	Hertz
IPA	2-Propanol
<i>i</i> PrOH	2-Propanol
<i>J</i>	Coupling constant
LDA	Lithium diisopropylamide
M	Molar [mol/L]
Me	Methyl-
MOFs	Metal-organic frameworks
MS	Molecular sieves
<i>n</i>	Normal
NHC	<i>N</i> -Heterocyclic carbenes
NMR	Nuclear magnetic resonance
ORD	Optical Rotatory Dispersion
Ph	Phenyl-
PMP	Para-methoxyphenyl-
ppm	Parts per million
Py	Pyridine
RIHT	Reactions involving hydrogen transfer
r.t.	Room temperature
SEC	Spectroelectrochemistry
TBDMS	tert-Butyldimethylsilyl-
TEA	Triethylamine
TES	Triethylsilyl-
TFA	Trifluoroacetic acid
TH	Transfer Hydrogenation
THF	Tetrahydrofuran
TIPS	Triisopropylsilyl-
TLC	Thin layer chromatography
TMS	Trimethylsilyl-
TOF	Turnover Frequency
TON	Turnover Number
TRIP	3,3'-Bis(2,4,6-triisopropyl-phenyl)-1,1'-binaphthyl-2,2'-diyl hydrogen phosphate
TS	Transition State
UV	Ultraviolet
XRD	X-ray Diffraction

List of papers deriving from this work of thesis

- (1) *Efficient Synthesis of Amines by Iron-Catalyzed C=N Transfer Hydrogenation and C=O Reductive Amination*. S. Vailati Facchini, M. Cettolin, X. Bai, G. Casamassima, L. Pignataro, C. Gennari, U. Piarulli, *Adv. Synth. Catal.* **2018**, 360, 1054-1059.
- (2) *Improving C=N Bond Reductions with (Cyclopentadienone)iron Complexes: Scope and Limitations*. M. Cettolin, X. Bai, D. Lübken, M. Gatti, S. V. Facchini, U. Piarulli, L. Pignataro, C. Gennari, *Eur. J. Org. Chem.* **2019**, 647-654.
- (3) *Chiral (Cyclopentadienone)iron Complexes with a Stereogenic Plane as Pre-catalysts for the Asymmetric Hydrogenation of Polar Double Bonds*. X. Bai, M. Cettolin, G. Mazzocanti, M. Pierini, U. Piarulli, V. Colombo, A. Dal Corso, L. Pignataro, C. Gennari, *Tetrahedron* **2019**, 75, 1415-1424.
- (4) *Hydrogen-Borrowing Amination of Secondary Alcohols Promoted by a (Cyclopentadienone)iron Complex*. X. Bai, F. Aiolfi, M. Cettolin, U. Piarulli, A. Dal Corso, L. Pignataro, C. Gennari, *Synthesis* **2019**, 51, 3545-3555.

Acknowledgements

I like to thank the China Scholarship Council for my Ph.D. fellowship (CSC No. 201608410107). I wholeheartedly acknowledge my supervisors, Prof. Cesare Gennari and Prof. Luca Pignataro, for giving me the opportunity to start my PhD project, for their kind and patient help and support, and for their tremendous contribution to my scientific education. In general, words can't express my gratitude for their excellent advice and support.

I'm grateful with Prof. F. Gasparrini, Dr. Marco Pierini and Dr. Giulia Mazzocanti for the significant collaboration which allowed me to carry out all the tests of chiral (cyclopentadienone)iron complexes with stereogenic plane in asymmetric hydrogenation of polar double bonds.

I'm proud of the important collaboration with Dr. Marco Ranocchiari (Paul Scherrer Institute) for the synthesis of MOF-supported (cyclopentadienone)iron complexes, which allowed me to obtain the catalytic MOFs and tested their catalytic activity in hydrogenation of C=O bonds.

I'm also proud of the important collaboration with Prof. Umberto Piarulli, Dr. Sofia Vailati Facchini, which allowed me to carry out all the research with the (cyclopentadienone)iron complex **9d**.

I thank Dr. Mattia Cettolin for giving me a lot of help and advice in my PhD project, and Dr. André Filipe Raposo Moreira Dias, Dr. Paula Lopez Rivas and Dr. Arianna Pina for giving me much help in my life and work.

In a word, thank all the kind and wonderful people I met during my PhD: Alberto Dal Corso, Giovanni Sacco, Francesco Aiolfi, Valentina Borlandelli, Franzisca Schirmer, Simone Grosso, Andrea Dell'Acqua, Eduard Figueras, Sabine Schuster, Simone Zanella, Dennis Lübken and so on.

And finally, a big thanks to my parents (谢谢你们对我的无私奉献与支持), my sister (谢谢你代我在家孝敬父母以及对我学业的支持), and to my beloved wife – Qiu Huili. Without Huili, this thesis wouldn't have been written, and even this PhD wouldn't have been started.

Last from the University of Milan, but absolutely not least. Every wonderful things experiencing during my three years PhD will become to be a memorable reminiscence.